

Synthesis and pharmacological characterization of new histamine H₁-/H₄-receptor ligands derived from the atypical antipsychotic drug Clozapine

Dissertation

zur Erlangung des Doktorgrades der Naturwissenschaften (Dr. rer. nat.) der
Naturwissenschaftlichen Fakultät IV – Chemie und Pharmazie –
der Universität Regensburg



vorgelegt von
Susanne Gobleder
aus Eichstätt

2014

Die vorliegende Arbeit entstand in der Zeit von Juli 2010 bis Mai 2014 unter der Leitung von Frau PD Dr. Andrea Straßer und Herrn Prof. Dr. Sigurd Elz am Institut für Pharmazie der Naturwissenschaftlichen Fakultät IV - Chemie und Pharmazie - der Universität Regensburg.

Das Promotionsgesuch wurde eingereicht im Mai 2014.

Tag der mündlichen Prüfung: 23. Mai 2014

Prüfungsausschuss:	Prof. Dr. A. Buschauer (Vorsitzender)
	PD Dr. A. Straßer (Erstgutachterin)
	Prof. Dr. S. Elz (Zweitgutachter)
	Prof. Dr. J. Heilmann (Drittprüfer)

Author's Declaration

The author declares that the work presented in this thesis was written by none other than herself. Apart from where indicated, all work was performed or supervised by the author.

Molecular dynamics simulations described in **Chapter 4.4.1.2** and **Figure 4.5** were performed by PD Dr. A. Straßer and Dr. H.-J. Wittmann (Department of Pharmaceutical / Medicinal Chemistry II, University of Regensburg, Germany; Faculty of Chemistry and Pharmacy, University of Regensburg, Germany).

Competition binding assays at dopamine, serotonin and muscarine receptors described in **Chapter 4.4.3** were performed by Prof. Dr. P. Gmeiner, Dr. H. Hübner and Coworkers (Department of Pharmaceutical Chemistry, Friedrich Alexander University Erlangen – Nürnberg, Germany).

Danksagungen

An dieser Stelle möchte ich mich bedanken bei:

Frau PD Dr. Andrea Straßer für die wissenschaftlichen Anregungen und die konstruktive Kritik bei der Durchsicht dieser Arbeit, für die Erstellung des Erstgutachtens sowie für die strukturierte, gewissenhafte und zielorientierte Betreuung während der gesamten Promotionszeit,

Herrn Prof. Dr. Sigurd Elz für die Vergabe des interessanten und herausfordernden Promotionsthemas, für seine geduldige Hilfestellung bei der Interpretation der organopharmakologischen Daten am Meerschweinchen-Ileum und für die Erstellung des Zweitgutachtens,

Herrn Prof. Dr. Jörg Heilmann für seine Bereitschaft, das Amt des Drittprüfers zu übernehmen,

Herrn Prof. Dr. Armin Buschauer für die Möglichkeit zur Teilnahme an den Lehrstuhlseminaren seines Arbeitskreises sowie zur Durchführung der pharmakologischen Arbeiten an seinem Lehrstuhl und dafür, dass er sich bereit erklärt hat, den Vorsitz der Prüfungskommission zu übernehmen,

Herrn Prof. Dr. Jens Schlossmann für die Zurverfügungstellung von Laborräumen und -verbrauchsmaterialien zur Durchführung der Radioligand-Bindungsassays an seinem Lehrstuhl,

Herrn Dr. Hans-Joachim Wittmann für die Erstellung der Molecular Dynamics Simulationen am Histamin H₁- und H₄-Rezeptor,

Frau Maria Beer-Krön für die Bereitstellung der Sf9-Zellen, ihre außerordentliche Hilfsbereitschaft bei der Membranpräparation sowie für ihre Unterstützung bei der Durchführung der steady-state [³³P]GTPase- und [³⁵S]GTPγS Assays,

Frau Christine Braun und Frau Kerstin Röhl für die zuverlässige Durchführung der organopharmakologischen Testungen am Meerschweinchen-Ileum,

Frau Gertraud Wilberg für die Bereitstellung der Sf9-Zellen sowie für ihre Hilfsbereitschaft in allen Bereichen der pharmakologischen Labortätigkeiten,

Frau Uta Hasselmann für ihre tatkräftige Unterstützung bei organisatorischen Problemen aller Art und für ihre ansteckende gute Laune,

allen Mitarbeitern der analytischen Abteilungen der Fakultät für die Aufnahme der NMR- und Massenspektren sowie für die Durchführung der Elementaranalysen,

allen Mitgliedern der Lehrstühle Pharmazeutische Chemie I und Pharmazeutische Chemie II für das angenehme Arbeitsklima, die kollegiale Zusammenarbeit und die stetige Hilfsbereitschaft bei chemischen Problemstellungen (hierbei gilt der Dank insbesondere Herrn Dr. Herwig Pongratz und Herrn Dr. Andreas Sellmer),

meinen Kollegen Frau Bernadette Streifinger und Herrn Michel Leonhard für die geduldige Hilfe bei der Formatierung dieser Arbeit,

meinem Kollegen Herrn Thomas Dang-Lieu für die Unterstützung bei Netzwerk- und Computerproblemen,

Frau Franziska Naporra für die engagierte Mitarbeit im Labor im Rahmen ihres Forschungspraktikums,

meinem Laborkollegen Herrn Steffen Pockes für eine fabelhafte musikalische Untermalung der gemeinsamen Laborzeit (möge sich die Discokugel immer drehen) sowie für die gute Freundschaft während der Promotion,

meinen Kolleginnen in der Marien Apotheke Schierling, die mir durch ihr herzliches Betriebsklima eine angenehme Abwechslung zum Laboralltag geboten haben,

meinen Eltern für ihre liebevolle Fürsorge, ihre Ermutigung und ihre Unterstützung während des Studiums und der Promotion,

und vor allem meinem Freund Tommy für seine Geduld, sein Verständnis und seinen bedingungslosen Rückhalt in allen Lebenslagen.

Scientific presentations

- **EFMC-ISMIC 21st International Symposium on Medicinal Chemistry, Brussels (Belgium), 05. – 09.09.2010**
Poster presentation. E. Wagner, S. Gobleder and A. Straßer. “Synthesis, pharmacological characterization and molecular modelling of dual Histamine H₁-/H₄-receptor antagonists.”
- **5th Summer School “Medicinal Chemistry”, Regensburg (Germany), 13. – 15.09.2010**
Poster presentation. E. Wagner, S. Gobleder and A. Straßer. “Synthesis, pharmacological characterization and molecular modelling of dual Histamine H₁-/H₄-receptor antagonists.”
- **Joint Meeting of the Austrian and German Pharmaceutical Societies, Innsbruck (Austria), 20. – 23.09.2011**
Poster presentation. S. Gobleder, S. Elz and A. Straßer. “Synthesis and pharmacology of Clozapine-derived Histamine H₁-/H₄-receptor ligands.”
- **6th Summer School “Medicinal Chemistry”, Regensburg (Germany), 26. – 28.09.2012**
Oral poster presentation. S. Gobleder, S. Elz and A. Straßer. “New Clozapine derived Histamine H₁-/H₄-receptor ligands as possible treatment of type-I-allergic diseases.”
- **Annual meeting of the German Pharmaceutical Society, Greifswald (Germany), 10. – 13.10.2012**
Poster presentation. S. Gobleder, H.-J. Wittmann, S. Elz and A. Straßer. “New Clozapine derived Histamine H₁-/H₄-receptor ligands as possible treatment of type-I-allergic diseases.”
- **Annual meeting of the German Pharmaceutical Society, Freiburg (Germany), 09. – 11.10.2013**
Poster presentation. S. Gobleder, H.-J. Wittmann, S. Elz and A. Straßer. “New Clozapine derived dimeric Histamine H₁-/H₄-receptor ligands and their pharmacological characterization.”

CONTENTS

1. INTRODUCTION	2
1.1. The G-Protein coupled receptors (GPCRs)	2
1.1.1. Structure and classification of GPCRs	2
1.1.2. GPCRs on a molecular level	3
1.1.3. The G-protein cycle	4
1.1.4. Signal transduction pathways of GPCRs	6
1.1.5. Receptor activation and ligand classification	8
1.1.6. GPCR oligomerization and dimerization: bivalent ligands and their interaction with the receptors	10
1.2. Histamine and the histamine receptor family	12
1.2.1. The histamine H ₁ receptor	13
1.2.2. The histamine H ₂ receptor	17
1.2.3. The histamine H ₃ receptor	19
1.2.4. The histamine H ₄ receptor	23
1.3. Antipsychotic drugs	26
1.3.1. Classification	26
1.3.2. Clozapine and its interaction with multiple molecular targets (“dirty drug” problem)	28
1.4. References	30
2. SCOPE AND OBJECTIVES	46
References	49
3. CHEMICAL SECTION	52
3.1. Ligand design related to VUF 6884 (Smits et al., 2006)	52
3.2. Synthesis of the “open” phenylbenzamidines: opening up the rigid aromatic ring system in the center of the molecule	53
3.2.1. VUF 6884 reduced to the core: (<i>E</i>)- <i>N</i> -(2-aminoethyl)- <i>N</i> -phenylbenzamidine derivatives	53
3.2.2. “Open” VUF 6884 derivatives with modified substitution pattern: detecting the influence of kind and position of the substituents	54
3.2.3. Acylated open VUF 6884 derivatives: an attempt to increase the hH ₄ R affinity	58
3.3. Synthesis of the closed VUF 6884 derivatives: return to a rigid aromatic ring system in the center of the molecule	61

Contents

3.3.1.	“Ring-closed” VUF 6884 derivatives with modified substitution pattern: determining the key role of the closed central heterocycle in synergy with the substitution pattern_____	62
3.3.2.	“Closed” VUF 6884 derivatives with a modified piperazine moiety: exchanging <i>N</i> -methylpiperazine by piperazine _____	65
3.4.	Dimeric dibenzo[<i>b,f</i>][1,4]oxazepines: an approach to address homo- and hetero-oligomeric histamine H₁ and H₄ receptors_____	66
3.4.1.	Dibenzo[<i>b,f</i>][1,4]oxazepines linked by nonpolar alkyl spacers at the piperazine moiety	69
3.4.2.	Dibenzo[<i>b,f</i>][1,4]oxazepines linked by polar spacers at the piperazine moiety _____	71
3.4.3.	Dibenzo[<i>b,f</i>][1,4]oxazepines linked by at the NH ₂ group in position 3 / 3' _____	74
3.5.	References_____	76
4.	PHARMACOLOGICAL SECTION_____	80
4.1.	Pharmacological parameters _____	80
4.1.1.	Schild equation _____	80
4.1.2.	Cheng-Prusoff equation _____	81
4.1.3.	GTPase activity_____	82
4.2.	Antagonist binding on a molecular level _____	83
4.3.	Pharmacological materials and methods_____	84
4.3.1.	The Sf9 / Baculovirus expression system (Schneider and Seifert, 2010)_____	84
4.3.2.	Generation of recombinant baculoviruses (Seifert et al., 2003, Seifert and Wieland, 2005, Schneider et al., 2009, Schnell et al., 2011) _____	85
4.3.3.	Membrane preparation out of Sf9 cells (Seifert et al., 1998) _____	86
4.3.4.	³ [H]MEP-/ ³ [H]HIS-competition-binding experiments at hH ₁ R and hH ₄ R (Seifert et al., 2003, Schneider et al., 2010) _____	87
4.3.5.	Steady-state [³³ P]GTPase activity assay at hH ₁ R (Preuss et al., 2007) _____	88
4.3.6.	[³⁵ S]GTPγS-binding assay at hH ₄ R (Schneider et al., 2009) _____	89
4.3.7.	[³⁵ S]GTPγS-binding assays at hH ₂ R and hH ₃ R (Schneider et al., 2009) _____	90
4.3.8.	Organ bath experiments at the isolated guinea pig ileum (Elz et al., 2000) _____	90
4.3.9.	Pharmacological characterization of selected compounds at dopamine, serotonin and muscarine receptors _____	91
4.3.9.1.	Determination of the binding affinity to dopamine and serotonin receptors _____	91
4.3.9.2.	Binding studies with muscarine receptors_____	92
4.3.9.3.	Data analysis for binding studies to dopamine, serotonin and muscarine receptors ____	92
4.4.	Pharmacological results _____	93
4.4.1.	[³ H]MEP-/ ³ [H]HIS-competition binding experiments at hH ₁ R and hH ₄ R_____	93

Contents

4.4.1.1.	Characterization of the (<i>E</i>)- <i>N</i> -(2-aminoethyl)- <i>N</i> -phenylbenzamidines: VUF 6884 reduced to the core _____	93
4.4.1.2.	Characterization of dibenzo[<i>b,f</i>][1,4]oxazepines: the key role of the closed central oxazepine ring _____	98
4.4.1.3.	Characterization of dimeric dibenzo[<i>b,f</i>][1,4]oxazepines _____	105
4.4.1.3.1.	Dibenzo[<i>b,f</i>][1,4]oxazepines linked by nonpolar alkylspacers _____	105
4.4.1.3.2.	Dibenzo[<i>b,f</i>][1,4]oxazepines linked by polar spacers of different type and length: compounds linked at the piperazine moiety _____	107
4.4.1.3.3.	Dibenzo[<i>b,f</i>][1,4]oxazepines linked by polar spacers of different type and length: compounds linked at the NH ₂ group in position 3 / 3' _____	111
4.4.2.	Isolated guinea pig ileum _____	114
4.4.2.1.	Characterization of the mono, di, and acylamino substituted open compounds _____	114
4.4.2.2.	Characterization of the closed dibenzo[<i>b,f</i>][1,4]-oxazepine derivatives _____	117
4.4.2.3.	Characterization of the dimeric dibenzo[<i>b,f</i>][1,4]-oxazepine derivatives _____	120
4.4.2.3.1.	Dimeric “ring-closed” VUF 6884 derivatives linked by nonpolar alkyl spacers at the piperazine moiety _____	120
4.4.2.3.2.	Dimeric “ring-closed” VUF 6884 derivatives linked by polar spacers at the piperazine moiety _____	121
4.4.2.3.3.	Dimeric “ring-closed” VUF 6884 derivatives linked at the NH ₂ group in position 3 / 3' _____	122
4.4.2.4.	Estimating the pA ₂ values for compounds with slope significantly ≠ 1 (<i>method A</i>) _____	124
4.4.2.5.	Estimating the pA ₂ values for compounds with slope significantly ≠ 1 (<i>method B</i>) _____	128
4.4.2.6.	Comparison of the pK _i (hH ₁ R) and the pA ₂ (gp-ileum) _____	137
4.4.2.6.1.	“Open” VUF 6884 derivatives _____	137
4.4.2.6.2.	“Ring-closed” VUF 6884 derivatives _____	138
4.4.2.6.3.	Dimeric “ring-closed” VUF 6884 derivatives linked by nonpolar alkyl spacers at the piperazine moiety _____	138
4.4.2.6.4.	Dimeric “ring-closed” VUF 6884 derivatives linked by polar spacers at the piperazine moiety _____	139
4.4.2.6.5.	Dimeric “ring-closed” VUF 6884 derivatives linked at the NH ₂ group in position 3 / 3' _____	140
4.4.3.	Pharmacological characterization of selected compounds at dopamine, serotonin and muscarine receptors _____	141
4.4.3.1.	Porcine and human dopamine receptors pD ₁ / hD ₁ _____	142
4.4.3.2.	Human dopamine receptors hD _{2short} , hD _{2long} and hD ₃ _____	142
4.4.3.3.	Human dopamine receptor hD _{4.4^a} _____	143
4.4.3.4.	Porcine serotonin receptors p5-HT _{1A} and p5-HT ₂ _____	143
4.4.3.5.	Human muscarine receptors hM ₁ , hM ₂ and hM ₃ _____	144

Contents

4.4.4.	Functional assays at human histamine receptors: pharmacological results of steady state [³³ P]GTPase activity assays and [³⁵ S]GTPγS binding assays _____	148
4.4.4.1.	Steady-state [³³ P]GTPase activity assays at hH ₁ R _____	148
4.4.4.2.	[³⁵ S]GTPγS binding assays at hH ₄ R _____	151
4.4.4.3.	[³⁵ S]GTPγS binding assays at hH ₂ R and hH ₃ R (selectivity studies) _____	152
4.5.	Discussion _____	155
4.5.1.	Structure activity relationships of a selected core compound prevalent within all series: compounds bearing Cl substituents in position 3 and 7 / <i>p</i> - position of the aniline and the benzoic acid moiety (related to 159) _____	155
4.5.2.	Structure activity relationships of H ₁ R and H ₄ R ligands _____	159
4.6.	References _____	165
5.	SUMMARY _____	170
6.	EXPERIMENTAL SECTION _____	176
6.1.	General chemical procedures _____	176
6.2.	General procedure A: Preparation of compounds 22, 23, 25 _____	177
6.3.	General procedure B: Preparation of compounds 4, 45 – 47, 53, 59, 65, 68, 71, 74, 77, 100, 104, 105, 176, 177 _____	179
6.4.	General procedure C: Preparation of compounds 28, 50, 55, 58, 61, 64, 67, 70, 73, 76, 79, 102, 108, 109, 180, 181 _____	187
6.5.	General procedure D: Preparation of compounds 52, 56, 62, 80, 103, 110, 111 _____	198
6.6.	General procedure E: Preparation of compounds 99, 112, 114 - 117 _____	203
6.7.	General procedure F: Preparation of compounds 84, 118, 145 _____	207
6.8.	General procedure G: Preparation of compounds 85, 89, 119, 120, 132, 138, 146, 152, 153 _____	209
6.9.	General procedure H: Preparation of compounds 86, 90, 122, 123, 133, 139, 147, 154, 155 _____	214
6.10.	General procedure I: Preparation of compounds 88, 92, 126, 127, 135, 141, 149, 158, 159 and 193, 196, 232 - 235 _____	218
6.11.	General procedure J: Preparation of compounds 128, 129, 136 _____	230

Contents

6.12.	General procedure K: Preparation of compounds 205 – 210, 212, 213 _____	232
6.13.	General procedure L: Preparation of compounds 217, 224 _____	239
6.14.	General procedure M: Preparation of compounds 225, 238 – 242, 244 _____	240
6.15.	General procedure N: Preparation of compounds 215, 221, 227, 229 – 231, 243 _____	246
6.16.	Overview _____	253
6.17.	Appendix _____	258
6.17.1.	HPLC parameters for compounds 243 and 244 _____	258
6.17.2.	HSQC-, HMBC- and COSY-NMR spectra of compound 88 _____	259
	Eidesstattliche Erklärung _____	265

List of abbreviations

List of abbreviations

5-HT	5-hydroxytryptamine
AC	adenylyl cyclase
ACN	acetonitrile
ADHD	attention deficit hyperactivity disorder
AMP	adenosine 5`-monophosphate
ATP	adenosine 5`-triphosphate
B _{max}	maximal specific binding of a ligand
Boc	<i>tert</i> -butoxycarbonyl
BRET	bioluminescence resonance energy transfer
BSA	bovine serum albumin
cAMP	cyclic adenosine 3`,5`-monophosphate
cGMP	cyclic guanosine 3`,5`-monophosphate
CHO cells	chinese hamster ovary cells
CI	chemical ionization
CLO	clozapine
CNS	central nervous system
COSY	correlation spectroscopy
CREB	cAMP response element binding protein
CTCM	cubic ternary complex model
DAG	1,2-diacylglycerol
DCM	dichloromethane
DIPEA	diisopropylethylamine
DMF	<i>N,N</i> -dimethylformamide
DMSO	dimethyl sulfoxide
EC ₅₀	concentration of agonist producing 50% of the maximal effect
ECL	extracellular loop of a G-protein coupled receptor
EI	electron (impact) ionization
ESI	electrospray ionization
EPS	extrapyramidal side effects
ERK	extracellular signal-regulated kinase
ETCM	extended ternary complex model

List of abbreviations

EtOAc	ethyl acetate
EtOH	ethanol
FRET	fluorescence resonance energy transfer
GC	guanylyl cyclase
GDP	guanosine 5'-diphosphate
GMP	guanosine 5'-monophosphate
GPCR	G-protein coupled receptor
GRK	G-protein coupled receptor kinase
GTP	guanosine 5'-triphosphate
GTP γ S	guanosine 5'-[γ -thio]triphosphate
G α_i	α -subunit of G-proteins that inhibits certain isoforms of adenylyl cyclase
G α_q	α -subunit of G-proteins that stimulates phospholipase C
G α_s	α -subunit of G-proteins that stimulates adenylyl cyclase
G $\beta\gamma$	$\beta\gamma$ -subunits of a heterotrimeric G-protein
h	hour(s)
H ₁ R, H ₂ R, H ₃ R, H ₄ R	histamine receptor subtypes
HEK cells	human embryonic kidney cells
HIS	histamine
HMBC	heteronuclear multiple bond correlation
HSQC	heteronuclear single quantum correlation
HPLC	high performance (pressure) liquid chromatography
HX	hexane
IC ₅₀	concentration of inhibitor producing 50% of inhibition
ICL	intracellular loop of a G-protein coupled receptor
IP ₃	inositol-1,4,5-trisphosphate
K _B	dissociation constant of receptor to antagonist
K _D	dissociation constant of a radioligand
K _i	dissociation constant of a competitive inhibitor and a receptor
LOX	loxapine
MAPK	mitogen-activated protein kinase
MD	molecular dynamics
MeOH	methanol

List of abbreviations

MEP	mepyramine
min	minute(s)
NEt ₃	triethylamine
NMR	nuclear magnetic resonance
NO	nitric oxide
pA ₂	-log of the dissociation constant K _B
PBS	phosphate buffered saline
PDE	phosphodiesterase
pEC ₅₀	-log of the EC ₅₀ value
PEI	polyethyleneimine
P _i	inorganic phosphate
PI ₃ K	phosphatidylinositol-3-kinase
PIP ₂	phosphatidylinositol-4,5-bisphosphate
PKA	protein kinase A
PKC	protein kinase C
pK _i	-log of the K _i value
PLA ₂	phospholipase A ₂
PLC	phospholipase C
PNS	peripheral nervous system
R	inactive state of a G-protein coupled receptor
R*	active state of a G-protein coupled receptor
RGS	regulator of G-protein signaling
Rho-GEFs	Ras homology guanine nucleotide exchange factors
rpm	revolutions per minute
RT	room temperature
SARs	structure-activity relationships
Sf9	insect cell line of <i>Spodoptera frugiperda</i>
TCM	ternary complex model
TFA	trifluoroacetic acid
THF	tetrahydrofuran
TM	transmembrane domain of a G-protein coupled receptor
TLC	thin-layer chromatography
TOL	toluene

Chapter 1

Introduction

1. Introduction

1.1. The G-Protein coupled receptors (GPCRs)

The G-Protein coupled receptors (GPCRs) represent the largest group of membrane integrated receptors in the human genome. (Lagerström and Schiöth, 2008) By now, roughly 800 GPCRs have been identified (Fredriksson et al., 2003) that are divided into two groups: about 400 GPCRs belong to the family of the endoGPCRs that are addressed by peptides, lipids, prostanoids, neurotransmitters, nucleosides and nucleotides, whereas about 400 GPCRs belong to the family of csGPCRs (chemosensory GPCRs) that respond to external signals like odors, tastes, photons or pheromones. (Vassilatis et al., 2003, Kristiansen, 2004) For more than 260 endoGPCRs endogenous ligands have been identified whereas the remaining 140 endoGPCRs are counted among the group of “orphan receptors” as their endogenous ligands have not yet been conclusively identified. (Sharman et al., 2013)

GPCRs are the target of about 30 % of the drugs prevalent on the current drug market (Overington et al., 2006, Stevens et al., 2013) and play important roles in a long row of physiological and pathophysiological processes. (Fang et al., 2003) Therefore, it is not surprising that GPCRs are still of major interest in pharmacological research and drug discovery.

1.1.1. Structure and classification of GPCRs

All GPCRs are characterized by a common architecture: an extracellular N-terminus, seven transmembrane α -helices (TM1 – TM7) and an intracellular C-terminus. The counter-clockwisely arranged transmembrane α -helices share a very high degree of sequence conservation and are linked by three intra- and three extracellular loops (ICL 1 – 3, ECL 1 -3) that distinctly differ in their size and complexity. Transmembrane and extracellular regions are involved in ligand binding, whereas the intracellular regions are responsible for the signal transduction in the cell. (Ji et al., 1998) The name G-protein coupled receptor results from the classical way of signaling that consists of coupling to heterotrimeric G-proteins located at the intracellular surface. (Fredriksson et al., 2003, Kobilka, 2007, Lagerström and Schiöth, 2008)

Due to structural differences, mammalian GPCRs are grouped into five receptor families, also known as “GRAFs system” (Fredriksson et al., 2003): rhodopsin, secretin, adhesion, glutamate and frizzled/taste2. A former GPCR classification system dividing the GPCRs into classes A – F (Kolakowski, 1994) is used by the International Union of Pharmacology, Committee on Receptor Nomenclature and Classification (NC-IUPHAR) (Foord et al., 2005). This system differs from the GRAFs system by comprising the adhesion and secretin family in class B and by dividing the taste receptors into two sections, one as part of the glutamate and a second as part of the frizzled/taste2 group.

The rhodopsin receptor family (class A) is subdivided in four groups (α , β , γ and δ) and represents the largest subfamily (672 GPCRs, including both endo- and csGPCRs). The secretin-like receptor family (class B) comprises 15 GPCRs that respond to peptides like secretin, calcitonin and parathyroid hormone. The adhesion receptor family (class B) represents with 33 members the second largest receptor family among which the majority is counted to the group of the “orphan receptors”. (Civelli et al., 2013, Sharman et al., 2013) The glutamate receptor family (class C) includes 22 GPCRs that contain very large C- and N-terminal tails. The latter was found to bear a cavity formed by two lobes of the region, a so called Venus flytrap module (Kunishima et al., 2000) that represents the binding site. Finally, the frizzled/taste2 receptor family comprises 10 frizzled and 25 taste GPCRs that are either involved in cell development and proliferation or in the detection of the bitter taste of compounds, respectively. (Fredriksson et al., 2003, Kristiansen, 2004, Jacoby et al., 2006, Lagerström and Schiöth, 2008, Luttrell, 2008, Davies et al., 2011)

In newer literature, the GPCRs are often referred to as “seven transmembrane receptors” (7 TM receptors) as in recent research G-protein independent signal pathways were described for some of these receptors (see [1.1.3](#)). (Ritter and Hall, 2009, Kenakin and Miller, 2010)

1.1.2. GPCRs on a molecular level

The crystal structure of bovine rhodopsin published in 2000 provided a first insight into the three dimensional structure of a representative class A GPCR on a molecular level

(Palczewski et al., 2000). However, as it was bound to the inverse agonist 11-cis retinal, this crystal structure represented an inactive receptor model.

In 2007, the crystal structure of the first aminergic GPCR, the β_2 -adrenergic receptor, was resolved, revealing specific differences with regard to the “ionic lock” of the inactive state of rhodopsin. (Cherezov et al., 2007) The first receptor that was crystallized in its active state was opsin, the ligand free form of rhodopsin. (Park et al., 2008, Scheerer et al., 2008) In 2011, Rasmussen et al. published the crystal structure of the active state of the β_2 -adrenergic receptor by replacing the G-protein by a nanobody (Rasmussen et al., 2011a) as well as in form of the active state ternary complex containing the nucleotide free heterotrimeric G-protein. (Rasmussen et al., 2011b) These milestones in GPCR research represented precursors for the in the meantime resolved 18 crystal structures of different class A GPCRs (Venkatakrishnan et al., 2013), among others the turkey β_1 -adrenergic receptor (Warne et al., 2008), the human dopamine D_3 receptor (Chien et al., 2010) and the human histamine H_1 receptor (Shimamura et al., 2011).

Regarding drug design and receptor investigation, the crystal structure of GPCRs bound to signaling proteins other than the G-protein will be of major interest in future research as it provides new starting points for the investigation of ligand-receptor interactions on a molecular level. (Granier and Kobilka, 2012)

1.1.3. The G-protein cycle

GPCR-mediated G-protein dependent intracellular signaling is prevalently known as the G-Protein cycle (figure [1.1](#)). By binding to either the extracellular loop or the transmembrane domain of the GPCR, the agonist evokes a conformational change of the intracellular surface of the receptor. As a consequence, heterotrimeric G-proteins (consisting of a G_α subunit, a $G_{\beta\gamma}$ complex and a GDP nucleotide (Gilman, 1987, Offermanns, 2003)) are able to bind to the GPCR. This binding evokes the release of the G-protein bound GDP nucleotide, forming a ternary complex of agonist, receptor and nucleotide-free G-protein that is characterized by a very high affinity for the agonist. In a next step, GTP binds to the G_α subunit, leading to a conformational change of the G-protein and thus to a disruption of the ternary complex. The G_α -GTP subunit dissociates from the $G_{\beta\gamma}$ complex and each interact with (different) effector

proteins (e.g., enzymes or ion channels) to give biochemical signals. After a certain period of time, the intrinsic GTPase activity of G_α terminates the G_α -induced signal and the bound GTP is hydrolyzed to GDP and inorganic phosphate (P_i). The now GDP-bound G_α -subunit re-associates with the $G_{\beta\gamma}$ -subunit to the inactive heterotrimeric state that leads over to the next G-protein cycle. (Hermans, 2003, Schneider and Seifert, 2010)

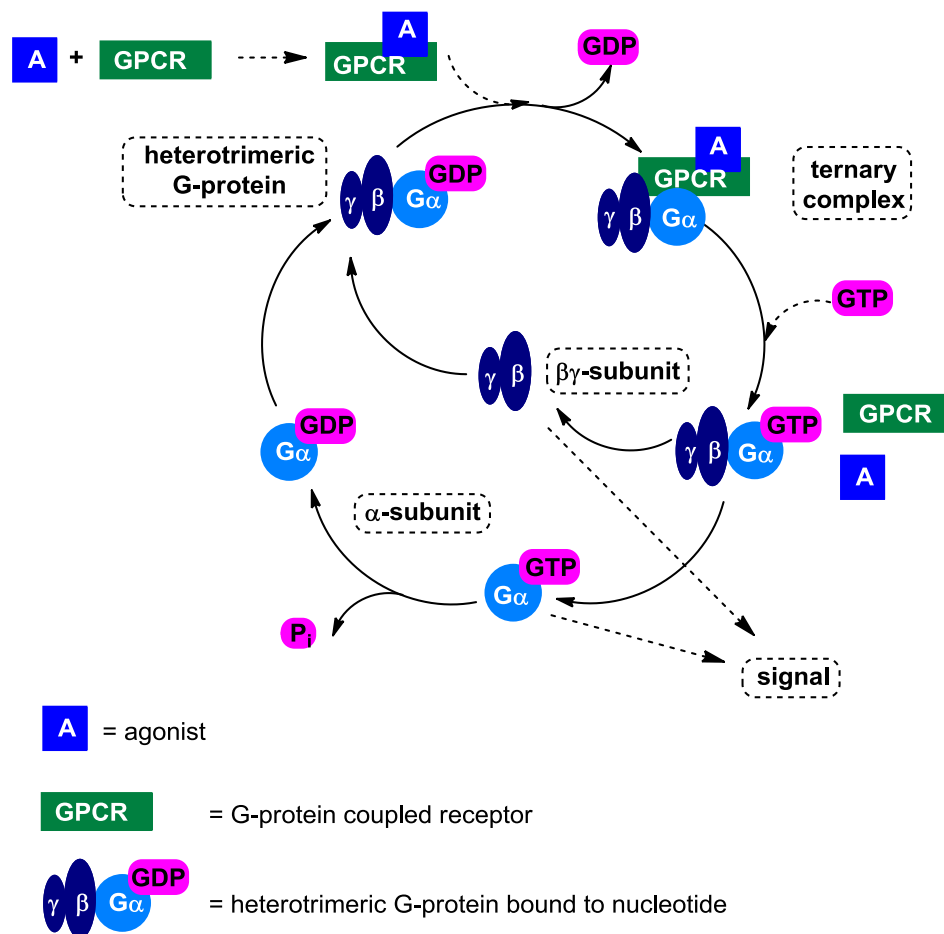


Figure 1.1. The G-protein cycle (adapted from Schneider and Seifert, 2010).

Some GPCRs turned out to reveal the active state although no agonist is bound. As a consequence, they bind to the G-protein complex and evoke biochemical signals, what is prevalently known as “constitutive activity” of a receptor. (Seifert and Wenzel-Seifert, 2002) The activity of G-proteins is moreover influenced by so called “regulators of G-protein signaling” proteins (Zhu et al., 2001) that stimulate the GTPase activity of the α -subunit. (Ross and Wilkie, 2000, De Vries et al., 2000, Neubig and Siderovski, 2002)

Based on the knowledge of the G-protein cycle, several approaches to investigate the GPCR activity on a molecular level are established: firstly, binding studies using fluorescent or radio-labeled ligands to determine the high-affinity binding to a GPCR (referred to as competition binding assay in this work), secondly, the application of radio-labeled non-hydrolysable GTP analogs like, e.g., guanosine 5'-[γ -thio]triphosphate to detect the dissociation of the ternary complex (referred to as [^{35}S]GTP γ S binding assay in this work) as well as thirdly, the measuring of the hydrolysis of radio-labeled GTP to GDP and P_i to determine the intrinsic GTPase activity of the G_α subunit (referred to as [^{33}P]GTPase activity assay in this work). (Schneider and Seifert, 2010)

In recent research not only the classical G-protein-dependent signaling of GPCRs was reported, but also other signal pathways independent from the G-protein (Luttrell, 2008) as, e.g., the GPCR signaling via β -arrestins 1 and 2 that are ubiquitously prevalent in tissues of the human body (Lefkowitz and Whalen, 2004). Although originally regarded as modulators of GPCR desensitization through internalization into clathrin-coated pits (Lefkowitz and Shenoy, 2005, Lefkowitz et al., 2005, Evans et al., 2010), important cellular processes like gene transcription, cell proliferation and differentiation are accounted to these molecules (Rajagopal et al., 2010) and β -arrestin signaling is considered to be pro-survival, cytoprotective and anti-apoptotic. (Violin and Lefkowitz, 2007)

1.1.4. Signal transduction pathways of GPCRs

Based on their structure and signaling pathway, G-proteins are grouped into four main families with regard to their G_α subunit: G_α_s , $\text{G}_{\alpha_{i/o}}$, $\text{G}_{\alpha_{q/11}}$ and $\text{G}_{\alpha_{12/13}}$. (Cabrera-Vera et al., 2003) The different signaling pathways are described in the following.

Characteristic of the G_α_s family is the activation of adenylyl cyclases (AC 1-9) what leads to an increase of the second messenger cAMP (3',5'-cyclic adenosine monophosphate) in the cell. By contrast, inverse effects are observed for the $\text{G}_{\alpha_{i/o}}$ family, as they are known to inhibit the activity of the adenylyl cyclases (AC 5 and AC 6). (Hanoune and Defer, 2001, Pavan et al., 2009) Derived from ATP, the second messenger cAMP is responsible, e.g., for the activation of the protein kinase A (PKA) or the mitogen-activated protein kinase (MAPK) pathway and as a consequence for the modulation of gene expression. (Marinissen and Gutkind, 2001) The signal

transduction is terminated by the inactivation of cAMP (e.g., through phosphodiesterases (PDE)).

The $G_{\alpha_{q/11}}$ family regulates the activity of phospholipase C (PLC_{β}) leading to the hydrolysis of phosphatidylinositol-4,5-bisphosphate (PIP_2) into inositol-1,4,5-trisphosphate (IP_3) and diacylglycerol (DAG), both second messengers that are responsible for various intracellular effects. For instance, the increase of IP_3 levels induces the release of Ca^{2+} ions into the cytosol (Mikoshiba, 2007) that, together with DAG, stimulate the protein kinase C (PKC) and thereby modulate the function of cellular proteins by phosphorylation. (Thomsen et al., 2005)

The last family, the $G_{\alpha_{12/13}}$ family, interferes with the cytoskeletal assembly by interaction with Rho-GEFs (Ras homology guanine nucleotide exchange factors). (Cabrera-Vera et al., 2003, Kristiansen, 2004, Birnbaumer, 2007, Luttrell, 2008)

Moreover, not only the G_{α} -subunit but also the $G_{\beta\gamma}$ -heterodimer can regulate certain effectors like PLC_{β} and ion channels (K^+ and Ca^{2+} regulated). (Cabrera-Vera et al., 2003)

An overview of the families, subtypes and evoked pharmacological effects is given in table 1.1.

Subunit	Family	Subtypes	Effector(s)
α	α_s	$G\alpha_s, G\alpha_{olf}$	AC \uparrow
	$\alpha_{i/o}$	$G\alpha_{i1}, G\alpha_{i2}, G\alpha_{i3}$	AC \downarrow
		$G\alpha_{oA}, G\alpha_{oB}$	K ⁺ channels \uparrow
		$G\alpha_{t1}, G\alpha_{t2}$	PDE \uparrow
		$G\alpha_z$	PDE \uparrow , AC \downarrow
	$\alpha_{q/11}$	$G\alpha_q, G\alpha_{11}, G\alpha_{14-16}$	PLC \uparrow
	$\alpha_{12/13}$	$G\alpha_{12}, G\alpha_{13}$	Rho-guanine-nucleotide-exchange factors \uparrow
β and γ	β_{1-5} and γ_{1-12}	various $\beta\gamma$ complexes	AC \uparrow/\downarrow , PLC \uparrow , PI ₃ K \uparrow , PKC and PKD \uparrow , GPCR kinases \uparrow , Ca ²⁺ and K ⁺ channels

Table 1.1. G-Protein subunits and their effectors according to Hermans, 2003, Worzfeld et al., 2008 and Smrcka, 2008, adapted from Brunskole (PhD Thesis, University of Regensburg, 2011).

1.1.5. Receptor activation and ligand classification

In the past, several models have been set up to describe the mechanism of the activation of GPCRs in dependence of appropriate ligands. A first model, the “ternary complex model” (TCM, figure 1.2 I) (De Lean et al., 1980), describes the agonist promoted interaction of the receptor and the transducer proteins (later identified as G-proteins) (Gilman, 1987). In this model, however, agonist binding to the receptor is necessary to activate the transducer and as a consequence, constitutive activity as well as inverse agonism cannot be explained.

The more suitable “extended ternary complex model” (ETCM, figure 1.2 II) (Samama et al., 1993, Leff, 1995) explains the pharmacodynamic activities of the majority of interacting ligands: receptors exist in both inactive (R) and active (R^{*}) conformations, whereby the latter couples to the transducer protein (R^{*}T) and induces signaling. Inactive receptors (R) are allowed to isomerize to the active conformation (R^{*}), be it

spontaneously or in complex with an agonist (LR^*). The spontaneous activation of the receptor independent from agonist binding is referred to as constitutive activity.

A third and thermodynamically more complex model, the “cubic ternary complex model” (CTCM, figure 1.2 III) (Weiss et al., 1996c, Weiss et al., 1996a, Weiss et al., 1996b) increases the number of conformations compared to the ETCM by including the interaction between the inactive receptor (R) and the transducer (RT) independent from agonist binding.

All three ternary complex models (TCM, ETCM and CTCM) are displayed in figure 1.2.

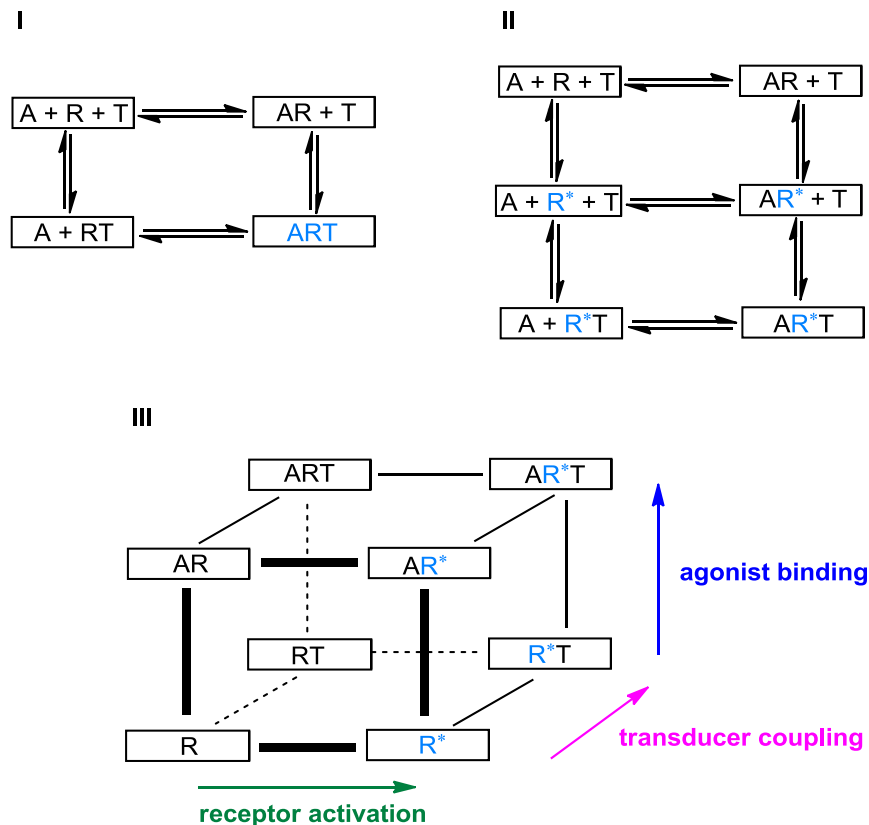


Figure 1.2. Models of GPCR signaling: I. ternary complex model (TCM); II. extended ternary complex model (ETCM); III. cubic ternary complex model (CTCM) (adapted from Rajagopal et al., 2010, Nordemann, PhD Thesis, University of Regensburg, 2013).

A further distinction is made with regard to the kind of the binding ligand and its influence on the equilibrium between the active and the inactive state of the receptor (figure 1.3): agonists reveal a higher affinity to the active receptor conformation (R^*), whereas inverse agonists prefer the interaction with the inactive state of the receptor

(R). Neutral antagonists bind to the active as well as to the inactive conformation with the same affinity without having an impact on the equilibrium. Partial (inverse) agonists are less effective than full (inverse) agonists as they only bind to some extent to the active or inactive state of the receptor, respectively. (Kenakin, 2002b, Kenakin, 2002a)

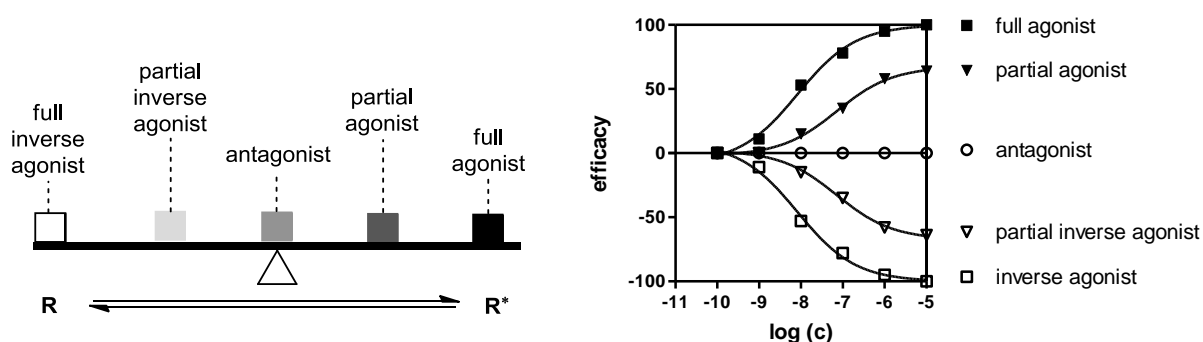


Figure 1.3. Ligand classification according to their impact on the equilibrium between both the active and the inactive receptor state as well as differential responses in an effector system upon binding of different ligand classes (full / partial (inverse) agonist and antagonist) (adapted from Seifert and Wenzel Seifert, 2002).

1.1.6. GPCR oligomerization and dimerization: bivalent ligands and their interaction with the receptors

GPCRs were identified to appear not only as monomers but also as homo-oligomers (two or more identical GPCRs forming a complex) and hetero-oligomers (two or more different GPCRs forming a complex). (Smith and Milligan, 2010) Although their physiological relevance could not yet be sufficiently proved, an important role for GPCRs' trafficking, folding, internalization and activation is postponed. (Nikbin et al., 2003)

In order to investigate this phenomenon on a molecular level, different techniques including cross-linking, immunoblotting and co-immunoprecipitations, radioligand binding studies as well as optical methods like FRET (fluorescence induced resonance energy transfer), BRET (bioluminescence induced resonance energy transfer) and atomic force microscopy were applied. Regarding the receptor-receptor interaction, three regions of interest are obvious: extracellular loops, transmembrane regions as well as intracellular loops that can all interact via covalent and non-covalent bonds. (George et al., 2002, Nikbin et al., 2003)

Several class A and C GPCRs were identified to form receptor homo-dimers, among others dopamine (D₂R, D₃R) (Nimchinsky et al., 1997, Lee et al., 2000), opioid (Cvejic and Devi, 1997, Jordan and Devi, 1999, McVey et al., 2001) and histamine receptors (H₁R, H₂R, H₃R, H₄R) (Fukushima et al., 1997, Carrillo et al., 2003, Bakker et al., 2004, Shenton et al., 2005, van Rijn et al., 2006) as well as the 5-HT_{1D} serotonin receptor (Lee et al., 2000). Furthermore, also receptor hetero-dimers like, e.g., the GABA_{B1}/GABA_{B2} receptors (Kaupmann et al., 1998) or the δ/κ -opioid receptors (Jordan and Devi, 1999) were found and interestingly, there is growing evidence that above all receptor-hetero-dimers reveal a modified signaling pathway as well as a modified ligand binding relative to the individual monomeric receptors. (George et al., 2000, Kristiansen, 2004)

Provided there is an adequate monomeric lead compound as well as a proper attachment point of a sufficiently long spacer, bivalent ligands represent a promising approach to either investigate the pharmacological profile of dimeric GPCRs as well as to improve the potency, selectivity and pharmacokinetic profile of compounds. (Halazy, 1999, Shonberg et al., 2011, Lezoualc'h et al., 2009) Characteristically, bivalent ligands are linked by a spacer and contain either two (different) pharmacophoric entities or, in the broader sense, one pharmacophoric group and a non-pharmacophoric recognition unit. (Portoghese, 1989, Portoghese, 2001)

In dependence of the spacer length, different binding modes are suggested (figure 1.4): if the spacer is too short to link two neighbored GPCRs (be it homo- or heterodimeric) (**I**), the binding to an accessory binding site next to the orthosteric binding site of the monomeric GPCR is postulated. If the spacer is of sufficient length to bridge the two neighbored GPCRs (**II**), each pharmacophoric entity of the bivalent ligand may interact with the (orthosteric) binding site of one receptor. (Portoghese, 1989, Jones et al., 1998, Halazy, 1999, Portoghese, 2001, Messer, 2004)

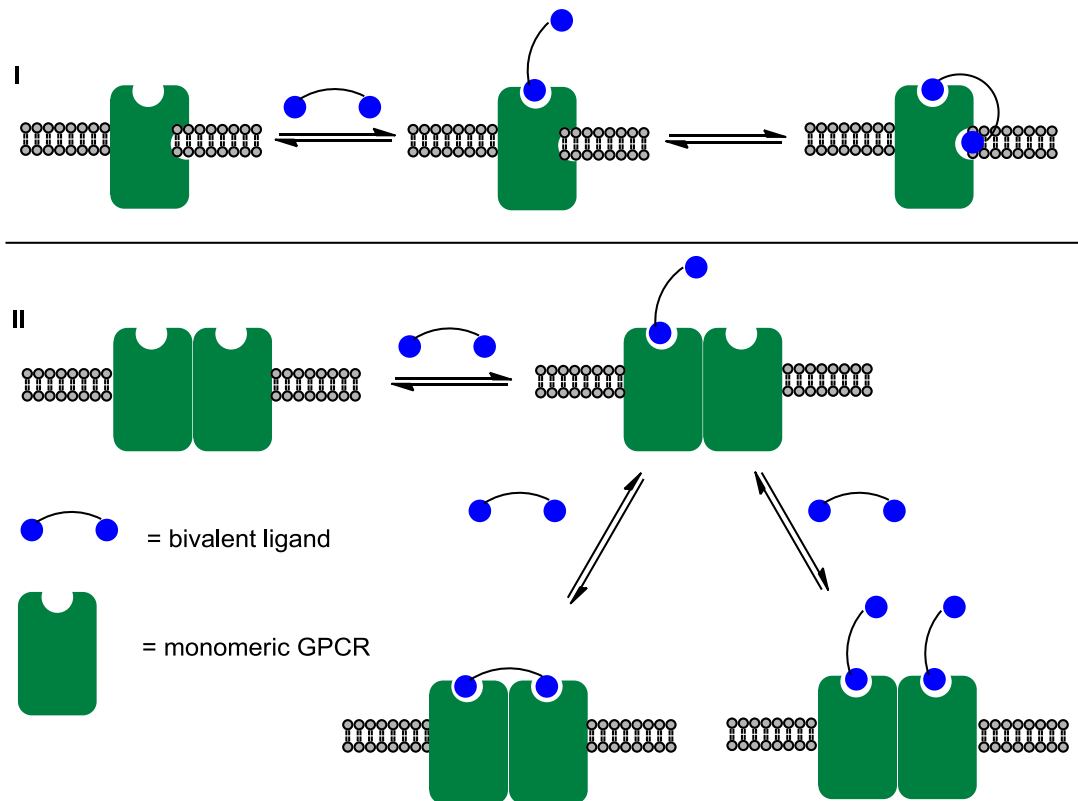


Figure 1.4. A bivalent ligand binding to a GPCR with an accessory binding site (I) or to a GPCR dimer (II). Adapted from Portoghese (1989), Portoghese (2001) and Igel (2008).

1.2. Histamine and the histamine receptor family

Reviewing more than 100 years of histamine research, beginning with the first technical histamine synthesis (Windaus and Vogt, 1908) plus the first isolation out of ergot (*Claviceps purpurea*) (Barger and Dale, 1910) and culminating in the first crystallization of an H₁R (Shimamura et al., 2011), histamine and its receptors have been intensively investigated. (Parsons and Ganellin, 2006)

As a biogenic amine, histamine (2-(1*H*-imidazol-4-yl)ethanamine) (figure 1.5) was found to be a local mediator, immunomodulator as well as a neurotransmitter targeting four histamine receptor subtypes that were successively discovered: the H₁R (Ash and Schild, 1966), the H₂R (Black et al., 1972), the H₃R (Arrang et al., 1983) and the recently and by several research groups more or less simultaneously found H₄R (Oda et al., 2000, Nakamura et al., 2000, Liu et al., 2001, Morse et al., 2001, Nguyen et al., 2001, Zhu et al., 2001). All four histamine receptor subtypes represent rhodopsin like

(class A) GPCRs with different signaling related to their G-protein coupling. A more detailed description of their signaling pathway as well as an overview over selected (selective) ligands will be given in the following.

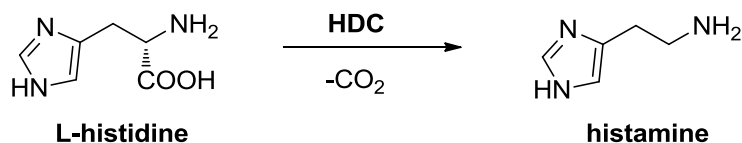


Figure 1.5. Biosynthesis of histamine (HDC = histidine decarboxylase) (Haas et al., 2008).

In the human body, histamine is synthesized from the amino acid L-histidine (figure 1.5) and plays a major role in physiological and pathophysiological processes like inflammatory reactions, the modulation of immune responses as well as the regulation of gastrointestinal and circulatory functions. (Dy and Schneider, 2004) Moreover, it was found to have impact on a number of brain functions as, e.g., the sleep-wake cycle, learning and memory processes, anxiety or neuroendocrine regulation (Passani et al., 2007). Histamine accumulates in tissues of the skin, the lungs and the gastrointestinal tract and is stored in neurons, endothelial cells, mast cells, basophil granulocytes as well as in the enterochromaffin like (ECL) cells in the stomach. (Riley and West, 1952, Graham et al., 1955, Hakanson et al., 1974, Karnushina et al., 1980, Schwartz et al., 1980, Saxena et al., 1989, Falcone et al., 2006)

During allergic conditions, histamine is released from the secretory granules in mast cells and basophiles, resulting in vasodilatation, smooth muscle contraction and an increase of vascular permeability. Histamine released from ECL cells regulates the secretion of gastric acid in the parietal cells. (Mössner and Caca, 2005) Macrophages, dendritic cells, neutrophils and T-cells were furthermore found to release histamine after *de novo* synthesis. (Thurmond et al., 2008)

1.2.1. The histamine H₁ receptor

The human histamine H₁R consists of 487 amino acids and is expressed in a huge number of tissues in the human body (smooth muscle cells of blood vessels, airways and the gastrointestinal tract, endothelial cells, lymphocytes, leukocytes, dendritic cells

as well as in the cardiovascular system and the brain). (Hill, 1990) It plays an important role in the pathophysiology of allergic and inflammatory reactions like, e.g., bronchial asthma, allergic rhinitis, urticaria and histamine induced itch, explained by the H₁R signaling pathway on a molecular level: as the H₁R couples to pertussis-toxin insensitive G $\alpha_{q/11}$ proteins, phospholipase C (PLC) is activated. Subsequently, Ca²⁺ is released from intracellular stores (leading to a contraction of smooth muscles like, e.g., of the airways) and the protein kinase C (PKC) is activated (regulating the gene expression by phosphorylation). (Leurs et al., 1995) The contraction of endothelial cells leads to an increase of vascular permeability and thus to typical allergic reactions like urticaria and itching. (Majno and Palade, 1961) Moreover, the release of nitric oxide (NO) from endothelial cells is induced, resulting in the dilatation of smooth muscles of the blood vessels and thus to the decrease of blood pressure. (Vandevorde and Leusen, 1983, Toda, 1984) (Figure 1.6)

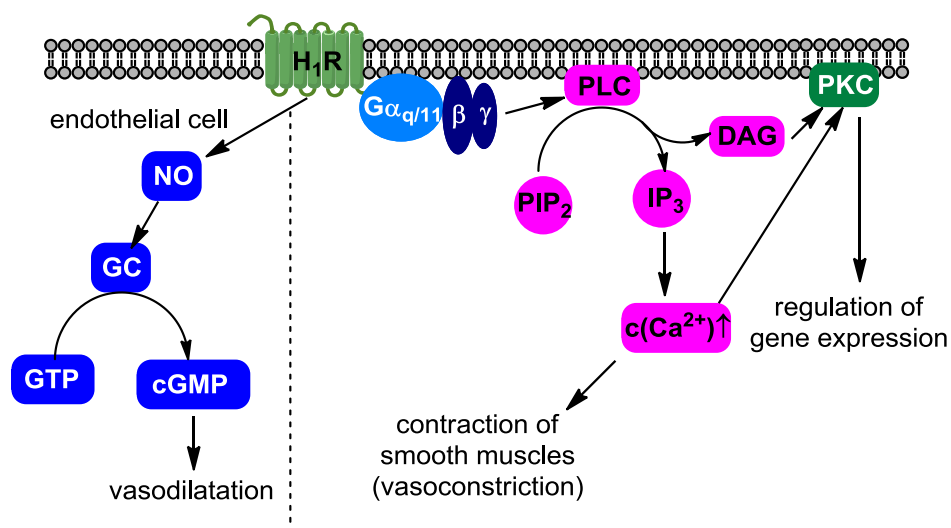


Figure 1.6. Signaling pathways of the H₁R.

Both agonists and antagonists addressing the H₁R are known: whereas agonists are rather used as pharmacological tools or in the pharmacotherapy of Menière's disease (inner ear disorder reflected in vertigo, tinnitus and hearing loss) (Barak, 2008), antagonists are widespread and well-known anti-allergic drugs (so called "antihistamines").

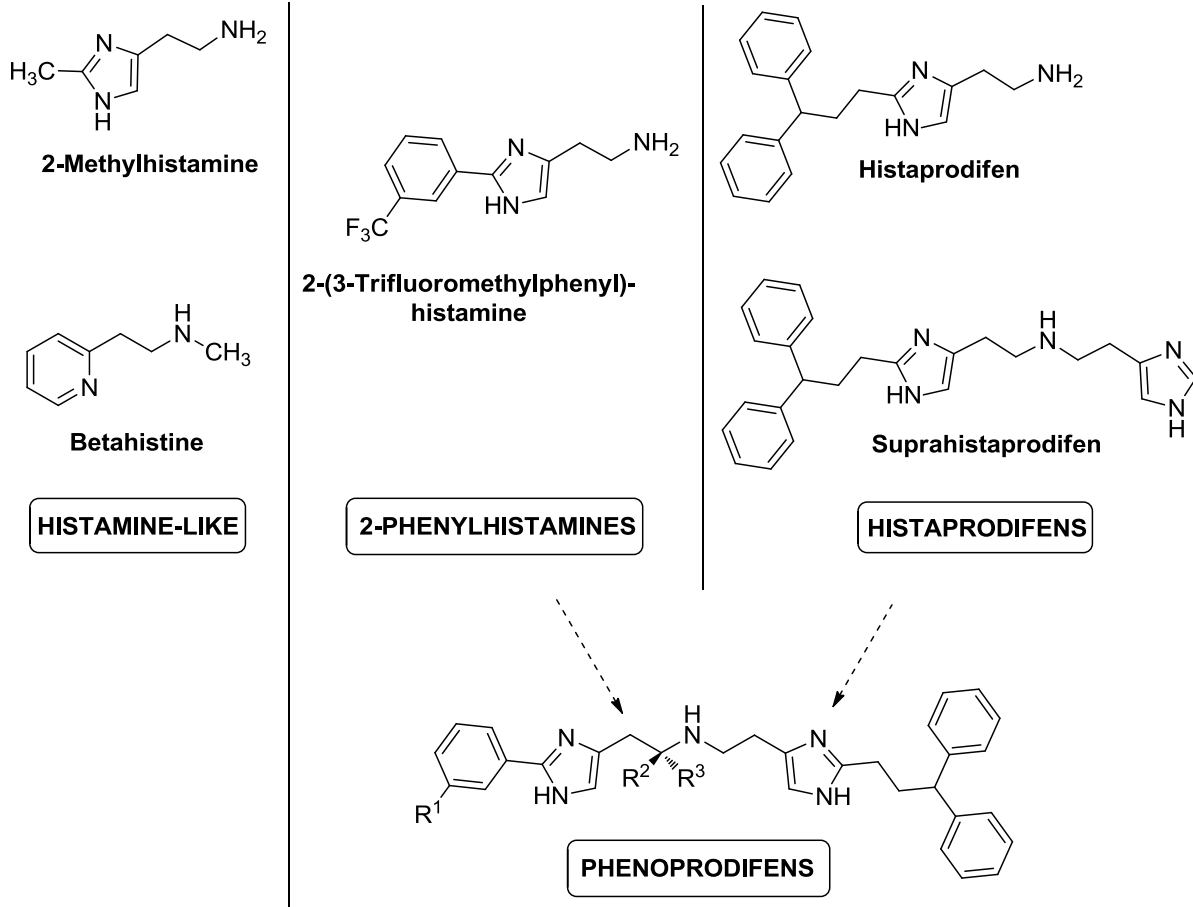
H₁R agonists can be divided into four classes: firstly, small histamine-like molecules like, e.g., 2-methylhistamine or the only therapeutically used H₁R agonist betahistine (Aequamen[®], treatment of Menière's disease) that reveal to some extent an H₁R subtype selectivity but a rather poor potency compared to histamine. (Durant et al.,

1976, Durant et al., 1975) Secondly, the so called “2-phenylhistamines”, histamine-derived molecules with aromatic substituents in position 2 of the imidazole ring like, e.g., 2-(3-trifluoromethylphenyl)histamine, that reveal a potency similar and in some cases superior to histamine. (Zingel et al., 1990, Leschke et al., 1995, Seifert et al., 2003b, Strasser et al., 2009) A third group comprises the highly potent and selective group of the histaprodifens, bearing a characteristic 3,3-diphenylpropyl substituent (Elz et al., 2000a, Elz et al., 2000b, Seifert et al., 2003b, Strasser et al., 2008a), among which suprahistaprodifen, consisting of histaprodifen and histamine, represents the most potent member, revealing a 36-fold higher potency than histamine. (Menghin et al., 2003) A fourth and last group represent hybrid compounds resulting from the coupling of phenylhistamines to a histaprodifen partial structure, the so called “phenoprodifens”. The potency of these compounds is comparable to suprahistaprodifen. (Strasser et al., 2008b, Strasser et al., 2009, Wittmann et al., 2011, Strasser et al., 2013)

For decades, H₁R antagonists have been successfully used in the treatment of allergic diseases like allergic rhinitis (so called “hay-fever”) or histamine induced itch and are divided into first and second generation antagonists: the first generation antagonists like mepyramine or diphenhydramine are known for more than 50 years, however, due to their high lipophilicity, penetration through the blood-brain barrier causes sedation as an undesired side effect. As a consequence, these drugs were replaced by the newer second generation antagonists like, e.g., cetirizine that are characterized by a more polar structure and thus a reduced sedating effect. (Hill et al., 1997) Nevertheless, radio-labeled mepyramine ([³H]mepyramine) still plays an important role as a pharmacological tool and is, e.g., used as radioligand in H₁R binding assays. (Hill et al., 1977, Seifert et al., 2003b)

An overview of selected H₁R ligands as well as their classification is provided in figure 1.7.

AGONISTS



ANTAGONISTS

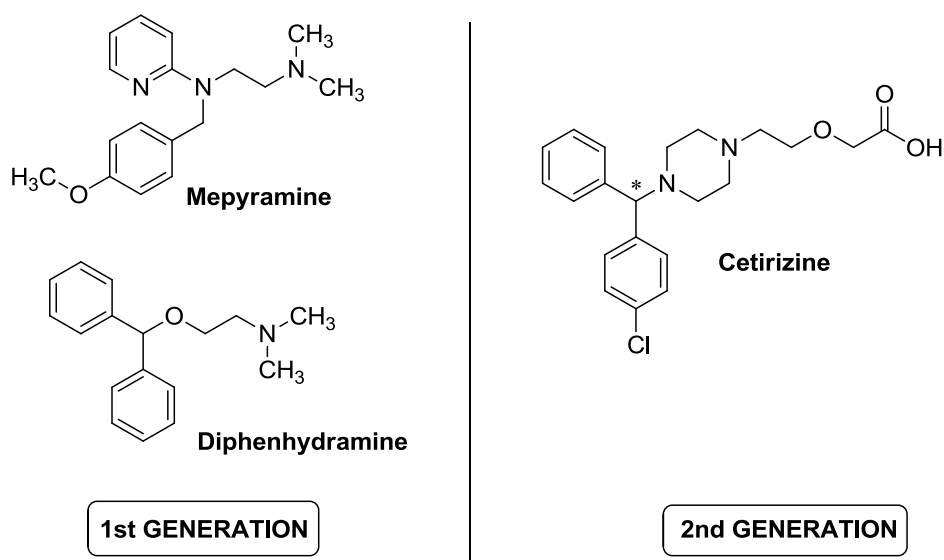


Figure 1.7. Selected H₁R ligands (agonists and antagonists).

1.2.2. The histamine H₂ receptor

The human histamine H₂R consists of 358 amino acids and is located on gastric parietal cells as well as in cells of the brain, the heart, the uterus and of the hematopoietic system. (Gantz et al., 1991, Hill et al., 1997, Dove et al., 2004) It regulates the histamine dependent secretion of gastric acid from parietal cells (Black et al., 1972, Gespach et al., 1982) and is known to have a positive inotropic and chronotropic effect (cardiac H₂Rs) in atrial and ventricular tissues (Levi and Alloatti, 1988). Moreover, it is involved in the immune system (Schneider et al., 2002, Akdis and Simons, 2006, Bäumer and Rossbach, 2010) as well as in the relaxation of smooth muscle cells in blood vessels, uterus and airway. (Black et al., 1972, Levi and Alloatti, 1988)

The histamine H₂R couples to G α_s proteins and therefore activates the formation of the second messenger cAMP through adenylyl cyclases (AC). (Hill et al., 1997) cAMP, in turn, activates protein kinase A (PKA), which is responsible for altered gene transcription by modulation of the transcription factor termed cAMP response element binding protein (CREB). (Bakker and Leurs, 2005) Moreover, the H₂R was found to couple to G $\alpha_{q/11}$ proteins in some specific cell systems. (Seifert et al., 1992, Kühn et al., 1996, Leopoldt et al., 1997, Wellner-Kienitz et al., 2003) As a consequence, the intracellular Ca²⁺-concentration increases mediated by the phospholipase C (PLC). (Figure 1.8)

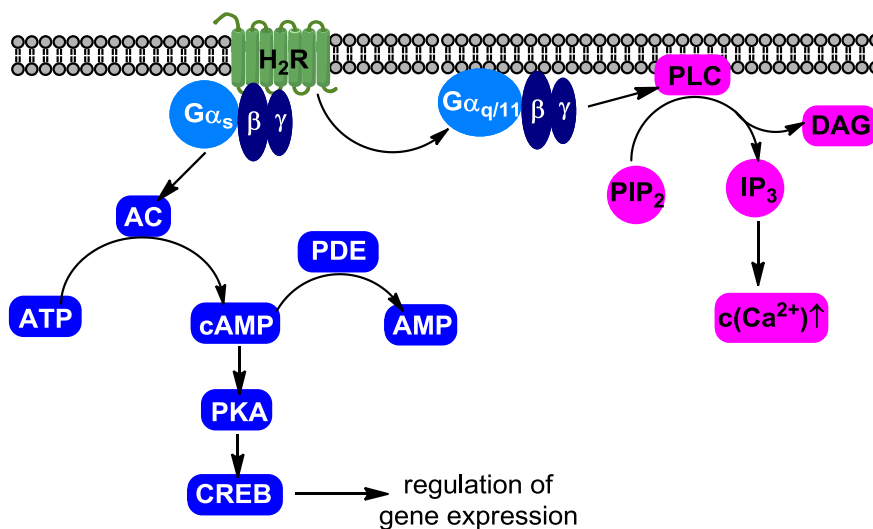


Figure 1.8. Signaling pathways of the H₂R (adapted from Brunskole (2011)).

According to their chemical structure, H₂R agonists can be divided into two groups: small amine-type agonists and guanidine-type agonists. 5-Methylhistamine as well as dimaprit (a non-imidazole) represent H₂R agonists of the small amine-type. (Parsons et al., 1977, Durant et al., 1977) Interestingly, 5-methylhistamine, the first H₂R agonist reported in literature that showed H₂R selectivity over the H₁R (Durant et al., 1975), was recently reported to be selective for the H₄R. (Lim et al., 2005) Highly potent and selective H₂R agonists like impromidine (Durant et al., 1985) and arpromidine (Buschauer, 1989, Buschauer et al., 1992) belong to the guanidine-type family, among which the imidazolylpropylguanidine moiety was found to be crucial for H₂R agonism. (Dove et al., 2004) Derived from this, the replacement of the highly basic guanidine group by an acylguanidine moiety resulted in a new group of H₂R agonists, termed the acylguanidine-type family (Ghorai et al., 2008, Kraus et al., 2009). Recently, the bivalent ligand approach was successfully applied to the acylguanidines, yielding highly selective and potent dimeric H₂R agonists. (Birnkammer et al., 2012)

By contrast to the - by now only as pharmacological tool used - H₂R agonists described above, the H₂R antagonists represent blockbuster drugs in the treatment of peptic ulcer and gastro-oesophageal reflux disease. (Parsons and Ganellin, 2006) The first H₂R antagonist available on the drug market was cimetidine, followed by more potent analogues like ranitidine or famotidine. (Hill et al., 1997) Moreover, radio-labeled [³H]tiotidine is used as pharmacological tool in radioligand binding studies. (van der Goot and Timmerman, 2000)

An overview of selected H₂R ligands as well as their classification is provided in figure 1.9.

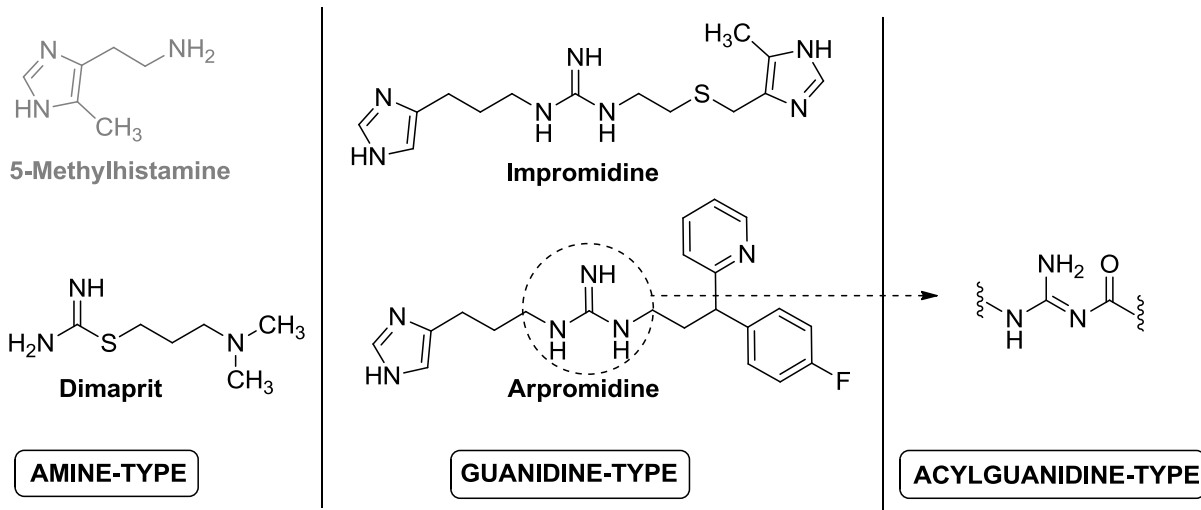
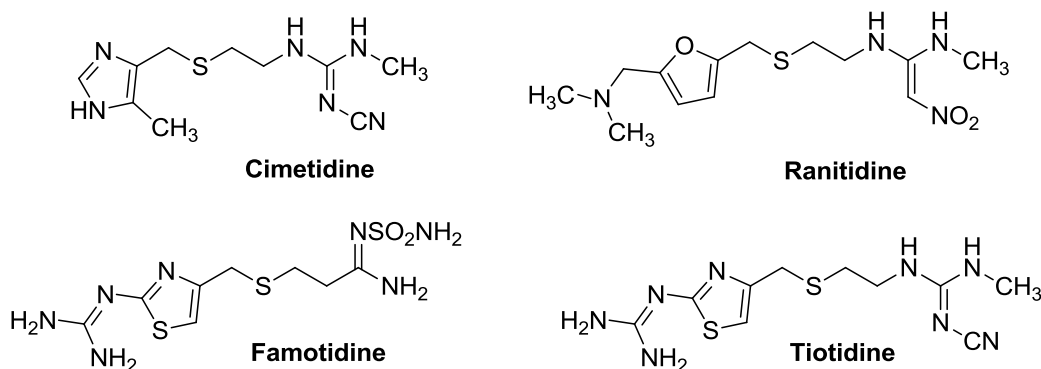
AGONISTS**ANTAGONISTS**

Figure 1.9. Selected H₂R ligands (agonists and antagonists).

1.2.3. The histamine H₃ receptor

The physiologically dominant human histamine H₃R isoform consists of 445 amino acids and is prevalent both in the central and the peripheral nervous system of the human body, however, about 20 isoforms have been found due to introns and exons in the H₃R encoding gene. (Lovenberg et al., 1999, Wiedemann et al., 2002, Leurs et al., 2005, Bongers et al., 2007, Berlin et al., 2011) Located in the hippocampus, the cortical area, basal ganglia (central nervous system (CNS), (Martinez-Mir et al., 1990)) as well as in cells of the gastrointestinal tract, the cardiovascular system and the airways (peripheral nervous system (PNS), (Wijtmans et al., 2007)) it plays an important role in the pathophysiology of sleep and cognitive disorders, obesity and

pain. (Leurs et al., 1998, Bakker, 2004, Parmentier et al., 2007) It acts both as a presynaptic autoreceptor regulating the release of histamine and as a heteroreceptor regulating the release of several non-histaminergic neurotransmitters, like, e.g., dopamine, serotonin and acetylcholine, among others. (Hill et al., 1997, Gemkow et al., 2009)

The H₃R couples to pertussis-toxin sensitive G $\alpha_{i/o}$ proteins, leading to an inhibition of adenylyl cyclase (AC). Moreover, it was found to interfere with phospholipase A₂ (PLA₂), mitogen-activated protein kinase (MAPK) and phosphatidyl inositol-3 kinase (PI₃K) as well as to inhibit the Na⁺/H⁺ exchanger and to lower intracellular Ca²⁺ levels (figure 1.10). (Clark and Hill, 1996, Leurs et al., 2005, Bongers et al., 2007)

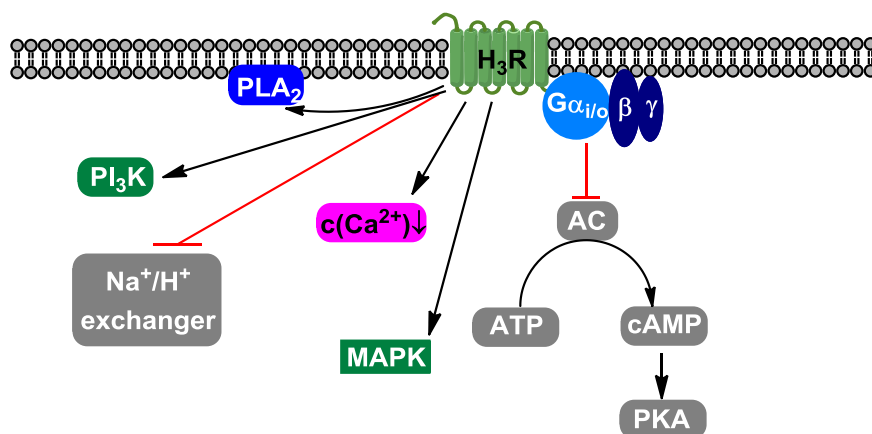


Figure 1.10. Signaling pathways of the H₃R.

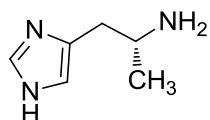
All H₃R agonists bear an imidazole moiety as it was found to be crucial for H₃R agonism. (Leurs et al., 2005) Examples are R- α -methylhistamine as well as N $^{\alpha}$ -methylhistamine or immapip. (Arrang et al., 1987, De Esch and Belzar, 2004) However, due to the high sequence homology with the H₄R (\approx 58% sequence identity in transmembrane α -helices (Nakamura et al., 2000, Oda et al., 2000, Coge et al., 2001)), no selectivity over the H₄R was revealed for these compounds. Structural modifications of immapip resulted in immethridine and methimmapip, both selective and potent H₃R agonists. (Kitbunnadaj et al., 2004) Nevertheless, radio-labeled [³H]N $^{\alpha}$ -methylhistamine is used in radioligand binding studies. (van der Goot and Timmerman, 2000).

Therapeutically, H₃R agonists could due to their auto- and hetero-regulatory properties be used for the treatment of pathophysiological conditions traced back to elevated neurotransmitter levels like, e.g., migraine, inflammation, insomnia or pain. (Berlin et al., 2011)

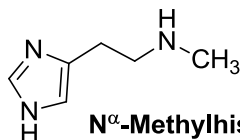
H₃R antagonists can be divided in imidazole-type and non-imidazole-type ligands: clobenpropit (van der Goot et al., 1992) and thioperamide (Arrang et al., 1987) represent imidazole-type H₃R antagonists. However, no selectivity over the H₄R is given as also the H₄R is addressed by these molecules. (Lim et al., 2005) Pitolisant, former known as BF 2.649, represents a non-imidazole H₃R antagonist / inverse agonist that is clinically used for the treatment of narcolepsy. (Schwartz, 2011) Furthermore, H₃R antagonists / inverse agonists undergo clinical evaluations for the treatment of mental diseases as, e.g., Alzheimer's disease, schizophrenia, ADHD (attention deficit hyperactivity disorder) or epilepsy. (Parmentier et al., 2007, Sander et al., 2008, Gemkow et al., 2009, Leurs et al., 2011, Berlin et al., 2011)

An overview of selected H₃R ligands as well as their classification is provided in figure 1.11.

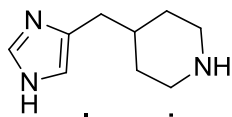
AGONISTS



R- α -Methylhistamine

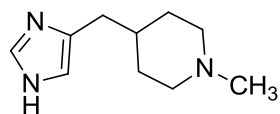


N α -Methylhistamine

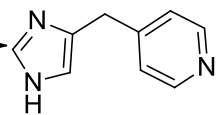


Immepip

NON-SELECTIVE



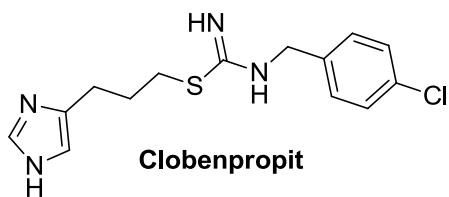
Methimnepip



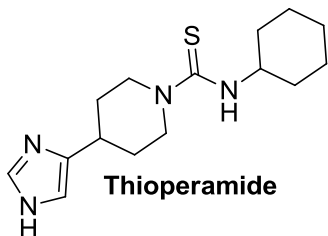
Immethridine

SELECTIVE

ANTAGONISTS / INVERSE AGONISTS

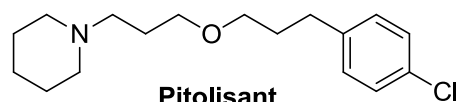


Clobenpropit



Thioperamide

IMIDAZOLE-TYPE



**Pitolisant
(BF 2.649)**

NON-IMIDAZOLE-TYPE

Figure 1.11. Selected H₃R ligands ((inverse) agonists and antagonists).

1.2.4. The histamine H₄ receptor

The human histamine H₄R consists of 390 amino acids and is mainly expressed in cells of the immune system such as neutrophils, eosinophils, basophils, dendritic cells, mast cells, monocytes, T-cells as well as in cells of the nasal mucosa and of the central and intrinsic nervous system. (Leurs et al., 2009) Two further non signaling isoforms of the H₄R were found on the intracellular surface of eosinophils and mast cells that are – alike already reported for the human H₃R – traced back to the existence of two introns and three exons in the encoding gene. (van Rijn et al., 2008) Also similar to the H₃R, it displays a high constitutive activity. (Morse et al., 2001, Schneider et al., 2009)

The H₄R plays a major role in immunological and inflammatory reactions and is involved in the chemotaxis of eosinophils, dendritic cells, mast cells and T-cells as well as in the cytokine release of cells of the immune system. (Morse et al., 2001, Takeshita et al., 2003, de Esch et al., 2005, Zhang et al., 2007, Damaj et al., 2007) As a consequence, inflammatory diseases like rheumatoid arthritis, systemic lupus erythematosus or multiple sclerosis as well as *type I* allergic diseases like bronchial asthma, rhinitis or conjunctivitis are supposed to be linked to the H₄R. (Jablonowski et al., 2004, Thurmond et al., 2008, Deml et al., 2009, Zampeli and Tiligada, 2009, Leurs et al., 2011)

The H₄R mediated signaling is coupled to pertussis-toxin sensitive G $\alpha_{i/o}$ proteins and inhibits adenylyl cyclase, resulting in reduced cAMP formation and CREB (cAMP response element binding protein) mediated gene-transcription. (Leurs et al., 2009) Moreover, it activates MAPK (mitogen activated protein kinase) pathways (Morse et al., 2001) and contributes to the intracellular Ca²⁺ mobilization in mast cells and eosinophils. (Hofstra et al., 2003, Buckland et al., 2003) Besides, G-protein independent signaling was recently reported for several ligands (β -arrestin pathway). (Seifert et al., 2011, Nijmeijer et al., 2012) (Figure [1.12](#))

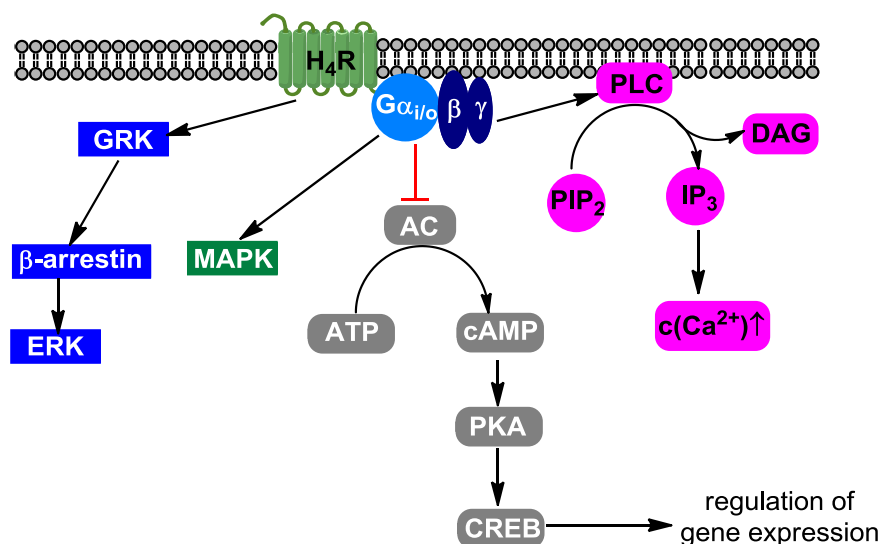


Figure 1.12. Signaling pathways of the H₄R (adapted from Brunskole (2011)).

Because of the high sequence homology of the H₃R and the H₄R, several above all imidazole-bearing compounds addressing the H₃R are often also targeting the H₄R. (Lim et al., 2005) However, with intent to investigate the pathophysiological role of the H₄R, selective H₄R ligands are needed.

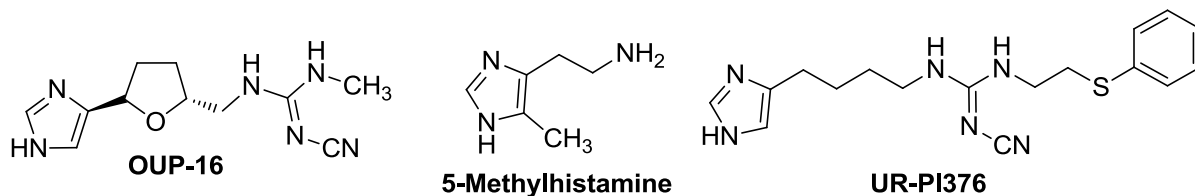
The first reported selective H₄R agonist was OUP-16, a chiral tetrahydrofuran analog derived from the H₃R agonist imifuramine. (Hashimoto et al., 2003) Moreover, 5-methylhistamine that was originally reported to be a selective H₂R agonist turned out to display a distinct H₄R selectivity over the other histamine receptor subtypes. (Lim et al., 2005) Recently, new cyanoguanidine-type H₄R agonists like UR-PI376 were developed and found to reveal a high potency and selectivity. (Igel et al., 2009, Geyer and Buschauer, 2011)

Thioperamide, an H₃R antagonist, was proved to be an imidazole-type inverse H₄R agonist. (Lim et al., 2005) The first non-imidazole-type selective H₄R antagonist was JNJ7777120, an indole-2-carboxamide discovered in a high throughput screening campaign of *Johnson & Johnson* laboratories. (Jablonowski et al., 2003) In radioligand binding studies at H₄R, radio-labeled [³H]JNJ7777120 is applied, among others. (Lim et al., 2005) Further highly potent and (to some extent) selective H₄R antagonists / inverse agonists represent the group of the 2-aminopyrimidines (Bacon et al., 2005, Altenbach et al., 2008, Sander et al., 2009, Smits et al., 2009) as well as the

quinazoline- and quinoxaline derived series developed by Smits et al.. (Smits et al., 2008a, Smits et al., 2008b)

An overview of selected H₄R ligands is provided in figure 1.13.

AGONISTS



ANTAGONISTS / INVERSE AGONISTS

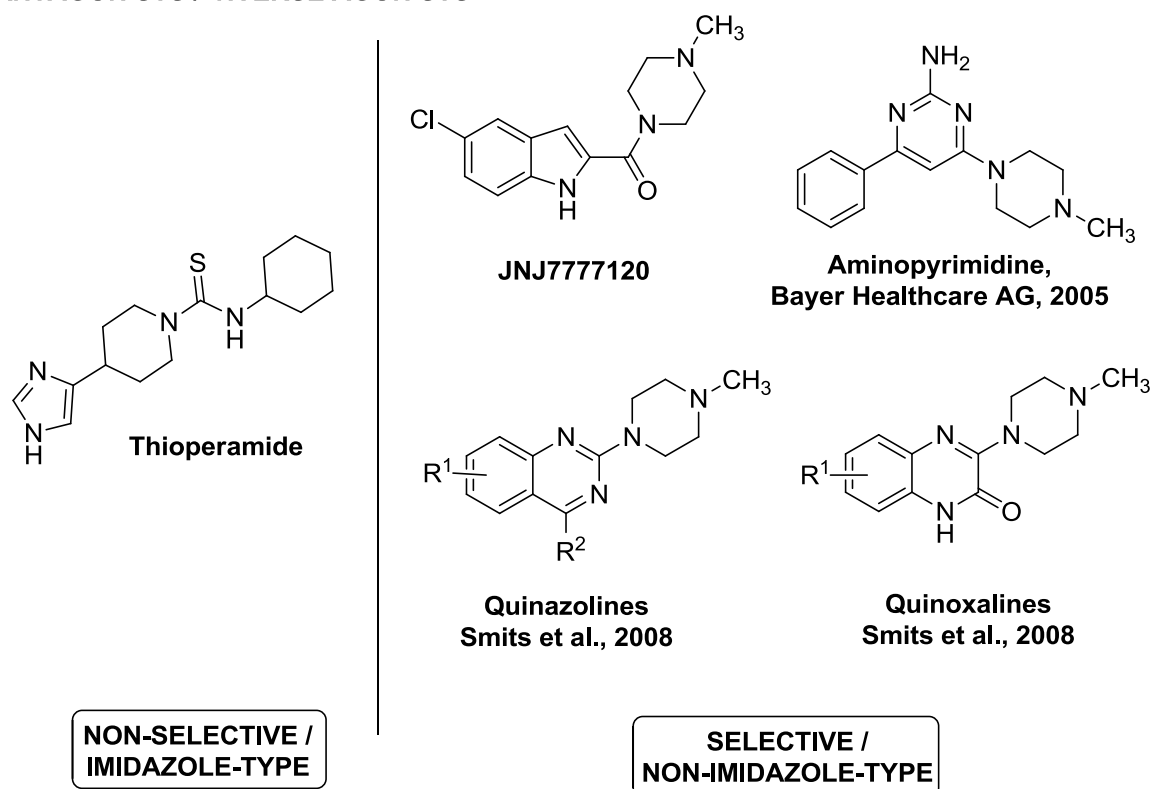


Figure 1.13. Selected H₄R ligands ((inverse) agonists and antagonists).

1.3. Antipsychotic drugs

Known as “antipsychotics” or “neuroleptics”, antipsychotic drugs are prevalently used for the treatment of mental disorders like schizophrenia or bipolar disorder. Derived from promethazine, an H₁R antihistamine, the first antipsychotic drug chlorpromazine was marketed for the pharmacotherapy of schizophrenia about sixty years ago (as a so called “major tranquillizer”). (Healy, 2004) On a molecular level, a dopaminergic hyperactivity in schizophrenic subjects is postulated and consequently, the suppression of dopamine activity via dopaminergic receptors (D_xRs, mostly D₂R and D₄R) is the target of antipsychotic treatment. (Carlsson, 1978)

Nevertheless, not only D_xRs are affected by antipsychotic drugs. For example, as all four H_xRs are expressed in the CNS (Hill et al., 1997, Connelly et al., 2009), antipsychotic drugs also reveal affinity to H_xRs, above all to the H₁R that was identified to be responsible for their sedative effects. (Richelson, 1979) Moreover, an involvement of histaminergic signaling in the pathophysiology of schizophrenia is suggested. (Haas et al., 2008, Appl et al., 2012)

The discovery of chlorpromazine was succeeded by the release of several drugs with functional enhancements concerning neuroleptic potency and efficacy, chemical structure and mode of action that will be described in the following.

1.3.1. Classification

According to their side effect profile, antipsychotic drugs are roughly divided into two groups: typical antipsychotics of the first generation that were found to reveal higher extrapyramidal side effects than the so called “atypical” antipsychotics of the second generation. (Ahmed et al., 2008) Examples for EPS are, e.g., dyskinesia, akinesia or akathisia, comprised as movement disorders of the human body.

The family of the typical antipsychotics is further divided into four subgroups: *phenothiazines* like, e.g., chlorpromazine that, besides D₂R antagonism, reveal distinct antihistaminergic and anticholinergic effects. Similar findings are reported for the group of the *thioxanthenes* like, e.g., chlorprothixene. Most pronounced EPS appear during the pharmacotherapy with *butyrophenones* (e.g., haloperidol) and

diphenylbutylpiperidines (e.g., pimozid) because of their high affinity to the D₂R. (Aktories et al., 2005) (Figure 1.14)

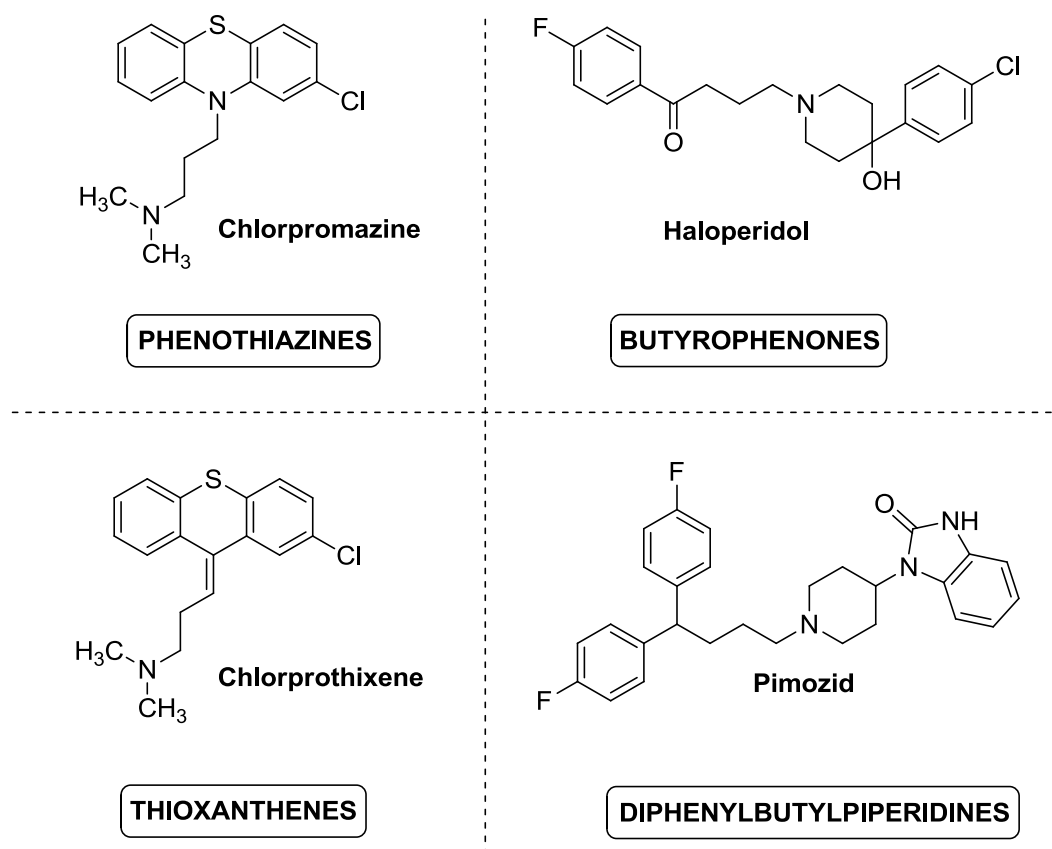
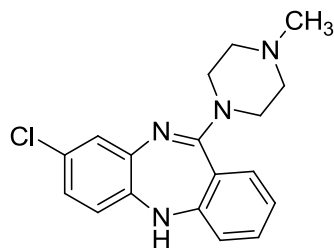
TYPICAL

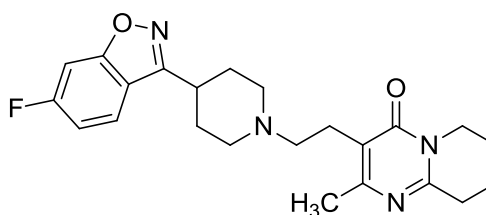
Figure 1.14. Selected typical antipsychotic drugs.

By contrast, atypical antipsychotics like, e.g., clozapine, olanzapine or risperidone are characterized by an improved side effect profile regarding the EPS rate. Although the molecular mode of action is by now not entirely understood, in case of clozapine this can be explained by the predominant interaction with D₄R and 5-HT_{2A}R and thus by a reduced influence on the D₂R that is supposed to cause EPS. (Aktories et al., 2005) (Figure 1.15)

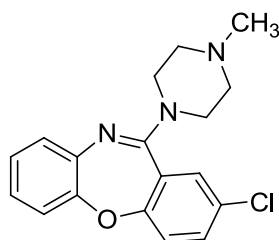
ATYPICAL



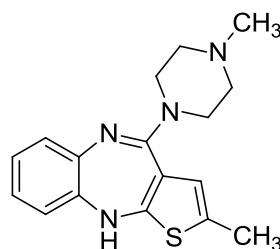
Clozapine



Risperidone



Loxapine



Olanzapine

Figure 1.15. Selected atypical antipsychotic drugs.**1.3.2. Clozapine and its interaction with multiple molecular targets (“dirty drug” problem)**

The binding of the multi-target drug clozapine to a broad variety of GPCRs as well as the associated both desired and adverse effects have been intensively investigated in the last years. (Fitzsimons et al., 2005, Flanagan and Dunk, 2008, Nooijen et al., 2011) For instance, binding data are reported for dopaminergic (D_{1-4}), adrenergic ($\alpha_{1,2}$), serotonergic ($5-HT_{2A,C}$), cholinergic (M_{1-5}) and histaminergic ($H_{1,4}$) receptors. (Baldessarini and Frankenburg, 1991, Zorn et al., 1994, Michal et al., 1999) The pharmacological discrepancies between the four histamine receptor subtypes $H_{1-4}R$ are intriguing: whereas it acts as an inverse agonist / antagonist on most GPCRs including the histamine H_1R , the H_2R and the H_3R , a partial agonism at the hH_4R was revealed recently. (Richelson and Nelson, 1984, Lim et al., 2005, Appl et al., 2012). Moreover, compared to the high affinity of clozapine to the H_1R (pK_i (hH_1R) = 8.59 ± 0.14 , (Appl et al., 2012)), the H_4R binding is by two to three orders of magnitude lower (pK_i (hH_4R) = 5.93 ± 0.12 , (Appl et al., 2012)). This can be traced back to a different orientation of clozapine in the binding pocket of the active hH_4R compared to the inactive hH_1R . (Appl et al., 2012)

Although clozapine is characterized by a good clinical efficacy as well as a decreased EPS rate, serious side effects like neutropenia or agranulocytosis were found to occur during the first weeks of clozapine pharmacotherapy. Agranulocytosis is an acute condition characterized by a lowered neutrophil count in the circulating blood, reflected in a severe suppression of the immune system. (Ryabik et al., 1993) As a consequence, its use is predominantly allowed for patients revealing unresponsiveness or intolerance regarding typical neuroleptics under strict surveillance of the neutrophil count in the blood (drug monitoring).

1.4. References

- AHMED, M. R., GUREVICH, V. V., DALBY, K. N., BENOVIĆ, J. L. & GUREVICH, E. V. **2008**. Haloperidol and clozapine differentially affect the expression of arrestins, receptor kinases, and extracellular signal-regulated kinase activation. *J Pharmacol Exp Ther*, **325**, 276-283.
- AKDIS, C. A. & SIMONS, F. E. R. **2006**. Histamine receptors are hot in immunopharmacology. *Eur J Pharmacol*, **533**, 69-76.
- AKTORIES, K., FÖRSTERMANN, U., HOFMANN, B. & STARKE, K. **2005**. *Allgemeine und spezielle Pharmakologie und Toxikologie*, München: Elsevier GmbH, Urban & Fischer.
- ALTENBACH, R. J., ADAIR, R. M., BETTENCOURT, B. M., BLACK, L. A., FIX-STENZEL, S. R., GOPALAKRISHNAN, S. M., HSIEH, G. C., LIU, H., MARSH, K. C., MCPHERSON, M. J., MILICIC, I., MILLER, T. R., VORTHERMS, T. A., WARRIOR, U., WETTER, J. M., WISHART, N., WITTE, D. G., HONORE, P., ESBENSHADE, T. A., HANCOCK, A. A., BRIONI, J. D. & COWART, M. D. **2008**. Structure-activity studies on a series of a 2-aminopyrimidine-containing histamine H₄ receptor ligands. *J Med Chem*, **51**, 6571-6580.
- APPL, H., HOLZAMMER, T., DOVE, S., HAEN, E., STRASSER, A. & SEIFERT, R. **2012**. Interactions of recombinant human histamine H₁R, H₂R, H₃R, and H₄R receptors with 34 antidepressants and antipsychotics. *Naunyn Schmiedeberg's Arch Pharmacol*, **385**, 145-170.
- ARRANG, J. M., GARBARG, M., LANCELOT, J. C., LECOMTE, J. M., POLLARD, H., ROBBA, M., SCHUNACK, W. & SCHWARTZ, J. C. **1987**. Highly potent and selective ligands for histamine H₃-receptors. *Nature*, **327**, 117-123.
- ARRANG, J. M., GARBARG, M. & SCHWARTZ, J. C. **1983**. Auto-inhibition of brain histamine release mediated by a novel class H₃ of histamine receptor. *Nature*, **302**, 832-837.
- ASH, A. S. & SCHILD, H. O. **1966**. Receptors mediating some actions of histamine. *Br J Pharmacol Chemother*, **27**, 427-439.
- BACON, K., FUKUSHIMA, K., GANTNER, F., SAKAI, K., SATO, H., SHIMAZAKI, M. & URBAN, K. **2005**. 2-Aminopyrimidine derivatives. Patent.
- BAKKER, R. A. **2004**. Histamine H₃-receptor isoforms. *Inflamm Res*, **53**, 509-516.
- BAKKER, R. A., DEES, G., CARRILLO, J. J., BOOTH, R. G., LOPEZ-GIMENEZ, J. F., MILLIGAN, G., STRANGE, P. G. & LEURS, R. **2004**. Domain swapping in the human histamine H₁ receptor. *J Pharmacol Exp Ther*, **311**, 131-138.
- BAKKER, R. A. & LEURS, R. **2005**. Constitutively active histamine receptors, in G-protein coupled receptors as drug targets. Analysis of activation and constitutive activity (Seifert R and Wieland T eds). *Wiley-VCH, Weinheim*, 195-222.
- BALDESSARINI, R. J. & FRANKENBURG, F. R. **1991**. Clozapine. A novel antipsychotic agent. *N Engl J Med*, **324**, 746-754.
- BARAK, N. **2008**. Betahistidine: what's new on the agenda? *Expert Opin Investig Drugs*, **17**, 795-804.

- BARGER, G. & DALE, H. H. **1910**. CCLXV.—4-β-Aminoethylglyoxaline (β-iminazolyethylamine) and the other active principles of ergot. *J Chem Soc, Transactions*, **97**, 2592-2595.
- BÄUMER, W. & ROSSBACH, K. **2010**. Histamine as an immunomodulator. *J Dtsch Dermatol Ges*, **8**, 495-504.
- BERLIN, M., BOYCE, C. W. & RUIZ MDE, L. **2011**. Histamine H₃ receptor as a drug discovery target. *J Med Chem*, **54**, 26-53.
- BIRNBAUMER, L. **2007**. Expansion of signal transduction by G proteins - The second 15 years or so: From 3 to 16 α subunits plus βγ dimers. *Biochimica Et Biophysica Acta-Biomembranes*, **1768**, 772-793.
- BIRNKAMMER, T., SPICKENREITHER, A., BRUNSKOLE, I., LOPUCH, M., KAGERMEIER, N., BERNHARDT, G., DOVE, S., SEIFERT, R., ELZ, S. & BUSCHAUER, A. **2012**. The Bivalent Ligand Approach Leads to Highly Potent and Selective Acylguanidine-Type Histamine H₂ Receptor Agonists. *J Med Chem*, **55**, 1147-1160.
- BLACK, J. W., DUNCAN, W. A., DURANT, C. J., GANELLIN, C. R. & PARSONS, E. M. **1972**. Definition and antagonism of histamine H₂-receptors. *Nature*, **236**, 385-390.
- BONGERS, G., BAKKER, R. A. & LEURS, R. **2007**. Molecular aspects of the histamine H₃ receptor. *Biochem Pharmacol*, **73**, 1195-1204.
- BRUNSKOLE, I. **2011**. Molecular and cellular analysis of aminergic G-protein coupled receptors: histamine H₂, H₄ and β₂-adrenergic receptors, a scientific paradigm. *PhD Thesis, University of Regensburg*.
- BUCKLAND, K. F., WILLIAMS, T. J. & CONROY, D. M. **2003**. Histamine induces cytoskeletal changes in human eosinophils via the H₄ receptor. *Br J Pharmacol*, **140**, 1117-1127.
- BUSCHAUER, A. **1989**. Synthesis and in vitro pharmacology of arpromidine and related phenyl(pyridylalkyl)guanidines, a potential new class of positive inotropic drugs. *J Med Chem*, **32**, 1963-1970.
- BUSCHAUER, A., LACHENMAYR, F. & SCHUNACK, W. **1992**. Synthesis and histamine H₂-receptor activity of heterocyclic impromidine analogues. *Pharmazie*, **47**, 86-91.
- CABRERA-VERA, T. M., VANHAUWE, J., THOMAS, T. O., MEDKOVA, M., PREININGER, A., MAZZONI, M. R. & HAMM, H. E. **2003**. Insights into G protein structure, function, and regulation. *Endocrine Rev.*, **24**, 765-781.
- CARLSSON, A. **1978**. Antipsychotic drugs, neurotransmitters, and schizophrenia. *Am J Psychiatry*, **135**, 165-173.
- CARRILLO, J. J., PEDIANI, J. & MILLIGAN, G. **2003**. Dimers of class A G protein-coupled receptors function via agonist-mediated trans-activation of associated G proteins. *J Biol Chem*, **278**, 42578-42587.
- CHEREZOV, V., ROSENBAUM, D. M., HANSON, M. A., RASMUSSEN, S. G. F., THIAN, F. S., KOBILKA, T. S., CHOI, H. J., KUHN, P., WEIS, W. I., KOBILKA, B. K. & STEVENS, R. C. **2007**. High-resolution crystal structure of an engineered human β₂-adrenergic G protein-coupled receptor. *Science*, **318**, 1258-1265.

- CHIEN, E. Y., LIU, W., ZHAO, Q., KATRITCH, V., HAN, G. W., HANSON, M. A., SHI, L., NEWMAN, A. H., JAVITCH, J. A., CHEREZOV, V. & STEVENS, R. C. **2010**. Structure of the human dopamine D₃ receptor in complex with a D₂/D₃ selective antagonist. *Science*, **330**, 1091-1095.
- CIVELLI, O., REINSCHIED, R. K., ZHANG, Y., WANG, Z. W., FREDRIKSSON, R. & SCHIOTH, H. B. **2013**. G Protein-Coupled Receptor Deorphanizations. *Annu Rev Pharmacol Toxicol*, **53**, 127-146.
- CLARK, E. A. & HILL, S. J. **1996**. Sensitivity of histamine H₃ receptor agonist-stimulated [³⁵S]GTPγS binding to pertussis toxin. *Eur J Pharmacol*, **296**, 223-225.
- COGE, F., GUENIN, S. P., RIQUE, H., BOUTIN, J. A. & GALIZZI, J. P. **2001**. Structure and expression of the human histamine H₄-receptor gene. *Biochem Biophys Res Commun*, **284**, 301-309.
- CONNELLY, W. M., SHENTON, F. C., LETHBRIDGE, N., LEURS, R., WALDVOGEL, H. J., FAULL, R. L., LEES, G. & CHAZOT, P. L. **2009**. The histamine H₄ receptor is functionally expressed on neurons in the mammalian CNS. *Br J Pharmacol*, **157**, 55-63.
- CVEJIC, S. & DEVI, L. A. **1997**. Dimerization of the delta opioid receptor: implication for a role in receptor internalization. *J Biol Chem*, **272**, 26959-26964.
- DAMAJ, B. B., BECERRA, C. B., ESBER, H. J., WEN, Y. & MAGHAZACHI, A. A. **2007**. Functional expression of H₄ histamine receptor in human natural killer cells, monocytes, and dendritic cells. *J Immunol*, **179**, 7907-7915.
- DAVIES, M. N., GLORIAM, D. E., SECKER, A., FREITAS, A. A., TIMMIS, J. & FLOWER, D. R. **2011**. Present Perspectives on the Automated Classification of the G-Protein Coupled Receptors (GPCRs) at the Protein Sequence Level. *Curr Top Med Chem*, **11**, 1994-2009.
- DE ESCH, I. J., THURMOND, R. L., JONGEJAN, A. & LEURS, R. **2005**. The histamine H₄ receptor as a new therapeutic target for inflammation. *Trends Pharmacol Sci*, **26**, 462-469.
- DE ESCH, I. J. P. & BELZAR, K. J. **2004**. Histamine H₃ receptor agonists. *Mini Rev Med Chem*, **4**, 955-963.
- DE LEAN, A., STADEL, J. M. & LEFKOWITZ, R. J. **1980**. A Ternary Complex Model Explains the Agonist-Specific Binding-Properties of the Adenylate Cyclase-Coupled β-Adrenergic-Receptor. *J Biol Chem*, **255**, 7108-7117.
- DEML, K. F., BEERMANN, S., NEUMANN, D., STRASSER, A. & SEIFERT, R. **2009**. Interactions of histamine H₁-receptor agonists and antagonists with the human histamine H₄-receptor. *Mol Pharmacol*, **76**, 1019-1030.
- DE VRIES, L., ZHENG, B., FISCHER, T., ELENKO, E. & FARQUHAR, M. G. **2000**. The regulator of G protein signaling family. *Annu Rev Pharmacol Toxicol*, **40**, 235-271.
- DOVE, S., ELZ, S., SEIFERT, R. & BUSCHAUER, A. **2004**. Structure-activity relationships of histamine H₂ receptor ligands. *Mini Rev Med Chem*, **4**, 941-954.
- DURANT, G. J., EMMETT, J. C., GANELLIN, C. R., ROE, A. M. & SLATER, R. A. **1976**. Potential histamine H₂-receptor antagonists. 3. Methylhistamines. *J Med Chem*, **19**, 923-928.
- DURANT, G. J., GANELLIN, C. R., HILLS, D. W., MILES, P. D., PARSONS, M. E., PEPPER, E. S. & WHITE, G. R. **1985**. The histamine H₂ receptor agonist impromidine: synthesis and structure-activity considerations. *J Med Chem*, **28**, 1414-1422.

- DURANT, G. J., GANELLIN, C. R. & PARSONS, M. E. **1975**. Chemical differentiation of histamine H₁- and H₂-receptor agonists. *J Med Chem*, **18**, 905-909.
- DURANT, G. J., GANELLIN, C. R. & PARSONS, M. E. **1977**. Dimaprit, (S-[3-(N,N-dimethylamino)propyl]isothiourea). A highly specific histamine H₂-receptor agonist. Part 2. Structure-activity considerations. *Agents and Actions*, **7**, 39-43.
- DY, M. & SCHNEIDER, E. **2004**. Histamine-cytokine connection in immunity and hematopoiesis. *Cytokine Growth Factor Rev*, **15**, 393-410.
- ELZ, S., KRAMER, K., LESCHKE, C. & SCHUNACK, W. **2000a**. Ring-substituted histaprodifen analogues as partial agonists for histamine H₁ receptors: synthesis and structure-activity relationships. *Eur J Med Chem*, **35**, 41-52.
- ELZ, S., KRAMER, K., PERTZ, H. H., DETERT, H., TER LAAK, A. M., KÜHNE, R. & SCHUNACK, W. **2000b**. Histaprodifens: synthesis, pharmacological in vitro evaluation, and molecular modeling of a new class of highly active and selective histamine H₁-receptor agonists. *J Med Chem*, **43**, 1071-1084.
- EVANS, B. A., SATO, M., SARWAR, M., HUTCHINSON, D. S. & SUMMERS, R. J. **2010**. Ligand-directed signalling at beta-adrenoceptors. *Br J Pharmacol*, **159**, 1022-1038.
- FALCONE, F. H., ZILLIKENS, D. & GIBBS, B. F. **2006**. The 21st century renaissance of the basophil? Current insights into its role in allergic responses and innate immunity. *Exp Dermatol*, **15**, 855-864.
- FANG, Y., LAHIRI, J. & PICARD, L. **2003**. G protein-coupled receptor microarrays for drug discovery. *Drug Discov Tod*, **8**, 755-761.
- FITZSIMONS, J., BERK, M., LAMBERT, T., BOURIN, M. & DODD, S. **2005**. A review of clozapine safety. *Expert Opin Drug Saf*, **4**, 731-744.
- FLANAGAN, R. J. & DUNK, L. **2008**. Haematological toxicity of drugs used in psychiatry. *Hum Psychopharmacol*, **23 Suppl 1**, 27-41.
- FOORD, S. M., BONNER, T. I., NEUBIG, R. R., ROSSER, E. M., PIN, J. P., DAVENPORT, A. P., SPEDDING, M. & HARMAR, A. J. **2005**. International Union of Pharmacology. XLVI. G protein-coupled receptor list. *Pharmacol Rev*, **57**, 279-288.
- FREDRIKSSON, R., LAGERSTRÖM, M. C., LUNDIN, L. G. & SCHIOTH, H. B. **2003**. The G-protein-coupled receptors in the human genome form five main families. Phylogenetic analysis, paralogon groups, and fingerprints. *Mol Pharmacol*, **63**, 1256-1272.
- FUKUSHIMA, Y., ASANO, T., SAITOH, T., ANAI, M., FUNAKI, M., OGIHARA, T., KATAGIRI, H., MATSUHASHI, N., YAZAKI, Y. & SUGANO, K. **1997**. Oligomer formation of histamine H₂ receptors expressed in Sf9 and COS7 cells. *FEBS Lett*, **409**, 283-286.
- GANTZ, I., MUNZERT, G., TASHIRO, T., SCHAFFER, M., WANG, L., DELVALLE, J. & YAMADA, T. **1991**. Molecular cloning of the human histamine H₂ receptor. *Biochem Biophys Res Commun*, **178**, 1386-1392.
- GEMKOW, M. J., DAVENPORT, A. J., HARICH, S., ELLENBROEK, B. A., CESURA, A. & HALLETT, D. **2009**. The histamine H₃ receptor as a therapeutic drug target for CNS disorders. *Drug Discov Tod*, **14**, 509-515.

- GEORGE, S. R., FAN, T., XIE, Z. D., TSE, R., TAM, V., VARGHESE, G. & O'DOWD, B. F. **2000**. Oligomerization of μ - and δ -opioid receptors - Generation of novel functional properties. *J Biol Chem*, **275**, 26128-26135.
- GEORGE, S. R., O'DOWD, B. F. & LEE, S. R. **2002**. G-protein-coupled receptor oligomerization and its potential for drug discovery. *Nat Rev Drug Discov*, **1**, 808-820.
- GESPACH, C., BOUHOURS, D., BOUHOURS, J. F. & ROSSELIN, G. **1982**. Histamine interaction on surface recognition sites of H_2 -type in parietal and non-parietal cells isolated from the guinea pig stomach. *FEBS Lett*, **149**, 85-90.
- GEYER, R. & BUSCHAUER, A. **2011**. Synthesis and histamine H_3 and H_4 receptor activity of conformationally restricted cyanoguanidines related to UR-PI376. *Arch Pharm (Weinheim)*, **344**, 775-785.
- GHORAI, P., KRAUS, A., KELLER, M., GOTTE, C., IGEL, P., SCHNEIDER, E., SCHNELL, D., BERNHARDT, G., DOVE, S., ZABEL, M., ELZ, S., SEIFERT, R. & BUSCHAUER, A. **2008**. Acylguanidines as bioisosteres of guanidines: NG-acylated imidazolylpropylguanidines, a new class of histamine H_2 receptor agonists. *J Med Chem*, **51**, 7193-7204.
- GILMAN, A. G. **1987**. G-Proteins - Transducers of Receptor-Generated Signals. *Annu Rev Biochem*, **56**, 615-649.
- GRAHAM, H. T., LOWRY, O. H., WHEELWRIGHT, F., LENZ, M. A. & PARISH, H. H., JR. **1955**. Distribution of histamine among leukocytes and platelets. *Blood*, **10**, 467-481.
- GRANIER, S. & KOBILKA, B. **2012**. A new era of GPCR structural and chemical biology. *Nat Chem Biol*, **8**, 670-673.
- HAAS, H. L., SERGEEVA, O. A. & SELBACH, O. **2008**. Histamine in the nervous system. *Physiol Rev*, **88**, 1183-1241.
- HAKANSON, R., LARSSON, L. I. & SUNDLER, F. **1974**. Endocrine-like cells in rat stomach: effects of 6-hydroxydopa on amine stores and amino acid decarboxylase activities. A chemical, fluorescence histochemical and electron microscopic study. *J Pharmacol Exp Ther*, **191**, 92-101.
- HALAZY, S. **1999**. G-protein coupled receptors bivalent ligands and drug design. *Exp Opin Ther Patents*, **9**, 431-446.
- HANOUNE, J. & DEFER, N. **2001**. Regulation and role of adenylyl cyclase isoforms. *Annu Rev Pharmacol Toxicol*, **41**, 145-174.
- HASHIMOTO, T., HARUSAWA, S., ARAKI, L., ZUIDERVELD, O. P., SMIT, M. J., IMAZU, T., TAKASHIMA, S., YAMAMOTO, Y., SAKAMOTO, Y., KURIHARA, T., LEURS, R., BAKKER, R. A. & YAMATODANI, A. **2003**. A selective human H_4 -receptor agonist: (-)-2-cyano-1-methyl-3-[(2R,5R)-5-[1H-imidazol-4(5)-yl]tetrahydrofuran-2-yl] methylguanidine. *J Med Chem*, **46**, 3162-3165.
- HEALY, D. **2004**. *The creation of psychopharmacology*, Harvard University Press.
- HERMANS, E. **2003**. Biochemical and pharmacological control of the multiplicity of coupling at G-protein-coupled receptors. *Pharmacology & Therapeutics*, **99**, 25-44.

- HILL, S. J. **1990**. Distribution, properties, and functional characteristics of three classes of histamine receptor. *Pharmacol Rev*, **42**, 45-83.
- HILL, S. J., GANELLIN, C. R., TIMMERMAN, H., SCHWARTZ, J. C., SHANKLEY, N. P., YOUNG, J. M., SCHUNACK, W., LEVI, R. & HAAS, H. L. **1997**. International Union of Pharmacology. XIII. Classification of histamine receptors. *Pharmacol Rev*, **49**, 253-278.
- HILL, S. J., YOUNG, J. M. & MARRIAN, D. H. **1977**. Specific binding of [³H]-mepyramine to histamine H₁ receptors in intestinal smooth muscle. *Nature*, **270**, 361-363.
- HOFSTRA, C. L., DESAI, P. J., THURMOND, R. L. & FUNG-LEUNG, W. P. **2003**. Histamine H₄ receptor mediates chemotaxis and calcium mobilization of mast cells. *J Pharmacol Exp Ther*, **305**, 1212-1221.
- IGEL, P. **2008**. Synthesis and structure-activity relationships of N^G-acylated arylalkylguanidines and related compounds as histamine receptor ligands: searching for selective H₄R agonists. *PhD Thesis, University of Regensburg*.
- IGEL, P., GEYER, R., STRASSER, A., DOVE, S., SEIFERT, R. & BUSCHAUER, A. **2009**. Synthesis and structure-activity relationships of cyanoguanidine-type and structurally related histamine H₄ receptor agonists. *J Med Chem*, **52**, 6297-6313.
- JABLONOWSKI, J. A., GRICE, C. A., CHAI, W., DVORAK, C. A., VENABLE, J. D., KWOK, A. K., LY, K. S., WEI, J., BAKER, S. M. & DESAI, P. J. **2003**. The first potent and selective non-imidazole human histamine H₄ receptor antagonists. *J Med Chem*, **46**, 3957-3960.
- JACOBY, E., BOUHELAL, R., GERSPACHER, M. & SEUWEN, K. **2006**. The 7TM G-protein-coupled receptor target family. *ChemMedChem*, **1**, 760-782.
- Jl, T. H., GROSSMANN, M. & JI, I. **1998**. G protein-coupled receptors I. Diversity of receptor-ligand interactions. *J Biol Chem*, **273**, 17299-17302.
- JONES, R. M., HJORTH, S. A., SCHWARTZ, T. W. & PORTOGHESE, P. S. **1998**. Mutational evidence for a common κ antagonist binding pocket in the wild-type κ and mutant μ [K303E] opioid receptors. *J Med Chem*, **41**, 4911-4914.
- JORDAN, B. A. & DEVI, L. A. **1999**. G-protein-coupled receptor heterodimerization modulates receptor function. *Nature*, **399**, 697-700.
- KARNUSHINA, I. L., PALACIOS, J. M., BARBIN, G., DUX, E., JOO, F. & SCHWARTZ, J. C. **1980**. Studies on a capillary-rich fraction isolated from brain: histaminic components and characterization of the histamine receptors linked to adenylate cyclase. *J Neurochem*, **34**, 1201-1208.
- KAUPMANN, K., MALITSCHKE, B., SCHULER, V., HEID, J., FROEST, W., BECK, P., MOSBACHER, J., BISCHOFF, S., KULIK, A., SHIGEMOTO, R., KARSCHIN, A. & BETTLER, B. **1998**. GABA(B)-receptor subtypes assemble into functional heteromeric complexes. *Nature*, **396**, 683-687.
- KENAKIN, T. **2002a**. Drug efficacy at G protein-coupled receptors. *Annu Rev Pharmacol Toxicol*, **42**, 349-379.
- KENAKIN, T. **2002b**. Efficacy at G-protein-coupled receptors. *Nat Rev Drug Discov*, **1**, 103-110.

- KENAKIN, T. & MILLER, L. J. **2010**. Seven Transmembrane Receptors as Shapeshifting Proteins: The Impact of Allosteric Modulation and Functional Selectivity on New Drug Discovery. *Pharmacol Rev*, **62**, 265-304.
- KITBUNNADAJ, R., ZUIDERVELD, O. P., CHRISTOPHE, B., HULSCHER, S., MENGE, W. M., GELENS, E., SNIP, E., BAKKER, R. A., CELANIRE, S., GILLARD, M., TALAGA, P., TIMMERMAN, H. & LEURS, R. **2004**. Identification of 4-(1H-imidazol-4(5)-ylmethyl)pyridine (immethridine) as a novel, potent, and highly selective histamine H₃ receptor agonist. *J Med Chem*, **47**, 2414-2417.
- KOBILKA, B. K. **2007**. G protein coupled receptor structure and activation. *Biochimica Et Biophysica Acta-Biomembranes*, **1768**, 794-807.
- KOLAKOWSKI, L. F. **1994**. Gcrdb - a G-Protein-Coupled Receptor Database. *Receptors & Channels*, **2**, 1-7.
- KRAUS, A., GHORAI, P., BIRNKAMMER, T., SCHNELL, D., ELZ, S., SEIFERT, R., DOVE, S., BERNHARDT, G. & BUSCHAUER, A. **2009**. N⁶-acylated aminothiazolylpropylguanidines as potent and selective histamine H₂ receptor agonists. *ChemMedChem*, **4**, 232-240.
- KRISTIANSEN, K. **2004**. Molecular mechanisms of ligand binding, signaling, and regulation within the superfamily of G-protein-coupled receptors: molecular modeling and mutagenesis approaches to receptor structure and function. *Pharmacology & Therapeutics*, **103**, 21-80.
- KÜHN, B., SCHMID, A., HARTENECK, C., GUDERMANN, T. & SCHULTZ, G. **1996**. G proteins of the Gq family couple the H₂ histamine receptor to phospholipase C. *Mol Endocrinol*, **10**, 1697-1707.
- KUNISHIMA, N., SHIMADA, Y., TSUJI, Y., SATO, T., YAMAMOTO, M., KUMASAKA, T., NAKANISHI, S., JINGAMI, H. & MORIKAWA, K. **2000**. Structural basis of glutamate recognition by a dimeric metabotropic glutamate receptor. *Nature*, **407**, 971-977.
- LAGERSTRÖM, M. C. & SCHIÖTH, H. B. **2008**. Structural diversity of G protein-coupled receptors and significance for drug discovery. *Nat Rev Drug Discov*, **7**, 339-357.
- LEE, S. P., O'DOWD, B. F., NG, G. Y. K., VARGHESE, G., AKIL, H., MANSOUR, A., NGUYEN, T. & GEORGE, S. R. **2000**. Inhibition of cell surface expression by mutant receptors demonstrates that D₂ dopamine receptors exist as oligomers in the cell. *Mol Pharmacol*, **58**, 120-128.
- LEFF, P. **1995**. The 2-State Model of Receptor Activation. *Trends Pharmacol Sci*, **16**, 89-97.
- LEFKOVITZ, Z., SHAPIRO, R., KOCH, S. & CAPPELL, M. S. **2005**. The emerging role of virtual colonoscopy. *Med Clin North Am*, **89**, 111-138, viii.
- LEFKOWITZ, R. J. & SHENOY, S. K. **2005**. Transduction of receptor signals by β -arrestins. *Science*, **308**, 512-517.
- LEFKOWITZ, R. J. & WHALEN, E. J. **2004**. β -arrestins: traffic cops of cell signaling. *Curr Opin Cell Biol*, **16**, 162-168.
- LEOPOLDT, D., HARTENECK, C. & NÜRNBERG, B. **1997**. G proteins endogenously expressed in Sf9 cells: interactions with mammalian histamine receptors. *Naunyn Schmiedebergs Arch Pharmacol*, **356**, 216-224.

- LESCHKE, C., ELZ, S., GARBARG, M. & SCHUNACK, W. **1995**. Synthesis and histamine H₁ receptor agonist activity of a series of 2-phenylhistamines, 2-heteroarylhistamines, and analogues. *J Med Chem*, **38**, 1287-1294.
- LEURS, R., BAKKER, R. A., TIMMERMAN, H. & DE ESCH, I. J. **2005**. The histamine H₃ receptor: from gene cloning to H₃ receptor drugs. *Nat Rev Drug Discov*, **4**, 107-120.
- LEURS, R., BLANDINA, P., TEDFORD, C. & TIMMERMAN, H. **1998**. Therapeutic potential of histamine H₃ receptor agonists and antagonists. *Trends Pharmacol Sci*, **19**, 177-183.
- LEURS, R., CHAZOT, P. L., SHENTON, F. C., LIM, H. D. & DE ESCH, I. J. **2009**. Molecular and biochemical pharmacology of the histamine H₄ receptor. *Br J Pharmacol*, **157**, 14-23.
- LEURS, R., SMIT, M. J. & TIMMERMAN, H. **1995**. Molecular pharmacological aspects of histamine receptors. *Pharmacol Ther*, **66**, 413-463.
- LEURS, R., VISCHER, H. F., WIJTMANS, M. & DE ESCH, I. J. **2011**. En route to new blockbuster anti-histamines: surveying the offspring of the expanding histamine receptor family. *Trends Pharmacol Sci*, **32**, 250-257.
- LEVI, R. C. & ALLOATTI, G. **1988**. Histamine modulates calcium current in guinea pig ventricular myocytes. *J Pharmacol Exp Ther*, **246**, 377-383.
- LEZOUALC'H, F., JOCKERS, R. & BERQUE-BESTEL, I. **2009**. Multivalent-based drug design applied to serotonin 5-HT₄ receptor oligomers. *Curr Pharm Des*, **15**, 719-729.
- LIM, H. D., VAN RIJN, R. M., LING, P., BAKKER, R. A., THURMOND, R. L. & LEURS, R. **2005**. Evaluation of histamine H₁-, H₂-, and H₃-receptor ligands at the human histamine H₄ receptor: identification of 4-methylhistamine as the first potent and selective H₄ receptor agonist. *J Pharmacol Exp Ther*, **314**, 1310-1321.
- LIU, C., MA, X., JIANG, X., WILSON, S. J., HOFSTRA, C. L., BLEVITT, J., PYATI, J., LI, X., CHAI, W., CARRUTHERS, N. & LOVENBERG, T. W. **2001**. Cloning and pharmacological characterization of a fourth histamine receptor H₄ expressed in bone marrow. *Mol Pharmacol*, **59**, 420-426.
- LOVENBERG, T. W., ROLAND, B. L., WILSON, S. J., JIANG, X., PYATI, J., HUVAR, A., JACKSON, M. R. & ERLANDER, M. G. **1999**. Cloning and functional expression of the human histamine H₃ receptor. *Mol Pharmacol*, **55**, 1101-1107.
- LUTTRELL, L. M. **2008**. Reviews in molecular biology and biotechnology: transmembrane signaling by G protein-coupled receptors. *Mol Biotechnol*, **39**, 239-264.
- MAJNO, G. & PALADE, G. E. **1961**. Studies on inflammation. 1. The effect of histamine and serotonin on vascular permeability: an electron microscopic study. *J Biophys Biochem Cytol*, **11**, 571-605.
- MARINISSEN, M. J. & GUTKIND, J. S. **2001**. G-protein-coupled receptors and signaling networks: emerging paradigms. *Trends Pharmacol Sci*, **22**, 368-376.
- MARTINEZ-MIR, M. I., POLLARD, H., MOREAU, J., ARRANG, J. M., RUAT, M., TRAIFFORT, E., SCHWARTZ, J. C. & PALACIOS, J. M. **1990**. Three histamine receptors (H₁, H₂ and H₃) visualized in the brain of human and non-human primates. *Brain Res*, **526**, 322-327.
- MCVEY, M., RAMSAY, D., KELLETT, E., REES, S., WILSON, S., POPE, A. J. & MILLIGAN, G. **2001**. Monitoring receptor oligomerization using time-resolved fluorescence resonance energy transfer and

- bioluminescence resonance energy transfer. The human δ opioid receptor displays constitutive oligomerization at the cell surface, which is not regulated by receptor occupancy. *J Biol Chem*, **276**, 14092-14099.
- MENGHIN, S., PERTZ, H. H., KRAMER, K., SEIFERT, R., SCHUNACK, W. & ELZ, S. **2003**. N $^{\alpha}$ -imidazolylalkyl and pyridylalkyl derivatives of histaprodifen: synthesis and in vitro evaluation of highly potent histamine H $_1$ -receptor agonists. *J Med Chem*, **46**, 5458-5470.
- MESSER, W. S., JR. **2004**. Bivalent ligands for G protein-coupled receptors. *Curr Pharm Des*, **10**, 2015-2020.
- MICHAL, P., LYSIKOVA, M., EL-FAKAHANY, E. E. & TUCEK, S. **1999**. Clozapine interaction with the M $_2$ and M $_4$ subtypes of muscarinic receptors. *Eur J Pharmacol*, **376**, 119-125.
- MIKOSHIBA, K. **2007**. IP $_3$ receptor/Ca $^{2+}$ channel: from discovery to new signaling concepts. *J Neurochem*, **102**, 1426-1446.
- MORSE, K. L., BEHAN, J., LAZ, T. M., WEST, R. E., JR., GREENFEDER, S. A., ANTHES, J. C., UMLAND, S., WAN, Y., HIPKIN, R. W., GONSIOREK, W., SHIN, N., GUSTAFSON, E. L., QIAO, X., WANG, S., HEDRICK, J. A., GREENE, J., BAYNE, M. & MONSMA, F. J., JR. **2001**. Cloning and characterization of a novel human histamine receptor. *J Pharmacol Exp Ther*, **296**, 1058-1066.
- MÖSSNER, J. & CACA, K. **2005**. Developments in the inhibition of gastric acid secretion. *Eur J Clin Invest*, **35**, 469-475.
- NAKAMURA, T., ITADANI, H., HIDAKA, Y., OHTA, M. & TANAKA, K. **2000**. Molecular cloning and characterization of a new human histamine receptor, hH $_4$ R. *Biochem Biophys Res Commun*, **279**, 615-620.
- NEUBIG, R. R. & SIDEROVSKI, D. R. **2002**. Regulators of G-protein signalling as new central nervous system drug targets. *Nat Rev Drug Discov*, **1**, 187-197.
- NGUYEN, T., SHAPIRO, D. A., GEORGE, S. R., SETOLA, V., LEE, D. K., CHENG, R., RAUSER, L., LEE, S. P., LYNCH, K. R., ROTH, B. L. & O'DOWD, B. F. **2001**. Discovery of a novel member of the histamine receptor family. *Mol Pharmacol*, **59**, 427-433.
- NIJMEIJER, S., VISCHER, H. F., ROSETHORNE, E. M., CHARLTON, S. J. & LEURS, R. **2012**. Analysis of multiple histamine H $_4$ receptor compound classes uncovers G α_i protein- and β -arrestin2-biased ligands. *Mol Pharmacol*, **82**, 1174-1182.
- NIKBIN, N., EDWARDS, C. & REYNOLDS, C. A. **2003**. G-protein coupled receptor dimerization. *IJPT*, **2**, 1-11.
- NIMCHINSKY, E. A., HOF, P. R., JANSSEN, W. G. M., MORRISON, J. H. & SCHMAUSS, C. **1997**. Expression of dopamine D $_3$ receptor dimers and tetramers in brain and in transfected cells. *J Biol Chem*, **272**, 29229-29237.
- NOOIJEN, P. M., CARVALHO, F. & FLANAGAN, R. J. **2011**. Haematological toxicity of clozapine and some other drugs used in psychiatry. *Hum Psychopharmacol*, **26**, 112-119.
- NORDEMANN, U. **2013**. Radioligand binding and reporter gene assays for histamine H $_3$ and H $_4$ receptor species orthologs. *PhD Thesis, University of Regensburg*.

- ODA, T., MORIKAWA, N., SAITO, Y., MASUHO, Y. & MATSUMOTO, S. **2000**. Molecular cloning and characterization of a novel type of histamine receptor preferentially expressed in leukocytes. *J Biol Chem*, **275**, 36781-36786.
- OFFERMANN, S. **2003**. G-proteins as transducers in transmembrane signalling. *Prog Biophys Mol Biol*, **83**, 101-130.
- OVERINGTON, J. P., AL-LAZIKANI, B. & HOPKINS, A. L. **2006**. Opinion - How many drug targets are there? *Nat Rev Drug Discov*, **5**, 993-996.
- PALCZEWSKI, K., KUMASAKA, T., HORI, T., BEHNKE, C. A., MOTOSHIMA, H., FOX, B. A., LE TRONG, I., TELLER, D. C., OKADA, T., STENKAMP, R. E., YAMAMOTO, M. & MIYANO, M. **2000**. Crystal structure of rhodopsin: A G protein-coupled receptor. *Science*, **289**, 739-745.
- PARK, J. H., SCHEERER, P., HOFMANN, K. P., CHOE, H. W. & ERNST, O. P. **2008**. Crystal structure of the ligand-free G-protein-coupled receptor opsin. *Nature*, **454**, 183-187.
- PARMENTIER, R., ANACLET, C., GUHENNEC, C., BROUSSEAU, E., BRICOUT, D., GIBOULOT, T., BOZYCZKO-COYNE, D., SPIEGEL, K., OHTSU, H., WILLIAMS, M. & LIN, J. S. **2007**. The brain H₃-receptor as a novel therapeutic target for vigilance and sleep-wake disorders. *Biochem Pharmacol*, **73**, 1157-1171.
- PARSONS, M. E. & GANELLIN, C. R. **2006**. Histamine and its receptors. *Br J Pharmacol*, **147 Suppl 1**, S127-S135.
- PARSONS, M. E., OWEN, D. A., GANELLIN, C. R. & DURANT, G. J. **1977**. Dimaprit -(S-[3-(N,N-dimethylamino)propyl]isothiourea) - a highly specific histamine H₂ -receptor agonist. Part 1. Pharmacology. *Agents and Actions*, **7**, 31-37.
- PASSANI, M. B., GIANNONI, P., BUCHERELLI, C., BALDI, E. & BLANDINA, P. **2007**. Histamine in the brain: beyond sleep and memory. *Biochem Pharmacol*, **73**, 1113-1122.
- PAVAN, B., BIONDI, C. & DALPIAZ, A. **2009**. Adenylyl cyclases as innovative therapeutic goals. *Drug Discov Tod*, **14**, 982-991.
- PORTOGHESE, P. S. **1989**. Bivalent Ligands and the Message-Address Concept in the Design of Selective Opioid Receptor Antagonists. *Trends Pharmacol Sci*, **10**, 230-235.
- PORTOGHESE, P. S. **2001**. From models to molecules: Opioid receptor dimers, bivalent ligands, and selective opioid receptor probes. *J Med Chem*, **44**, 2259-2269.
- RAJAGOPAL, S., RAJAGOPAL, K. & LEFKOWITZ, R. J. **2010**. Teaching old receptors new tricks: biasing seven-transmembrane receptors. *Nat Rev Drug Discov*, **9**, 373-386.
- RASMUSSEN, S. G. F., CHOI, H. J., FUNG, J. J., PARDON, E., CASAROSA, P., CHAE, P. S., DEVREE, B. T., ROSENBAUM, D. M., THIAN, F. S., KOBILKA, T. S., SCHNAPP, A., KONETZKI, I., SUNAHARA, R. K., GELLMAN, S. H., PAUTSCH, A., STEYAERT, J., WEIS, W. I. & KOBILKA, B. K. **2011a**. Structure of a nanobody-stabilized active state of the β_2 -adrenoceptor. *Nature*, **469**, 175-180.
- RASMUSSEN, S. G. F., DEVREE, B. T., ZOU, Y. Z., KRUSE, A. C., CHUNG, K. Y., KOBILKA, T. S., THIAN, F. S., CHAE, P. S., PARDON, E., CALINSKI, D., MATHIESEN, J. M., SHAH, S. T. A., LYONS, J. A., CAFFREY, M., GELLMAN, S. H., STEYAERT, J., SKINIOTIS, G., WEIS, W. I., SUNAHARA, R. K. & KOBILKA, B. K. **2011b**. Crystal structure of the β_2 -adrenergic receptor-Gs protein complex. *Nature*, **477**, 549-555.

- RICHELSON, E. **1979**. Tricyclic antidepressants and histamine H₁ receptors. *Mayo Clin Proc*, **54**, 669-674.
- RICHELSON, E. & NELSON, A. **1984**. Antagonism by neuroleptics of neurotransmitter receptors of normal human brain in vitro. *Eur J Pharmacol*, **103**, 197-204.
- RILEY, J. F. & WEST, G. B. **1952**. Histamine in tissue mast cells. *J Physiol*, **117**, 72P-73P.
- RITTER, S. L. & HALL, R. A. **2009**. Fine-tuning of GPCR activity by receptor-interacting proteins. *Nat Rev Mol Cell Biol*, **10**, 819-830.
- ROSS, E. M. & WILKIE, T. M. **2000**. GTPase-activating proteins for heterotrimeric G proteins: Regulators of G protein signaling (RGS) and RGS-like proteins. *Annu Rev Biochem*, **69**, 795-827.
- RYABIK, B. M., NGUYEN, V. T., MANN, R. M., SMITH, J. D. & LIPPMANN, S. B. **1993**. Clozapine-induced agranulocytosis and colony-stimulating cytokines. *Gen Hosp Psychiatry*, **15**, 263-265.
- SAMAMA, P., COTECCHIA, S., COSTA, T. & LEFKOWITZ, R. J. **1993**. A Mutation-Induced Activated State of the β_2 -Adrenergic Receptor - Extending the Ternary Complex Model. *J Biol Chem*, **268**, 4625-4636.
- SANDER, K., KOTTKE, T. & STARK, H. **2008**. Histamine H₃ receptor antagonists go to clinics. *Biol Pharm Bull*, **31**, 2163-2181.
- SANDER, K., KOTTKE, T., TANRIKULU, Y., PROSCHAK, E., WEIZEL, L., SCHNEIDER, E. H., SEIFERT, R., SCHNEIDER, G. & STARK, H. **2009**. 2,4-Diaminopyrimidines as histamine H₄ receptor ligands-- Scaffold optimization and pharmacological characterization. *Bioorg Med Chem*, **17**, 7186-7196.
- SAXENA, S. P., BRANDES, L. J., BECKER, A. B., SIMONS, K. J., LABELLA, F. S. & GERRARD, J. M. **1989**. Histamine is an intracellular messenger mediating platelet aggregation. *Science*, **243**, 1596-1599.
- SCHEERER, P., PARK, J. H., HILDEBRAND, P. W., KIM, Y. J., KRAUSS, N., CHOE, H. W., HOFMANN, K. P. & ERNST, O. P. **2008**. Crystal structure of opsin in its G-protein-interacting conformation. *Nature*, **455**, 497-502.
- SCHNEIDER, E., ROLLI-DERKINDEREN, M., AROCK, M. & DY, M. **2002**. Trends in histamine research: new functions during immune responses and hematopoiesis. *Trends Immunol*, **23**, 255-263.
- SCHNEIDER, E. H., SCHNELL, D., PAPA, D. & SEIFERT, R. **2009**. High constitutive activity and a G-protein-independent high-affinity state of the human histamine H₄-receptor. *Biochemistry*, **48**, 1424-1438.
- SCHNEIDER, E. H. & SEIFERT, R. **2010**. Sf9 cells: a versatile model system to investigate the pharmacological properties of G protein-coupled receptors. *Pharmacol Ther*, **128**, 387-418.
- SCHWARTZ, J. C. **2011**. The histamine H₃ receptor: from discovery to clinical trials with pitolisant. *Br J Pharmacol*, **163**, 713-721.
- SCHWARTZ, J. C., POLLARD, H. & QUACH, T. T. **1980**. Histamine as a neurotransmitter in mammalian brain: neurochemical evidence. *J Neurochem*, **35**, 26-33.

- SEIFERT, R., HOER, A., SCHWANER, I. & BUSCHAUER, A. **1992**. Histamine increases cytosolic Ca^{2+} in HL-60 promyelocytes predominantly via H_2 receptors with an unique agonist/antagonist profile and induces functional differentiation. *Mol Pharmacol*, **42**, 235-241.
- SEIFERT, R., SCHNEIDER, E. H., DOVE, S., BRUNSKOLE, I., NEUMANN, D., STRASSER, A. & BUSCHAUER, A. **2011**. Paradoxical stimulatory effects of the "standard" histamine H_4 -receptor antagonist JNJ7777120: the H_4 receptor joins the club of 7 transmembrane domain receptors exhibiting functional selectivity. *Mol Pharmacol*, **79**, 631-638.
- SEIFERT, R. & WENZEL-SEIFERT, K. **2002**. Constitutive activity of G-protein-coupled receptors: cause of disease and common property of wild-type receptors. *Naunyn Schmiedebergs Arch Pharmacol*, **366**, 381-416.
- SEIFERT, R., WENZEL-SEIFERT, K., BÜCKSTÜMMER, T., PERTZ, H. H., SCHUNACK, W., DOVE, S., BUSCHAUER, A. & ELZ, S. **2003**. Multiple differences in agonist and antagonist pharmacology between human and guinea pig histamine H_1 -receptor. *J Pharmacol Exp Ther*, **305**, 1104-1115.
- SHARMAN, J. L., BENSON, H. E., PAWSON, A. J., LUKITO, V., MPAMHANGA, C. P., BOMBAIL, V., DAVENPORT, A. P., PETERS, J. A., SPEDDING, M., HARMAR, A. J. & NC-IUPHAR **2013**. IUPHAR-DB: updated database content and new features. *Nucleic Acids Research*, **41**, D1083-D1088.
- SHENTON, F. C., HANN, V. & CHAZOT, P. L. **2005**. Evidence for native and cloned H_3 histamine receptor higher oligomers. *Inflamm Res*, **54**, S48-S49.
- SHIMAMURA, T., SHIROISHI, M., WEYAND, S., TSUJIMOTO, H., WINTER, G., KATRITCH, V., ABAGYAN, R., CHEREZOV, V., LIU, W., HAN, G. W., KOBAYASHI, T., STEVENS, R. C. & IWATA, S. **2011**. Structure of the human histamine H_1 receptor complex with doxepin. *Nature*, **475**, 65-82.
- SHONBERG, J., SCAMMELLS, P. J. & CAPUANO, B. **2011**. Design strategies for bivalent ligands targeting GPCRs. *ChemMedChem*, **6**, 963-974.
- SMITH, N. J. & MILLIGAN, G. **2010**. Allostery at G Protein-Coupled Receptor Homo- and Heteromers: Uncharted Pharmacological Landscapes. *Pharmacol Rev*, **62**, 701-725.
- SMITS, R. A., DE ESCH, I. J., ZUIDERVELD, O. P., BROEKER, J., SANSUK, K., GUAITA, E., CORUZZI, G., ADAMI, M., HAAKSMA, E. & LEURS, R. **2008a**. Discovery of quinazolines as histamine H_4 receptor inverse agonists using a scaffold hopping approach. *J Med Chem*, **51**, 7855-7865.
- SMITS, R. A., LEURS, R. & DE ESCH, I. J. **2009**. Major advances in the development of histamine H_4 receptor ligands. *Drug Discov Tod*, **14**, 745-753.
- SMITS, R. A., LIM, H. D., HANZER, A., ZUIDERVELD, O. P., GUAITA, E., ADAMI, M., CORUZZI, G., LEURS, R. & DE ESCH, I. J. **2008b**. Fragment based design of new H_4 receptor-ligands with anti-inflammatory properties in vivo. *J Med Chem*, **51**, 2457-2467.
- SMRCKA, A. V. **2008**. G protein beta gamma subunits: Central mediators of G protein-coupled receptor signaling. *Cell Mol Life Sci*, **65**, 2191-2214.
- STEVENS, R. C., CHEREZOV, V., KATRITCH, V., ABAGYAN, R., KUHN, P., ROSEN, H. & WUTHRICH, K. **2013**. The GPCR Network: a large-scale collaboration to determine human GPCR structure and function. *Nat Rev Drug Discov*, **12**, 25-34.

- STRASSER, A., STRIEGL, B., WITTMANN, H. J. & SEIFERT, R. **2008a**. Pharmacological profile of histaprodifens at four recombinant histamine H₁ receptor species isoforms. *J Pharmacol Exp Ther*, **324**, 60-71.
- STRASSER, A., WITTMANN, H. J., BUSCHAUER, A., SCHNEIDER, E. H. & SEIFERT, R. **2013**. Species-dependent activities of G-protein-coupled receptor ligands: lessons from histamine receptor orthologs. *Trends Pharmacol Sci*, **34**, 13-32.
- STRASSER, A., WITTMANN, H. J., KUNZE, M., ELZ, S. & SEIFERT, R. **2009**. Molecular basis for the selective interaction of synthetic agonists with the human histamine H₁-receptor compared with the guinea pig H₁-receptor. *Mol Pharmacol*, **75**, 454-465.
- STRASSER, A., WITTMANN, H. J. & SEIFERT, R. **2008b**. Ligand-specific contribution of the N terminus and E2-loop to pharmacological properties of the histamine H₁-receptor. *J Pharmacol Exp Ther*, **326**, 783-791.
- TAKESHITA, K., SAKAI, K., BACON, K. B. & GANTNER, F. **2003**. Critical role of histamine H₄ receptor in leukotriene B₄ production and mast cell-dependent neutrophil recruitment induced by zymosan in vivo. *J Pharmacol Exp Ther*, **307**, 1072-1078.
- THOMSEN, W., FRAZER, J. & UNETT, D. **2005**. Functional assays for screening GPCR targets. *Curr Opin Biotech*, **16**, 655-665.
- THURMOND, R. L., GELFAND, E. W. & DUNFORD, P. J. **2008**. The role of histamine H₁ and H₄ receptors in allergic inflammation: the search for new antihistamines. *Nat Rev Drug Discov*, **7**, 41-53.
- TODA, N. **1984**. Endothelium-dependent relaxation induced by angiotensin II and histamine in isolated arteries of dog. *Br J Pharmacol*, **81**, 301-307.
- VAN DER GOOT, H., SCHEPERS, M. J. P., STERK, G. J. & TIMMERMAN, H. **1992**. Isothiourea Analogs of Histamine as Potent Agonists or Antagonists of the Histamine H₃ Receptor. *Eur J Med Chem*, **27**, 511-517.
- VAN DER GOOT, H. & TIMMERMAN, H. **2000**. Selective ligands as tools to study histamine receptors. *Eur J Med Chem*, **35**, 5-20.
- VAN RIJN, R. M., CHAZOT, P. L., SHENTON, F. C., SANSUK, K., BAKKER, R. A. & LEURS, R. **2006**. Oligomerization of recombinant and endogenously expressed human histamine H₄ receptors. *Mol Pharmacol*, **70**, 604-615.
- VAN RIJN, R. M., VAN MARLE, A., CHAZOT, P. L., LANGEMEIJER, E., QIN, Y., SHENTON, F. C., LIM, H. D., ZUIDERVELD, O. P., SANSUK, K., DY, M., SMIT, M. J., TENSEN, C. P., BAKKER, R. A. & LEURS, R. **2008**. Cloning and characterization of dominant negative splice variants of the human histamine H₄ receptor. *Biochem J*, **414**, 121-131.
- VANDEVOORDE, J. & LEUSEN, I. **1983**. Role of the Endothelium in the Vasodilator Response of Rat Thoracic Aorta to Histamine. *Eur J Pharmacol*, **87**, 113-120.
- VASSILATIS, D. K., HOHMANN, J. G., ZENG, H., LI, F. S., RANCHALIS, J. E., MORTTRUD, M. T., BROWN, A., RODRIGUEZ, S. S., WELLER, J. R., WRIGHT, A. C., BERGMANN, J. E. & GAITANARIS, G. A. **2003**. The G protein-coupled receptor repertoires of human and mouse. *Proc Nat Acad Sci U.S.A.*, **100**, 4903-4908.

- VENKATAKRISHNAN, A. J., DEUPI, X., LEBON, G., TATE, C., SCHERTLER, G. F., BABU, M. M. **2013**. Molecular signatures of G-Protein coupled receptors. *Nature*, **494**, 185-94.
- VIOLIN, J. D. & LEFKOWITZ, R. J. **2007**. β -arrestin-biased ligands at seven-transmembrane receptors. *Trends Pharmacol Sci*, **28**, 416-422.
- WARNE, T., SERRANO-VEGA, M. J., BAKER, J. G., MOUKHAMETZIANOV, R., EDWARDS, P. C., HENDERSON, R., LESLIE, A. G. W., TATE, C. G. & SCHERTLER, G. F. X. **2008**. Structure of a β_1 -adrenergic G-protein-coupled receptor. *Nature*, **454**, 486-491.
- WEISS, J. M., MORGAN, P. H., LUTZ, M. W. & KENAKIN, T. P. **1996a**. The cubic ternary complex receptor-occupancy model . 1. Model description. *J Theor Biol*, **178**, 151-167.
- WEISS, J. M., MORGAN, P. H., LUTZ, M. W. & KENAKIN, T. P. **1996b**. The cubic ternary complex receptor-occupancy model . 2. Understanding apparent affinity. *J Theor Biol*, **178**, 169-182.
- WEISS, J. M., MORGAN, P. H., LUTZ, M. W. & KENAKIN, T. P. **1996c**. The cubic ternary complex receptor-occupancy model . 3. Resurrecting efficacy. *J Theor Biol*, **181**, 381-397.
- WELLNER-KIENITZ, M. C., BENDER, K., MEYER, T. & POTT, L. **2003**. Coupling to G_s and $G_{q/11}$ of histamine H_2 receptors heterologously expressed in adult rat atrial myocytes. *Biochim Biophys Acta*, **1642**, 67-77.
- WIEDEMANN, P., BONISCH, H., OERTERS, F. & BRUSS, M. **2002**. Structure of the human histamine H_3 receptor gene (HRH3) and identification of naturally occurring variations. *J Neur Trans*, **109**, 443-453.
- WIJTMANS, M., LEURS, R. & DE ESCH, I. **2007**. Histamine H_3 receptor ligands break ground in a remarkable plethora of therapeutic areas. *Expert Opin Investig Drugs*, **16**, 967-985.
- WINDAUS, A. & VOGT, W. **1908**. Synthesis of Imidazolyethylamine. *Ber Dtsch Chem Ges*, **40**, 3685 - 3691.
- WITTMANN, H. J., SEIFERT, R. & STRASSER, A. **2011**. Influence of the N-terminus and the E2-loop onto the binding kinetics of the antagonist mepyramine and the partial agonist phenoprodifen to H_1R . *Biochem Pharmacol*, **82**, 1910-1918.
- WORZFELD, T., WETTSCHURECK, N. & OFFERMANN, S. **2008**. G_{12}/G_{13} -mediated signalling in mammalian physiology and disease. *Trends Pharmacol Sci*, **29**, 582-589.
- ZAMPELI, E. & TILIGADA, E. **2009**. The role of histamine H_4 receptor in immune and inflammatory disorders. *Br J Pharmacol*, **157**, 24-33.
- ZHANG, M., THURMOND, R. L. & DUNFORD, P. J. **2007**. The histamine H_4 receptor: a novel modulator of inflammatory and immune disorders. *Pharmacol Ther*, **113**, 594-606.
- ZHU, Y., MICHALOVICH, D., WU, H.-L., TAN, K., DYTOKO, G. M., MANNAN, I. J., BOYCE, R., ALSTON, J., TIERNEY, L. A. & LI, X. **2001**. Cloning, expression, and pharmacological characterization of a novel human histamine receptor. *Mol Pharmacol*, **59**, 434-441.
- ZINGEL, V., ELZ, S. & SCHUNACK, W. **1990**. Histamine Analogs .33. 2-Phenylhistamines with High Histamine H_1 -Agonistic Activity. *Eur J Med Chem*, **25**, 673-680.

Introduction

ZORN, S. H., JONES, S. B., WARD, K. M. & LISTON, D. R. **1994**. Clozapine is a potent and selective muscarinic M₄ receptor agonist. *Eur J Pharmacol*, **269**, R1-2.

Chapter 2

Scope and objectives

2. Scope and objectives

Both, the H₁R and the H₄R were recently reported to play an important role in allergic inflammation. (Thurmond et al., 2008) A study on the acute murine asthma model performed by Deml et al. revealed that the combined application of mepyramine (H₁R-antagonist) and JNJ7777120 (H₄R-antagonist) had a synergistic inhibitory effect on the eosinophil-accumulation in the bronchoalveolar lavage fluid. (Deml et al., 2009) These results indicate an involvement of both, the H₁R and H₄R in *type I* allergic diseases like, e.g., chronic pruritus or bronchial asthma. As a consequence, a synergy between H₁R and H₄R antagonists in the form of molecules bearing pharmacophores that address both, the H₁R and the H₄R are in great demand for future research.

With regard to the design of this kind of ligands, two different strategies of molecule design can be pursued: firstly, an H₁R antagonist can be linked to an H₄R antagonist by spacers of different type and length, obtaining bivalent hybrid compounds. Examples can be found in the work of Wagner et al.: therein, the H₄R antagonist JNJ7777120 was linked with different kinds of spacers to (parts of) either mepyramine or astemizole. (Wagner et al., 2011) However, the resulting molecules did not show the desired affinity to both targets. Although some of the resulting hybrid compounds revealed high affinity to H₁R, the effects at the H₄R were rather of a lower range.

A second strategy consists of either the screening for molecules that already address the H₁R and the H₄R and as a consequence contain a (as the case may be common) H₁R and H₄R pharmacophore, or of the development of new compounds meeting these conditions. These lead structures can then be further modified and refined in order to get ligands with the desired pharmacological effects.

The antipsychotic drug clozapine exhibits (among others) antagonistic affinity to the H₁R and partial agonistic affinity to the H₄R (Appl et al., 2012). Related to this, a dutch group around Leurs developed the optimized compound VUF 6884 with on the first sight only minor structural modifications compared to clozapine (Smits et al., 2006): the nitrogen in position 5 was replaced by an oxygen and the Cl substituent in position 8 was shifted to position 7 (figure [2.1](#)). As a consequence, this optimized ligand revealed a distinctly increased partial agonistic affinity to H₄R as well as a constantly high antagonistic affinity to H₁R. (Smits et al., 2006)

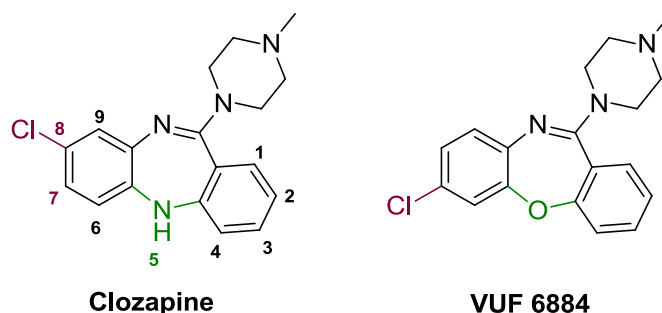


Figure 2.1. Clozapine and the “optimized” clozapine derivative VUF 6884.

Based on this, the aim of this work was to prepare a series of VUF 6884 derived compounds that were modified regarding their substitution pattern, the rigidization of the piperazine moiety and the central heterocycle in the molecule.

In a first part of the project, the VUF 6884 molecule was reduced to the core: the central oxazepine ring was opened and the rigid basic amine moiety consisting of an *N*-methylpiperazine on top of the molecule was replaced by different flexible ethylenediamine derivatives with varying alkyl substituents (**1**) (figure 2.2). A further series of these “opened” compounds contained a rigid *N*-methylpiperazine moiety as well as various modifications of the substitution pattern (**2**). The highest analogy to VUF 6884 was given within a third series of compounds (**3**), however, by a modification of either the substitution pattern or the piperazine moiety the pharmacological behaviour could be distinctly influenced. (Figure 2.2)

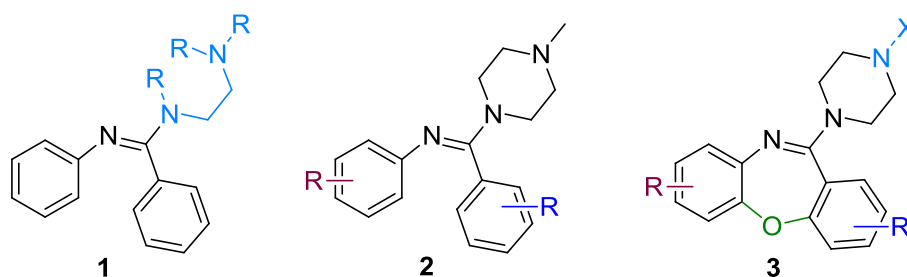


Figure 2.2. Structural modifications of VUF 6884.

Furthermore, the compounds showing the most promising pharmacological results were, in accordance with the work of McRobb et al., transferred into dimeric molecules, linked by different spacer types and lengths in different positions of the molecule (**4**). (McRobb et al., 2012) (Figure 2.3).

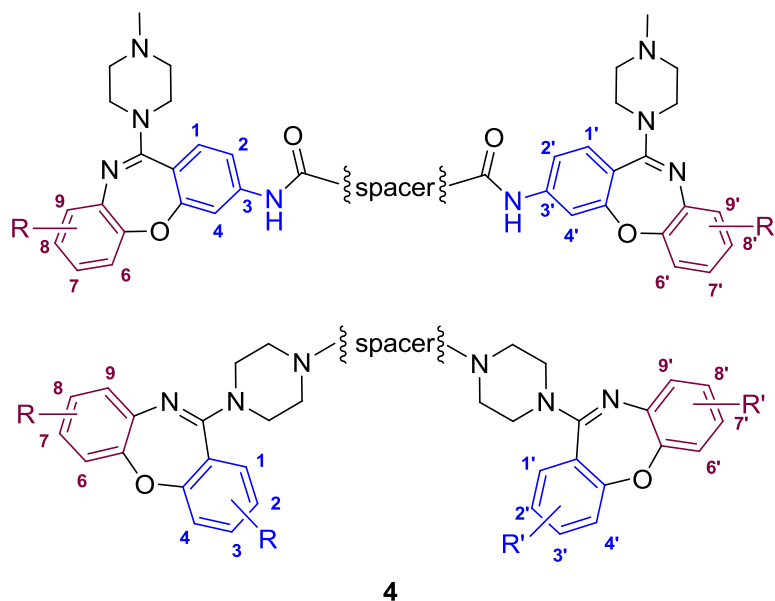


Figure 2.3. Dimeric VUF 6884 derivatives.

Pharmacological characterization of the resulting compounds in several different testing systems provided a closer insight into structure activity relationships (SARs) at H_1R and H_4R .

References

- APPL, H., HOLZAMMER, T., DOVE, S., HAEN, E., STRASSER, A. & SEIFERT, R. **2012**. Interactions of recombinant human histamine H₁R, H₂R, H₃R, and H₄R receptors with 34 antidepressants and antipsychotics. *Naunyn Schmiedeberg's Arch Pharmacol*, **385**, 145-170.
- DEML, K. F., BEERMANN, S., NEUMANN, D., STRASSER, A. & SEIFERT, R. **2009**. Interactions of histamine H₁-receptor agonists and antagonists with the human histamine H₄-receptor. *Mol Pharmacol*, **76**, 1019-1030.
- MCROBB, F. M., CROSBY, I. T., YURIEV, E., LANE, J. R. & CAPUANO, B. **2012**. Homobivalent ligands of the atypical antipsychotic clozapine: design, synthesis, and pharmacological evaluation. *J Med Chem*, **55**, 1622-1634.
- SMITS, R. A., LIM, H. D., STEGINK, B., BAKKER, R. A., DE ESCH, I. J. & LEURS, R. **2006**. Characterization of the histamine H₄ receptor binding site. Part 1. Synthesis and pharmacological evaluation of dibenzodiazepine derivatives. *J Med Chem*, **49**, 4512-4516.
- THURMOND, R. L., GELFAND, E. W. & DUNFORD, P. J. **2008**. The role of histamine H₁ and H₄ receptors in allergic inflammation: the search for new antihistamines. *Nat Rev Drug Discov*, **7**, 41-53.
- WAGNER, E., WITTMANN, H. J., ELZ, S. & STRASSER, A. **2011**. Mepyramine-JNJ7777120-hybrid compounds show high affinity to hH₁R, but low affinity to hH₄R. *Bioorg Med Chem Lett*, **21**, 6274-6280.

Chapter 3
Chemical section

3. Chemical section

3.1. Ligand design related to VUF 6884 (Smits et al., 2006)

The chemical section of this work aimed at the modification and structural investigation of molecules related to VUF 6884, a potent histamine H₁-/ H₄-receptor ligand that was developed by Smits et al. (2006) (figure 3.1). Several modifications of either the substitution pattern, the piperazine moiety, the heterocycle in the center of the molecule or the molecule size (i.e., dimerization of the modified molecules) were carried out with intent to get a closer insight into structure-activity relationships at hH₁R and hH₄R as well as at other GPCRs that were described in the pharmacological section.

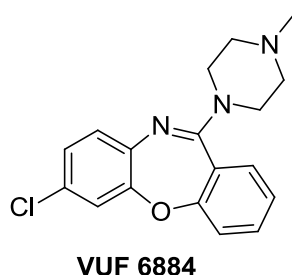


Figure 3.1. Lead structure VUF 6884.

Starting from fairly simplified VUF 6884 derivatives, the molecule was re-built bit by bit so that pharmacological effects related to the respective parts of the molecule could be investigated. Furthermore, several series of different VUF 6884 derived dimeric molecules were prepared with intent to address either homo- and hetero-oligomeric histamine H₁ / H₄ receptors (provided a sufficient spacer length) or to address a further binding pocket in the extracellular region of the receptors. (Figure 3.2)

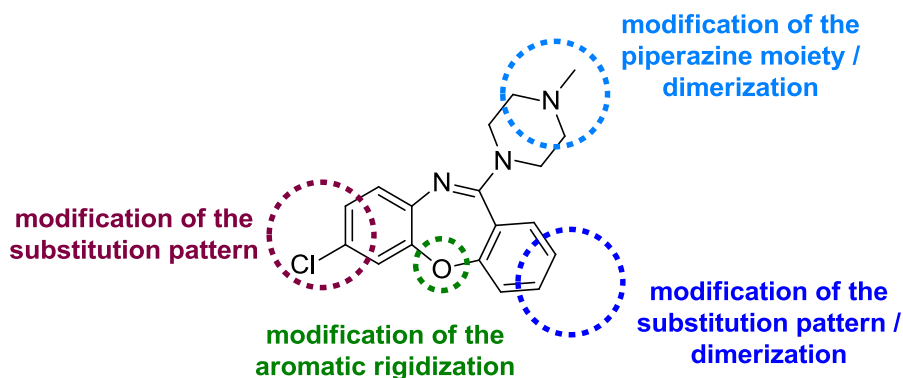


Figure 3.2. Structural modifications of the lead structure VUF 6884.

3.2. Synthesis of the “open” phenylbenzamidines: opening up the rigid aromatic ring system in the center of the molecule

A first series of truncated compounds was prepared that will be referred to as “open” compounds in the following. Formally, they are derived from the tricyclic parent compounds by ring-opening of the central heterocycle. As a consequence, the two aromatic rings in the central core of the molecule are released from rigidisation and thus able to rotate around the single bonds adjacent to the imino-bond. Hence, the respective substituents in, e.g., *m*-position of the rings are able to possess different positions in the binding pocket of the target receptors.

A map of the resulting molecules was set up to provide an overview of the modifications of the substitution pattern (figure 3.3). The substituents were inserted in *para* (*p*-) or *meta* (*m*-) position of either the **aniline** or the **benzoic acid** moiety, terms that are derived from the pursued synthesis strategy that will be described in 3.2.2.

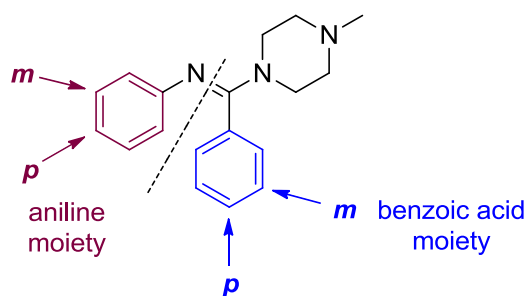


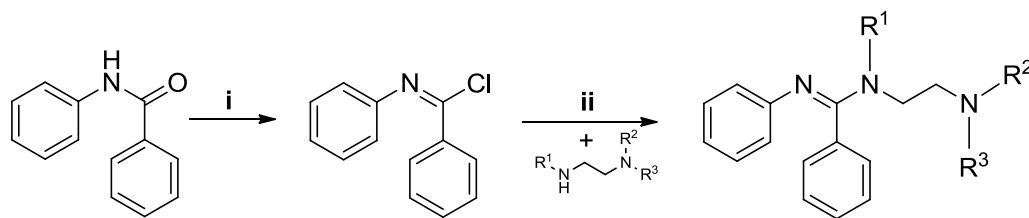
Figure 3.3. Molecule map of the “open” VUF 6884 derivatives.

3.2.1. VUF 6884 reduced to the core: (*E*)-*N*-(2-aminoethyl)-*N'*-phenylbenzamidines derivatives

Among the “open” series of compounds, three of them focused on the very basic elements of VUF 6884: with intent to provide an increase of flexibility in the central core as well as in the basic amine part of the molecule, the “open” phenylbenzamidines-core was linked to differently substituted ethylenediamine derivatives instead of the rigid *N*-methypiperazine moiety.

The desired compounds were easily accessible pursuing the following synthesis strategy: firstly, commercially available benzanilide was converted in-situ to the imide chloride by using PCl_5 , to which in a second step and without further purification the

pertinent ethylenediamine derivatives (**22**: *N,N*-dimethylethylenediamine, **23**: *N,N*-diethylethylenediamine and **25**: *N,N,N'*-trimethylethylenediamine) were added (Wu et al., 2005). (Figure 3.4)



i: benzene, PCl_5 , 2 h reflux; ii: benzene, 2 h RT

Figure 3.4. Synthesis pathway of the (*E*)-*N*-(2-aminoethyl)-*N*-phenylbenzamidines derivatives.

The resulting ethylenediamine substituted phenylbenzamidines **22**, **23**, and **25** were purified by column chromatography over silica gel (EtOAc / NH_3 (7 N in MeOH) 9:1) and were obtained as colorless solids. (Table 3.1)

	R^1	R^2	R^3	Cpd.
	H	-CH ₃	-CH ₃	22
	H	-C ₂ H ₅	-C ₂ H ₅	23
	-CH ₃	-CH ₃	-CH ₃	25

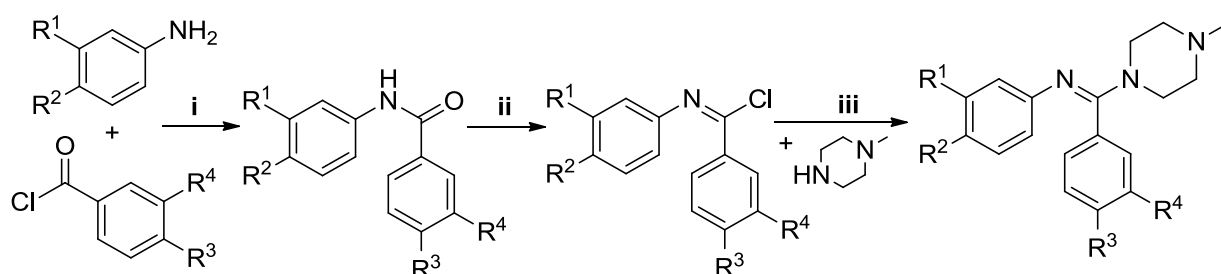
Table 3.1. “Open” VUF 6884 derivatives with ethylenediamine moiety.

3.2.2. “Open” VUF 6884 derivatives with modified substitution pattern: detecting the influence of kind and position of the substituents

By analogy with the above described procedure and in the style of Jensen and Pedersen (1979), the “open” VUF 6884 analogues carrying a rigid *N*-methylpiperazine moiety were obtained from the corresponding benzanilide building blocks which were either commercially available or conveniently accessible by coupling substituted

benzoic acid chlorides (**benzoic acid moiety**) with substituted aniline derivatives (**aniline moiety**) under nitrogen atmosphere in the presence of NEt₃ (Sun et al., 2009). The resulting amines revealed different colors depending on their substitution pattern and were all obtained as crystalline solids after re-crystallization from acetone.

After converting the amides with PCl₅ in situ to the corresponding imide chlorides, *N*-methylpiperazine was added in the presence of NEt₃ and, as soon as the reaction was completed, purified by column chromatography over silica gel (EtOAc : MeOH 1:1). Except from NO₂-substituted molecules that invariably revealed shades of yellow, all compounds were obtained as colorless solids. (Figure 3.5)



i: NEt₃, N₂, DCM, 6 h RT, 12 h reflux; ii: PCl₅, benzene / ACN, 2 h reflux; iii: NEt₃, benzene / ACN, 12 h reflux

Figure 3.5. Synthesis pathway of the “open” VUF 6884 derivatives with *N*-methylpiperazine moiety.

As VUF 6884 and clozapine both carry a Cl-substituent in different positions of the molecule, this kind of substituent found itself in the spotlight of interest and was introduced in various positions at both the aniline and the benzoic acid moiety. Nevertheless, also other halide (Br) and pseudohalide (CN) substituents as well as NH₂ groups were introduced with intent to get a closer insight into the structure activity relationships (SARs) in dependence of the kind of substituent and the resulting substitution pattern. Mono- as well as di-substituted compounds were prepared and, referred to the map of the molecule shown in figure 3.3, are summarized in table 3.2.

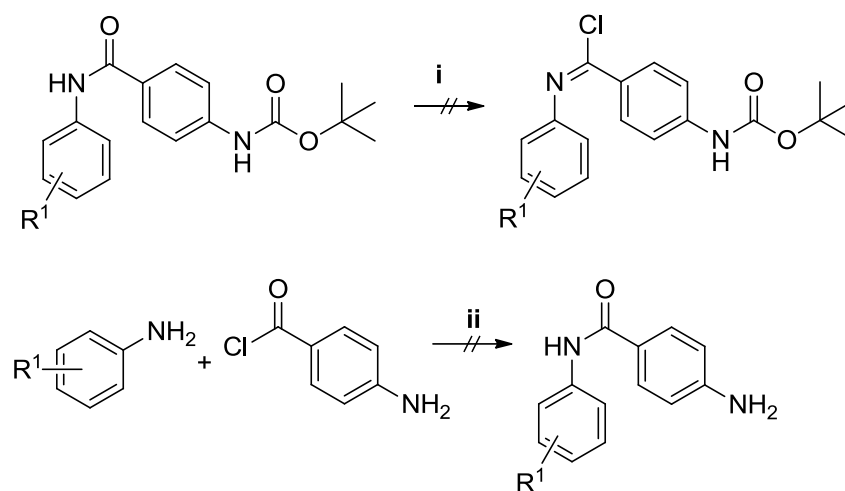
	R	Cpd.		R	Cpd.
	H	28		<i>p</i>-CN	58
	<i>p</i>-Br	64		<i>p</i>-Cl	70
	<i>p</i>-Cl	67		<i>p</i>-NO₂	55
	<i>p</i>-NO₂	50		<i>m</i>-Cl	76
	<i>m</i>-Cl	73			

	R	Cpd.		R	Cpd.
	<i>p</i>-Cl	79		<i>p</i>-Cl	108
	<i>p</i>-Br	61		<i>m</i>-Cl	109
	<i>m</i>-Cl	102			

	R	Cpd.		
	<i>p</i>-Cl	180		
	<i>m</i>-Cl	181		

Table 3.2. Mono- and di-substituted “open” VUF 6884 analogues with modified substitution pattern.

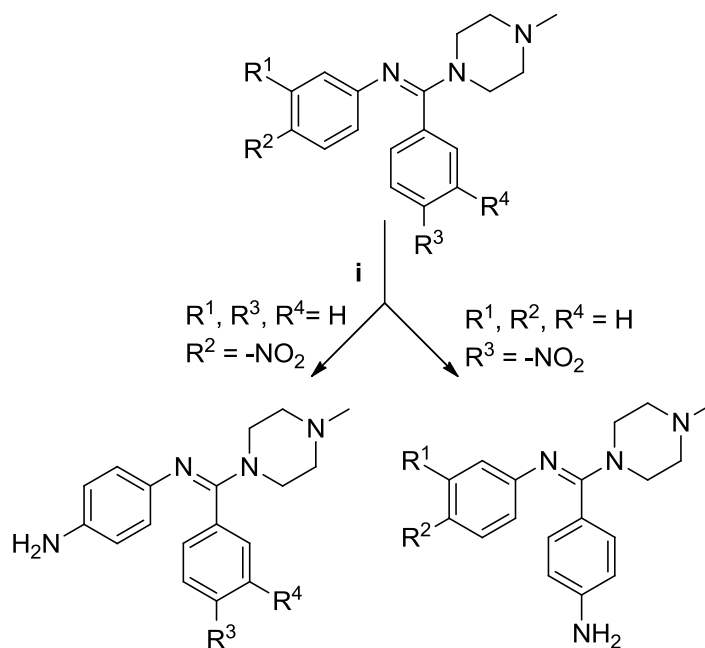
For the compounds bearing an NO₂ substituent, a final reduction step was added to obtain the desired NH₂ substitution. Attempts using BOC-protected NH₂-substituted starting material failed as well as the use of NH₂-substituted aniline or benzoyl chloride derivatives (figure 3.6). However, the insertion and later reduction of NO₂-substituted starting material provided a convenient method to obtain the desired compounds.



i: PCl_5 , benzene / ACN, 2 h reflux; ii: NEt_3 , DCM, 6 h RT, 12 h reflux

Figure 3.6. Failed synthetic attempts on the way to NH_2 -substituted “open” compounds.

Using SnCl_2 to reduce the NO_2 -substituted molecules according to Chao et al. (2009) resulted in the desired NH_2 -substituted compounds (figure 3.7). The compounds were purified by column chromatography over silica gel (EtOAc : MeOH 1:1) and were obtained as slightly yellow solids.



i: $\text{SnCl}_2 \cdot 2 \text{H}_2\text{O}$, EtOH, 12 h reflux

Figure 3.7. General procedure for the reduction of the NO_2 -substituted compounds according to Chao et al. (2009).

An overview of the synthesized mono- and di-substituted NH₂-bearing compounds is provided in table 3.3:

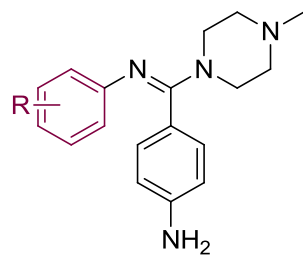
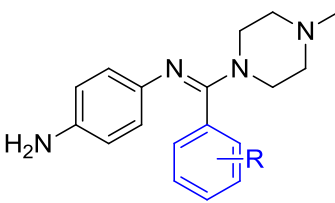
	R	Cpd.		R	Cpd.
	H	56		H	52
	<i>p</i> -Br	62		<i>m</i> -Cl	110
	<i>p</i> -Cl	80		<i>p</i> -Cl	111
	<i>m</i> -Cl	103			

Table 3.3. Mono- and di- substituted NH₂-bearing “open” VUF 6884 analogues.

3.2.3. Acylated open VUF 6884 derivatives: an attempt to increase the hH₄R affinity

Within a series of several quinoxaline and quinazoline derived compounds, an increase of hH₄R affinity was determined that could be traced back to the insertion of an additional aromatic substituent located at the central core of the respective molecules. (Smits et al., 2008a, Smits et al., 2008b) Based on this and on the flexible alignment study of two further structurally related hH₄R ligands (JNJ7777120 and VUF 6884), a three-pocket pharmacophore model for the hH₄R was postulated: therein, the two pockets for the *N*-methylpiperazine moiety and the central aromatic heterocycle are completed by a third, hydrophobic pocket to which the additional aromatic substituent is suggested to bind to. (Smits et al., 2008a).

As the “open” VUF 6884 derived compounds show analogy to the molecules described above, a short series of compounds was prepared in which a similar strategy was pursued in order to increase the affinity to the hH₄R (figure 3.8):

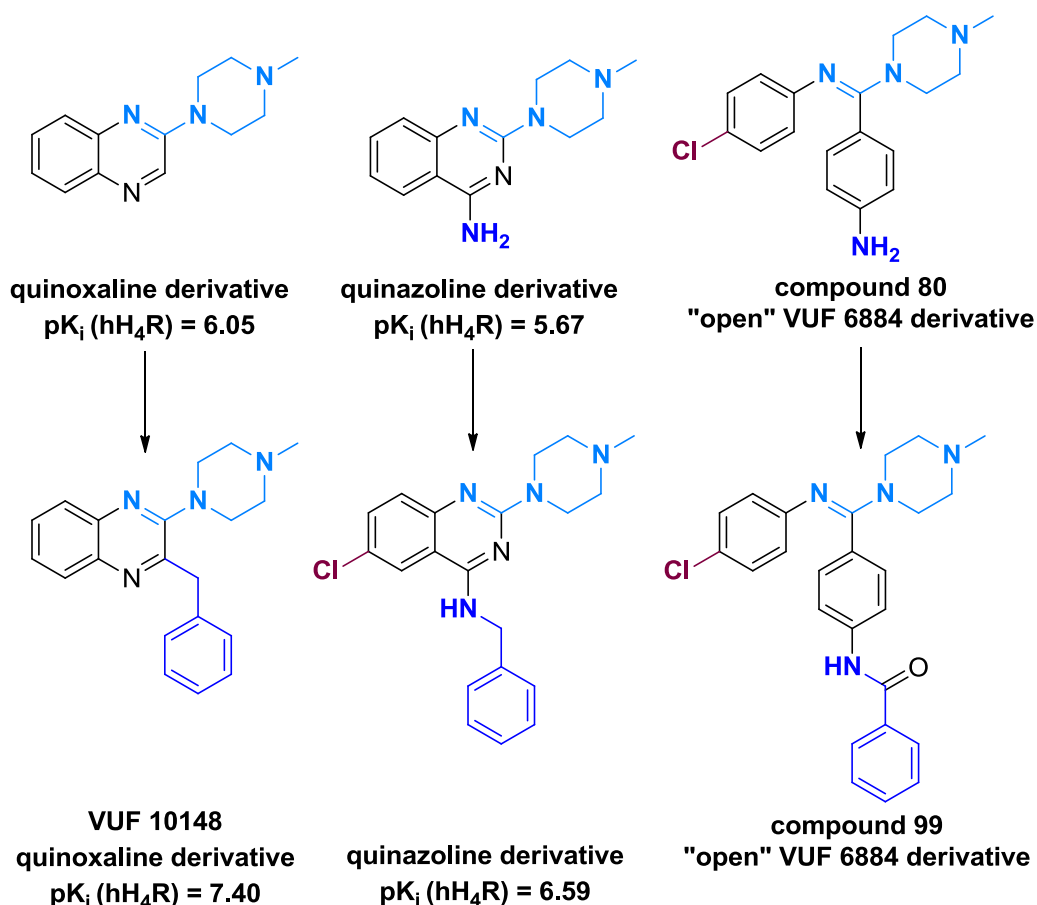
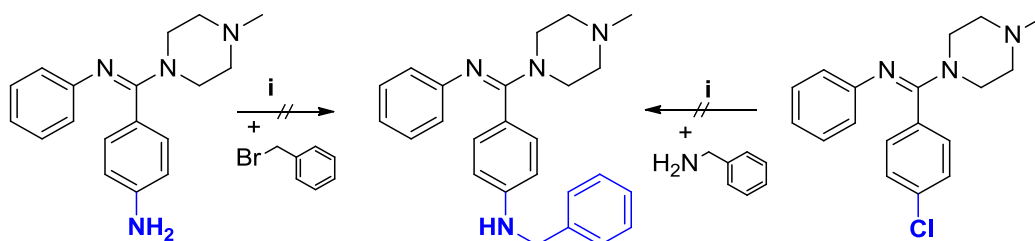


Figure 3.8. Structural similarities between quinoxaline / quinazoline derived hH_4R ligands and the acylated "open" VUF 6884 analogues. (Smits et al., 2008a, Smits et al., 2008b)

According to literature (Smits et al., 2008a), the above described quinazolines were linked to the aromatic substituent by nucleophilic displacement in a microwave reaction. However, due to the structural conditions prevalent in the "open" VUF 6884 analogues, neither NH_2 - nor Cl -substituted starting material led to the desired compounds (figure 3.9).

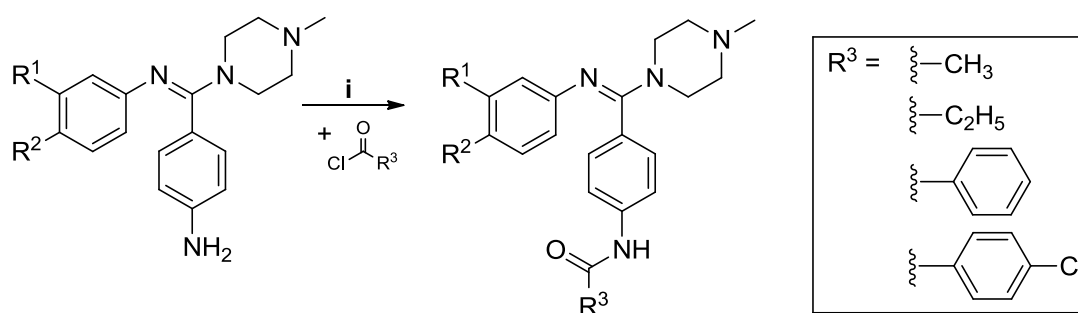


i: DIPEA, EtOAc; 120 °C, 25 min microwave reaction

Figure 3.9. Failed synthetic attempts to add a benzyl substituent to the "open" VUF 6884 analogues.

Therefore, in order to stick to a similar chain-length of the substituent, an amide coupling between NH₂-substituted “open” VUF 6884 derivatives and pertinent acid chlorides was performed (figure 3.10). The acylated compounds were easily accessible: in the presence of NEt₃, different acid chlorides were added to the respective compounds bearing an NH₂ substitution in *p*-position of the benzoic acid moiety (Sun et al., 2009) with intent to interact with the free amine of the NH₂ group by amide coupling.

Two different kinds of acid chlorides were therefore used: firstly, short linear carboxylic acid chlorides (**114**, **116**: acetylchloride, **115**: propionylchloride) and secondly, benzoic acid chlorides (**99**, **117**: benzoylchloride, **112**: 4-chlorobenzoylchloride) which were all commercially available. The reaction was performed under nitrogen atmosphere and the resulting compounds were purified by column chromatography over silica gel (EtOAc : MeOH 1:1).



i: NEt₃, N₂, DCM, 6 h RT, 12 h reflux

Figure 3.10. General procedure for the preparation of the acylated open VUF 6884 derivatives.

Acylated compounds with Cl-substitution in *p*- as well as in *m*- position of the aniline moiety were prepared and are summarized in table 3.4.

R¹	<i>p</i> -Cl	<i>p</i> -Cl	<i>p</i> -Cl	<i>p</i> -Cl	<i>m</i> -Cl	<i>m</i> -Cl
R²						
Cpd.	99	112	114	115	116	117

Table 3.4. Acylated “open” VUF 6884 analogues bearing Cl substituents in *p*- and *m*-position of the aniline moiety.

3.3. Synthesis of the closed VUF 6884 derivatives: return to a rigid aromatic ring system in the center of the molecule

In order to determine the role of the central heterocycle in the SARs, a series of compounds was synthesized that were directly derived from VUF 6884 and differ only with respect to their substitution pattern and piperazine moiety. Due to their closed and thus rigid central heterocyclic core these compounds will be referred to as the “ring-closed” compounds in the following. (Figure [3.11](#))

Again, Cl substitution was in the spotlight of interest and therefore intensively investigated in several positions of the molecule. Moreover, with regard to the dimerization project described in [3.4](#), compounds bearing an NH₂ substituent in position 3 were prepared to enable the connection with different kinds of spacers by amide coupling.

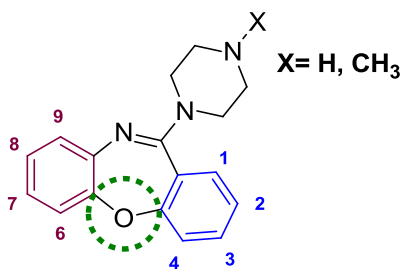


Figure 3.11. Molecule map of the “closed” VUF 6884 derivatives.

3.3.1. “Ring-closed” VUF 6884 derivatives with modified substitution pattern: determining the key role of the closed central heterocycle in synergy with the substitution pattern

All VUF 6884 derived “ring-closed” compounds were synthesized according to a slightly modified synthesis pathway described by Smits et al. (2006) (figure 3.12). The modifications refer to the reaction conditions during the last nucleophilic displacement step as well as to slight changes in the composition of the used solvents.

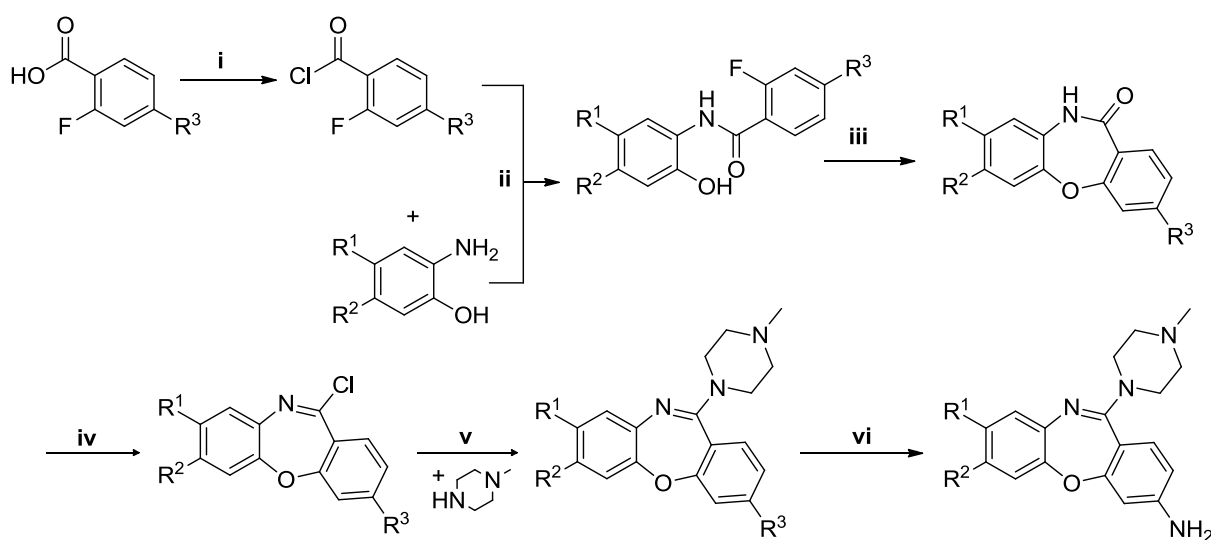
The first step of the reaction consisted of an amide coupling of a (substituted) commercially available 2-aminophenol with a (substituted) commercially available 2-fluorobenzoic acid chloride in the presence of NEt_3 in THF under nitrogen atmosphere. In some cases, the 2-fluorobenzoic acid chloride was not commercially available and had to be converted from the corresponding commercially available 2-fluorobenzoic acid by the use SOCl_2 in THF prior to the amide coupling. The resulting 2-fluorobenzoic acid chlorides were then used without further purification.

After the amide coupling was successfully carried out, water was added to stop the reaction. The pH-dependently precipitated amide could be separated by filtration and was used without further purification in the next reaction step. This consisted of a ring closure that was carried out by the addition of freshly pulverized NaOH and heating at reflux in DMF. To stop the reaction, the mixture was poured into water and the precipitated dibenzo[*b,f*][1,4]-oxazepin-11(10*H*)-one could be separated by filtration.

Copious amounts of water were bound to the precipitate that had to be completely removed before the in-situ conversion to the iminochloride, as the required POCl_3 and the desired product are known to be very sensitive to contact with water. It turned out to be very important that this reaction step is carried out for at least 12 - 15 hours, as

otherwise the nucleophilic displacement in the next step did not take place to a satisfying degree.

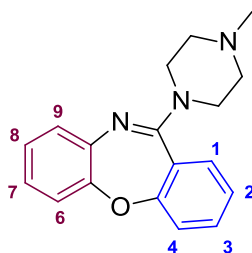
Finally, nucleophilic displacement of chloride with a 10-fold excess of *N*-methylpiperazine, that had to be carried out for at least 4 hours, resulted in the desired VUF 6884 derived compounds. If the last step was stopped earlier (e.g., after 2 hours as reported by Smits et al. (2006)), the yield was significantly decreased. After the completion of the reaction, the mixture was partitioned between EtOAc and a solution of Na₂CO₃ in water to separate excess *N*-methylpiperazine, and the organic layer was concentrated and purified by column chromatography over silica gel (EtOAc : MeOH 1:1). The resulting “ring-closed” VUF 6884 derivatives were obtained as colorless to light yellow solids (depending on the substitution pattern). (Table 3.5)



i: SOCl₂, THF, 2 h reflux; ii: NEt₃, THF, 12 h RT, iii: NaOH, DMF, 5 h reflux; iv: POCl₃, TOL / ACN, 12 h reflux; v: TOL / ACN, 4 h reflux; vi: SnCl₂ · 2H₂O, EtOH, 5 h reflux (for R³ = NO₂)

Figure 3.12. Synthesis pathway for the preparation of the “ring-closed” VUF 6884 derivatives bearing an *N*-methylpiperazine moiety.

Compounds bearing an NO₂ substituent were converted to the corresponding NH₂ substitution by reduction with SnCl₂ · 2 H₂O (Chao et al., 2009) as already described in [3.2.2.](#)



R	H	H	H	3-Cl	3-NO ₂	3-NO ₂	3-NO ₂	3-Cl	3-Cl
	H	8-Cl	7-Cl	H	H	7-Cl	8-Cl	8-Cl	8-Cl
Cpd.	141	88	92	149	135	127	126	158	159

Table 3.5. “Closed” VUF 6884 analogues bearing an *N*-methylpiperazine moiety.

As for all “ring-closed” compounds described above a pertinent “open” counterpart was synthesized and pharmacologically characterized, the SAR evoked by the ring-closure in the central core of the molecule could distinctly be investigated and will be reported in the pharmacological section (4.4).

R	Cpd.
H	136
7-Cl	128
8-Cl	129

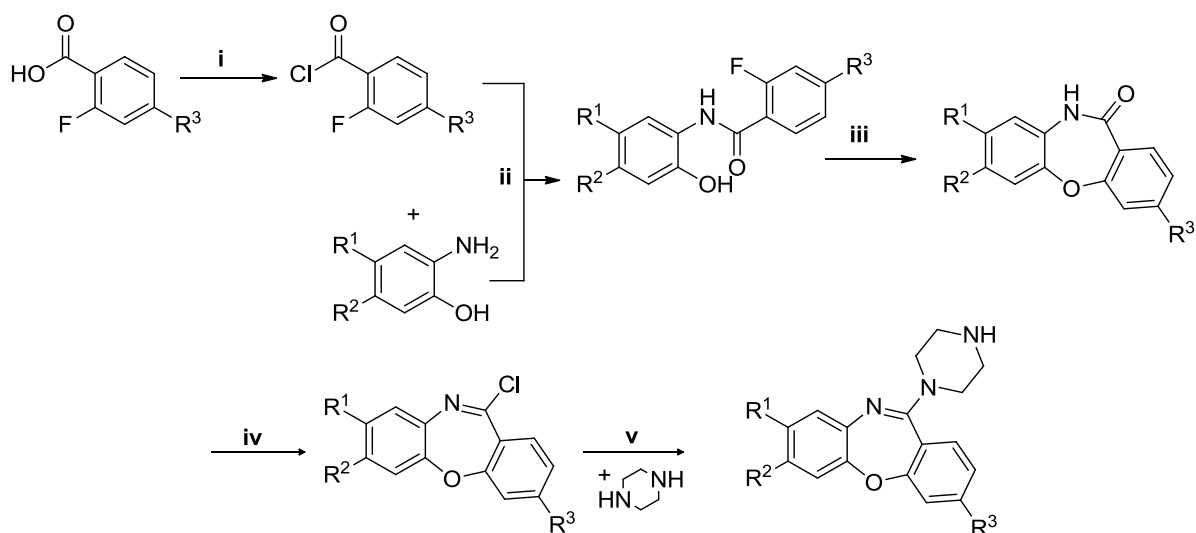
Table 3.6. “Closed” VUF 6884 analogues carrying NH₂ groups in 3-position.

Compounds with NH₂ substitution are summarized in table 3.6 and were *inter alia* used to prepare a series of dimeric molecules linked at this position with different spacers (see section 3.4).

3.3.2. “Closed” VUF 6884 derivatives with a modified piperazine moiety: exchanging *N*-methylpiperazine by piperazine

A short series of compounds was prepared in which the *N*-methypiperazine moiety was replaced by piperazine with intent to get a closer insight into the role of either a tertiary or a secondary amine in hH₁R and hH₄R binding, respectively. Moreover, these compounds were used to prepare a series of dimeric compounds that were linked at the piperazine moiety with either polar or nonpolar spacers of different types and lengths (3.4).

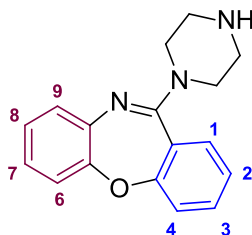
All piperazine-bearing “ring-closed” VUF 6884 derivatives were synthesized by analogy with the synthesis pathway described above for the *N*-methylpiperazine bearing compounds (figure 3.13). Instead of *N*-methylpiperazine, piperazine was added in the last nucleophilic displacement step, again in a 10-fold excess to improve the yield. The reaction conditions as well as the modifications regarding the reaction time described above remained equal. However, before the addition of piperazine, it had to be dissolved in MeOH *quantum satis* as it was not soluble in reasonable amounts of the reaction solvent mixture acetonitrile / toluene.



i: SOCl₂, THF, 2 h reflux; ii: NEt₃, THF, 12 h RT, iii: NaOH, DMF, 5 h reflux; iv: POCl₃, TOL / ACN, 12 h reflux; v: TOL / ACN, 4 h reflux

Figure 3.13. Synthesis pathway of the “ring closed” VUF 6884 derivatives bearing a piperazine moiety.

Except compounds with NH₂ group in position 3, for all *N*-methylpiperazine bearing compounds described in 3.3.1 a piperazine bearing counterpart was synthesized with intent to determine the effect of the rigid basic amine moiety in dependence of the substitution pattern. Furthermore, as the free amine of the piperazine moiety allowed dimerization by either nucleophilic displacement or amide coupling, a series of dimeric compounds was accessible from these molecules (see section 3.4). A summary of the piperazine bearing molecules with modified substitution pattern is provided in table 3.7.



R	H H	H 8-Cl	H 7-Cl	3-Cl H	3-Cl 7-Cl	3-Cl 8-Cl
Cpd.	233	234	235	232	193	196

Table 3.7. “Ring-closed” VUF 6884 analogues bearing a piperazine moiety.

3.4. Dimeric dibenzo[*b,f*][1,4]oxazepines: an approach to address homo- and hetero-oligomeric histamine H₁ and H₄ receptors

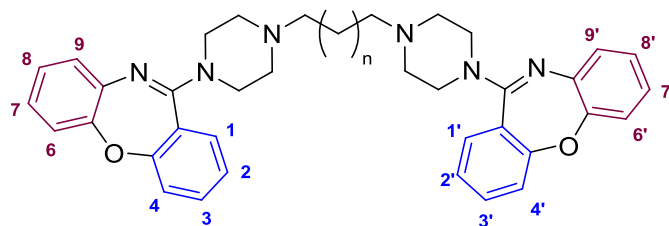
Both the hH₁R and the hH₄R are known to generate receptor homo-oligomers at physiological expression levels (Bakker et al., 2004, van Rijn et al., 2006). Furthermore, H₁R-H₄R hetero-oligomers were reported to be formed. Although the detection of H₁R-H₄R hetero-oligomers was achieved only at higher H₁R expression levels and as a consequence they are most likely not physiologically relevant (van Rijn et al., 2006), these results provide an important account to pharmacological research.

Due to their molecule size, all previously described compounds are supposed to address only monomeric histamine H₁ and H₄ receptors by binding to specific binding pockets. With intent to bind to the binding pockets of the receptors belonging to the above described receptor homo- or hetero-oligomers or to bind to the binding pocket as well as to the extracellular surface of the respective histamine receptors, a series of

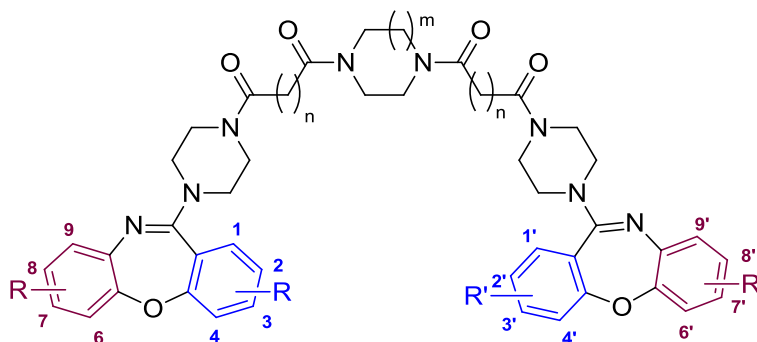
“ring-closed” VUF 6884 derived compounds was prepared that were linked with spacers of different type and length.

The spacers, consisting of either nonpolar alkyl chains or polar piperazine / homopiperazine bearing di-carboxylic acids, were inserted in different positions of the molecule (i.e., at the piperazine moiety or the NH₂ group in position 3, yielding new differently substituted dimeric molecules with high molecular weight (M_r 806.65 – 988.76). The molecule size and the resulting difficulties in solubility may not lead to physiologically and therapeutically relevant new compounds, however, in principle, they can be used as pharmacological tools to investigate the receptor homo- and hetero-dimerization of a broad variety of GPCRs.

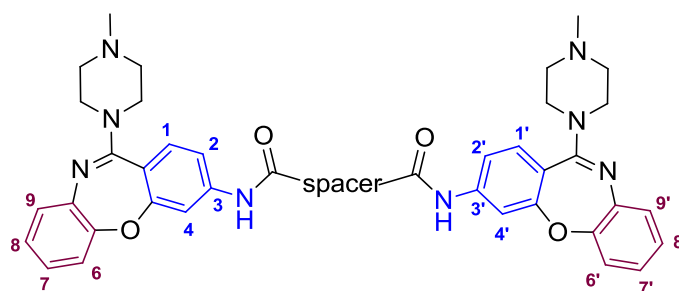
A map of the resulting different dimeric compounds is provided in figure 3.14.



Dibenzo[*b,f*][1,4]-oxazepines linked with nonpolar spacers at the piperazine moiety



Dibenzo[*b,f*][1,4]-oxazepines linked with polar spacers at the piperazine moiety



Dibenzo[*b,f*][1,4]-oxazepines linked with polar spacers at the NH₂ group in position 3 / 3'

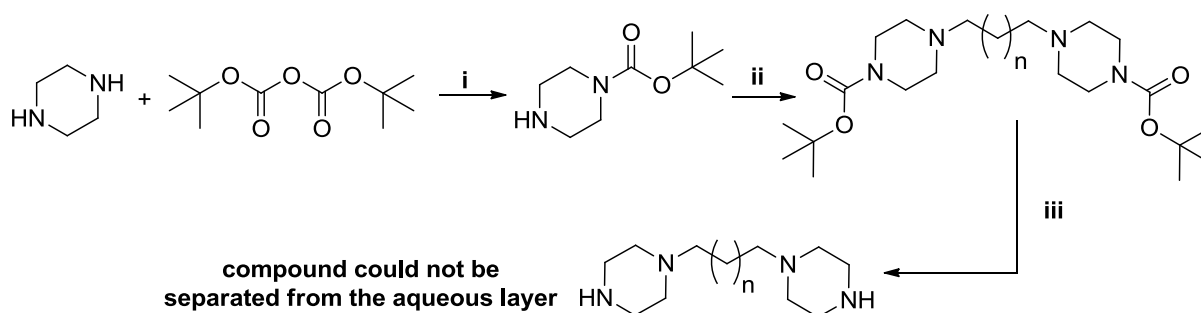
Figure 3.14. Map of the dimeric dibenzo[*b,f*][1,4]oxazepines linked in different positions of the molecule.

3.4.1. Dibenzo[*b,f*][1,4]oxazepines linked by nonpolar alkyl spacers at the piperazine moiety

The pharmacologically most promising “ring-closed” VUF 6884 derivatives bearing a di-Cl substitution in either position 3 and 7 (**159**) or 3 and 8 (**158**) were developed further by transferring them into dimeric molecules. Therefore, two different strategies were pursued to link the molecules at the piperazine moiety: the spacer was linked to the piperazine moiety before (figure 3.15) and after it was added to the tricyclic core (figure 3.16).

The first strategy, however, at least did not successfully lead to the desired compounds. Piperazine was protected by a BOC-group giving tert-butyl-piperazine-1-carboxylate (Sengmany et al., 2007) that was sufficiently pure to be used in the next step without further purification and was linked by a di-halide substituted alkyl spacer (Zhang et al., 2011) to give dimeric molecules. Di-chloro-substituted reagents did not lead to the desired compounds in a satisfying amount and were thus replaced by di-bromo or di-iodo derivatives.

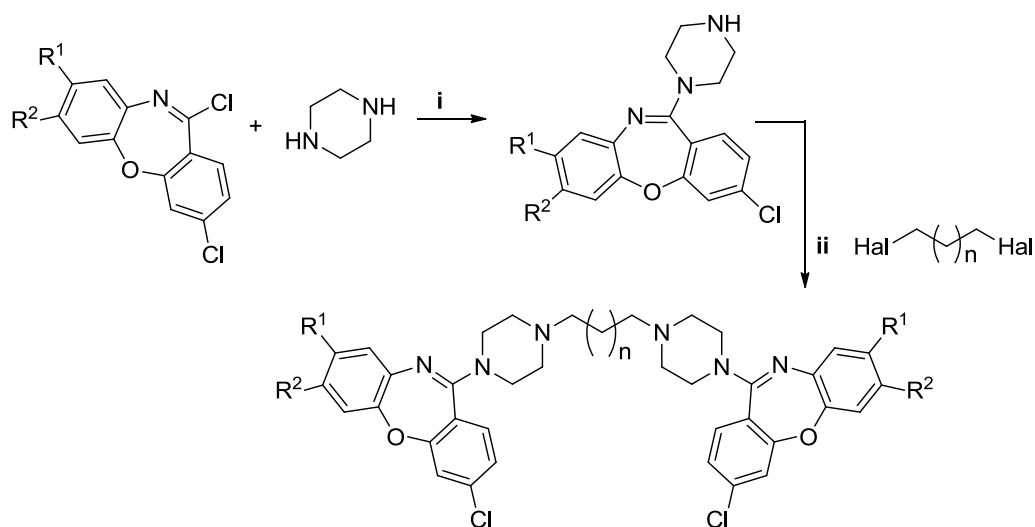
De-protection of the BOC-protected dimeric piperazine derivatives was carried out as usual adding TFA and DCM while being stirred for 2 hours at room temperature (Wang et al., 2007). However, after partitioning the reaction mixture between a solution of Na₂CO₃ in water and EtOAc, the dimeric de-protected piperazine molecules were not able to be removed from the aqueous layer and could thus not be linked to the tricyclic core (figure 3.15).



i: DCM, 0°C, 1.5 h; ii: di-halide substituted alkyl spacer, K₂CO₃, EtOH, reflux 12 h; iii: TFA, DCM, 2 h RT

Figure 3.15. Failed synthetic attempt on the way to dimeric VUF 6884 derivatives.

In the second and more successful strategy, the piperazine bearing counterparts of **158** and **159** (i.e. **196** and **193**) were linked by nucleophilic displacement with alkyl halides of different length ($n = 6 - 8, 10$) (figure [3.16](#)) (Tanaka et al., 2011).

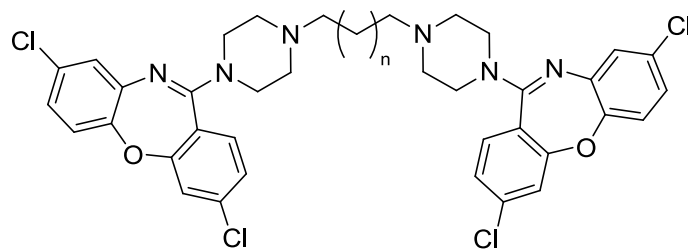


i: TOL / ACN, 4 h reflux; ii: K₂CO₃, MeCN, 12 h reflux

Figure 3.16. Synthesis of the dimeric “ring-closed” VUF 6884 derivatives linked by nonpolar alkyl spacers.

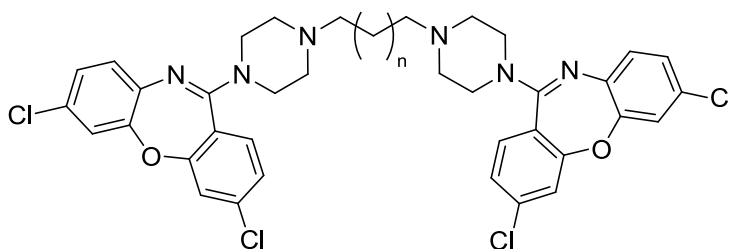
For the nucleophilic displacement reaction at the free secondary amine of the piperazine moiety, different alkyl halides were used: for $n = 6$ or 8 , di-iodo- and for $n = 7$ or 10 , di-bromo-substituted derivatives were applied.

All synthesized dimeric compounds linked by nonpolar alkyl spacers were purified by column chromatography over silica gel (EtOAc / HX (3 : 2); EtOAc; EtOAc / NH₃ (7 N in MeOH) (9 : 1)) and were obtained as colorless to light brown solids. Classified in relation to the substitution pattern, they are summarized in tables [3.8](#) and [3.9](#).



n	6	7	8	10
Cpd.	212	205	208	207

Table 3.8. Dimeric dibenzo[*b,f*][1,4]oxazepines derived from **158** linked by nonpolar alkyl spacers at the piperazine moiety.



n	6	7	8	10
Cpd.	213	206	210	209

Table 3.9. Dimeric dibenzo[*b,f*][1,4]oxazepines derived from **159** linked by nonpolar alkyl spacers at the piperazine moiety.

3.4.2. Dibenzo[*b,f*][1,4]oxazepines linked by polar spacers at the piperazine moiety

A further series of dimeric compounds was prepared based on all the above mentioned piperazine bearing “ring-closed” VUF 6884 derivatives **193**, **196**, **232 – 235** that were linked at the piperazine moiety by polar di-carboxylic acid spacers. The spacers were prepared from either succinic or glutaric anhydride and piperazine or homopiperazine

according to the synthesis pathway described in figure 3.17 (Liu et al., 2002, McRobb et al., 2012). After re-crystallization from EtOH they were obtained as colorless solids and used in the next reaction steps without further purification.

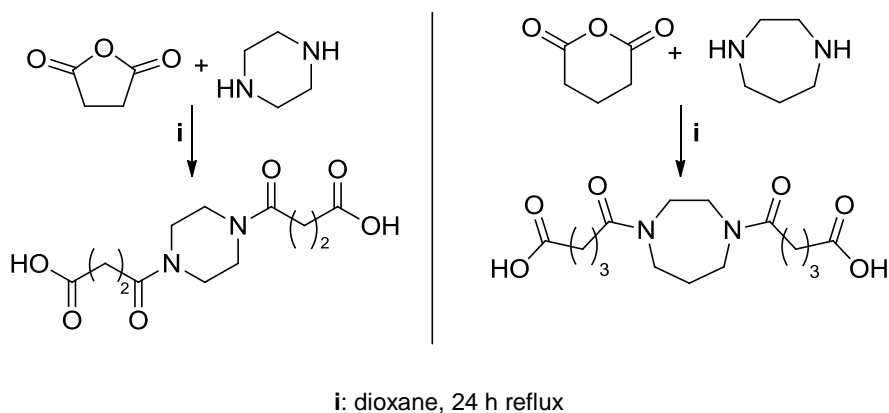


Figure 3.17. Synthesis pathway of the polar spacers containing either piperazine or homopiperazine.

Before use, the spacers were converted into the corresponding reactive di-acid chlorides by treatment with oxalyl chloride in DCM (figure 3.18)

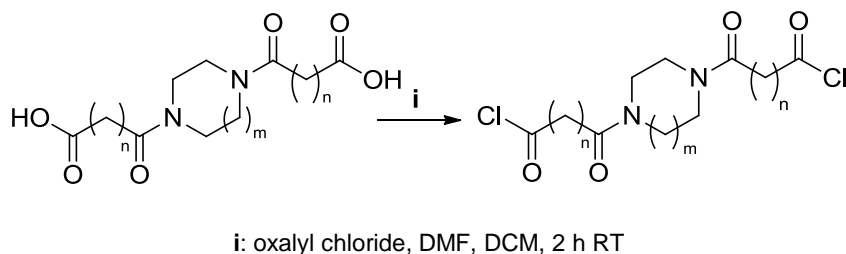
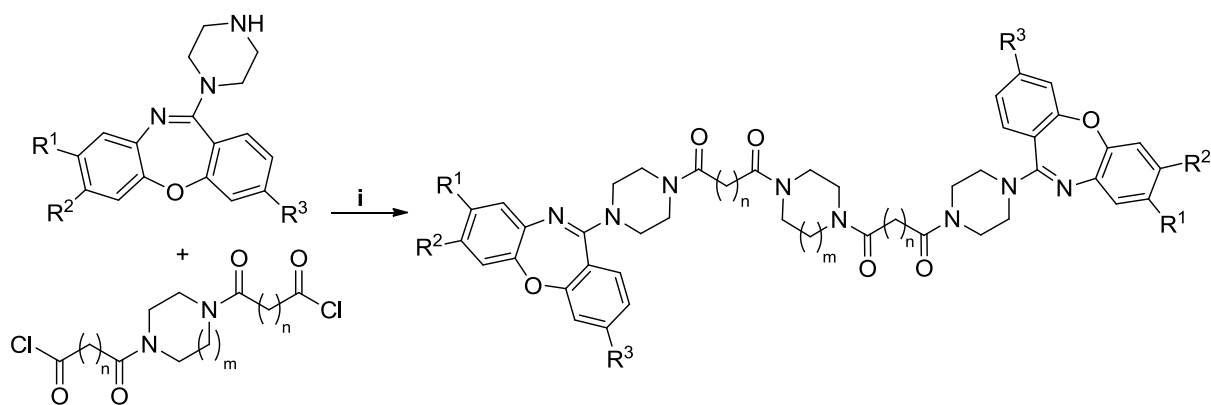


Figure 3.18. Conversion of the polar spacers into the reactive acid chlorides.

The reactive di-acid chloride spacers were then added dropwisely to the piperazine bearing “ring-closed” VUF 6884 derivatives with intent to interact with the free secondary amine of the piperazine moiety by amide coupling (figure 3.19). All reactions were carried out in the presence of 0.2 equivalents of pyridine.

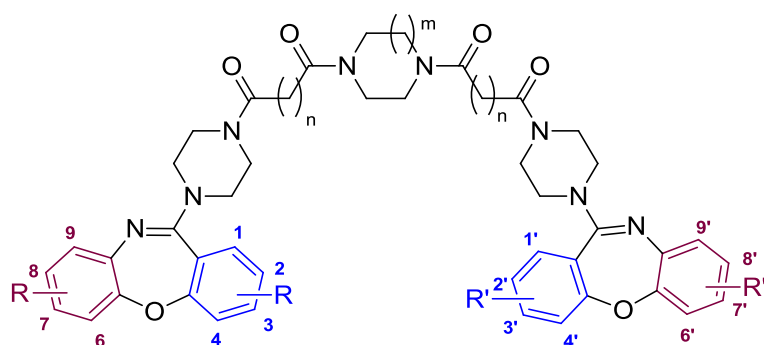
The resulting compounds were purified by column chromatography over silica gel (EtOAc / HX (3 : 2); EtOAc; MeOH) and obtained as colorless solids.



i: DIPEA, pyridine, DCM, 6 h RT

Figure 3.19. Synthesis pathway of the amide coupling between the reactive di-acid chloride spacers and the piperazine bearing “ring closed” VUF 6884 derivatives.

An overview of the dimeric compounds linked by polar spacers at the piperazine moiety is provided in table [3.10](#).

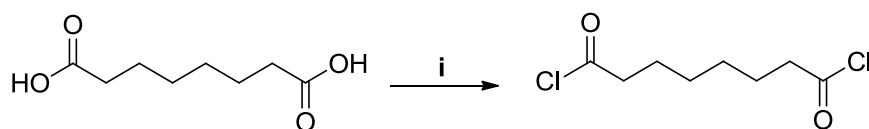


R / R'	H / H	8 / 8'-Cl	7 / 7'-Cl	H / H	8 / 8'-Cl	7 / 7'-Cl	7 / 7'-Cl
	H / H	H / H	H / H	3 / 3'-Cl	3 / 3'-Cl	3 / 3'-Cl	3 / 3'-Cl
m	1	1	1	1	1	1	2
n	2	2	2	2	2	2	3
Cpd.	240	241	242	238	225	239	244

Table 3.10. Dimeric dibenzo[*b,f*][1,4]oxazepines linked by polar spacers at the piperazine moiety.

3.4.3. Dibenzo[*b,f*][1,4]oxazepines linked by at the NH₂ group in position 3 / 3'

Derived from the “ring-closed” VUF 6884 derivatives bearing an NH₂-group in position 3 (**128**, **129**, **136**), a series of dimeric compounds was prepared that were linked by differently constituted spacers. Spacers containing piperazine or homopiperazine were prepared according to the procedure described above (figures [3.17](#), [3.18](#)) (Liu et al., 2002, McRobb et al., 2012). The spacer in compound **215** was easily accessible by converting the commercially available 1,8-octanedioic acid to the corresponding di-acid chloride using oxalyl chloride (figure [3.20](#)).

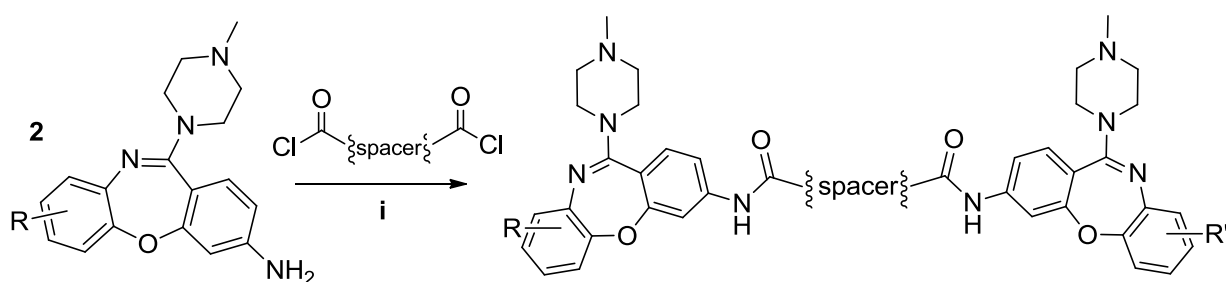


i: oxalyl chloride, DMF, DCM, 2 h RT

Figure 3.20. Conversion of the 1,8-octanedioic acid spacer into the reactive acid chloride.

The addition of the reactive acid chloride spacers to the free amine in position 3 was carried out by amide coupling (figure [3.21](#)). All reactions were performed in the presence of 0.2 equivalents of pyridine.

With regard to the reaction time, a dependence on the spacer type could be observed: whereas spacers consisting of either a linear or a piperazine bearing dicarboxylic acid were less reactive (reaction time 3 – 6 hours), spacers bearing a homopiperazine component revealed a higher reactivity and thus a shorter reaction time (1 – 1.5 hours).

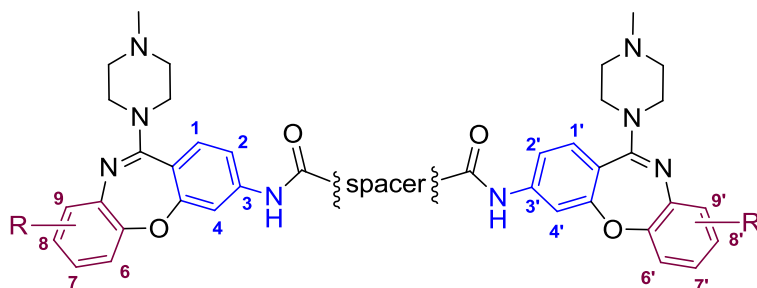


i: DIPEA, pyridine, DCM, 1 – 6 h RT

Figure 3.21. Synthesis pathway of the amide coupling between the reactive di-acid chloride spacers and the NH₂ group in position 3 of the “ring-closed” VUF 6884 derivatives.

The compounds were purified by column chromatography over silica gel (MeOH; NH₃ (7 N in MeOH)) and obtained as colorless solids.

A summary of the resulting compounds linked at the NH₂ group in position 3 / 3' is provided in table 3.11.



R / R'	spacer	Cpd.
7 / 7'-Cl		215
7 / 7'-Cl		227
7 / 7'-Cl		231
8 / 8'-Cl		229
8 / 8'-Cl		230
H / H		221
H / H		243

Table 3.11. Dimeric dibenzo[*b,f*][1,4]oxazepines linked at the free NH₂ group in position 3 / 3'.

3.5. References

- BAKKER, R. A., DEES, G., CARRILLO, J. J., BOOTH, R. G., LOPEZ-GIMENEZ, J. F., MILLIGAN, G., STRANGE, P. G. & LEURS, R. **2004**. Domain swapping in the human histamine H₁ receptor. *J Pharmacol Exp Ther*, **311**, 131-138.
- CHAO, Q., SPRANKLE, K. G., GROTZFELD, R. M., LAI, A. G., CARTER, T. A., VELASCO, A. M., GUNAWARDANE, R. N., CRAMER, M. D., GARDNER, M. F., JAMES, J., ZARRINKAR, P. P., PATEL, H. K. & BHAGWAT, S. S. **2009**. Identification of N-(5-tert-butyl-isoxazol-3-yl)-N'-(4-[7-(2-morpholin-4-yl-ethoxy)imidazo[2,1-b][1,3]benzothiazol-2-yl]phenyl)urea dihydrochloride (AC220), a uniquely potent, selective, and efficacious FMS-like tyrosine kinase-3 (FLT3) inhibitor. *J Med Chem*, **52**, 7808-7816.
- JENSEN, K. G. & PEDERSEN, E. B. **1979**. Phosphoramides .11. Phosphoramides as Reagents in the Synthesis of Benzamidines from Benzophenone Oxime. *Acta Chemica Scandinavica Series B-Organic Chemistry and Biochemistry*, **33**, 319-321.
- LIU, C. H., HUDSON, R. H. E. & PETERSEN, N. O. **2002**. Convergent and sequential synthesis of dendritic, multivalent complexing agents. *Synthesis*, 1398-1406.
- MCROBB, F. M., CROSBY, I. T., YURIEV, E., LANE, J. R. & CAPUANO, B. **2012**. Homobivalent ligands of the atypical antipsychotic clozapine: design, synthesis, and pharmacological evaluation. *J Med Chem*, **55**, 1622-1234.
- SENGMANY, S., LE GALL, E., LE JEAN, C., TROUPEL, M. & NEDELEC, J. Y. **2007**. Straightforward three-component synthesis of diarylmethylpiperazines and 1,2-diarylethylpiperazines. *Tetrahedron*, **63**, 3672-3681.
- SMITS, R. A., DE ESCH, I. J., ZUIDERVELD, O. P., BROEKER, J., SANSUK, K., GUAITA, E., CORUZZI, G., ADAMI, M., HAAKSMA, E. & LEURS, R. **2008a**. Discovery of quinazolines as histamine H₄ receptor inverse agonists using a scaffold hopping approach. *J Med Chem*, **51**, 7855-7865.
- SMITS, R. A., LIM, H. D., HANZER, A., ZUIDERVELD, O. P., GUAITA, E., ADAMI, M., CORUZZI, G., LEURS, R. & DE ESCH, I. J. **2008b**. Fragment based design of new H₄ receptor-ligands with anti-inflammatory properties in vivo. *J Med Chem*, **51**, 2457-2467.
- SMITS, R. A., LIM, H. D., STEGINK, B., BAKKER, R. A., DE ESCH, I. J. & LEURS, R. **2006**. Characterization of the histamine H₄ receptor binding site. Part 1. Synthesis and pharmacological evaluation of dibenzodiazepine derivatives. *J Med Chem*, **49**, 4512-4516.
- SUN, Y., GUOFENG, W. & WEI, G. **2009**. Colorimetric detection of cyanide with N-nitrophenyl benzamide derivatives. *Tetrahedron*, **65**, 3480-3485.
- TANAKA, M., SAWAGUCHI, T., SATO, Y., YOSHIOKA, K. & NIWA, O. **2011**. Surface modification of GC and HOPG with diazonium, amine, azide, and olefin derivatives. *Langmuir*, **27**, 170-178.
- VAN RIJN, R. M., CHAZOT, P. L., SHENTON, F. C., SANSUK, K., BAKKER, R. A. & LEURS, R. **2006**. Oligomerization of recombinant and endogenously expressed human histamine H₄ receptors. *Mol Pharmacol*, **70**, 604-615.

- WANG, H. L., KATON, J., BALAN, C., BANNON, A. W., BERNARD, C., DOHERTY, E. M., DOMINGUEZ, C., GAVVA, N. R., GORE, V., MA, V., NISHIMURA, N., SURAPANENI, S., TANG, P., TAMIR, R., THIEL, O., TREANOR, J. J. & NORMAN, M. H. **2007**. Novel vanilloid receptor-1 antagonists: 3. The identification of a second-generation clinical candidate with improved physicochemical and pharmacokinetic properties. *J Med Chem*, **50**, 3528-3539.
- WU, K. M., HUANG, C. A., PENG, K. F. & CHEN, C. T. **2005**. Palladacycles bearing pendant benzamidinate ligands as catalysts for the Suzuki and Heck coupling reactions. *Tetrahedron*, **61**, 9679-9687.
- ZHANG, R., WU, X., YALOWICH, J. C. & HASINOFF, B. B. **2011**. Design, synthesis, and biological evaluation of a novel series of bisintercalating DNA-binding piperazine-linked bisanthrapyrazole compounds as anticancer agents. *Bioorg Med Chem*, **19**, 7023-7032.

Chapter 4

Pharmacological section

4. Pharmacological section

4.1. Pharmacological parameters

All previously described compounds were characterized in several different pharmacological testing systems at hH_1 , hH_4 , gpH_1 , pD_1 / hD_1 , hD_{2short} , hD_{2long} , hD_3 , $hD_{4.4}$, $p5-HT_{1A}$, $p5-HT_2$, hM_1 , hM_2 and hM_3 receptors. Both competition binding and functional assays were performed at in-vitro testing systems (organ bath experiments as well as receptor binding studies based on Sf9 / CHO / HEK293 membranes). The respective equations that were used to determine the reported pharmacological parameters of the compounds are explained in the following.

4.1.1. Schild equation

The Schild equation provides an established method to characterize antagonists in functional assays as, e.g., the organ bath experiments at the isolated guinea pig ileum (Arunlakshana and Schild, 1959, Jenkinson et al., 1995):

$$\log K_B = \log c(B) - \log (r-1)$$

or:

$$pA_2 = -\log c(B) + \log (r-1)$$

K_B	dissociation constant (of antagonist to receptor)
$c(B)$	concentration of the antagonist*
r	$10^{\Delta pEC_{50}}$
ΔpEC_{50}	$pEC_{50} (His) - pEC_{50} (His/B)$
EC_{50}	concentration of agonist producing 50 % of the maximal effect
pA_2	-log of the dissociation constant (antagonist to receptor) at a concentration evoking a rightward shift of the concentration effect curve of the agonist

(* = with $pEC_{50}(His)$ measured in the absence and $pEC_{50}(His/B)$ in the presence of a defined concentration c of antagonist B)

The Schild equation holds true in case of a strictly competitive and reversible antagonism that can be determined by conducting the experiments in a wide concentration range. As long as the slope in the Schild plot is close to unity (slope = 1) and the maximal effect of the dose response curve is not significantly depressed, a competitive and reversible antagonism can be assumed.

Nevertheless, in some cases the slope in the Schild plot is significantly different from 1 or – prevalent in a huge number of experiments – the dose response curve shows depression at higher antagonist concentrations. In these cases, no distinct conclusion regarding the antagonism mode can be drawn and as a consequence, the Schild equation is not suitable to calculate the pA₂ values. If so, pA₂ values have to be estimated for every concentration range (described in section [4.4.2.4](#) and [4.4.2.5](#)).

4.1.2. Cheng-Prusoff equation

The radioligand competition binding assays were analyzed based on the Cheng-Prusoff equation derived from the law of mass action. (Cheng and Prusoff (1973))

$$K_i = \frac{IC_{50}}{1 + \frac{[A]}{K_D}}$$

K _i	dissociation constant of a competitive inhibitor and a receptor, expressed in Sf9 membrane fragments in competition to a radioligand
K _D	dissociation constant of a radioligand
IC ₅₀	concentration of inhibitor producing 50 % of inhibition
[A]	concentration of the applied radioligand

This equation is valid for the following assumptions: firstly, both the ligand and the radioligand bind to the same binding site in a reversible competitive mode. Secondly, an equilibrium reaction is postulated and the concentration of free ligand and free radioligand is known and remains on a constant level during the experiment.

The K_D values of the pertinent radioligands were determined in saturation binding experiments and were reported recently ($K_D = 4.49 \pm 0.35$ nM for [3 H]Mepyramine at hH₁R (Seifert et al. 2003); $K_D = 9.7 \pm 1.7$ nM for [3 H]Histamine at hH₄R (Schneider et al. 2009)).

4.1.3. GTPase activity

For selected compounds, steady state GTPase assays for the hH₁R were performed as described in [4.3.5](#). GTPase activities (as pmol P_i released per mg of protein per minute) of membranes were calculated according to the following equation:

$$GTPase\ activity = \frac{(cpm\ reaction - cpm\ blank) \cdot pmol\ unlabeled\ GTP \cdot 1.67}{cpm\ total \cdot mg\ protein \cdot min\ incubation} \left[\frac{pmol}{mg \cdot min} \right]$$

cpm reaction	radioactivity counted in 600 µl of samples except those with 1 mM unlabeled GTP
cpm blank	radioactivity counted in 600 µl of samples containing 1 mM unlabeled GTP; spontaneous hydrolysis of [γ - 33 P]-GTP
pmol unlabeled GTP	absolute amount of GTP present in the assay tubes (10 pmol)
1.67	factor accounting for the fact that only 600 µl of the 1000 µl samples were counted
cpm total	counts resulting from total added to each tube (no charcoal addition)
mg protein	amount of membrane protein present in each tube (10 µg)
min incubation	incubation period (20 min)

4.2. Antagonist binding on a molecular level

The aim of this work was to develop new compounds that evoke an antagonistic effect at both the histamine hH_1R and hH_4R . To characterize the range of evoked pharmacological effects, several pharmacological testing systems were performed that will be described closely in section [4.3](#). However, before discussing the detected pharmacological effects, it is necessary to define the term “antagonistic effect” on a molecular level.

More than half a century ago, a first differentiation between *competitive* and *non-competitive antagonism* was made (Gaddum et al., 1955). However, these terms can only be used in case of co-incubation of antagonist and agonist. As soon as the antagonist is pre-incubated before the agonist comes to operation (e.g. in organ bath experiments at the isolated guinea pig ileum), further definitions have to be taken into consideration: *surmountable antagonism* occurs, if the alteration of the maximal agonist dose-response curve is not affected, by contrast, *insurmountable antagonism* occurs, if the maximal effect of the dose-response curve is depressed. (Vauquelin et al., 2002)

The Schild-equation mentioned in [4.1.1](#) provides an established method to determine the pharmacological potency of strictly competitive, surmountable and reversibly bound antagonists. For insurmountable antagonists, further pharmacological effects have to be considered, as, e.g., the longevity of the antagonist-receptor complex, allosteric binding sites or receptor internalization. (Vauquelin et al., 2002) Above all the allosteric binding represents an intriguing expression of insurmountable antagonism, as the antagonist interacts with a site of the receptor that is distinct from the agonist binding site. Explained on a molecular level, the antagonist binding, be it reversible or irreversible, evokes a change in the receptor conformation, to which the agonist is no more capable to bind to.

In pre-incubating organ bath experiments, the longevity of the antagonist-receptor complex poses a challenge for the determination of surmountable or insurmountable antagonism. In some cases the dissociation of the antagonist-receptor complex may take place so slowly, that the dose-response curve of the agonist is depressed. As a consequence, surmountable antagonists can misleadingly be identified as insurmountable antagonists, because no proper equilibrium between antagonist, agonist and receptor could be established during the time of the experiment (hemi-

equilibrium conditions). (Kenakin et al., 2006) The extent of the depression is dependent on the “receptor reserve” that is directly linked to the receptor density of the tissue, the intrinsic activity of the agonist and the coupling of the receptor to the respective effector proteins. Thus, in tissues with a high receptor reserve, the alteration of the agonist dose-response curve will only be affected in case of higher antagonist concentrations. (Kenakin et al., 2006)

4.3. Pharmacological materials and methods

4.3.1. The Sf9 / Baculovirus expression system (Schneider and Seifert, 2010)

The Sf9 cell/baculovirus expression system is prevalently used for high-level protein expression and provides several advantages compared to mammalian cells. (Schneider and Seifert, 2010) The viruses used in the baculovirus expression system (*Autographa californica*) are not infectious to vertebrates and their promoters are inactive in mammalian cells (Carbonell et al., 1985, Carbonell and Miller, 1987).

Insect cells derived from *Spodoptera frugiperda* (American fall army worm) pupal ovarian tissue grown in suspension culture are infected with genetically modified baculoviruses carrying the genes of interest. GPCRs herein can freely be combined with different G-proteins: for example, co-infections with up to four different types of baculoviruses have been reported for the histamine H₄R (Schneider and Seifert, 2009). As a consequence, in the Sf9 cell environment interactions between the respective GPCRs and G-proteins can be investigated without the influence of other interfering GPCRs and G-proteins like in mammalian cells (e.g., receptor cross talk, receptor-hetero-dimerization).

Additionally, the Sf9 cell environment provides the possibility to investigate G-protein selectivity: only very few endogenous G-proteins are expressed in Sf9 cells. G-protein-like forms of G α_q and G α_s were reported to appear in Sf9 cells as well as one isoform of G α_i , however, coupling to mammalian GPCRs could be observed only meagrely. (Kühn et al., 1996, Houston et al., 2002, Knight and Grigliatti, 2004, Dolby et al., 2004) Fusion proteins, added to the Sf9 cells at infection, can amplify the coupling between a GPCR and the respective G-protein. For example, to obtain Sf9 cell membranes for use in a steady state [³³P]GTPase assay at hH₁R, the RGS4-protein (regulator of G-protein signaling) has to be coexpressed to ensure the coupling of the endogenous

G α_i -like protein to the GPCR. By contrast, for the preparation of membranes expressing the hH₄R, it is necessary to coexpress G α_{i2} as well as G $\beta_{1\gamma 2}$, as the endogenous G α_i -like protein does not couple to the mammalian GPCRs. (Schneider et al., 2009)

Further advantages of the Sf9 / baculovirus expression system are the expression of a much higher level of both recombinant GPCRs and G-proteins in Sf9 cells than in mammalian cells as well as the absence of constitutively active receptors, leading to an excellent signal-to-noise ratio in functional assays (as, e.g., steady state [³³P]GTPase- or [³⁵S]GTP γ S-binding assays). As Sf9 cells provide a variety of endogenous signal transduction components that are similar to pathways in mammalian cells, the gain of comparable results can be performed more easily. (Schneider and Seifert, 2010)

4.3.2. Generation of recombinant baculoviruses (Seifert et al., 2003, Seifert and Wieland, 2005, Schneider et al., 2009, Schnell et al., 2011)

Sf9 cells were cultured in 250 or 500 ml disposable Erlenmeyer flasks at 28 °C under rotation at 150 rpm in Insect Xpress medium supplemented with 5% (v/v) fetal calf serum and 0.1 mg/ml gentamicin without CO₂ supplementation. Cells were maintained at a density of 0.5-6.0 × 10⁶ cells/ml.

Recombinant baculoviruses encoding the hH₁R+RGS4, hH₂R-G α_{sA} S, hH₃R+G α_{i2} +G $\beta_{1\gamma 2}$ or hH₄R+G α_{i2} +G $\beta_{1\gamma 2}$ were generated in Sf9 cells using the BaculoGOLD transfection kit (BDPharmingen, San Diego, CA) according to the manufacturer's instructions. (Seifert and Wieland, 2005) After initial transfection, high-titer virus stocks were generated by two sequential virus amplifications. In the first amplification, cells were seeded at 2.0 × 10⁶ cells/ml and infected with a 1:100 dilution of the supernatant fluid from the initial transfection. Cells were cultured for 7 days, resulting in death of virtually the entire cell population. The supernatant of this infection was harvested and stored under light protection at 4 °C. In a second amplification, cells were seeded at 3.0 × 10⁶ cells/ml and infected with a 1:20 dilution of the supernatant fluid from the first amplification. Cells were cultured for 48 hours and afterwards, the supernatant fluid was harvested. After the 48 hours culture period, the most of cells showed signs of infection (e.g., altered morphology, viral inclusion bodies), but the majority of cells was still intact. The

supernatant fluid from the second amplification was stored under light protection at 4 °C and used as routine virus stock for membrane preparations.

Before infection, Sf9 cells were sedimented by centrifugation and suspended in fresh medium. Cells were seeded at 3.0×10^6 cells/ml and infected with a 1:100 dilution of the respective high-titer baculovirus stocks encoding hH₁R and RGS4 (hH₁R+RGS4 membranes), hH₂R-GsαS (hH₂R-GsαS membranes), hH₃R, G_{αi2} and G_{β1γ2} (hH₃R+G_{αi2}+G_{β1γ2} membranes), or hH₄R, G_{αi2} and G_{β1γ2} (hH₄R+G_{αi2}+G_{β1γ2} membranes) (1 mL of baculovirus stock to 100 mL of cell suspension). Cells were cultured for 48h at 28 °C under constant rotation (150 rpm) before membrane preparation. Sf9 membranes were prepared as described in the following.

4.3.3. Membrane preparation out of Sf9 cells (Seifert et al., 1998)

In a 250 ml flask, cells were seeded at a density of 3.0×10^6 cells / ml in 200 ml fresh medium and infected with high titer baculovirus stock carrying the genes encoding the desired GPCRs and G-proteins described above. After the infection, the cells were incubated for 48 h at 28 °C under constant rotation (150 rpm) without CO₂ supplementation (Schnell et al., 2011).

After 48 h, the membrane preparation was performed as described at 4 °C (Seifert et al., 1998). Therefore, the infected Sf9-cells were partitioned in Falcon tubes of 100 ml and sedimented by centrifugation (1000 rpm, 10 min) after which the supernatant was discarded. The remaining pellet was re-suspended in 50 ml of PBS-Buffer (100 mM NaCl, 80 mM Na₂HPO₄, 20 mM NaH₂PO₄; pH = 7.4) and again sedimented by centrifugation (1000 rpm, 10 min). The supernatant was discarded as previously described and to the remaining pellet of infected Sf9 cells 30 ml of Lysis-Buffer (10 mM Tris/HCl, 1 mM EDTA, containing 0.2 mM phenylmethylsulfonyl fluoride, 10 µg/mL benzamidine and 10 µg/ml leupeptine as protease inhibitors; pH = 7.4) were added. The solution was homogenized in a Dounce homogenizer with 25 strokes on ice and afterwards again sedimented by centrifugation (500 rpm, 5 min). The supernatant (containing the desired membrane fragments) was carefully separated from the pellet (containing nuclei and non-broken cells), added to a plastic tube and sedimented by centrifugation using a Sorvall centrifuge (18000 rpm, 20 min). As high G was applied, the tubes had to be carefully tared before use. The supernatant was discarded and the

pellet was re-suspended in 20 ml of Lysis-Buffer and one last time sedimented by centrifugation in the Sorvall centrifuge (18000 rpm, 20 min). To the remaining pellet 25 ml of Binding-Buffer (12.5 mM MgCl₂, 1 mM EDTA, 75 mM Tris/HCl; pH = 7.4) were added, after which the solution was homogenized on ice by a syringe (0.4 mm) with 20 strokes. Aliquots (1 ml) were separated in Eppendorf Cups and stored at -80 °C until use.

To determine the protein concentration of the obtained membranes, a DC-Protein Assay of Bio Rad was performed (Hercules, CA).

4.3.4. ³[H]MEP-/³[H]HIS-competition-binding experiments at hH₁R and hH₄R (Seifert et al., 2003, Schneider et al., 2010)

All [³H]Mepyramine ([³H]MEP) and [³H]Histamine ([³H]HIS) competition-binding experiments at hH₁R and hH₄R were carried out in disposable 6 ml vials. For competition binding experiments, 6 cups (6 ml) of the previously prepared Sf9 cell-membranes of each type (hH₁R + RGS4, hH₄R + G_{αi2} + G_{β1γ2}, containing 1 – 2 mg/ml of protein) were thawed, homogenized and sedimented by centrifugation (10 min, 13000 rpm, 4 °C). Afterwards, the resulting membrane pellet was re-suspended in 1.5 ml (hH₁R-assay) or 3 ml (hH₄R assay) of binding buffer (12.5 mM MgCl₂, 1 mM EDTA and 75 mM Tris/HCl, pH 7.4) and kept at 4 °C until being added to the prepared competition binding assay in the last step.

For the preparation of the assay, binding buffer was added to the vials (hH₁R assay: 400 µl binding buffer; hH₄R assay: 350 µl binding buffer containing 6.7 % BSA). In a second step, increasing concentrations (1 nM – 1 mM final concentration, doublets) of the respective unlabeled ligands (hH₁R assay: 25 µl; hH₄R assay: 50 µl) were added as well as reference cups for the determination of the unspecific binding and solvent cups as blank values for each ligand (depending on the solubility of the ligand, H₂O : DMSO proportionately 3 : 1 or 1 : 1).

All competition binding experiments were performed in the presence of 5 nM ([³H]MEP) (hH₁R) or 10 nM ([³H]HIS) (hH₄R). In a last step, the prepared and carefully homogenized membranes were added to the assay mixture (hH₁R: 25 µl, hH₄R: 50 µl) and the completed assay mixture (475 µl for hH₁R, consisting of 400 µl binding buffer, 25 µl unlabeled ligand, 25 µl [³H]Mepyramine (stock solution, 100 nM), 25 µl

membrane; 500 μ l for hH₄R, consisting of 350 μ l binding buffer, 50 μ l unlabeled ligand, 50 μ l [³H]Histamine (stock solution, 100 nM) and 50 μ l membrane) was incubated at room temperature for 90 min at 250 rpm.

Bound radioligand was separated from free radioligand by filtration through GF/C filters using a Brandel Harvester. In case of the hH₄R assay the GF/C filter was pre-treated with 0.3 % polyethyleneimine. After harvesting the assay mixture, two washes with 2 ml of cold binding buffer (4 °C) were performed and the filter-bound radioactivity was determined after an equilibration phase of at least 4 h by liquid scintillation counting using a β -counter.

Every ligand was characterized at each receptor in at least three different assays using different membranes in each case.

4.3.5. Steady-state [³³P]GTPase activity assay at hH₁R (Preuss et al., 2007)

All steady-state [³³P]GTPase activity assays at hH₁R were carried out in disposable 1.5 ml Eppendorf cups. Sf9 membranes expressing hH₁R + RGS4 were thawed, sedimented by centrifugation (4 °C, 13000 rpm, 10 min) and re-suspended in a defined volume of 10 mM Tris/HCl (pH 7.4) with intent to obtain a concentration of membrane protein of 0.5 μ g/ml. The reaction vials contained 10 μ l of hH₁R ligands at increasing concentrations (1 nM – 10 μ M final concentration, triplicates) as well as 50 μ l of REA-Mix (final concentration after the addition of [γ -³³P]GTP: 1.0 mM MgCl₂, 0.1 mM EDTA, 0.1 mM ATP, 100 nM GTP, 0.1 mM adenylyl imidodiphosphate, 5 mM creatine phosphate, 40 μ g of creatine kinase, and 0.2% (w/v) bovine serum albumin in 50 mM Tris/HCl, pH 7.4) and 20 μ l of the earlier prepared Sf9 membrane (10 μ g of protein/tube). For the determination of K_B values (antagonist mode of the [³³P]GTPase activity assay) histamine was added to the reaction mixture (final concentration 200 nM).

Reaction mixtures (80 μ l) were pre-incubated at 25 °C for 2 minutes before 20 μ l of [γ -³³P]GTP (0.1 μ Ci/tube) were added. All stock and work dilutions of [γ -³³P]GTP were prepared in 20 mM Tris/HCl, pH 7.4 as solutions in H₂O (millipore) turned out to be instable due to hydrolysis. Reactions were conducted for 20 min at 25 °C and were afterwards terminated by adding 900 μ l of slurry consisting of 5% (w/v) activated charcoal and 50 mM NaH₂PO₄ (pH 2.0). Charcoal absorbs nucleotides but not P_i.

Charcoal-quenched reaction mixtures were centrifuged for 7 min at room temperature at 15000 rpm. After the centrifugation was completed, 600 μ l of the supernatant fluid of reaction mixtures were removed, and $^{33}\text{P}_i$ was determined by liquid scintillation counting. Spontaneous $[\gamma\text{-}^{33}\text{P}]\text{GTP}$ degradation was determined in tubes containing all components listed above and in addition to that a high concentration of unlabeled GTP (1 mM) that prevents $[\gamma\text{-}^{33}\text{P}]\text{GTP}$ hydrolysis by enzymatic activities present in Sf9 membranes due to competition with $[\gamma\text{-}^{33}\text{P}]\text{GTP}$. Spontaneous $[\gamma\text{-}^{33}\text{P}]\text{GTP}$ degradation was $< 1\%$ of the total amount of radioactivity added. The experimental conditions chosen ensured that not more than 10% of the total amount of $[\gamma\text{-}^{33}\text{P}]\text{GTP}$ added was converted to $^{33}\text{P}_i$. All experimental data were analyzed by non-linear regression with PRISM 5.0. (GraphPad Software, San Diego, CA).

4.3.6. $^{35}\text{S}[\text{GTP}\gamma\text{S}]$ -binding assay at hH₄R (Schneider et al., 2009)

All $^{35}\text{S}[\text{GTP}\gamma\text{S}]$ -binding experiments at hH₄R were carried out in disposable 96 well plates. Before the experiments, Sf9 membranes expressing hH₄R + G α_{i2} + G $\beta_{1\gamma 2}$ were thawed and sedimented by centrifugation (4 °C, 13000 rpm, 10 min). Membranes were re-suspended in 1060 μ l REA-Mix (Binding Buffer plus 1.25 μ M GDP, 125 mM NaCl, and 0.063 % (w/v) bovine serum albumin (BSA)) and stored at 4 °C until use.

Every reaction well contained 70 μ l of REA-Mix, 10 μ l of the respective ligands at increasing concentrations (1 nM – 1 mM final concentration, triplicates), 10 μ l of radioligand ($^{35}\text{S}[\text{GTP}\gamma\text{S}]$, 2 nM final concentration) and 10 μ l of the before carefully homogenized Sf9 membrane suspension. Furthermore, histamine was used as reference ligand (final concentration 10 μ M, triplicates) as well as cold GTP γ S (final concentration 10 μ M) to determine the unspecific binding. The plates were incubated at room temperature for 120 min (450 rpm). Afterwards, bound radioligand was separated from free radioligand by filtration through a GF/C-filter and washed 5 times with cold binding buffer (4 °C) using a Brandel Harvester. Filter-bound radioactivity was determined after an equilibration phase of at least 12 h by liquid scintillation counting using a β -counter.

4.3.7. [³⁵S]GTPγS-binding assays at hH₂R and hH₃R (Schneider et al., 2009)

With intent to determine the receptor selectivity of some selected compounds, [³⁵S]GTPγS-binding assays were performed at hH₂R and hH₃R using disposable 6 ml vials. Therefore, membranes carrying hH₂R-G_{sα}S and hH₃R + G_{αi2} + G_{β1γ2} were used.

Before the experiments, the respective Sf9 membranes were thawed and sedimented by centrifugation (4 °C, 13000 rpm, 10 min). Membranes were re-suspended in 1400 µl REA-Mix (Binding Buffer plus 1.25 µM GDP, 125 mM NaCl, and 0.063 % (w/v) bovine serum albumin (BSA)) and stored at 4 °C until use.

Every reaction vial contained 175 µl of REA-Mix, 25 µl of the ligands at increasing concentrations (100 nM – 1 mM final concentration, triplicates), 25 µl of radio ligand ([³⁵S]GTPγS, 2 nM final concentration) and 25 µl of the earlier carefully homogenized Sf9 membrane suspension. Furthermore, histamine was used as reference ligand (final concentration 10 µM, triplicate) and one vial containing cold GTPγS was measured to determine the unspecific binding. The protein content of the samples was 15 µg/ml of membrane protein per 250 µL. The vials were incubated at room temperature for 240 min (250 rpm). Afterwards, bound radioligand was separated from free radioligand by filtration through a GF/C-filter and washed with 2 ml of cold binding buffer (4 °C) using a Brandel Harvester. Filter-bound radioactivity was determined after an equilibration phase of at least 12 h by liquid scintillation counting using a β-counter.

4.3.8. Organ bath experiments at the isolated guinea pig ileum (Elz et al., 2000)

For the preparation of the guinea pig ileum segments, guinea pigs of either sex (250 – 500 g) were stunned by a blow on the head and exsanguinated by cutting the carotid artery. After slicing the abdominal wall, the ileum was removed, rinsed and cut into segments of 1.5 – 2.5 cm length. The ileum segments were mounted isotonicly in 20 ml organ baths containing aqueous Tyrode's solution (NaCl 137 mM, KCl 2.7 mM, CaCl₂ 1.8 mM, MgCl₂ 1.0 mM, NaH₂PO₄ 0.4 mM, NaHCO₃ 11.9 mM and glucose 5.0 mM) (Pertz and Elz, 1995) and were connected to a Transducer (Type TIT 1100, FMI GmbH, Seeheim, preload 5 mN). The contraction was measured by means of an amplifier (Transducer coupler 4711, FMI GmbH, Seeheim) and recorded by a 6-channel-x/t-writer (Kompensograph C 1015, Siemens). The solution was aerated with carbogen (95% O₂, 5% CO₂) and warmed to a constant temperature of 37 °C. After an

equilibration period of about 30 min, the tissues were pre-stimulated three times with histamine (1 μ M, then 10 μ M) followed by washout (8 minutes) and recovery (10 minutes), during which atropine at a concentration not affecting H₁ receptors (0.05 μ M) was added in order to block cholinergic M receptors (Leschke et al., 1995).

For every tissue, a cumulative concentration-response curve of histamine (0.01 – 30 μ M) was recorded, followed by at most three cumulative concentration-response curves of histamine (0.01 – up to 1000 or 2000 μ M) in the presence of increasing concentrations of antagonist (incubation time 15 minutes). (Elz et al., 2000)

4.3.9. Pharmacological characterization of selected compounds at dopamine, serotonin and muscarine receptors

4.3.9.1. Determination of the binding affinity to dopamine and serotonin receptors

Receptor binding studies were carried out as described previously (Hübner et al., 2000). In brief, the dopamine D₁ receptor assay was done with porcine and human striatal membranes at a final protein concentration of 20 μ g/assay tube and the radioligand [³H]SCH 23390 (specific activity = 60 Ci/mmol, Biotrend, Cologne, Germany) at 0.50 nM (K_D = 0.67 nM, B_{max} = 625 fmol/mg protein). For competition binding experiments with human D_{2long}, D_{2short} (Hayes et al. 1992), D₃ (Sokoloff et al., 1992) and D_{4.4} (Asghari et al., 1995) receptors, preparations of membranes from CHO cells stably expressing the corresponding receptor were used together with [³H]spiperone (specific activity = 81 Ci/mmol, PerkinElmer, Rodgau, Germany) at a final concentration of 0.20-0.30 nM. The assays were carried out at a protein concentration of 2-10 μ g/assay tube, K_D values of 0.12-0.15 nM, 0.092-0.12 nM, 0.14-0.18 nM, and 0.17-0.23 nM and corresponding B_{max} values of 510 fmol/mg, 2600-4800 fmol/mg, 2300-4200 fmol/mg, and 1300-2600 fmol/mg for the D_{2long}, D_{2short}, D₃ and D_{4.4} receptors, respectively. Binding studies with the porcine serotonin receptors were carried out as described (Hübner et al., 2000, Bettinetti et al., 2002). Homogenates from porcine cerebral cortex were prepared and assays were run with membranes at a protein concentration per each assay tube of 60 and 80-100 μ g/mL for 5-HT_{1A} and 5-HT₂, respectively, in the presence of the radioligands [³H]WAY100635 (specific activity = 80 Ci/mmol, Biotrend, Cologne, Germany) (0.15 nM final concentration, K_D = 0.062-0.088 nM, B_{max} = 80 fmol/mg) and [³H]ketanserin (specific activity = 53 Ci/mmol,

PerkinElmer, Rodgau, Germany) (0.50 nM final concentration, $K_D = 1.8$ nM, $B_{max} = 100$ -200 fmol/mg). Protein concentration was established by the method of Lowry using bovine serum albumin as standard (Lowry et al., 1951).

4.3.9.2. Binding studies with muscarine receptors

Receptor binding studies with the human muscarine receptor subtypes M_1 , M_2 and M_3 were carried out utilizing homogenates of membranes from HEK293 cells which were transiently transfected with the pcDNA3.1 vector containing the human M_1 , M_2 or M_3 receptor (all purchased from Missouri S&T cDNA Resource Center, Rolla, MO), respectively, by the calcium phosphate method (Jordan et al., 1996). The binding assays were run according to the protocol described above when membranes were incubated at a final concentration of 4-20 μ g/well together with 0.10-0.20 nM of [3 H]N-methylscopolamine (specific activity = 80 Ci/mmol, Biotrend, Cologne, Germany) at K_D values of 0.050-0.095 nM, 0.087-0.20 nM, and 0.080 nM and B_{max} values of 350-1100 fmol/mg, 140-490 fmol/mg, and 1800 fmol/mg protein for M_1 , M_2 and M_3 , respectively. For all muscarine receptor systems unspecific binding was determined in the presence of 10 μ M atropin.

4.3.9.3. Data analysis for binding studies to dopamine, serotonin and muscarine receptors

The resulting competition curves of the receptor binding experiments were analyzed by nonlinear regression using the algorithms in PRISM 3.0 (GraphPad Software, San Diego, CA). The data were initially fit using a sigmoid model to provide an IC_{50} value, representing the concentration corresponding to 50% of maximal inhibition. IC_{50} values were transformed to K_i values according to the equation of Cheng and Prusoff. (Cheng and Prusoff, 1973) In the case of two individual measurements, K_i was calculated as mean value in nM with the standard deviation (SD), while analyzing more than two single values the standard error of mean (SEM) was calculated.

4.4. Pharmacological results

4.4.1. [³H]MEP-/ [³H]HIS-competition binding experiments at hH₁R and hH₄R

Competition binding assays at hH₁R and hH₄R were routinely performed for all synthesized compounds. Therefore, increasing ligand concentrations of 1 nM – 1 mM (final) were incubated together with the respective Sf9 membrane and radioligand. The detailed experimental parameters were described in [4.3.4](#). Each compound was characterized at least in triplicates in the presence of three different Sf9 membrane charges. The standard deviation (SD) was calculated and is quoted as “± SD” in the tables of results. The resulting competition curves of the receptor binding experiments were analyzed by nonlinear regression using the algorithms in PRISM 5.0 (GraphPad Software, San Diego, CA)

4.4.1.1. Characterization of the (*E*)-*N*-(2-aminoethyl)-*N*-phenylbenzamidines: VUF 6884 reduced to the core

The results of the binding assays at hH₁R and hH₄R revealed significant pharmacological differences between the (*E*)-*N*-(2-aminoethyl)-*N*-phenylbenzamidines (**22**, **23**, **25**, **28**, **52**, **56**, **58**, **62**, **64**, **67**, **70**, **73**, **76**, **80**, **99**, **103**, **110**, **111**, **112**, **114** – **117**, **180**, **181**, referred to as the “open” compounds in the following) and the corresponding dibenzo-annulated oxazepines **88**, **92**, **128**, **129**, **136**, **141**, **149**, **158**, **159**, **193**, **196**, **232** – **235**, as well as specific structure activity relationships (SARs) within both series of compounds.

The open compounds have to be partitioned into two sections: firstly, compounds **22**, **23** and **25**, that carry no substituents at the aromatic core and within which the rigid basic *N*-methylpiperazine moiety was replaced by variously alkylated ethylenediamine derivatives, and secondly, compounds **28**, **52**, **56**, **58**, **62**, **64**, **67**, **70**, **73**, **76**, **80**, **99**, **103**, **110**, **111**, **112**, **114** – **117**, **180**, **181** bearing an unchanged rigid *N*-methylpiperazine moiety as well as various modifications of the substitution pattern of the aromatic core.

Compounds lacking the rigid *N*-methylpiperazine-moiety (**22**, **23**, **25**) showed in direct comparison to the corresponding *N*-methylpiperazine bearing counterpart **28**, that above all the hH₄R is very sensitive to changes in this area of the molecule. (Table [4.1](#)) However, except compound **25**, the affinity to the hH₁R was not mentionably affected.

Interestingly, compound **25** showed compared to the other two ethylenediamine-substituted compounds **22** and **23** a significant decrease of hH₁R affinity (p (**25/22, 23**) < 0.0001) that – as described in 4.4.2 – could be reproduced at the guinea pig ileum.

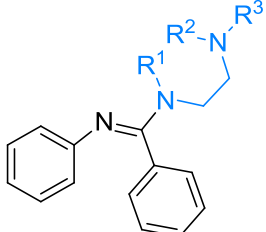
	R ¹	R ²	R ³		pK _i (hH ₁ R)	pK _i (hH ₄ R)
	H	-CH ₃	-CH ₃	22	5.08 ± 0.18	3.89 ± 0.23
	H	-C ₂ H ₅	-C ₂ H ₅	23	5.07 ± 0.13	3.30 ± 0.18
	-CH ₃	-CH ₃	-CH ₃	25	3.58 ± 0.12	3.91 ± 0.24

Table 4.1. Binding data of the open compounds lacking the piperazine moiety.

For the open compounds with rigid basic piperazine moiety, compound **28** serves as reference due to the lack of influences that can be traced back to substituents. Differences can be made with regard to the part of the molecule at which the substituent is located (**aniline moiety** or **benzoic acid moiety**) or the position (*p*- or *m*-position). As already described in the chemical section, the terms “aniline moiety” and “benzoic acid moiety” are derived from the synthesis strategy that was pursued to obtain the described compounds and serve to provide a better orientation as to be seen in the molecule map (figure 4.1).

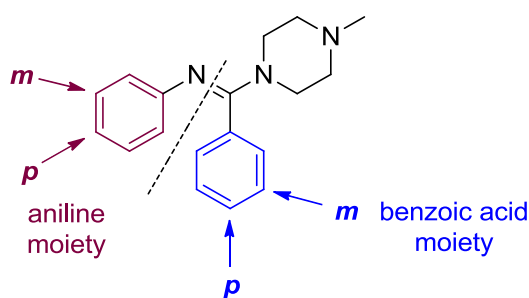


Figure 4.1. Molecule map of the open compounds.

Compounds are separated into mono- (**52, 56, 58, 64, 67, 70, 72, 76**) and di-substituted molecules (**62, 80, 99, 103, 110 – 112, 114 – 117, 180, 181**). Among the mono-substituted compounds, those bearing Cl substituents (**67, 70, 73, 76**) revealed the

most pronounced pharmacological effects that could also be transferred to the oxazepine-derived compounds later in this section. (Table 4.2)

With regard to the hH₁R affinity, *p*-substitution of the aniline moiety with Cl, Br or NH₂ substituents (**52**, **64**, **67**) turned out to be detrimental compared to the reference compound **28**, whereas the hH₄R affinity could be slightly increased. For the *p*-substitution at the benzoic acid moiety it is necessary to distinguish between the different types of substituents: whereas Cl substitution (**70**) revealed a significant increase in hH₁R and hH₄R affinity (p (**70/28**) < 0.0001), for CN and NH₂ substitution (**56**, **58**) a decrease of affinity to both, the hH₁R and the hH₄R, could be observed. Substitution with Cl in *m*-position at the aniline or the benzoic acid moiety (**73**, **76**) increased the affinity to the hH₁R (**73/28**: p < 0.0001; **76/28**: p = 0.0026) as well as the affinity to the hH₄R (p (**73**, **76/28**) < 0.0001). The reported pharmacological effects of the mono-substituted compounds are summarized in table 4.2 in which compound **28** serves as a reference.

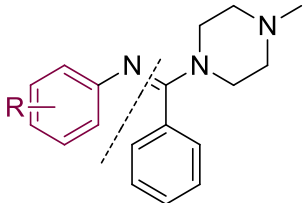
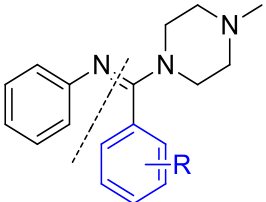
	R		pK _i (hH ₁ R)	pK _i (hH ₄ R)
	H	28	5.20 ± 0.14	4.07 ± 0.07
	<i>p</i> -NH ₂	52	4.41 ± 0.21	5.25 ± 0.17
	<i>p</i> -Br	64	3.80 ± 0.10	5.16 ± 0.09
	<i>p</i> -Cl	67	4.35 ± 0.15	5.20 ± 0.18
	<i>m</i> -Cl	73	5.99 ± 0.19	4.91 ± 0.15
	<i>p</i> -NH ₂	56	4.19 ± 0.17	3.63 ± 0.11
	<i>p</i> -CN	58	4.28 ± 0.07	3.82 ± 0.12
	<i>p</i> -Cl	70	6.07 ± 0.13	4.67 ± 0.12
	<i>m</i> -Cl	76	5.61 ± 0.21	4.82 ± 0.14

Table 4.2. Binding data of the mono-substituted open compounds at hH₁R and hH₄R.

With intent to combine the SARs detected when bearing only one substituent, a series of compounds was prepared (**62**, **80**, **103**, **110**, **111**, **180**, **181**) that were substituted at both, the aniline and the benzoic acid moiety. Again, compound **28** serves as a reference.

Among the di-substituted molecules, the di-chlorinated compounds **180** and **181** revealed by approximately 1.5 orders of magnitude a significantly higher affinity to the hH₄R compared to **28** ($p(\mathbf{180}, \mathbf{181}/\mathbf{28}) < 0.0001$), whereas only minor changes in hH₁R affinity were determined. The combination of halide substituents in favourable positions for hH₁R and hH₄R binding with a *p*-NH₂ group at the aniline moiety (**110**, **111**) evoked no increase in affinity compared to **28**. A *p*-NH₂ group at the benzoic acid moiety combined with a halide substituent at the aniline moiety resulted at least in a moderate increase of the hH₄R affinity (**62**, **80**, **103**). The reported pharmacological effects of the di-substituted compounds are shown in table 4.3, in which compound **28** is mentioned as a reference.

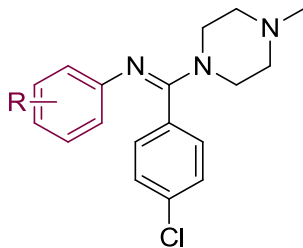
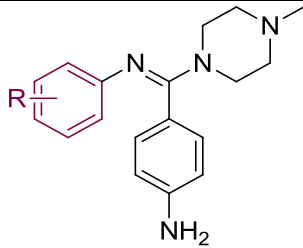
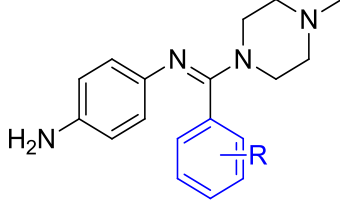
	R		pK _i (hH ₁ R)	pK _i (hH ₄ R)
	H	28	5.20 ± 0.14	4.07 ± 0.07
	<i>p</i> -Cl	180	4.74 ± 0.04	5.60 ± 0.09
	<i>m</i> -Cl	181	5.75 ± 0.03	5.28 ± 0.04
	<i>p</i> -Br	62	3.69 ± 0.23	4.60 ± 0.06
	<i>p</i> -Cl	80	4.07 ± 0.05	4.51 ± 0.11
	<i>m</i> -Cl	103	5.49 ± 0.23	4.40 ± 0.21
	<i>m</i> -Cl	110	3.91 ± 0.06	4.12 ± 0.17
	<i>p</i> -Cl	111	3.70 ± 0.24	4.02 ± 0.10

Table 4.3. Binding data of the di-substituted “open” compounds at hH₁R and hH₄R.

A further series derived from the di-substituted compounds **80** and **103** was prepared that contained various acylamino groups in *p*-position of the benzoic acid moiety as

well as Cl substituents in *p*-position (**99**, **112**, **114**, **115**) or *m*-position (**116**, **117**) of the aniline moiety. The intent was to increase the affinity to hH₄R as described by Smits et al. for quinoxaline and quinazoline derived molecules (Smits et al., 2008a; Smits et al., 2008b). For all compounds, the affinity to hH₁R decreased compared to **28**, and the hH₄R affinity remained on the same level (**99**, **114** - **117**) or was increased (**112**). A summary of the binding data of the acylamino-substituted compounds is shown in table 4.4.

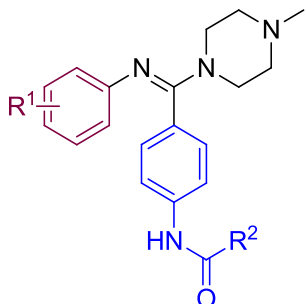
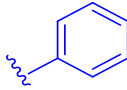
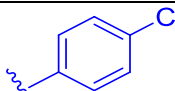
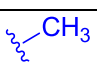
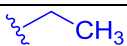
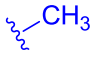
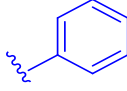
	R ¹	R ²		pK _i (hH ₁ R)	pK _i (hH ₄ R)
	<i>p</i> -Cl		99	4.36 ± 0.19	4.54 ± 0.11
	<i>p</i> -Cl		112	4.61 ± 0.09	5.29 ± 0.20
	<i>p</i> -Cl		114	4.00 ± 0.09	4.38 ± 0.18
	<i>p</i> -Cl		115	3.22 ± 0.23	4.16 ± 0.06
	<i>m</i> -Cl		116	4.42 ± 0.05	4.29 ± 0.16
	<i>m</i> -Cl		117	4.34 ± 0.22	4.41 ± 0.08

Table 4.4. Binding data of the di-substituted acylamino substituted compounds at hH₁R and hH₄R.

4.4.1.2. Characterization of dibenzo[*b,f*][1,4]oxazepines: the key role of the closed central oxazepine ring

A fairly minor structural modification lead to a distinct improvement of pharmacological affinity at both the hH₁R and hH₄R: according to Smits et al. (2006), for some selected open compounds a series of dibenzo[*b,f*][1,4]oxazepine-derived counterparts with piperazine- or *N*-methylpiperazine-moiety was prepared. (Figure 4.2).

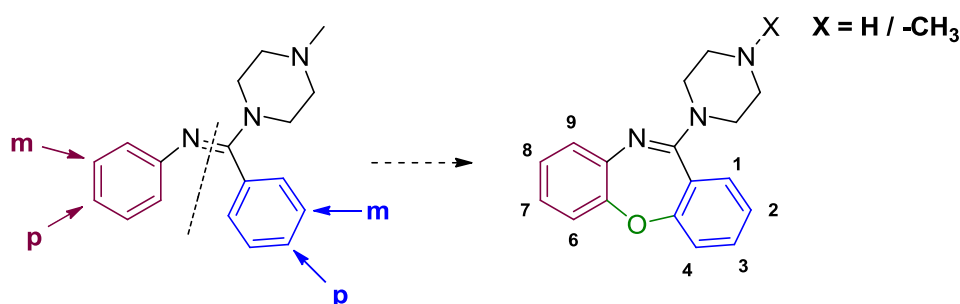


Figure 4.2. Molecule map of the dibenzo[*b,f*][1,4]oxazepine-derived counterparts: the fusion of both phenyl moieties by an oxygen bridge results in a closed central oxazepine ring.

In general, all synthesized dibenzo[*b,f*][1,4]oxazepine-derived compounds (**88**, **92**, **128**, **129**, **136**, **141**, **149**, **158**, **159**, **193**, **196**, **232** - **235**) showed very high affinity to the hH₁R (pK_i 7.66 – 9.25) and – depending on the substitution pattern and the piperazine-moiety – moderate to high affinity to the hH₄R. For compounds synthesized by Smits et al. (**88**, **92**, **141**, **158**) the published pK_i values could not be reproduced and showed a difference of -0.2 to -0.8 log units. A possible reason for the detected deflections could be the disparity of the testing systems.

Alike within the series of the open compounds, a reference compound **141** without any substituents was prepared with intent to determine the pharmacological effects of the core molecule. Moreover, a comparison between the two reference compounds of the open (**28**) and the closed group (**141**) was made: the central oxazepine ring causes a significant increase in hH₁R and hH₄R affinity (hH₁R: +3 orders of magnitude, *p* (**28/141**) < 0.0001; hH₄R: + 2 orders of magnitude, *p* (**28/141**) < 0.0001), suggesting a key role of this part of the molecule for interactions with hH₁R and hH₄R. (Figure 4.3)

	R		pK _i (hH ₁ R)	pK _i (hH ₄ R)
	H	141	8.16 ± 0.22	6.19 ± 0.23 ¹
	8-Cl	88	8.19 ± 0.13	6.64 ± 0.14 ²
	7-Cl	92	7.76 ± 0.11 ³	6.99 ± 0.03 ³
	3-Cl	149	8.97 ± 0.04	6.13 ± 0.09
	3-NH ₂	136	7.92 ± 0.13	5.11 ± 0.06
	3-NH ₂ , 7-Cl	129	7.66 ± 0.19	6.48 ± 0.09
	3-NH ₂ , 8-Cl	128	8.18 ± 0.16	6.11 ± 0.13
	3-Cl, 8-Cl	158	8.52 ± 0.05	6.27 ± 0.23 ⁴
	3-Cl, 7-Cl	159	9.25 ± 0.16	6.96 ± 0.16
	2-Cl	LOX ⁵	8.64 ± 0.08	5.06 ± 0.07

Table 4.5. hH₁R/hH₄R- binding data of the dibenzo[*b,f*][1,4]oxazepine-derived compounds bearing an *N*-methylpiperazine moiety.

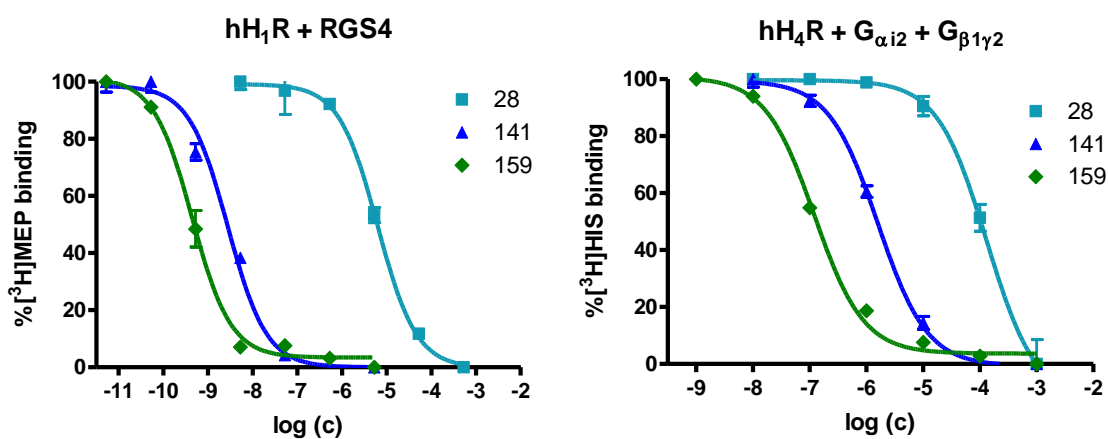


Figure 4.3. Pharmacological effect of the closed central oxazepine ring and the modification of the substitution pattern at hH₁R and hH₄R.

¹ Smits et al. (2006): pK_i (hH₄R) = 6.88 ± 0.1

² Smits et al. (2006): pK_i (hH₄R) = 7.37 ± 0.1

³ Smits et al. (2006): pK_i (hH₁R) = 8.11 ± 0.1; pK_i (hH₄R) = 7.55 ± 0.1

⁴ Smits et al. (2006): pK_i (hH₄R) = 6.51 ± 0.1

⁵ hH₁R and hH₄R binding data of **LOX** (loxapine) from Appl et al. (2012)

Similar effects could be detected for the pairs **67 / 92**, **70 / 149** and **103 / 128**. Moreover, for both the hH₁R and the hH₄R, an overview of the pK_i values of all “open” and “ring-closed” counterparts is given in figure 4.4.

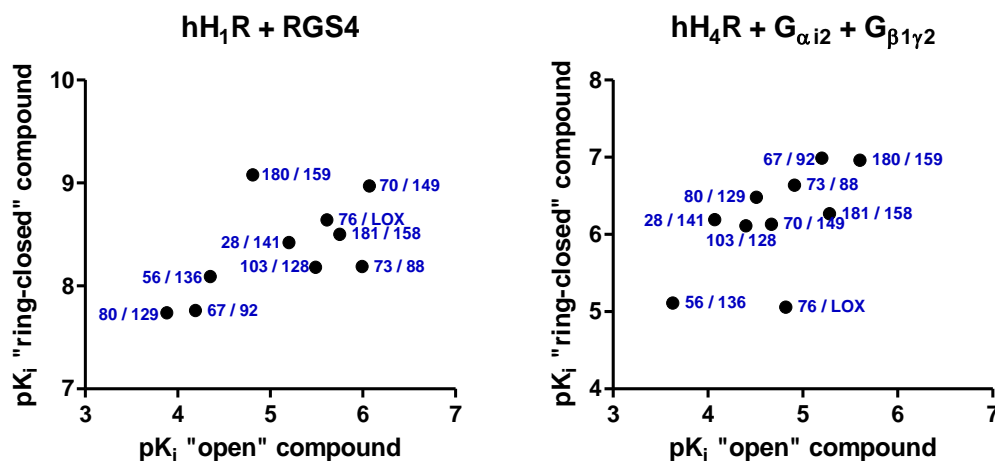


Figure 4.4 Overview of the pK_i values of all “open” and “ring-closed” counterparts at hH₁R and hH₄R.

For the majority of compounds, the SARs of the substituents determined within the series of the open compounds could be transferred to the closed compounds. All results are quoted in comparison to the reference compound **141**.

The introduction of a Cl substituent in position 7 (**92**) turned out to be significantly beneficial for hH₄R affinity (p (**92/141**) < 0.0001), whereas the introduction of a Cl substituent in position 3 (**149**) led to a significantly increased affinity to hH₁R (p (**149/141**) < 0.0001). Di-substituted compounds bearing an NH₂ group in position 3 and a Cl substituent in position 7 (**129**) or 8 (**128**) showed no remarkable change in the high hH₁R and the moderate hH₄R affinity. The introduction of only one NH₂ group in position 3 without any further substituent led to a significant loss of affinity to hH₄R (**136**) (p (**136/141**) < 0.0001). However, the high hH₁R affinity was not affected.

In some cases, the SARs determined at the open compounds could not be transferred to the closed compounds one-to-one. For example, the hH₁R-beneficial effect of a Cl substituent in *m*-position of the aniline moiety (**73**) could not to the same extent be reproduced for the corresponding closed counterpart **88**, as only an increase of hH₄R affinity was revealed in comparison to the unsubstituted reference compound **141**. The

hH₁R affinity, however, was not at all influenced. A possible explanation could be that in the open compound **73** the lack of rigidization of the two aromatic rings (aniline and benzoic acid moiety) allows rotation around the single bonds adjacent the imino-bond. As a consequence, substituents in *m*-position are able to possess different positions in the binding pocket. Transferred to the hH₄R, similar effects were observed for the pair **76** / **LOX**: *m*-Cl substitution of the benzoic acid moiety (**76**) increased the hH₄R affinity compared to the “open” reference compound **28**, whereas for the corresponding “ring-closed” counterpart **LOX** the affinity was distinctly decreased compared to the “ring-closed” reference compound **141**.

For the di-Cl-substituted compound **159**, the beneficial effects of Cl substitution in position 7 (hH₄R ↑) and position 3 (hH₁R ↑) could be combined, resulting in a significantly increased affinity to both the hH₁R (pK_i 9.25 ± 0.16, (**159/141**) *p* < 0.0001) and the hH₄R (pK_i 6.96 ± 0.16, *p* (**159/141**) < 0.0001). The corresponding open counterpart **180** showed the same tendencies regarding the hH₄R affinity, however, the pharmacological effects were not as pronounced as expected. All reported pharmacological effects are summarized in table 4.5.

Figure 4.5 shows a snapshot of the molecular dynamics simulation of compound **88** (A) and loxapine (**LOX**, B) in the binding pocket of hH₄R. The hH₄R model was constructed as recently described by homology modeling, using the crystal structure of the inactive hH₁R as template. (Wagner et al., 2014) For both molecules, an electrostatic interaction between the protonated distal nitrogen of the *N*-methylpiperazine moiety and the highly conserved Asp^{3.32} in TM 3 is suggested. As **88** and **LOX** differ only in their substitution pattern of the aromatic tricycle, a closer focus on this region of the molecule is necessary to explain the differences in the affinity to hH₄R. Embedded in a pocket between TM 3, TM 5, TM 6 and the E2-loop, the aromatic core is suggested to interact with several amino acids, mainly Phe¹⁶⁸, Phe¹⁶⁹, Tyr^{3.33} and Trp^{6.48}. Moreover, the Cl substituent in position 8 (**88**) is most likely to interact with further sub-pockets in TM 6 of the hH₄R binding site, resulting in an increased hH₄R affinity (pK_i (hH₄R) = 6.64 ± 0.14) By contrast, due to the Cl substituent in position 2 it is speculated that a sterical clash with Trp^{6.48} in TM 7 prevents the ligand from optimally fitting into the binding pocket and thus leads to a decreased hH₄R affinity of **LOX** (pK_i (hH₄R) = 5.06 ± 0.07). (personal communication, Strasser et al., 2014)

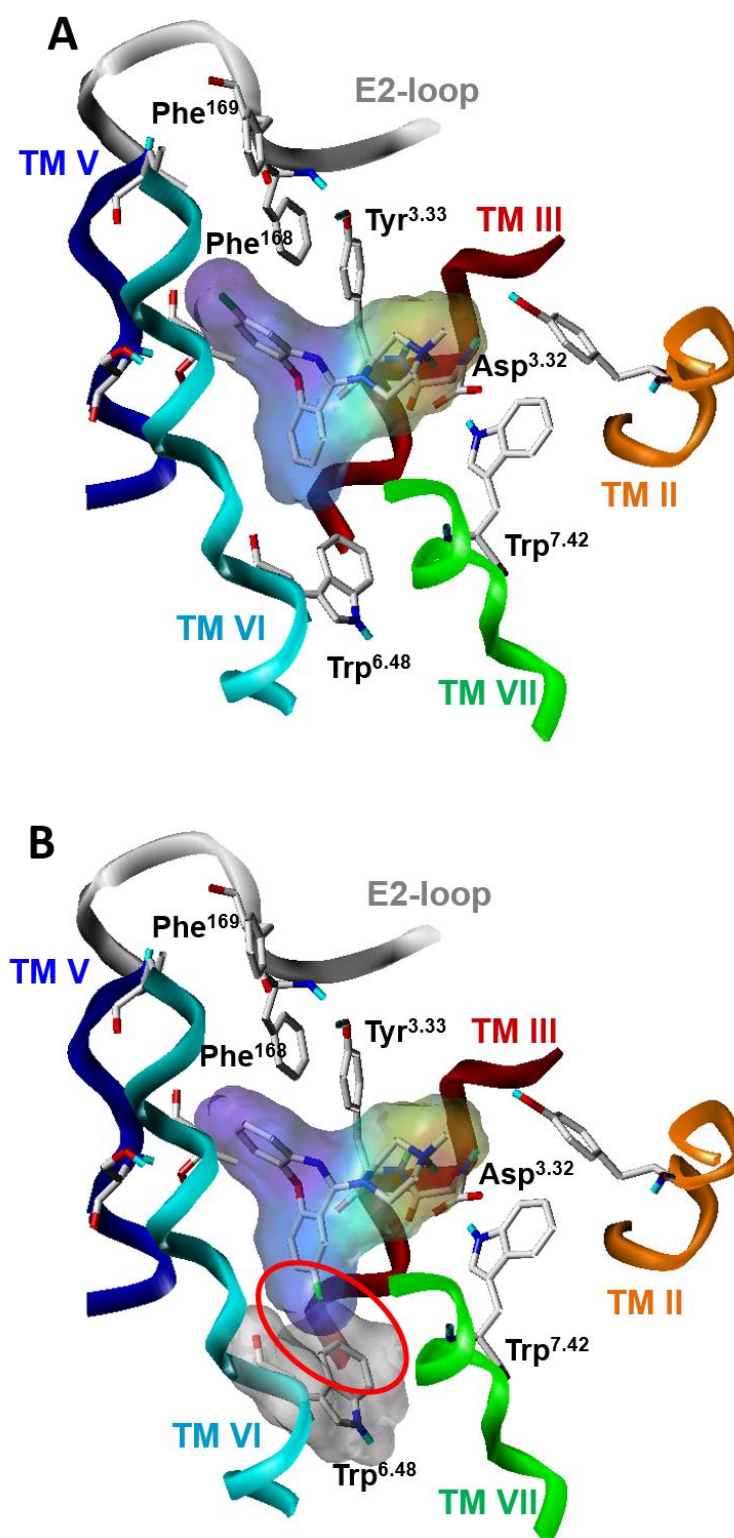


Figure 4.5. Interaction of **88** (A) and LOX (B) with amino acids in the binding pocket of hH4R (snapshot of MD simulation, Strasser et al., 2014)

Among the dibenzo[*b,f*][1,4]oxazepine-derived compounds, a small series was prepared, in which the *N*-methylpiperazine moiety was replaced by piperazine (**193**, **196**, **232** – **235**). For all compounds, the high affinity to hH₁R was not remarkably influenced, however, the hH₄R affinity was in all cases significantly decreased (0.5 – 1 orders of magnitude, $p < 0.0001$) compared to their “ring closed” *N*-methylpiperazine counterparts (figure 4.6). This phenomenon was also observed in the laboratories of the Leurs group (Smits et al., 2006): a reduced basicity of the distal nitrogen as in the piperazine-bearing compounds caused a distinctly decreased hH₄R affinity. Moreover, as ethylated piperazine analogues also revealed a decreased hH₄R affinity, an important role of the steric component is suggested. Regarding the aromatic core of the piperazine-bearing VUF 6884 derived molecules, the SARs determined for the substitution pattern within the group of the *N*-methylpiperazine bearing compounds could be reproduced.

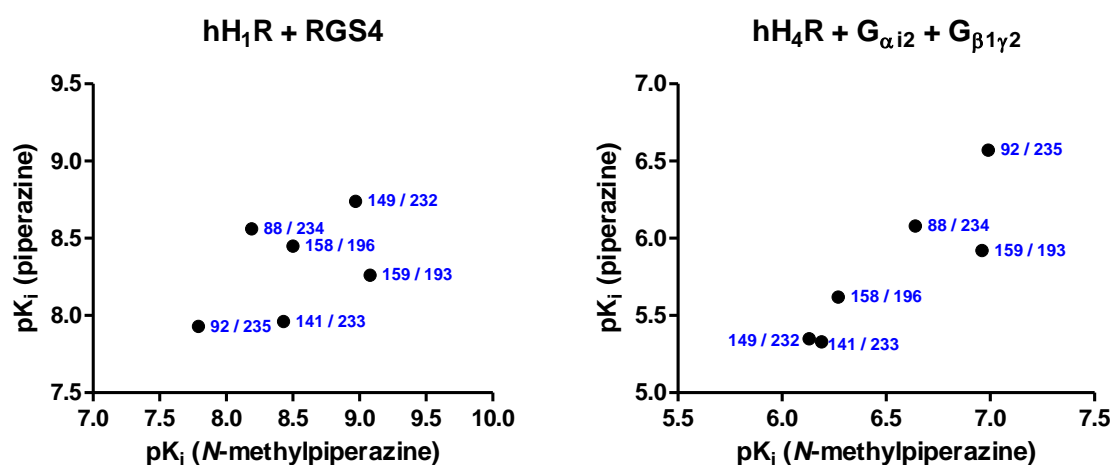


Figure 4.6. Comparison of the hH₁R-/ hH₄R affinity of the corresponding *N*-methylpiperazine-/ piperazine-bearing counterparts.

All reported pharmacological effects are summarized in table 4.6.

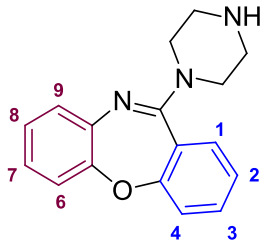
	R		pK _i (hH ₁ R)	pK _i (hH ₄ R)
	H	233	7.96 ± 0.03	5.33 ± 0.02
	8-Cl	234	8.40 ± 0.02	6.08 ± 0.10
	7-Cl	235	8.04 ± 0.12	6.57 ± 0.02
	3-Cl	232	8.74 ± 0.08	5.35 ± 0.03
	3-Cl, 7-Cl	193	8.23 ± 0.11	5.92 ± 0.12
	3-Cl, 8-Cl	196	8.52 ± 0.03	5.62 ± 0.06

Table 4.6. hH₁R/hH₄R binding data of the dibenzo[*b,f*][1,4]oxazepine-derived compounds bearing a piperazine moiety.

As a conclusion it is suggested, that the fusion of the central oxazepine ring causes an increase of hH₁R affinity in a range of, in general, about 3 log units, and about 2 log units of hH₄R affinity. These pharmacological results emphasize that not only the substitution pattern, but more importantly, the closed central heterocycle and above all the oxygen as fusion atom plays a key role in the ligand-receptor interaction at both the hH₁R and hH₄R. As previously reported crystallographic data of modified fusion atoms revealed, the 3D structure of the clozapine-like molecule is strongly determined by the nature of the atom that fuses the phenyl rings (e.g. sulfur, carbon, oxygen or nitrogen). (Liégeois et al., 2002) This can be traced back to the conformational differences due to the dihedral angle between the planes of both aromatic rings. (Liégeois et al., 2002, Smits et al., 2006) Furthermore, the hH₄R turned out to be very sensitive to changes in the rigid basic *N*-methylpiperazine moiety: the replacement of the *N*-methylpiperazine ring by either a flexible ethylenediamine moiety or a piperazine-ring caused a distinct drop of hH₄R affinity that can be traced back to steric components as well as to the loss of basicity. (Smits et al., 2006)

The detected SARs are summarized in figure [4.7](#).

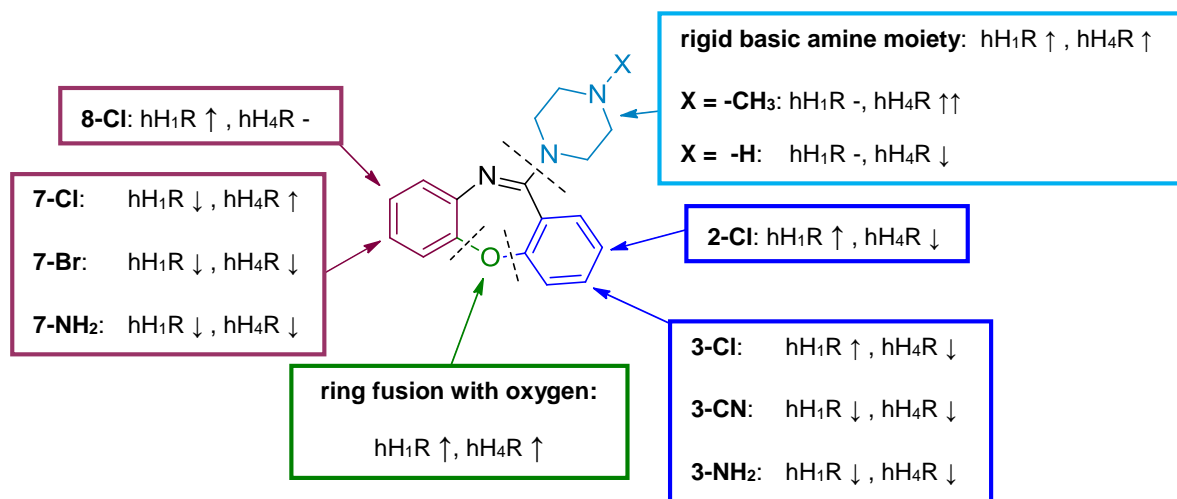


Figure 4.7. SARs of the open and “ring-closed” compounds at hH₁R and hH₄R.

4.4.1.3. Characterization of dimeric dibenzo[*b,f*][1,4]oxazepines

4.4.1.3.1. Dibenzo[*b,f*][1,4]oxazepines linked by nonpolar alkylspacers

As compounds **158** and **159** showed the most promising pharmacological profile with regard to both the hH₁R and the hH₄R, a series of dimeric compounds derived from these molecules was prepared. Due to matters of synthesis, nonpolar alkyl spacers of different length ($n = 6, 7, 8, 10$) were used to link the respective piperazine bearing counterparts of **158** and **159** (compounds **196** and **193**) at the free amine of the piperazine moiety. A map of the resulting molecules is shown in figure 4.8.

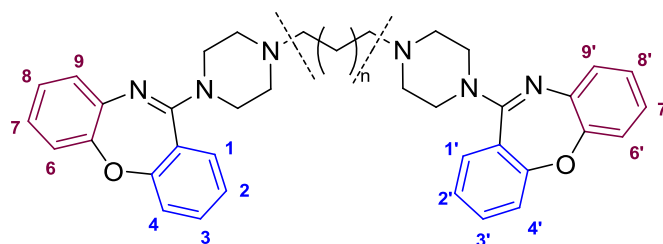


Figure 4.8. Molecule map of the dimeric dibenzo[*b,f*][1,4]oxazepine derivatives linked by nonpolar alkyl spacers.

In all cases, the affinity to hH₁R and hH₄R was significantly decreased compared to the monomeric compounds **158** or **159** ($p < 0.0001$). All dimeric compounds linked by nonpolar spacers showed very weak affinity to the hH₄R ($pK_i < 5$), which can be traced

back to the recently described sensitivity of the hH₄R to changes in the area of the rigid basic piperazine moiety. (Smits et al., 2006) Moreover, a decrease in hH₁R affinity in a range of approximately 3 - 4 log units was observed compared to the respective monomers. However, a differentiation regarding the spacer length is necessary:

Compounds bearing spacers with $n = 6$ (**212**, **213**), $n = 8$ (**208**, **210**) and $n = 10$ (**207**, **209**) showed no mentionable difference in the moderate affinity that could be related to modifications of the substitution pattern or the spacer length. By contrast, for compounds linked by a spacer with $n = 7$ (**205**, **206**), a distinct difference in hH₁R affinity depending on the position of the Cl substituents was detected: for substituents in position 8 / 8' and 3 / 3' (**205**), the hH₁R affinity remained on the same level as already reported for spacer lengths $n = 6, 8, 10$. For substituents in position 7 / 7' and 3 / 3' (**206**), the hH₁R affinity was significantly increased by approximately 2 orders of magnitude (p (**205/206**) < 0.0001). (Figure 4.9) These data, in combination with molecular modelling studies at hH₁R indicate that this compound binds only at one hH₁R, but does not address dimeric hH₁Rs. The first pharmacophor binds specifically in the binding pocket of hH₁R, whereas the second pharmacophor binds on the extracellular surface of hH₁R. As it will be reported later in this section (4.4.2), the results determined for compounds **205** and **206** could be confirmed at the isolated guinea pig ileum.

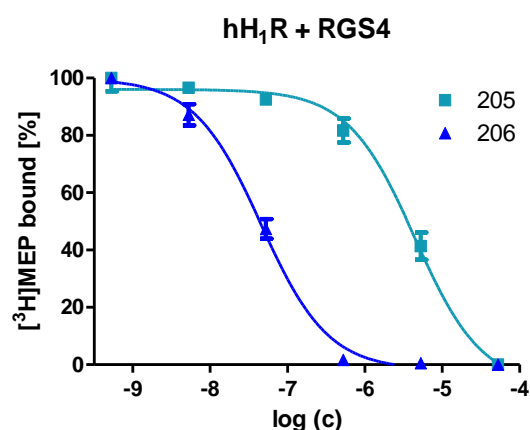
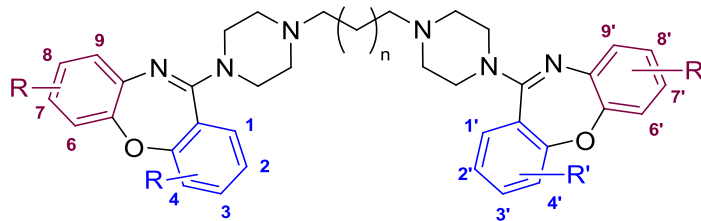


Figure 4.9. Competition binding assay at hH₁R: compound **206** with substitution in positions 3 / 3' and 7 / 7' clearly superior to its 3 / 3' and 8 / 8' substituted analogue **205**.

The competition binding data discussed above are summarized in table 4.7.



R / R'	n		pK _i (hH ₁ R)	pK _i (hH ₄ R)
8 / 8' -Cl, 3 / 3' -Cl	6	212	5.86 ± 0.10	< 5
8 / 8' -Cl, 3 / 3' -Cl	7	205	5.63 ± 0.22	< 5
8 / 8' -Cl, 3 / 3' -Cl	8	208	5.42 ± 0.23	< 5
8 / 8' -Cl, 3 / 3' -Cl	10	207	5.69 ± 0.10	< 5
7 / 7' -Cl, 3 / 3' -Cl	6	213	5.87 ± 0.16	< 5
7 / 7' -Cl, 3 / 3' -Cl	7	206	7.44 ± 0.10	< 5
7 / 7' -Cl, 3 / 3' -Cl	8	210	5.02 ± 0.20	< 5
7 / 7' -Cl, 3 / 3' -Cl	10	209	5.84 ± 0.09	< 5

Table 4.7. hH₁R / hH₄R binding data of dimeric dibenzo[*b,f*][1,4]oxazepine derivatives linked by nonpolar spacers.

4.4.1.3.2. Dibenzo[*b,f*][1,4]oxazepines linked by polar spacers of different type and length: compounds linked at the piperazine moiety

Derived from the dibenzo[*b,f*][1,4]oxazepine compounds that carry a piperazine moiety (**193**, **196**, **232** – **235**) a further series of dimeric compounds was prepared that were linked by different types of polar spacers. The spacers, containing a piperazine- or a homopiperazine component, were linked to the respective monomeric compounds at the free secondary amine of the piperazine moiety by amide coupling. A map of the resulting molecules is shown in figure [4.10](#).

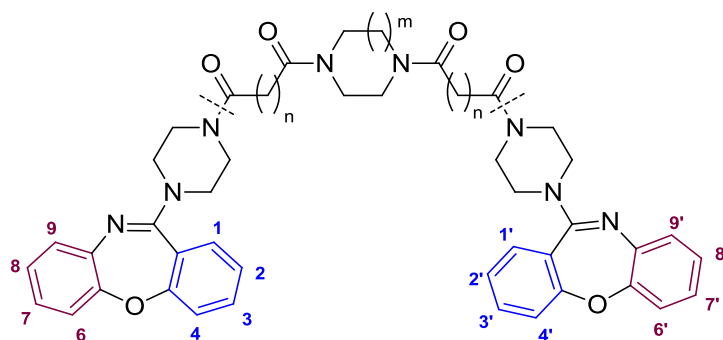


Figure 4.10. Molecule map of the dibenzo[*b,f*][1,4]oxazepine derivatives linked by polar spacers containing piperazine or homopiperazine components.

Compared to the monomeric compounds **193**, **196**, **232** - **235**, the affinity to hH₁R and hH₄R was in all cases decreased. As the hH₄R affinity of the monomers was itself low due to the lack of an *N*-methylpiperazine moiety, the resulting dimeric compounds did not surprise with their low hH₄R affinity ($pK_i < 5$). This can again be quoted to the sensitivity of the hH₄R to changes at the rigid basic *N*-methylpiperazine moiety that was already observed for the compounds linked by nonpolar spacers.

However, a different observation could be made for the hH₁R: among all dimeric compounds linked at the piperazine moiety (be it by polar or nonpolar spacers), the hH₁R revealed a slight preference to compounds linked by polar spacers. Although decreased in a range of about 2 log units in comparison to the corresponding monomeric counterparts, the loss of hH₁R affinity was not as pronounced as reported for the nonpolarly linked compounds. As a consequence, based on the fact that the aromatic core and the proximal part of the piperazine moiety within the molecule remained equal, the reason for the differences in affinity arises from the spacer type and its connection to the monomers. The spacers within this series of compounds contain a piperazine- or a homopiperazine-component that is linked to the piperazine-moiety of the respective monomers by amide coupling with a dioic acid. Due to the amide bond, the piperazine components lack a basic amine, what usually represents an important element for hH₁R binding (e.g. protonated amine-components of agonists and antagonists interacting with Asp^{3.32}). (Ohta et al., 1994, Wieland et al., 1999, Jongejan et al., 2005) However, as amide bonds reveal a polar character, interaction with the amino acids in the binding pocket (e.g., water bridges) of the hH₁R can be suggested, what could be an explanation for the improved interaction with the hH₁R

compared to the recently described compounds linked by nonpolar alkyl spacers. SARs that can be related to a change of the substitution pattern occur only in tendencies, however, they are in general congruent with the findings within the corresponding group of monomers: compounds bearing four Cl substituents (**225**, **239**) were slightly superior to compounds bearing only two (**238**, **241**, **242**) or even no Cl substituent (**240**). (Figure 4.11)

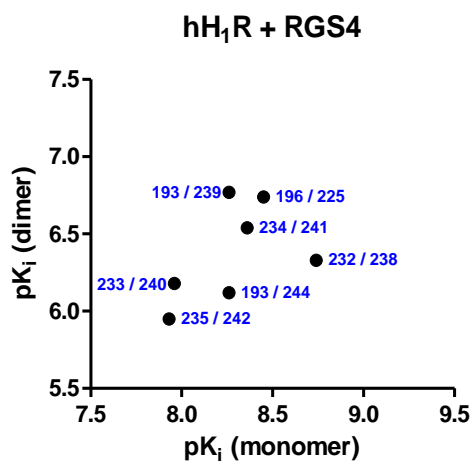
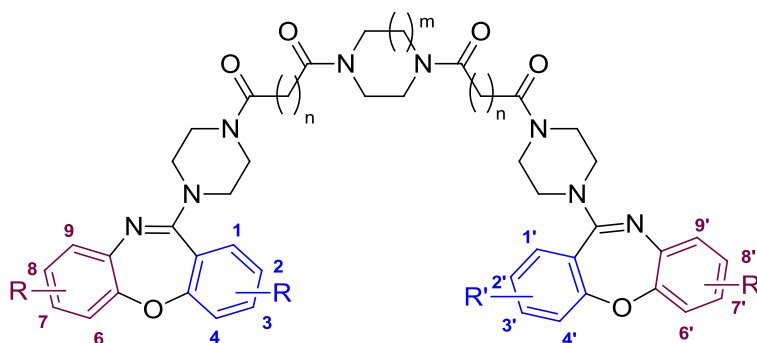


Figure 4.11. Comparison of the hH₁R affinity of the corresponding monomeric and dimeric counterparts.

The reported pharmacological effects at hH₁R and hH₄R are summarized in table 4.8.



R / R'	m	n		pK _i (hH ₁ R)	pK _i (hH ₄ R)
H / H	1	2	240	6.18 ± 0.09	< 5
8 / 8' -Cl	1	2	241	6.54 ± 0.04	< 5
7 / 7' -Cl	1	2	242	5.95 ± 0.06	< 5
3 / 3' -Cl	1	2	238	6.33 ± 0.11	< 5
8 / 8' -Cl, 3 / 3' -Cl	1	2	225	6.74 ± 0.10	< 5
7 / 7' -Cl, 3 / 3' -Cl	1	2	239	6.77 ± 0.09	< 5
7 / 7' -Cl, 3 / 3' -Cl	2	3	244	6.12 ± 0.05	< 5

Table 4.8. hH₁R-/ hH₄R- competition binding data of dimeric dibenzo[*b*,*7*][1,4]-oxazepine derivatives linked by polar spacers.

4.4.1.3.3. Dibenzo[*b,f*][1,4]oxazepines linked by polar spacers of different type and length: compounds linked at the NH₂ group in position 3 / 3'

Derived from the dibenzo[*b,f*][1,4]oxazepine compounds that carry an NH₂ group in position 3 (**128**, **129**, **136**), a further series of dimeric compounds was prepared that were linked by different types of spacers. The spacers, consisting either of an alkyl chain or a piperazine or homopiperazine component, were linked to the respective monomeric compounds at the free amine in position 3 by amide coupling. As a consequence, the *N*-methylpiperazine moiety in the resulting molecules was not modified, providing the possibility to interact with the hH₄R.

A map of the molecules is shown in figure [4.12](#).

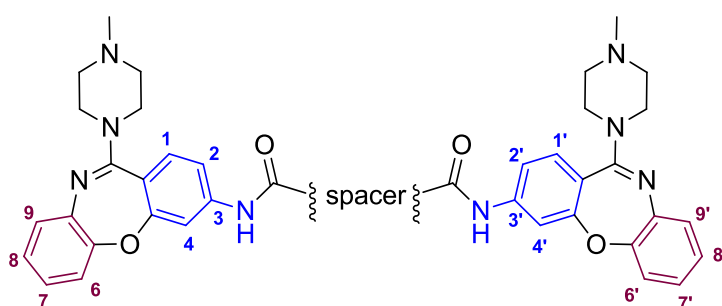


Figure 4.12. Molecule map of the dibenzo[*b,f*][1,4]oxazepine derivatives linked by spacers containing alkyl chains or piperazine or homopiperazine components.

Compared to the monomeric compounds **128** and **129**, the affinity of the corresponding dimeric compounds (**215**, **227 – 231**) to both, the hH₁R and hH₄R, was in all cases significantly decreased in a range of 1 to 1.5 log units ($p < 0.0001$). Compounds derived from **136** (**221**, **243**) revealed – alike the monomeric compound – a very weak hH₄R affinity and the hH₁R affinity was decreased in a range of about 1 order of magnitude compared to the monomer. (Figures [4.13](#), [4.14](#))

Regarding the hH₁R, a slight preference could be determined for compounds bearing a homopiperazine spacer (**229**, **231**): the observed pK_i-values were significantly increased up to 0.5 log units compared to their analogues bearing a piperazine-spacer (**230**, **227**) (p (**227/231**) = 0.0011; p (**229/230**) = 0.0153) With regard to the hH₄R, Cl substitution in position 7 / 7' (**227**, **231**) again turned out to be slightly favourable for

hH₄R affinity. This, in combination with a homopiperazine spacer (**231**) revealed a significantly increased hH₄R affinity (p (**227/231**) < 0.0001; p (**229/231**) < 0.0001).

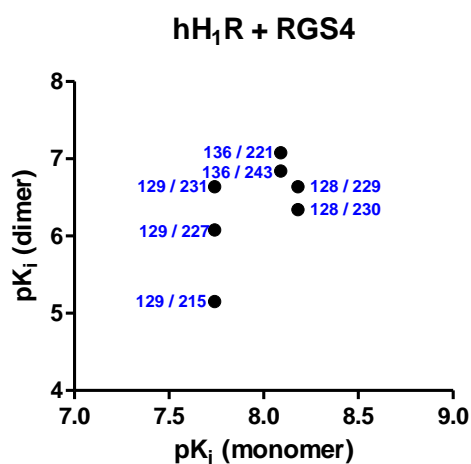


Figure 4.13. Comparison of the hH₁R affinity of the corresponding monomeric and dimeric counterparts.

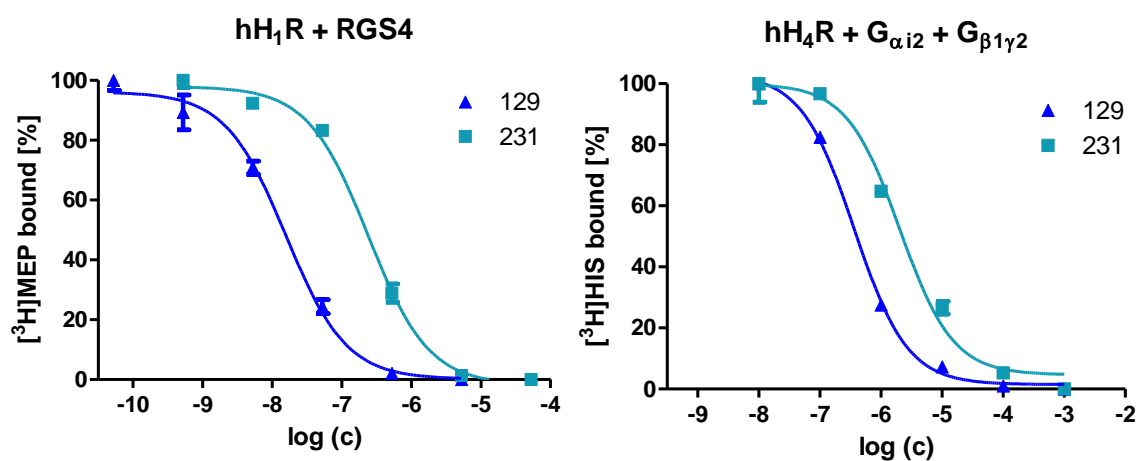
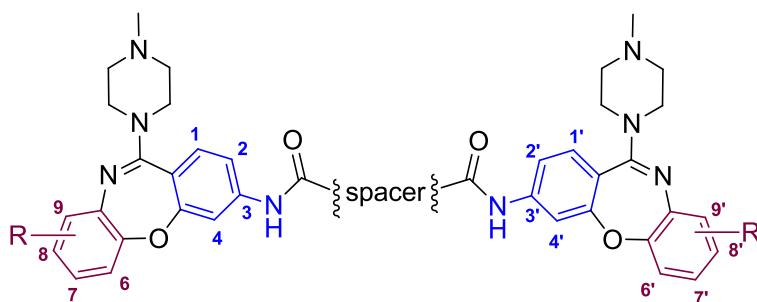


Figure 4.14. Competition binding assays at hH₁R and hH₄R for the corresponding monomeric and dimeric counterparts **129** and **231**.

The pharmacological data resulting from the competition binding assays at hH₁R and hH₄R are summarized in table [4.9](#).



R / R'	spacer		pK _i (hH ₁ R)	pK _i (hH ₄ R)
7 / 7' -Cl		215	5.15 ± 0.10	5.06 ± 0.18
7 / 7' -Cl		227	6.17 ± 0.22	5.10 ± 0.09
7 / 7' -Cl		231	6.64 ± 0.02	5.74 ± 0.21
8 / 8' -Cl		229	6.64 ± 0.10	4.92 ± 0.15
8 / 8' -Cl		230	6.34 ± 0.23	4.89 ± 0.12
H / H		221	7.08 ± 0.23	4.49 ± 0.15
H / H		243	6.84 ± 0.09	4.84 ± 0.13

Table 4.9. hH₁R-/ hH₄R competition binding data of the dibenzo[*b,f*][1,4]-oxazepine derivatives linked by polar spacers at the free NH₂ group in position 3 / 3'.

4.4.2. Isolated guinea pig ileum

All compounds were additionally characterized at the isolated guinea pig ileum in the presence of histamine. In all cases, the concentration effect curve was shifted rightward and at higher antagonist concentrations (concentration depending on the compound), the maximum of the curve was depressed. Experimental details of the organ bath experiments were described in section [4.3.8](#).

Figure [4.15](#) shows a histamine concentration-effect curve described above: the first curve on the left represents histamine in the absence of an antagonist, all further curves on the right represent the histamine concentration-effect curve in the presence of increasing concentrations of **141** (3.16 nM – 316 nM). From 31.6 nM on, a depression of the concentration effect curve can be observed.

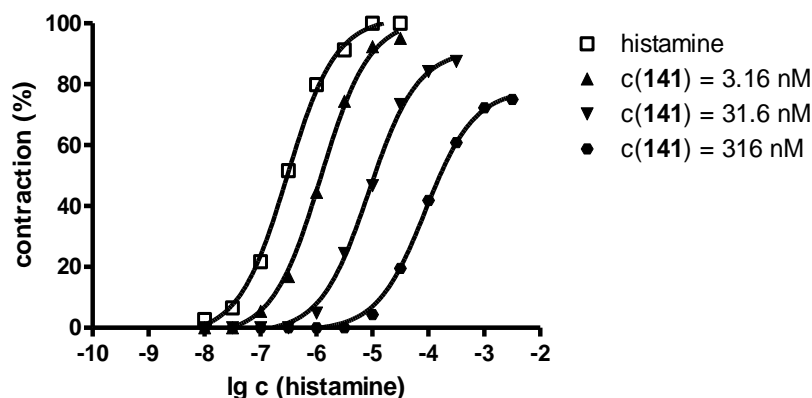


Figure 4.15. Concentration effect curve of histamine revealing depression at higher concentrations of **141**.

4.4.2.1. Characterization of the mono, di, and acylamino substituted open compounds

With intent to compare pA_2 values on the same background, all pA_2 values in the following were calculated via Schild plot analysis suggesting slope = 1. For cases in which the slope significantly differs from 1, more reliable pA_2 values depending on the concentration range of the incubated antagonist were estimated in section [4.4.2.4](#) (*method A*) and [4.4.2.5](#) (*method B*).

Among the unsubstituted compounds **22**, **23**, **25**, and **28**, no distinct decrease of affinity to $g_{pH_1}R$ was detected by replacing the *N*-methylpiperazine moiety by an

ethylenediamine moiety (**22**, **23**), a fact that points out a less important role of the rigid basic amine structure in gpH₁R binding. Again, compound **25** revealed the lowest gpH₁R affinity among the compounds with modified ethylenediamine moiety. This was already observed in competition binding assays at hH₁R, however, in a much more pronounced way.

For the open compounds bearing an *N*-methylpiperazine moiety, the unsubstituted compound **28** serves as a reference due to its lack of substituent influences. Cl substitution in *m*-position at both the aniline and the benzoic acid moiety (**73**, **76**) turned out to be beneficial for gpH₁R affinity (p (**73/28**) < 0.0001, p (**76/28**) = 0.0014), affirmed by a distinct increase of the pA₂ value. Among all open compounds, **73** marks the most potent representative, pointing out that a Cl substituent in *m*-position of the aniline moiety plays an important role in the ligand receptor interaction at gpH₁R. A differentiation is necessary for Cl substitution in *p*-position: *p*-Cl substitution at the benzoic acid moiety proved to be advantageous for the gpH₁R affinity (**70**), whereas *p*-Cl substitution at the aniline moiety was rather detrimental (**67**). In general it can be postulated, that *p*-substitution at the aniline moiety has a harmful effect on the gpH₁R affinity, independent from the kind of the substituent (**52**, **64**, **67**). At the *p*-position of the benzoic acid moiety, all other substituents except Cl had no distinct influence on the pharmacological effect (**56**, **58**).

Open compounds bearing more than one substituent (**62**, **80**, **103**, **110**, **111**, **180**, **181**) showed – compared to the respective mono-substituted open compounds – either no or a slightly decreased pharmacological effect at gpH₁R. Compounds **103** and **181** (derived from **73**) represent the most potent di-substituted open compounds, again emphasizing the gpH₁R-advantageous effect of Cl substitution in *m*-position of the aniline moiety. By contrast, substituents in *p*-position of the aniline moiety again turned out to have very negative influence on the gpH₁R affinity, most significant for **110** as weakest representative of the open compounds (p (**110/28**) = 0.0006). The discussed pharmacological effects are summarized in table [4.10](#).

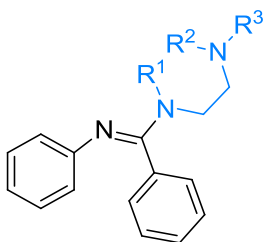
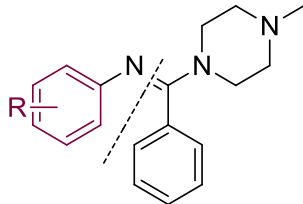
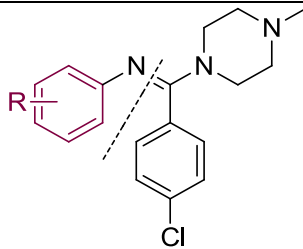
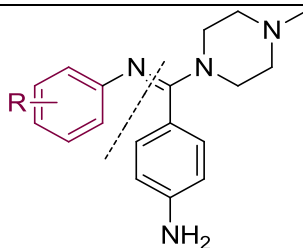
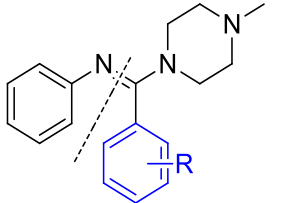
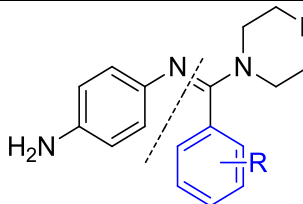
			pA₂ (gp-ileum), slope = 1
	R¹ = H R² = R³ = -CH₃	22	5.80 ± 0.05
	R¹ = H R² = R³ = -C₂H₅	23	5.73 ± 0.09
	R¹ = R² = R³ = -CH₃	25	5.21 ± 0.14
	H	28	5.87 ± 0.08
	p-NH₂	52	5.03 ± 0.11
	p-Br	64	5.08 ± 0.06
	p-Cl	67	5.22 ± 0.10
	m-Cl	73	6.89 ± 0.07
	p-Cl	180	5.46 ± 0.10
	m-Cl	181	6.26 ± 0.07
	p-Br	62	5.59 ± 0.18
	p-Cl	80	4.95 ± 0.13
	m-Cl	103	6.22 ± 0.07
	p-NH₂	56	5.56 ± 0.07
	p-CN	58	5.38 ± 0.08
	p-Cl	70	6.58 ± 0.07
	m-Cl	76	6.46 ± 0.03
	m-Cl	110	4.74 ± 0.12
	p-Cl	111	5.27 ± 0.10

Table 4.10. pA₂ values at the isolated guinea pig ileum (mono- and di-substituted open compounds).

The series of acylamino substituted compounds (**99**, **112** – **117**) revealed pA_2 values of only a moderate range (table 4.11). Unlike observed at the mono-substituted compounds, the position of the Cl substituent at the aniline moiety turned out to have no distinct influence on the pharmacological behaviour at gpH₁R when combined with a bigger acylamino group in *p*-position of the benzoic acid moiety. For example, **99** represents the most potent acylamino derivative, although a Cl substituent in the gpH₁R-detrimental *p*-position of the aniline moiety is contained. Furthermore, compounds bearing a Cl substituent in the gpH₁R-advantageous *m*-position of the aniline moiety (**116**, **117**) did not show any improved affinity to the receptor.

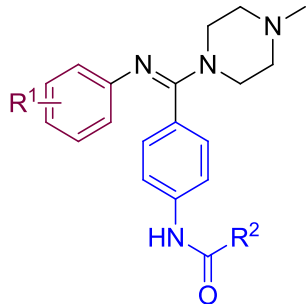
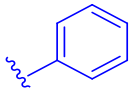
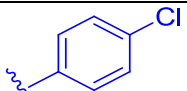
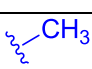
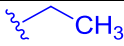
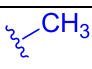
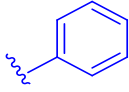
	R ¹	R ²		pA_2 (gp-ileum), slope = 1
	p-Cl		99	5.81 ± 0.09
	p-Cl		112	5.10 ± 0.16
	p-Cl		114	5.06 ± 0.14
	p-Cl		115	4.68 ± 0.19
	m-Cl		116	5.24 ± 0.09
	m-Cl		117	5.13 ± 0.14

Table 4.11. pA_2 values at the isolated guinea pig ileum (acylamino substituted compounds).

4.4.2.2. Characterization of the closed dibenzo[*b,f*][1,4]-oxazepine derivatives

With regard to the pA_2 values, the dibenzo[*b,f*][1,4]-oxazepine derivatives were clearly superior to the corresponding open counterparts and the dimeric derivatives. For all determined SARs, the unsubstituted closed compound **141** serves as a reference (table 4.12). The insertion of an NH₂ group in position 3 had a slightly detrimental

influence on the affinity to the gpH₁R (**136**). Cl substitution in position 3 had beneficial effects (**149**), resulting in the most potent “ring-closed” VUF 6884 derivative at the isolated guinea pig ileum (p (**149/141**) = 0.0034). By contrast, Cl substitution in position 8 and above all position 7 revealed detrimental effects (**88**, **92**). For compound **88**, this describes a discrepancy to the corresponding open counterpart **73**. As already described for hH₁R, a possible explanation could be, that due to the lack of rigidization of the two aromatic rings (aniline and benzoic acid moiety) substituents in *m*-position are – other than substituents in position 8 of a closed and thus rigid dibenzo[*b,h*][1,4]-oxazepine ring system – able to possess different positions in the binding pocket. Di-substitution had no effect on the pharmacological behaviour of the respective closed compounds (**128**, **158**, **159**), however, the striking decrease of gpH₁R affinity detected for compound **129** can be explained with a combination of the two detrimental influences of a 3-NH₂ group and a 7-Cl substituent (table 4.12). Compounds in which the *N*-methylpiperazine moiety was replaced by a piperazine-moiety showed – independent from the substitution pattern – a slight decrease in their affinity to gpH₁R (**193**, **196**, **232** – **235**) (table 4.13).

	R		pA ₂ (gp-ileum), slope = 1
	H	141	8.78 ± 0.04
	8-Cl	88	8.95 ± 0.09
	7-Cl	92	7.63 ± 0.06
	3-Cl	149	9.90 ± 0.12
	3-NH ₂	136	8.23 ± 0.06
	3-NH ₂ , 7-Cl	129	7.88 ± 0.10
	3-NH ₂ , 8-Cl	128	8.88 ± 0.06
	3-Cl, 8-Cl	158	8.78 ± 0.09
	3-Cl, 7-Cl	159	8.80 ± 0.09

Table 4.12. pA₂ values at the isolated guinea pig ileum (“ring-closed” compounds bearing an *N*-methylpiperazine moiety).

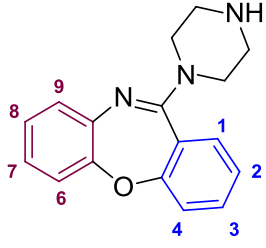
	R		pA ₂ (gp-ileum), slope = 1
	H	233	7.77 ± 0.06
	8-Cl	234	8.64 ± 0.06
	7-Cl	235	7.97 ± 0.08
	3-Cl	232	8.91 ± 0.08
	3-Cl, 7-Cl	193	8.04 ± 0.04
	3-Cl, 8-Cl	196	8.59 ± 0.05

Table 4.13. pA₂ values at the isolated guinea pig ileum (“ring-closed” compounds bearing a piperazine moiety).

In summary, the reported SARs of the open and “ring-closed” VUF 6884 derivatives at the isolated guinea pig ileum are shown in figure 4.16.

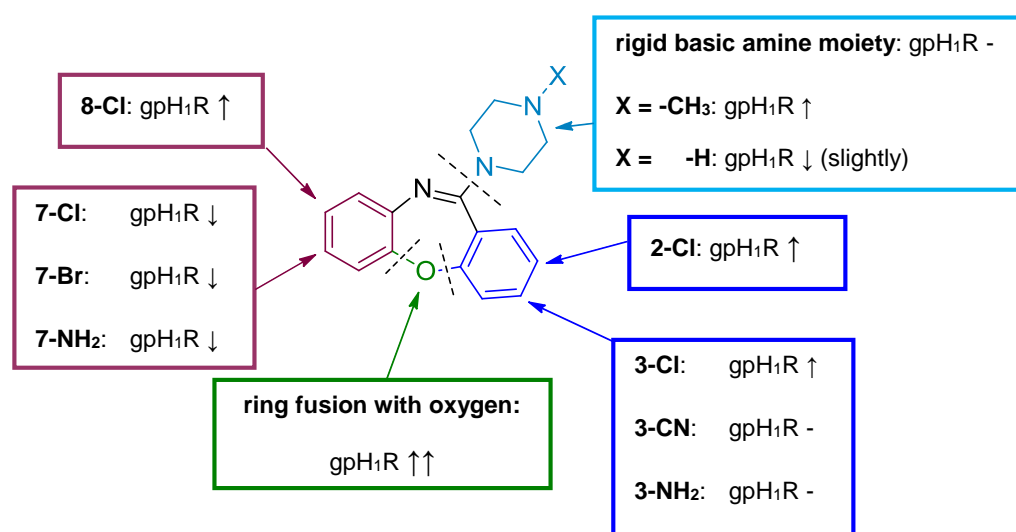


Figure 4.16. SARs of the open and “ring-closed” compounds at the isolated guinea pig ileum.

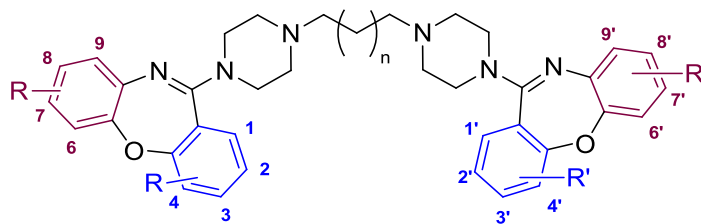
4.4.2.3. Characterization of the dimeric dibenzo[*b,f*][1,4]-oxazepine derivatives

The dimeric compounds revealed pA_2 values in the center span between the “open” and the “ring-closed” compounds, reflected in pA_2 values in a range of 5.93 – 7.89. Although the pA_2 values were in all cases decreased compared to the respective monomeric “ring-closed” compounds, it can be suggested that the gpH_1R is less sensitive to modifications of the molecule size (i.e., dimerization) than to modifications of the central heterocycle. Specific deflections between the different compounds (depending on the spacer type or the linking position) are discussed in the following.

4.4.2.3.1. Dimeric “ring-closed” VUF 6884 derivatives linked by nonpolar alkyl spacers at the piperazine moiety

Compared to the respective monomeric “ring-closed” compounds (**158** and **159**), all derived dimeric compounds (**205 – 210**, **212**, **213**) revealed a distinct decrease of affinity to the gpH_1R , reflected in pA_2 values in a range of 5.93 – 7.16. Independent of the substitution pattern a slight indisposition of compounds linked by spacers with $n = 8$ (**208**, **210**) could be observed: the detected pA_2 values were by approximately 0.5 orders of magnitude lower.

By contrast, alike already observed in the binding studies at hH_1R , compounds linked by a spacer with $n = 7$ (**205**, **206**) revealed a dependence on the position of the Cl substituents: again, for substituents in position 7 / 7' and 3 / 3' (**206**) the hH_1R affinity was by approximately 2 orders of magnitude higher compared to its 8 / 8' and 3 / 3' substituted analogue (**205**) (table [4.14](#))

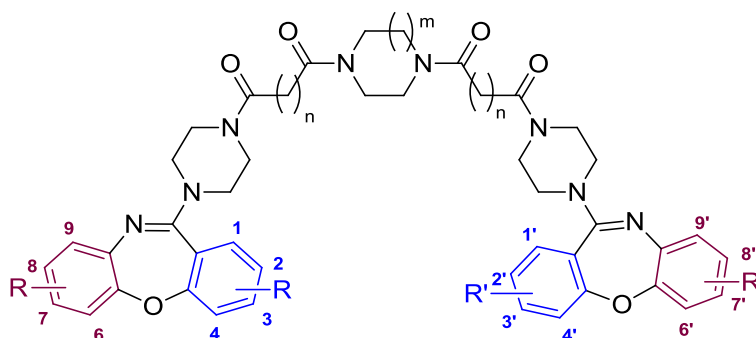


R / R'	n		pA ₂ (gp-ileum, slope = 1)
8 / 8' -Cl, 3 / 3' -Cl	6	212	6.70 ± 0.08
8 / 8' -Cl, 3 / 3' -Cl	7	205	6.75 ± 0.06
8 / 8' -Cl, 3 / 3' -Cl	8	208	5.93 ± 0.08
8 / 8' -Cl, 3 / 3' -Cl	10	207	6.14 ± 0.06
7 / 7' -Cl, 3 / 3' -Cl	6	213	6.55 ± 0.06
7 / 7' -Cl, 3 / 3' -Cl	7	206	7.21 ± 0.06
7 / 7' -Cl, 3 / 3' -Cl	8	210	6.20 ± 0.06
7 / 7' -Cl, 3 / 3' -Cl	10	209	6.49 ± 0.05

Table 4.14. pA₂ values at the isolated guinea pig ileum (dimeric “ring-closed” compounds linked by nonpolar alkyl spacers at the piperazine moiety).

4.4.2.3.2. Dimeric “ring-closed” VUF 6884 derivatives linked by polar spacers at the piperazine moiety

Among the group of the dimeric “ring-closed” VUF 6884 derivatives linked by polar spacers at the piperazine moiety, a preference of compounds bearing a 3 / 3'-Cl substituent was revealed, reflected in pA₂ values in a range of 7.03 – 7.37 (**225**, **238**, **239**, **244**). Moreover, their gpH₁R affinity was slightly superior compared to the above described dimeric “ring-closed” VUF 6884 derivatives linked by nonpolar alkyl spacers. Nevertheless, with regard to the potency of the monomeric counterparts, a distinctly dropped gpH₁R affinity was observed, reflected in a decrease of 1.5 – 2.5 log units. (Table 4.15)



R / R'	m	n		pA ₂ (gp-ileum, slope = 1)
H / H	1	2	240	6.72 ± 0.06
8 / 8' -Cl	1	2	241	6.63 ± 0.05
7 / 7' -Cl	1	2	242	6.08 ± 0.08
3 / 3' -Cl	1	2	238	7.22 ± 0.04
8 / 8' -Cl, 3 / 3' -Cl	1	2	225	7.44 ± 0.08
7 / 7' -Cl, 3 / 3' -Cl	1	2	239	7.15 ± 0.08
7 / 7' -Cl, 3 / 3' -Cl	2	3	244	7.12 ± 0.06

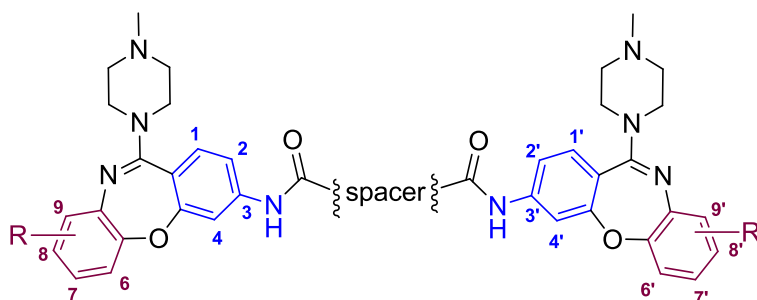
Table 4.15. pA₂ values at the isolated guinea pig ileum (dimeric “ring-closed” compounds linked by polar spacers at the piperazine moiety).

4.4.2.3.3. Dimeric “ring-closed” VUF 6884 derivatives linked at the NH₂ group in position 3 / 3'

Except from compound **215**, the dimeric “ring-closed” VUF 6884 derivatives linked at the NH₂ group in position 3 / 3' revealed pA₂ values in a range ≥ 6.7. Regarding the substitution pattern, a slight preference for compounds bearing an 8 / 8'-Cl substituent was observed. Moreover, in direct comparison of two compounds bearing the same substitution pattern that differ only in their spacer type (piperazine vs. homopiperazine), a preference for the homopiperazine spacer type was shown (**227** / **231**, **229** / **230**, **221** / **243**).

The drop of gpH₁R affinity compared to the corresponding monomeric “ring-closed” VUF 6884 derivatives adds up to 1 – 1.5 log units. This is less distinct than described

for dimeric compounds linked at the piperazine moiety in comparison to their monomeric counterparts. (Table 4.16)



R / R'	spacer		pA ₂ (gp-ileum, slope = 1)
7 / 7' -Cl		215	6.04 ± 0.11
7 / 7' -Cl		227	6.70 ± 0.10
7 / 7' -Cl		231	7.22 ± 0.10
8 / 8' -Cl		229	7.99 ± 0.03
8 / 8' -Cl		230	7.56 ± 0.08
H / H		221	7.05 ± 0.06
H / H		243	7.14 ± 0.05

Table 4.16. pA₂ values at the isolated guinea pig ileum (dimeric “ring-closed” compounds linked at the NH₂ group in position 3 / 3').

4.4.2.4. Estimating the pA₂ values for compounds with slope significantly ≠ 1 (*method A*)

A series of compounds revealed a slope that was significantly ≠ 1 in the Schild plot. Thus, the Schild plot is not suitable to calculate the pA₂ values. For these compounds pA₂ values had to be estimated for every concentration range using the following formula:

$$K_B = \frac{c(B)}{(r - 1)}$$

$$pA_2 \text{ (estimated)} = \log K_B$$

K_B dissociation constant (antagonist to receptor)

c(B) concentration of the antagonist

r 10^{ΔpEC₅₀}

ΔpEC₅₀ pEC₅₀ (His) – pEC₅₀ (His/B)*

(* = with pEC₅₀(His) measured in the absence and pEC₅₀(His/B) in the presence of a defined concentration c of antagonist B)

The calculations of *method A* do not include concentration ranges with depression (< 95%) of the maximal effect of the histamine dose-response curve (higher concentrations of the incubated antagonist; concentration differs from compound to compound). As a consequence, the estimated and the calculated pA₂ values were determined only for lower concentration ranges without depression of the maximal effect.

In the following table, the differences between the estimated pA₂ values (slope ≠ 1) of each single concentration and the calculated pA₂ values (slope = 1) are listed (table [4.17](#))

Cpd.	no depression c(B)	depression c(B)	pA ₂ (estimated)	n	pA ₂ (calculated)	slope
52	1 µM	> 100 µM	5.83 ± 0.33	6	5.19 ± 0.12	0.40
	3.16 µM		5.19 ± 0.47	4		
	10 µM		5.28 ± 0.20	6		
	31.6 µM		4.33 ± 0.15	3		
	100 µM		4.75 ± 0.16	4		
64*	1 µM	> 3.16 µM	5.77 ± 0.09	3	5.24 ± 0.33	1.65
	3.16 µM		4.44 ± 0.06	2		
73	100 nM	> 3.16 µM	7.16 ± 0.29	5	7.08 ± 0.06	0.74
	316 nM		7.02 ± 0.33	5		
	1 µM		7.15 ± 0.19	5		
	3.16 µM		6.84 ± 0.19	5		
76*	1 µM	> 3.16 µM	6.68 ± 0.10	6	6.55 ± 0.05	0.47
	3.16 µM		6.42 ± 0.14	6		
80	316 nM	> 31.6 µM	6.08 ± 0.29	4	5.22 ± 0.18	0.01
	1 µM		5.78 ± 0.36	3		
	3.16 µM		4.98 ± 0.52	5		
	10 µM		4.80 ± 0.44	4		
	31.6 µM		4.04 ± 0.06	2		
99	316 nM	> 3.16 µM	6.14 ± 0.23	3	5.87 ± 0.23	-0.04
	1 µM		5.93 ± 0.00	1		
	3.16 µM		5.02 ± 0.00	1		
110	1 µM	> 100 µM	5.30 ± 0.35	6	4.76 ± 0.17	0.31
	3.16 µM		5.18 ± 0.16	2		
	10 µM		4.89 ± 0.29	4		
	31.6 µM		4.18 ± 0.26	4		
	100 µM		4.39 ± 0.15	2		

Pharmacological section

114	316 nM	> 10 μ M	6.19 \pm 0.18	4	5.48 \pm 0.17	0.19
	1 μ M		5.05 \pm 0.28	3		
	3.16 μ M		5.45 \pm 0.43	4		
	10 μ M		4.73 \pm 0.02	2		
115	1 μ M	> 10 μ M	5.89 \pm 0.07	3	5.16 \pm 0.20	-0.16
	3.16 μ M		4.93 \pm 0.54	4		
	10 μ M		4.73 \pm 0.46	3		
141	3.16 nM	> 316 nM	8.97 \pm 0.19	6	8.89 \pm 0.04	0.85
	10 nM		8.98 \pm 0.05	6		
	31.6 nM		8.85 \pm 0.07	4		
	100 nM		8.91 \pm 0.35	3		
	316 nM		8.67 \pm 0.28	3		
149	0,316 nM	> 3.16 nM	9.34 \pm 0.22	5	9.59 \pm 0.10	1.67
	1 nM		9.70 \pm 0.19	4		
	3.16 nM		10.00 \pm 0.09	2		
158	0.316 nM	> 31.6 nM	9.26 \pm 0.44	4	8.86 \pm 0.12	0.48
	1 nM		9.05 \pm 0.19	4		
	3.16 nM		8.69 \pm 0.44	6		
	10 nM		8.80 \pm 0.49	3		
	31.6 nM		7.74 \pm 0.00	1		
207	100 nM	> 10 μ M	6.48 \pm 0.13	4	5.93 \pm 0.08	0.70
	316 nM		5.77 \pm 0.35	5		
	1 μ M		5.96 \pm 0.33	5		
	3.16 μ M		5.73 \pm 0.34	5		
	10 μ M		5.76 \pm 0.12	3		
208	100 nM	> 3.16 μ M	6.58 \pm 0.26	4	6.17 \pm 0.07	0.61
	316 nM		6.11 \pm 0.29	7		
	1 μ M		6.21 \pm 0.22	7		
	3.16 μ M		5.82 \pm 0.12	4		

Chapter 4

215	31.6 nM	> 10 μ M	6.90 ± 0.32	4	6.14 ± 0.12	0.50
	100 nM		6.72 ± 0.36	4		
	316 nM		5.70 ± 0.56	4		
	1 μ M		5.90 ± 0.22	4		
	3.16 μ M		5.85 ± 0.09	4		
	10 μ M		5.68 ± 0.02	3		
221	31.6 nM	> 10 μ M	7.24 ± 0.37	4	7.08 ± 0.06	0.85
	100 nM		7.21 ± 0.22	4		
	316 nM		7.16 ± 0.13	4		
	1 μ M		6.96 ± 0.25	4		
	3.16 μ M		6.88 ± 0.34	4		
	10 μ M		6.99 ± 0.04	3		
225	10 nM	> 316 nM	7.97 ± 0.27	2	7.37 ± 0.08	0.68
	31.6 nM		7.19 ± 0.02	2		
	100 nM		7.26 ± 0.18	7		
	316 nM		7.34 ± 0.27	6		
227	10 nM	> 1 μ M	7.89 ± 0.39	5	6.96 ± 0.12	0.33
	31.6 nM		7.19 ± 0.23	4		
	100 nM		6.81 ± 0.36	5		
	316 nM		6.77 ± 0.16	5		
	1 μ M		6.32 ± 0.42	4		
235	1 nM	> 316 nM	8.76 ± 0.39	6	8.11 ± 0.09	0.59
	3.16 nM		8.54 ± 0.20	6		
	10 nM		7.87 ± 0.55	4		
	31.6 nM		7.91 ± 0.25	6		
	100 nM		7.78 ± 0.24	6		
	316 nM		7.54 ± 0.17	3		
243	31.6 nM	> 10 μ M	7.53 ± 0.30	4	7.23 ± 0.06	0.85
	100 nM		7.38 ± 0.36	4		

	316 nM		7.23 ± 0.21	4		
	1 μ M		7.18 ± 0.10	4		
	3.16 μ M		6.91 ± 0.23	3		
	10 μ M		7.77 ± 0.07	3		

* as for compounds **64** and **76** no depression of the concentration – effect curve was observed only within two concentration ranges, a Schild plot analysis is not realizable. Within the observed concentration ranges, the pA_2 is estimated to be < 5.0 for compound **64** and ≤ 6.5 for compound **76**.

Table 4.17. Comparison of the estimated and the calculated pA_2 values (n = number of experiments).

Depending on the concentration of the antagonist, the estimated pA_2 values are settled in a broad range that often differ a lot from the calculated values. Moreover, due to the strict restriction criteria of *method A*, many experimental data had to be excluded and did not contribute to the pharmacological overall view of the characterized compounds. Although the estimation of pA_2 values at different concentrations according to *method A* provides a more detailed insight into the pharmacological effects of the characterized compounds above all at lower antagonist concentrations, a further *method B* was pursued to include the pharmacological data detected within higher antagonist concentrations.

4.4.2.5. Estimating the pA_2 values for compounds with slope significantly $\neq 1$ (*method B*)

The previously described *method A* to determine the estimated pA_2 values for compounds with slope significantly $\neq 1$ revealed some specific disadvantages. For example, a huge amount of pharmacologically valuable data had to be excluded from the calculations due to the depression of the maximal effect of the concentration – effect curve ($E_{\max} < 95\%$). Moreover, as a consequence of this limitation, for some compounds the actual concentration range to estimate the pA_2 value comprised at most one log unit in the lower section. The resulting Schild plots revealed to some extent a negative slope and were thus not suitable to draw a significant conclusion.

With intent to provide more reliable estimated pA_2 values, a further *method B* was pursued: therefore, the focus was set on the rightward shift of the concentration – effect curves. In case of a significant rightward-shift (in general ≥ 0.5 log units), all concentration ranges were included in the calculations regardless of a potential depression of the maximal effect. If at all, the lowest concentration ranges were excluded from the calculations due to the lack of control organs and significant rightward shifts of the concentration–effect curves (< 0.5 log units). Although at higher concentrations a significant rightward shift of the concentration–effect curve is assured, in some cases the highest concentration ranges had to be excluded from the calculations due to a huge depression of the maximal effect ($E_{\max} < 10\%$).

The resulting Schild plots of the majority of compounds still revealed a slope significantly $\neq 1$, however, the analyzed data to estimate the pA_2 values are settled in a central and thus more reliable concentration range. The results of this alternate *method B* to estimate the pA_2 value will be summarized in the following table (4.18). A more detailed table comprising the rightward shift of the concentration–effect curves and the resulting pA_2 values sorted by the concentration range will be given for one representative compound (**73**) in table 4.19. Moreover, the results of the two different methods *A* and *B* to estimate the pA_2 values including the resulting Schild plots will be discussed.

Pharmacological section

Cpd.	c(B)	pA ₂ (estimated)	n	pA ₂ (calculated)	slope	intercept (absc.)	pA ₂ (est.)
52	31.6 µM	4.51 ± 0.38	4	4.52 ± 0.09	0.72	4.73	< 5.0
	100 µM	4.73 ± 0.14	6				
	316 µM	4.23 ± 0.25	4				
64*	10 µM	5.00 ± 0.26	4	4.90 ± 0.09	0.62	5.00	< 5.0
	31.6 µM	4.80 ± 0.25	4				
73	316 nM	7.24 ± 0.25	3	6.90 ± 0.07	0.75	7.37	≤ 7.0
	1 µM	7.15 ± 0.19	5				
	3.16 µM	6.84 ± 0.19	5				
	10 µM	7.03 ± 0.22	6				
	31.6 µM	6.43 ± 0.43	5				
76	1µM	6.68 ± 0.10	6	6.47 ± 0.03	0.86	6.69	≤ 6.5
	3.16 µM	6.42 ± 0.14	6				
	10 µM	6.47 ± 0.12	6				
	31.6 µM	6.38 ± 0.27	6				
	100 µM	6.36 ± 0.10	6				
80	10 µM	5.14 ± 0.03	2	4.69 ± 0.12	0.83	4.74	< 5.0
	31.6 µM	4.68 ± 0.10	4				
	100 µM	4.74 ± 0.33	6				
99	1 µM	6.02 ± 0.07	3	5.71 ± 0.09	0.80	5.85	< 5.5
	3.16 µM	5.46 ± 0.06	3				
	10 µM	5.54 ± 0.10	3				
	31.6 µM	5.80 ± 0.00	1				
110	31.6 µM	4.69 ± 0.32	4	4.62 ± 0.07	0.99	4.63	< 5.0
	100 µM	4.49 ± 0.15	4				
	316 µM	4.66 ± 0.23	5				
114	10 µM	4.64 ± 0.10	4	4.55 ± 0.06	0.82	4.55	< 5.0
	31.6 µM	4.60 ± 0.35	4				

	100 μ M	4.40 ± 0.02	4				
115	3.16 μ M	4.48 ± 0.24	2	4.66 ± 0.12	0.96	4.65	< 5.0
	10 μ M	4.87 ± 0.24	5				
	31.6 μ M	4.20 ± 0.31	2				
	100 μ M	4.74 ± 0.15	2				
141	3.16 nM	8.97 ± 0.29	6	8.78 ± 0.04	0.82	9.22	> 8.5
	10 nM	8.98 ± 0.06	6				
	31.6 nM	8.88 ± 0.07	6				
	100 nM	8.95 ± 0.25	6				
	316 nM	8.81 ± 0.25	7				
	1 μ M	8.77 ± 0.15	6				
	3.16 μ M	8.71 ± 0.22	6				
	10 μ M	8.17 ± 0.23	6				
149**	1 nM	9.70 ± 0.17	5	10.13 ± 0.09	1.00	10.14	> 10.0
	3.16 nM	9.96 ± 0.32	5				
	10 nM	10.51 ± 0.55	5				
	31.6 nM	10.82 ± 0.12	5				
	100 nM	10.24 ± 0.10	5				
	316 nM	9.69 ± 0.40	5				
	1 μ M	9.84 ± 0.09	3				
158	1 nM	9.05 ± 0.19	4	8.74 ± 0.09	0.72	9.12	> 8.5
	3.16 nM	8.80 ± 0.33	5				
	10 nM	8.93 ± 0.48	4				
	31.6 nM	8.86 ± 0.19	5				
	100 nM	8.61 ± 0.53	5				
	316 nM	8.17 ± 0.12	2				
207	1 μ M	5.96 ± 0.33	5	5.83 ± 0.08	0.84	5.89	> 5.5
	3.16 μ M	5.73 ± 0.34	5				
	10 μ M	5.81 ± 0.14	4				

Pharmacological section

208	316 nM	6.17 ± 0.26	6	6.06 ± 0.06	0.72	6.13	≤ 6.0
	1 μ M	6.21 ± 0.22	7				
	3.16 μ M	5.96 ± 0.32	5				
	10 μ M	5.84 ± 0.23	4				
215	1 μ M	5.90 ± 0.22	4	5.73 ± 0.05	0.73	5.91	> 5.5
	3.16 μ M	5.85 ± 0.09	4				
	10 μ M	5.67 ± 0.03	4				
	31.6 μ M	5.50 ± 0.22	4				
221	100 nM	7.21 ± 0.21	4	7.04 ± 0.06	0.85	7.22	≥ 7.0
	316 nM	7.16 ± 0.13	4				
	1 μ M	6.96 ± 0.25	4				
	3.16 μ M	6.88 ± 0.39	4				
	10 μ M	6.98 ± 0.04	4				
225	100 nM	7.26 ± 0.18	7	7.32 ± 0.06	1.04	7.29	> 7.0
	316 nM	7.39 ± 0.25	8				
	1 μ M	7.26 ± 0.28	7				
	3.16 μ M	7.37 ± 0.28	5				
227	316 nM	6.77 ± 0.16	5	6.40 ± 0.06	0.73	6.75	> 6.0
	1 μ M	6.43 ± 0.23	4				
	3.16 μ M	6.37 ± 0.15	5				
	10 μ M	6.30 ± 0.04	5				
	31.6 μ M	6.17 ± 0.22	6				
235	31.6 nM	7.91 ± 0.25	6	7.72 ± 0.06	0.85	7.91	> 7.5
	100 nM	7.78 ± 0.24	6				
	316 nM	7.53 ± 0.13	6				
	1 μ M	7.62 ± 0.15	4				
	3.16 μ M	7.66 ± 0.22	4				
243	100 nM	7.45 ± 0.12	3	7.04 ± 0.05	0.84	7.36	≥ 7.0
	316 nM	7.23 ± 0.21	4				

	1 μ M	7.18 ± 0.10	4				
	3.16 μ M	6.93 ± 0.19	4				
	10 μ M	7.03 ± 0.27	5				
	31.6 μ M	6.89 ± 0.16	5				

* As for compound **64** a significant rightward shift of the concentration – effect curve was only observed within two concentration ranges, a Schild plot analysis is not realizable. Within the observed concentration ranges, the pA_2 is estimated to be < 5.0 .

** The pA_2 of compound **149** is most likely ≥ 10.0 . Thus, further organ bath experiments at lower antagonist concentrations were performed in which a longer incubation time (> 15 min) prior to the experiment was carried out in order to achieve equilibrium conditions. However, despite the prolonged incubation time of 1 and 1.5 h, respectively, the pA_2 of compound **149** remained on the same level (10.16 ± 0.05 , slope = 0.7196)

Table 4.18. Comparison of the estimated and the calculated pA_2 values (*method B*); *intercept (absc.)*: calculated intercept point of the Schild plot with the axis of abscissae (slope $\neq 1$).

With intent to give a closer insight into both *method A* and *method B*, for compound **73** a more detailed derivation of the estimated pA_2 value is provided in table [4.19](#). Herein, the restriction criteria of both methods (rightward shift (ΔpEC_{50} , *method B*) and maximal effect (E_{max} , *method A*) of the concentration – effect curves) are listed and for each concentration range, the resulting pA_2 value is quoted. Obviously, above all lower concentration ranges (100 nM – 316 nM) reveal a rather weakly pronounced rightward shift of the concentration effect curve, whereas at higher concentrations ($> 1 \mu$ M) the rightward shift turns more and more distinct. In return, within lower concentration ranges almost no depression of the maximal effect is observed ($< 10 \mu$ M). Higher concentrations $\geq 10 \mu$ M are always attended by a more or less frapping drop of the maximal effect of the concentration–effect curve.

Pharmacological section

	ΔpEC_{50}	$\log (r-1)$	E_{max}	pA_2	$\bar{x} (pA_2) \pm SD$	slope	pA_2 (est.)
100 nM	0.51	0.36	99	7.36	7.29 ± 0.07	0.70	≤ 7.0
	0.50	0.33	100	7.33			
	0.42	0.21	97	7.21			
	0.51	0.35	101	7.35			
	0.43	0.23	99	7.23			
316 nM	0.45	0.26	100	6.76	7.04 ± 0.32		
	0.43	0.23	100	6.73			
	0.92	0.87	96	7.37			
	0.95	0.89	98	7.39			
	0.58	0.45	100	6.95			
1 μM	1.08	1.04	101	7.04	7.15 ± 0.19		
	0.93	0.88	102	6.88			
	1.29	1.26	98	7.26			
	1.28	1.26	97	7.26			
	1.34	1.32	99	7.32			
3.16 μM	1.47	1.45	96	6.95	6.84 ± 0.19		
	1.57	1.56	98	7.06			
	1.12	1.09	97	6.59			
	1.23	1.20	96	6.70			
	1.40	1.38	97	6.88			
10 μM	2.38	2.38	93	7.38	7.03 ± 0.22		
	1.84	1.83	92	6.83			
	1.80	1.80	91	6.80			
	1.92	1.91	84	6.91			
	2.10	2.09	86	7.09			
	2.16	2.15	86	7.15			
31.6 μM	1.92	1.91	70	6.41	6.43 ± 0.43		

	2.22	2.21	66	6.71			
	1.49	1.47	74	5.97			
	1.57	1.56	50	6.06			
	2.50	2.50	77	7.00			
100 μM	2.32	2.32	15	6.32	6.30 \pm 0.13		
	2.46	2.46	1	6.46			
	2.23	2.23	14	6.23			
	2.17	2.17	11	6.17			

Table 4.19. Detailed derivation of the estimated pA₂ value of compound **73**.

The disparity of the different methods becomes more clear by analyzing the resulting Schild plots shown in figure 4.17: **A.** represents the Schild plot comprising all concentration ranges (100 nM – 100 μ M), **B.** represents the Schild plot resulting from *method A* (concentration ranges without depression of the maximal effect, 100 nM – 3.16 μ M) and **C.** represents the Schild plot resulting from *method B* (concentration ranges with significant rightward shift of the concentration–effect curve, 316 nM – 31.6 μ M).

Whereas *method A* focuses on a fairly small region settled at the lower border of the whole concentration range and thus excludes the results of more than one third of the experiments, *method B* comprises a broader field of pharmacological valuable data. These are settled above all in the center span of the whole concentration range. With intent to draw reliable pharmacological conclusions regarding the pA₂ values of compounds with slope \neq 1 in the Schild plot, a combination of both *methods A* and *B* represents a suitable approach. Therefore, the calculations are based on the centrally located concentration ranges with significant rightward shift of the concentration–effect curve that reveal an E_{max} \geq 10 %.

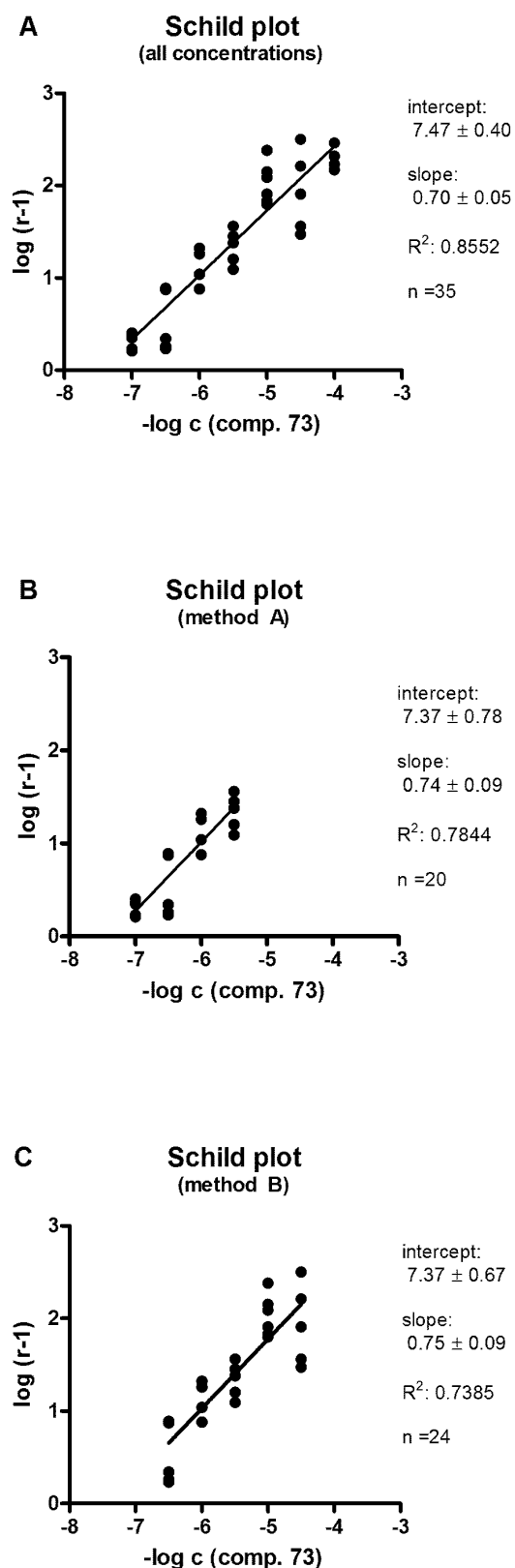


Figure 4.17. Comparison of the Schild plots of compounds **73** resulting from the different methods to determine a reasonable pA_2 value.

4.4.2.6. Comparison of the pK_i (hH₁R) and the pA_2 (gp-ileum)

The SARs determined at hH₁R and gpH₁R are – as reported in the previous sections – in general very similar. Nevertheless, with regard to, e.g., the substitution pattern of the open compounds, the gpH₁R turned out to be more permissive than hH₁R. Due to species differences between the hH₁R and the gpH₁R and the disparity of the testing systems (competition binding assay vs. organ bath experiments), the pA_2 values determined at gpH₁R were in the majority of cases higher than the pK_i values determined at hH₁R. However, exceptions and specific deflections within the different series of compounds will be discussed in the following.

4.4.2.6.1. “Open” VUF 6884 derivatives

All open compounds were characterized to have pK_i values at hH₁R in a range of 3.22 – 6.07, whereas the pA_2 values determined at the isolated guinea pig ileum (gpH₁R) were settled in a range of 4.76 – 7.08. In all cases, the pA_2 values were higher than the pK_i values, what is most pronounced for compounds **25**, **62**, **111**, and **115** ($\Delta \geq 1.5$ log units, $p < 0.0001$). In general, the difference between the determined pA_2 and pK_i values is reflected in a range of 0.5 – 1.8 log units (figure 4.18).

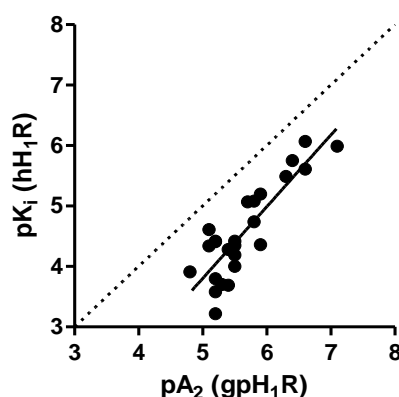


Figure 4.18. Comparison of the pK_i and the pA_2 values at hH₁R and gpH₁R; linear fit, $R^2 = 0.7437$; slope = 1.19 ± 0.15 ; dotted line: line of identity.

4.4.2.6.2. “Ring-closed” VUF 6884 derivatives

Among the series of the “ring-closed” VUF 6884 derivatives the comparison of the pK_i and the pA_2 values revealed some specific particularities: as the pK_i values were innately very high (7.66 – 9.25), the increase of pA_2 values turned out to be less distinct than reported above for the series of the “open” compounds, reflected in a range of 7.59 – 9.59. No significant difference between the pK_i and the pA_2 could be determined for compounds **88**, **232**, and **235**. Some compounds (**92**, **159**, **193**, **196**, **233**) revealed a pA_2 value even lower than the pK_i value (in a range of 0.2 – 0.7 log units). This is most significant for compounds bearing a Cl substituent in position 7 (**92**, **159**, **193**) (**92**: $p = 0.0042$; **159**: $p < 0.0001$; **193**: $p = 0.0247$), what was already reported to have a more detrimental effect on the gpH_1R than on the hH_1R (figure 4.19).

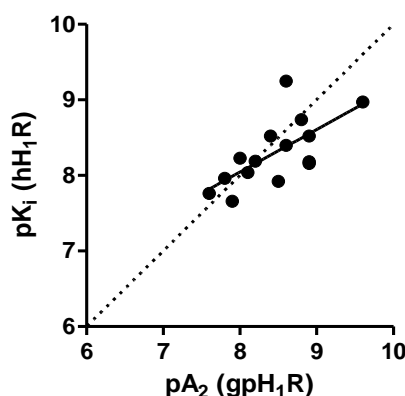


Figure 4.19. Comparison of the pK_i and the pA_2 values at hH_1R and gpH_1R ; linear fit, $R^2 = 0.4566$; slope = 0.56 ± 0.17 ; dotted line: line of identity.

4.4.2.6.3. Dimeric “ring-closed” VUF 6884 derivatives linked by nonpolar alkyl spacers at the piperazine moiety

Within the series of the dimeric compounds linked by nonpolar alkyl spacers at the piperazine moiety the determined pA_2 values (5.93 – 7.16) were in the majority of cases higher than the pK_i values (5.02 – 7.44), reflected in a difference between pA_2 and pK_i values in a range of 0.7 – 1.2 log units. However, compound **206** marks an exception from these findings as the extraordinarily high pK_i value of compound **206** could not to the same extent be reproduced at the isolated guinea pig ileum. The detected pA_2 value was by approximately 0.3 orders of magnitude lower than the pK_i found in the

binding studies at hH₁R. However, in both cases this compound is characterized by a significantly increased affinity to either the hH₁R or the gpH₁R compared to the spare compounds of this series ($p < 0.0001$) (figure 4.20).

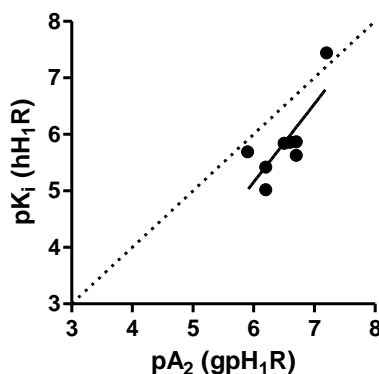


Figure 4.20. Comparison of the pK_i and the pA_2 values at hH₁R and gpH₁R; linear fit, $R^2 = 0.6155$; slope = 1.38 ± 0.45 ; dotted line: line of identity.

4.4.2.6.4. Dimeric “ring-closed” VUF 6884 derivatives linked by polar spacers at the piperazine moiety

Among the group of the dimeric “ring-closed” VUF 6884 derivatives linked by polar spacers at the piperazine moiety the pA_2 values (6.06 – 7.37) were in a range of 0.1 – 1.0 orders of magnitude higher than the determined pK_i values (5.95 – 6.77). Whereas compounds **241** and **242** showed no distinct difference in their affinity to either the hH₁R or the gpH₁R ($\Delta \approx 0.1$), for compounds **238** and **244** a significant difference between the pA_2 and the pK_i value in a range of $\Delta \approx 1.0$ orders of magnitude was revealed ($p < 0.0001$). (Figure 4.21)

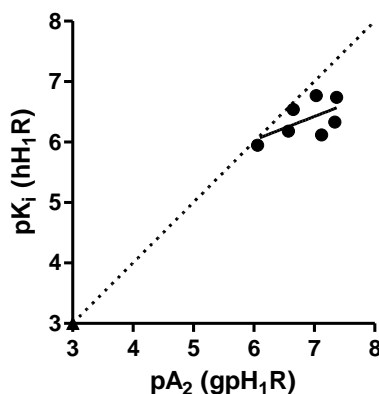


Figure 4.21. Comparison of the pK_i and the pA₂ values at hH₁R and gpH₁R; linear fit, $R^2 = 0.3411$; slope = 0.39 ± 0.24 ; dotted line: line of identity.

4.4.2.6.5. Dimeric “ring-closed” VUF 6884 derivatives linked at the NH₂ group in position 3 / 3’

The group of the dimeric “ring-closed” VUF 6884 derivatives linked at the NH₂ group in position 3 / 3’ is characterized by the highest affinity to the gpH₁R among the dimeric molecules (pA₂ values 6.14 – 7.89). Except from compound **215**, that was already reported to have a significantly lower pK_i value than the spare compounds within this series ((pK_i (hH₁R) = 5.15); $p < 0.0001$), all compounds revealed pA₂ values ≥ 6.7 . Compound **221** strikes with an equal affinity to the hH₁R and the gpH₁R. In general, a difference between the pA₂ values and the pK_i values in a range of 0.4 – 1.2 orders of magnitude is revealed. (Figure 4.22)

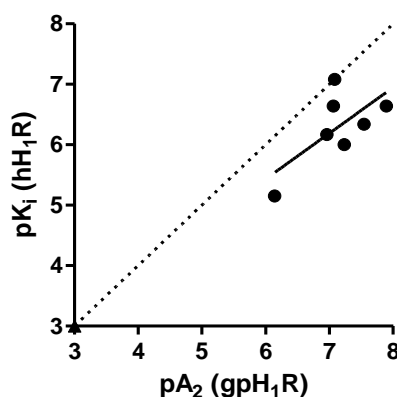


Figure 4.22. Comparison of the pK_i and the pA₂ values at hH₁R and gpH₁R; linear fit, $R^2 = 0.4481$; slope = 0.76 ± 0.38 ; dotted line: line of identity.

4.4.2.6.6. Discussion

The comparison of the pK_i values determined at hH_1R and the pA_2 values determined at gpH_1R revealed in the majority of cases that the characterized compounds were more affine to gpH_1R than to hH_1R (exceptions mentioned above). On the one hand, this can be related to the discrepancy of the testing systems and thus to the different conditions prevalent in the binding- and the organ bath assay, respectively. On the other hand, the different affinities can be traced back to species differences and as a consequence, to significant differences in the pharmacological properties of the receptors: within the TM regions, the identity of the amino acid sequence identity adds up to about 92 %, whereas, e.g., in the extracellular loops, the amino acid sequence identity of hH_1R and gpH_1R accounts for about 70 %. (Strasser et al., 2008, Strasser et al., 2013) In total, they show an overall sequence identity of about 72 %. (Strasser et al., 2008) As transmembrane and extracellular regions are involved in ligand binding (Ji et al., 1998), the discrepancies of the amino acid sequences within these regions are suggested to cause the determined deflections of the affinity to hH_1R and gpH_1R .

4.4.3. Pharmacological characterization of selected compounds at dopamine, serotonin and muscarine receptors

As clozapine is known to show affinity to several GPCRs (Baldessarini and Frankenburg, 1991), for clozapine as well as for selected open (**67**, **70**, **73**, **76**, **56**, **80**, **103**, **99**, **110**, **111**), closed (**88**, **92**, **128**, **129**, **136**, **141**, **149**, **158**, **159**), and dimeric compounds (**205 – 210**, **212**, **213**) competition binding assays at pD_1 / hD_1 , hD_{2short} , hD_{2long} , hD_3 , $hD_{4.4}$, $p5-HT_{1A}$, $p5-HT_2$, hM_1 , hM_2 and hM_3 receptors were performed in cooperation with Prof. Dr. Peter Gmeiner and Dr. Harald Hübner of the Friedrich Alexander University Erlangen. The experimental details were described in 4.3.9.1 (dopamine and serotonin receptors) and 4.3.9.2 (muscarine receptors).

The series of compounds with the pharmacologically most interesting and pronounced effects was, due to the analogy to the clozapine molecule, the monomeric closed dibenzo[*b,f*][1,4]-oxazepine derived series. For all SARs determined among this series,

the unsubstituted compound **141** serves as a reference. Interestingly, one specific SAR was observed for all dopamine, serotonin and muscarine receptors: the significant beneficial effect of a Cl substituent in position 8 (**88**). As clozapine bears the same substitution pattern, this part of the molecule is suggested to be – among others – responsible for its interaction with such a broad variety of GPCRs. Furthermore it is suggested, that alike already observed at histamine receptors (hH₁R, hH₄R, gpH₁R), a closed central oxazepine ring plays an important role and is essential above all for the affinity to dopamine and serotonin receptors.

As the plenty of compounds and receptor subtypes provides a huge amount of pharmacological data, the detailed pharmacological results for each compound and receptor subtype are summarized in tables [4.20](#) – [4.22](#). However, notable specific preferences of the respective receptor subtypes are reported in the following.

4.4.3.1. Porcine and human dopamine receptors pD₁ / hD₁

With regard to the *porcine* D₁R, only the closed compounds evoked pharmacologically interesting effects on a moderate to high level depending on the substitution pattern. Modifications in position 3, either by the insertion of an NH₂ group (**136**) or a Cl substituent (**149**, **159**) led to a decrease in affinity. Cl substitution in position 7, however, slightly improved the affinity to the pD₁R (**92**). Due to its apparent structural similarity to clozapine, compound **88** revealed the highest affinity to the pD₁R.

The dimeric compounds were characterized at the *human* D₁R, however, the observed pharmacological effects were only of a lower range (pK_i ≤ 5).

4.4.3.2. Human dopamine receptors hD_{2short}, hD_{2long} and hD₃

The determined SARs at these three human dopamine receptors were in good agreement. Although the group of the open compounds in general turned out to have a very low affinity to the respective receptors, a beneficial effect of a Cl substituent in *p*- or *m*-position of the benzoic acid moiety was observed (**70**, **76**). Among the dimeric compounds, independent of the substitution pattern a slight preference for compounds linked by a spacer with chain length *n* = 7 was observed (**205**, **206**). Dimeric compounds linked by spacers with chain length *n* = 6 and *n* = 8 showed a dependence

on their substitution pattern (**208, 212**: beneficial effect of a Cl substituent in position 8 / 8').

Regarding the monomeric closed compounds, the insertion of an NH₂ group in position 3 was detrimental (**129, 136**). By contrast, Cl substitution in positions 3 (**149**), 7 (**92**) or 8 (**88, 158**) increased the receptor affinity. Interestingly, the combination of substituents in position 3 and 7 led to a dropped affinity to the hD₃R (**128, 159**).

4.4.3.3. Human dopamine receptor hD_{4.4}^a

The hD_{4.4}R turned out to be very sensitive regarding modifications of the molecule size or the substitution pattern. In the group of the open compounds, only Cl substitution in *p*-position of the benzoic acid moiety was tolerated (**70**). Dimeric compounds showed in general a very weak affinity.

With regard to the monomeric closed compounds, the insertion of an NH₂ group in position 3 turned again out to be detrimental to the receptor affinity (**136, 129**). Compounds bearing a Cl substituent in position 8 (**88, 128, 158**) revealed an increased affinity to the hD_{4.4}, however, further modifications of the substitution pattern had no effects.

(^a: the D₄R shows polymorphism (VNTR) reflected in 2 – 11 repeats of 16 amino acid long sequences within the IL-3. The D_{4.4}R represents the most frequently occurring type, bearing 4 repeats)

4.4.3.4. Porcine serotonin receptors p5-HT_{1A} and p5-HT₂

All “ring-closed” and dimeric compounds showed significantly lower affinity to the p5-HT_{1A} than to p5-HT₂ receptor. Open and dimeric compounds showed almost no pharmacological effects at p5-HT_{1A} (pK_i ≤ 5), and with regard to the monomeric closed compounds substituents other than 8-Cl were not tolerated.

Focussing on the p5-HT₂, the open compounds again revealed almost no pharmacological effect. The dimeric compounds, however, showed in all cases a significantly higher affinity than to p5-HT_{1A}. Among them, similar tendencies as already observed at human dopamine receptors hD_{2short}, hD_{2long} and hD₃ (section 4.4.3.2) were exhibited: compounds linked by a spacer with chain length n = 7 (**205, 206**) showed, independent of the substitution pattern, a slightly increased affinity. Compounds linked

by spacers with chain length $n = 6$ and $n = 8$ showed a dependence on their substitution pattern (**208**, **212**: increased affinity of compounds bearing Cl substituents in position 8 / 8').

The group of the closed monomeric compounds moreover revealed beneficial effects for Cl substitution in position 3 (**149**, **158**, **159**) and 7 (**92**, **159**). As in the majority of receptor subtypes characterized in this study, the insertion of an NH_2 group in position 3 decreased the affinity to p5-HT_{1A} and p5-HT_2 (**136**).

4.4.3.5. Human muscarine receptors hM_1 , hM_2 and hM_3

The role of the closed central oxazepine ring observed for dopamine and serotonin receptors turned out to be less important with regard to human muscarine receptors, what is reflected in a moderate affinity of all open compounds. This is emphasized by a further intriguing finding concerning the nature of the fusion atom between the two phenyl rings: whereas compound **88** (oxygen as fusion atom) was more affine than clozapine (**CLO**) (nitrogen as fusion atom) within the group of the dopamine and serotonin receptors, the human muscarine receptors revealed a preference for clozapine. As a consequence it can be suggested that the effects of oxygen as fusion atom (e.g., 3D structure of the molecule, electronic and steric effects) are of a secondary importance for the interaction with muscarine receptors. Modifications regarding the size of the molecule (e.g., dimerization), however, proved to have detrimental effects on the affinity ($\text{pK}_i \leq 5$).

Focussing on the monomeric closed compounds, an interesting effect was observed: while being responsible for the significant decrease of affinity to all dopamine and serotonin receptors, the insertion of an NH_2 group in position 3 proved to be beneficial for the affinity to all three human muscarine receptors (**136**, **128**, **129**).

↑ open ↓										
	pd ₁	hD ₂ long	hD ₂ short	hD ₃	hD _{4,4^a}	p5-HT _{1A}	p5-HT ₂	hM ₁	hM ₂	hM ₃
CLO	7.45 ± 0.33	7.48 ± 0.13	7.64 ± 0.14	6.62 ± 0.14	7.98 ± 0.13	6.74 ± 0.28	7.81 ± 0.27	8.97 ± 0.15	7.41 ± 0.22	8.10 ± 0.16
67	5.23 ± 0.10	≤ 5	≤ 5	5.59 ± 0.00	≤ 5	≤ 5	≤ 5	6.23 ± 0.07	5.55 ± 0.03	5.78 ± 0.11
70	≤ 5	6.42 ± 0.01	6.46 ± 0.06	6.62 ± 0.21	6.09 ± 0.13	≤ 5	5.53 ± 0.07	6.48 ± 0.23	6.52 ± 0.36	6.14 ± 0.17
73	≤ 5	≤ 5	≤ 5	5.32 ± 0.13	5.51 ± 0.21	≤ 5	≤ 5	6.15 ± 0.00	5.33 ± 0.18	5.50 ± 0.04
76	≤ 5	5.78 ± 0.08	6.06 ± 0.24	6.88 ± 0.17	≤ 5	≤ 5	5.18 ± 0.11	6.62 ± 0.06	6.24 ± 0.45	6.28 ± 0.13
56	≤ 5	≤ 5	≤ 5	5.11 ± 0.02	5.39 ± 0.04	5.12 ± 0.11	≤ 5	6.54 ± 0.16	5.84 ± 0.10	6.59 ± 0.08
80	≤ 5	≤ 5	≤ 5	≤ 5	≤ 5	≤ 5	≤ 5	6.64 ± 0.03	5.80 ± 0.09	6.56 ± 0.10
103	≤ 5	≤ 5	≤ 5	5.10 ± 0.03	≤ 5	≤ 5	≤ 5	6.53 ± 0.07	5.55 ± 0.31	6.37 ± 0.07
99	≤ 5	≤ 5	5.07 ± 0.08	5.25 ± 0.04	5.31 ± 0.11	≤ 5	≤ 5	6.37 ± 0.33	5.61 ± 0.30	5.59 ± 0.04
110	≤ 5	≤ 5	≤ 5	5.09 ± 0.28	≤ 5	≤ 5	≤ 5	5.42 ± 0.17	5.13 ± 0.11	5.17 ± 0.08
111	≤ 5	5.06 ± 0.04	5.68 ± 0.03	6.83 ± 0.08	5.09 ± 0.13	≤ 5	≤ 5	5.11 ± 0.12	5.19 ± 0.43	5.13 ± 0.17

Table 4.20. Pharmacological data of selected open compounds at dopamine, serotonin and muscarine receptor subtypes

closed										
	pD ₁	hD ₂ long	hD ₂ short	hD ₃	hD _{4,4} ^a	p5-HT _{1A}	p5-HT ₂	hM ₁	hM ₂	hM ₃
CLO	7.45 ± 0.33	7.48 ± 0.13	7.64 ± 0.14	6.62 ± 0.14	7.98 ± 0.13	6.74 ± 0.28	7.81 ± 0.27	8.97 ± 0.15	7.41 ± 0.22	8.10 ± 0.16
88	8.17 ± 0.16	7.86 ± 0.12	7.89 ± 0.12	7.24 ± 0.10	8.69 ± 0.22	7.34 ± 0.28	8.63 ± 0.06	8.65 ± 0.06	7.20 ± 0.04	8.06 ± 0.23
92	7.69 ± 0.15	6.85 ± 0.00	7.05 ± 0.08	6.30 ± 0.33	7.04 ± 0.46	6.03 ± 0.13	8.24 ± 0.16	7.21 ± 0.08	6.79 ± 0.29	6.87 ± 0.21
141	7.24 ± 0.05	6.21 ± 0.13	6.23 ± 0.02	6.18 ± 0.07	6.85 ± 0.04	7.07 ± 0.21	7.81 ± 0.07	7.59 ± 0.31	6.70 ± 0.24	7.31 ± 0.34
149	6.78 ± 0.06	6.68 ± 0.09	6.72 ± 0.03	6.58 ± 0.16	6.81 ± 0.06	5.71 ± 0.08	8.72 ± 0.15	7.48 ± 0.26	6.65 ± 0.01	6.74 ± 0.03
158	7.21 ± 0.14	7.65 ± 0.01	7.71 ± 0.16	7.29 ± 0.12	7.36 ± 0.07	5.44 ± 0.09	9.35 ± 0.10	7.82 ± 0.23	6.54 ± 0.34	7.02 ± 0.20
159	6.57 ± 0.28	6.68 ± 0.06	6.94 ± 0.14	6.43 ± 0.27	6.33 ± 0.07	5.30 ± 0.13	8.74 ± 0.18	7.06 ± 0.14	6.34 ± 0.38	6.40 ± 0.16
128	7.12 ± 0.16	6.67 ± 0.10	6.69 ± 0.01	6.33 ± 0.04	7.30 ± 0.13	5.83 ± 0.39	7.98 ± 0.10	9.54 ± 0.26	8.12 ± 0.29	9.13 ± 0.18
129	7.04 ± 0.53	5.44 ± 0.13	5.60 ± 0.00	5.48 ± 0.04	5.24 ± 0.66	5.24 ± 0.13	7.61 ± 0.01	8.30 ± 0.03	7.02 ± 0.28	8.32 ± 0.15
136	6.19 ± 0.10	≤ 5	≤ 5	5.27 ± 0.75	5.51 ± 0.10	5.53 ± 0.13	7.14 ± 0.12	8.39 ± 0.20	7.23 ± 0.20	8.22 ± 0.23

Table 4.21. Pharmacological data of selected “ring-closed” compounds at dopamine, serotonin and muscarine receptor subtypes

↑ dimeric ↓										
	hD ₁	hD ₂ long	hD ₂ short	hD ₃	hD _{4,4^a}	p5-HT _{1A}	p5-HT ₂	hM ₁	hM ₂	hM ₃
CLO	7.45 ± 0.33	7.48 ± 0.13	7.64 ± 0.14	6.62 ± 0.14	7.98 ± 0.13	6.74 ± 0.28	7.81 ± 0.27	8.97 ± 0.15	7.41 ± 0.22	8.10 ± 0.16
205	≤ 5	6.25 ± 0.22	6.29 ± 0.17	6.22 ± 0.17	5.28 ± 0.31	≤ 5	7.23 ± 0.08	≤ 5	≤ 5	≤ 5
206	≤ 5	6.06 ± 0.19	6.40 ± 0.05	6.16 ± 0.09	5.67 ± 0.26	≤ 5	7.40 ± 0.07	5.19 ± 0.34	≤ 5	≤ 5
207	≤ 5	5.32 ± 0.27	5.49 ± 0.32	5.49 ± 0.34	≤ 5	≤ 5	6.47 ± 0.15	≤ 5	≤ 5	≤ 5
208	≤ 5	5.93 ± 0.26	6.10 ± 0.09	5.81 ± 0.11	≤ 5	≤ 5	6.95 ± 0.17	≤ 5	≤ 5	≤ 5
209	≤ 5	≤ 5	≤ 5	≤ 5	≤ 5	≤ 5	6.87 ± 0.06	≤ 5	5.41 ± 0.06	≤ 5
210	≤ 5	≤ 5	≤ 5	5.14 ± 0.18	≤ 5	≤ 5	6.29 ± 0.10	≤ 5	≤ 5	≤ 5
212	≤ 5	6.44 ± 0.38	6.84 ± 0.15	6.45 ± 0.14	5.55 ± 0.29	≤ 5	7.17 ± 0.11	≤ 5	≤ 5	≤ 5
213	≤ 5	5.65 ± 0.07	5.44 ± 0.29	5.52 ± 0.20	≤ 5	≤ 5	6.65 ± 0.25	≤ 5	≤ 5	≤ 5

Table 4.22. Pharmacological data of selected dimeric compounds at dopamine, serotonin and muscarine receptor subtypes

4.4.4. Functional assays at human histamine receptors: pharmacological results of steady state [^{33}P]GTPase activity assays and [^{35}S]GTP γ S binding assays

For all closed compounds as well as for the most promising dimeric compounds functional assays at hH₁R and hH₄R were performed. Furthermore, for a small series among this selection, selectivity investigations were performed with regard to the four human histamine receptor subtypes (hH₁₋₄R).

4.4.4.1. Steady-state [^{33}P]GTPase activity assays at hH₁R

All assays were carried out using Sf9 cell membranes co-expressing hH₁R and the regulator of G-protein coupling RGS4. Alike the results reported for the functional assays at gpH₁R, all characterized compounds revealed a functional antagonism at hH₁R that was determined in the “agonist mode” of the steady-state [^{33}P]GTPase activity assay (figure 4.23).

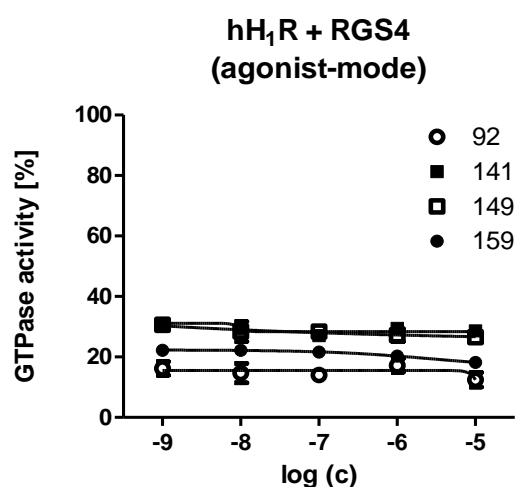


Figure 4.23. Agonist mode of the steady-state [^{33}P]GTPase activity assay at hH₁R proving functional antagonism of the tested compounds **92** (7-Cl), **141** (*not substituted*), **149** (3-Cl), **159** (3-Cl, 7-Cl).

In most cases the pK_B values determined in the steady-state [^{33}P]GTPase activity assays were lower than the pK_i values determined in the binding studies at hH₁R (table 4.23). The SARs that were detected in the binding assays in dependence of the

substitution pattern could be reproduced, however, in a more alleviated way. Among the dimeric compounds, no distinct difference of affinity between compounds linked at the piperazine moiety (**225**, **239**) and compounds linked at the free NH₂ group in position 3 / 3' (**229**, **231**) could be observed.

Figure 4.24 shows the data obtained in the antagonist mode of the steady-state [³³P]GTPase activity assay for compounds **159**, **193** and **239**, as they form a successional series within the tested compounds. Both, **159** and its marginally modified analogue **193** revealed an almost identical pK_B value (**159**: 7.97 ± 0.10; **193**: 7.81 ± 0.14), emphasizing a less important role of the basic piperazine-moiety. However, dimerization with a polar spacer (**239**) led to a significant decrease of the pK_B value (**239**: 6.51 ± 0.20; p (**239/159**, **193**) < 0.0001).

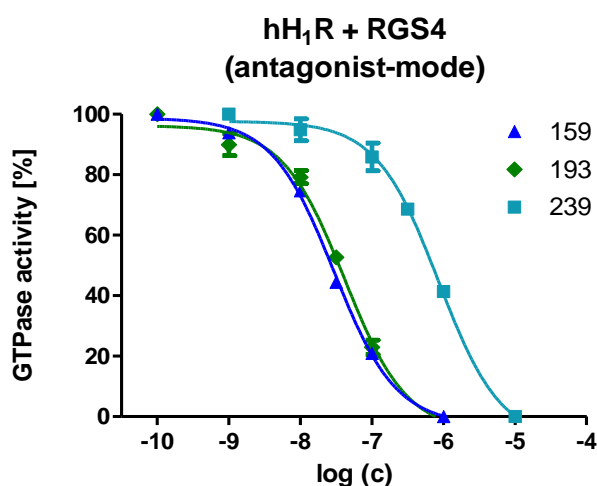


Figure 4.24. Antagonist mode of the steady-state [³³P]GTPase activity assay at hH₁R for compounds **159** (3-Cl, 7-Cl), **193** (*piperazine bearing analogue of 159*) and **239** (*dimeric analogue of 159, linked by a polar spacer*); 10⁻¹⁰ molar ligand concentration + 200 nM histamine was set to 100 %.

Cpd.	pK_i^a	pK_B^b	Hill slope^b
88	8.19 ± 0.13	8.03 ± 0.20	-1.48 ± 0.65
92	7.76 ± 0.11	7.85 ± 0.11	-0.96 ± 0.29
128	8.18 ± 0.16	8.24 ± 0.20	-0.94 ± 0.31
129	7.66 ± 0.19	7.71 ± 0.26	-0.69 ± 0.39
141	8.16 ± 0.22	8.35 ± 0.26	-0.66 ± 0.18
149	8.97 ± 0.04	8.67 ± 0.10	-1.10 ± 0.49
158	8.52 ± 0.05	8.27 ± 0.25	-1.40 ± 0.68
159	9.25 ± 0.16	7.97 ± 0.10	-1.04 ± 0.47
193	8.23 ± 0.11	7.81 ± 0.14	-1.40 ± 0.37
196	8.52 ± 0.03	8.26 ± 0.22	-0.98 ± 0.40
225	6.74 ± 0.10	6.50 ± 0.14	-1.15 ± 0.26
229	6.64 ± 0.10	6.59 ± 0.21	-0.69 ± 0.67
231	6.64 ± 0.02	6.45 ± 0.11	-1.01 ± 0.31
232	8.74 ± 0.08	8.39 ± 0.22	-1.06 ± 0.29
233	7.96 ± 0.03	8.03 ± 0.16	-1.66 ± 0.44
234	8.40 ± 0.02	8.20 ± 0.23	-1.29 ± 0.14
235	8.04 ± 0.12	7.96 ± 0.24	-1.09 ± 0.22
239	6.77 ± 0.09	6.51 ± 0.20	-1.18 ± 0.52

Table 4.23. pK_B values determined for selected compounds in the steady-state [³³P]GTPase activity assay at hH₁R + RGS4 (^a = data obtained from the competition binding assay at hH₁R + RGS4; ^b = data obtained from the steady-state [³³P]GTPase activity assay at hH₁R + RGS4)

4.4.4.2. [³⁵S]GTPγS binding assays at hH₄R

With intent to get a closer insight into the functional activity of some selected compounds at hH₄R, [³⁵S]GTPγS binding assays were carried out using Sf9 cell membranes co-expressing hH₄R + G_{αi2} + G_{β1γ2}. In all cases, a partial agonism could be observed, what is in good agreement with the data published for clozapine (Appl et al., 2012) and VUF 6884 (Smits et al., 2006). The partial agonistic effects (E_{\max}) are quoted in relation to histamine that was determined at a concentration of 10 μM and set to 1.0. All compounds revealed partial agonistic effects in a range of 0.34 – 0.68 of the histamine effect. The pEC₅₀ values detected in the [³⁵S]GTPγS binding assays at hH₄R were either lower or equal to the pK_i values determined in the competition binding assays at hH₄R. In addition to that, the SARs in dependence of the substitution pattern could be reproduced, above all with regard to the known hH₄R beneficial Cl substitution in position 7 (**92**, **129**, **159**, **235**). Figure 4.25 shows the [³⁵S]GTPγS binding assay at hH₄R for compounds **92**, **129**, **159**, and **231**, as they are all characterized by a Cl substituent in position 7 and a free *N*-methylpiperazine moiety. The most potent representative within this series, compound **159** (pEC₅₀: 6.96 ± 0.15) additionally carries a Cl substituent in position 3. The insertion of an NH₂ group (**129**) or the dimerization by spacers linked in this position (**231**) led to a decreased pEC₅₀ value (**129**: 6.40 ± 0.13; **231**: 5.73 ± 0.20). As expected, the exchange of the *N*-methylpiperazine moiety by piperazine (**193**, **196**, **232** – **235**) had a detrimental effect on the hH₄R affinity, reflected in pEC₅₀ values decreased in a range of 0.5 – 1.0 log units. (Table 4.24)

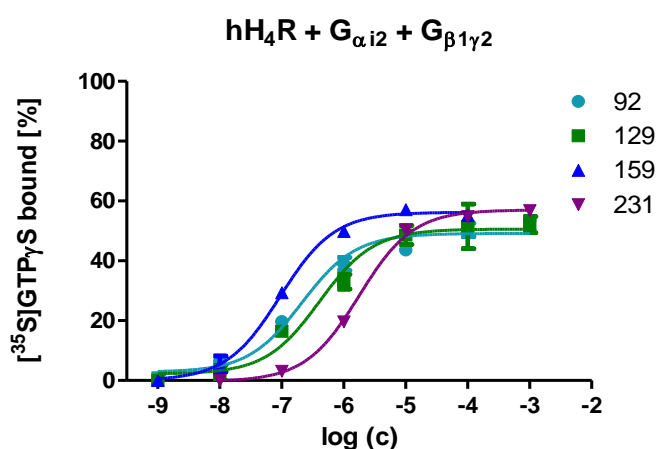


Figure 4.25. [³⁵S]GTPγS binding assay of compounds **92** (7-Cl), **129** (3-NH₂, 7-Cl), **159** (3-Cl, 7-Cl) and **231** (*dimeric analogue of 129, linked in position 3*) at hH₄R.

Cpd.	pK _i ^a	pEC ₅₀ ^b	E _{max} ^{b, c}
88	6.64 ± 0.14	6.20 ± 0.05	0.55 ± 0.19
92	6.99 ± 0.03	6.58 ± 0.19	0.45 ± 0.19
128	6.11 ± 0.13	6.11 ± 0.16	0.35 ± 0.08
129	6.48 ± 0.09	6.40 ± 0.13	0.35 ± 0.14
141	6.19 ± 0.23	6.16 ± 0.04	0.62 ± 0.14
149	6.13 ± 0.09	6.08 ± 0.05	0.68 ± 0.20
158	6.27 ± 0.23	6.20 ± 0.24	0.57 ± 0.16
159	6.96 ± 0.16	6.96 ± 0.15	0.55 ± 0.12
193	5.92 ± 0.12	5.87 ± 0.12	0.50 ± 0.18
196	5.62 ± 0.06	5.39 ± 0.09	0.48 ± 0.10
231	5.74 ± 0.21	5.73 ± 0.20	0.61 ± 0.01
232	5.35 ± 0.03	5.35 ± 0.19	0.40 ± 0.07
233	5.33 ± 0.16	5.21 ± 0.15	0.37 ± 0.09
234	6.08 ± 0.06	5.76 ± 0.10	0.38 ± 0.12
235	6.57 ± 0.16	6.11 ± 0.07	0.34 ± 0.11

Table 4.24. pEC₅₀ values and E_{max} data determined for selected compounds in the [³⁵S]GTPγS binding assay at hH₄R + G_{αi2} + G_{β1γ2}; (^a = data obtained from the competition binding assay at hH₄R + G_{αi2} + G_{β1γ2}; ^b = data obtained from the [³⁵S]GTPγS binding assay at hH₄R + G_{αi2} + G_{β1γ2}; ^c = the efficacy of histamine was determined at a concentration of 10 μM and set to 100 % (= 1.0).

4.4.4.3. [³⁵S]GTPγS binding assays at hH₂R and hH₃R (selectivity studies)

With regard to the human histamine receptor subtype selectivity, [³⁵S]GTPγS binding assays at hH₂R and hH₃R were performed. Therefore, Sf9 cell membranes co-expressing hH₂R-G_{sαS} and hH₃R + G_{αi2} + G_{β1γ2} were used, respectively. All characterized compounds revealed an inverse agonism at both the hH₂R and the hH₃R. The determined pEC₅₀ values at either the hH₂R or the hH₃R were significantly lower than the pK_B and pEC₅₀ values detected in the steady-state [³³P]GTPase activity assay at hH₁R and in the [³⁵S]GTPγS binding assay at hH₄R, indicating a distinct preference for the target receptors. The inverse agonistic efficacies (inv. eff.) are

quoted in relation to histamine that was determined at a concentration of 10 μM and set to 1.0. As a result, all compounds revealed inverse agonistic efficacies in a range of -0.31 to -0.15 at hH_2R and -0.39 to -0.19 at hH_3R . Interestingly, compound **128** revealed the highest inverse agonistic efficacy to both the hH_2R and the hH_3R , whereas compound **136** revealed in both cases the lowest inverse agonistic efficacies. Moreover, compound **159** turned out to have the highest potencies at hH_2R and hH_3R , however, regarding the high hH_1R and hH_4R affinity (pK_B (hH_1R) = 7.54 ± 0.10 ; pEC_{50} (hH_4R) = 6.96 ± 0.15), a selectivity towards the target receptors is still given. (Figures 4.26, 4.27, table 4.25)

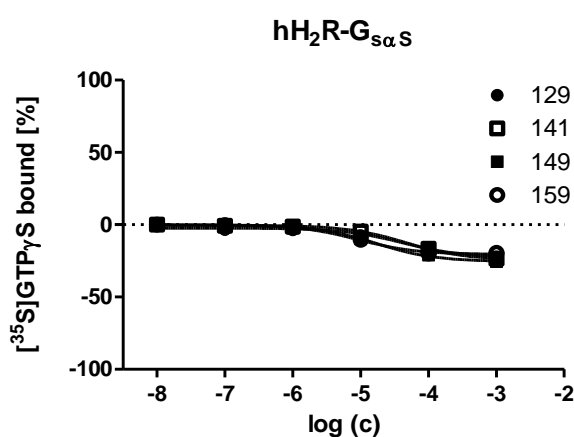


Figure 4.26. [³⁵S]GTP_γS binding assay of compounds **129** (3-NH₂, 7-Cl), **141** (*no substitution*), **149** (3-Cl) and **159** (3-Cl, 7-Cl) at $\text{hH}_2\text{R-G}_{\text{s}\alpha\text{S}}$ revealing an inverse agonism.

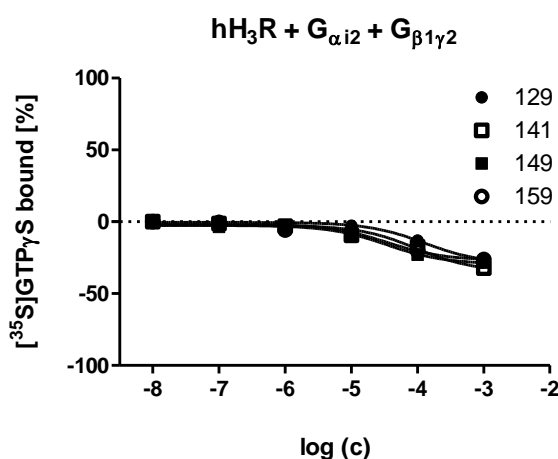


Figure 4.27. [³⁵S]GTP_γS binding assay of compounds **129** (3-NH₂, 7-Cl), **141** (*no substitution*), **149** (3-Cl) and **159** (3-Cl, 7-Cl) at $\text{hH}_3\text{R} + \text{G}_{\alpha\text{i}2} + \text{G}_{\beta1\gamma2}$ revealing an inverse agonism.

Cpd.	hH ₂ R		hH ₃ R	
	pEC ₅₀	Inv. eff. ^a	pEC ₅₀	Inv. eff. ^a
128	3.96 ± 0.11	-0.31 ± 0.03	3.73 ± 0.21	-0.39 ± 0.01
129	4.37 ± 0.04	-0.24 ± 0.02	3.97 ± 0.11	-0.32 ± 0.03
136	4.20 ± 0.05	-0.15 ± 0.03	4.42 ± 0.19	-0.19 ± 0.03
141	3.98 ± 0.34	-0.26 ± 0.02	4.01 ± 0.08	-0.32 ± 0.03
149	4.84 ± 0.10	-0.22 ± 0.06	4.40 ± 0.08	-0.28 ± 0.01
158	4.74 ± 0.12	-0.21 ± 0.04	4.20 ± 0.17	-0.28 ± 0.01
159	5.01 ± 0.06	-0.19 ± 0.02	4.46 ± 0.02	-0.26 ± 0.01

Table 4.25. pEC₅₀ values and E_{max} data determined for selected compounds in the [³⁵S]GTPγS binding assay at hH₂R-G_{sαS} and hH₃R + G_{αi2} + G_{β1γ2}; ^a the efficacy of histamine was determined at a concentration of 10 μM and set to 100 % (= 1.0).

4.5. Discussion

4.5.1. Structure activity relationships of a selected core compound prevalent within all series: compounds bearing Cl substituents in position 3 and 7 / *p*- position of the aniline and the benzoic acid moiety (related to 159)

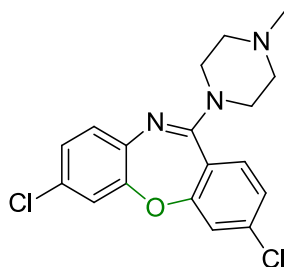
The pharmacologically most promising compound **159** finds itself within all structurally modified series described above. In the course of the different structural conversions, specific structure-activity as well as structure-selectivity relationships could be observed that contribute to a better understanding of the interaction of VUF 6884 derived ligands with the H₁R and the H₄R on a molecular level.

As already reported in previous sections, Cl substitution in *p*-position of the aniline moiety revealed a beneficial effect on the affinity to the H₄R. However, regarding the H₁R affinity, no effect on the affinity related to the substituents could be observed. Moreover, the central molecule core lacks rigidization and thus the affinities remain in general on a moderate level (figure 4.28).

180	pK_i (hH₁R) = 4.74 ± 0.04	pK_i (hH₄R) = 5.60 ± 0.09	pA₂ (gpH₁R) = 5.75 ± 0.13
------------	--	--	---

Figure 4.28. Pharmacological data of compound **180** (“open” analogue of **159**).

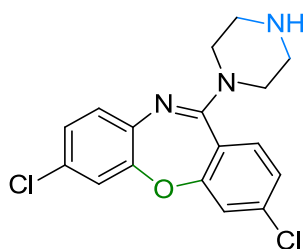
The closure of the central oxazepine ring evokes an increase of affinity to the hH₁R in a range of about 4.5 orders of magnitude and to the hH₄R in a range of about 1.4 orders of magnitude. With regard to the gpH₁R, an increase of affinity of about 3 orders of magnitude was observed. These results point out that the part of the molecule marked in green (e.g., the central oxazepine ring) plays a key role in the ligand-receptor interaction (figure 4.29).



159	pK_i (hH₁R) = 9.25 ± 0.16	pK_i (hH₄R) = 6.96 ± 0.16	pA₂ (gpH₁R) = 8.63 ± 0.13
------------	--	--	---

Figure 4.29. Pharmacological data of compound **159**.

But not only the central oxazepine ring plays an important role in the interaction with the target receptors, also the *N*-methylpiperazine moiety was found to be crucial at least for the affinity to the hH₄R. When replaced by piperazine, the hH₄R affinity drops down to almost the level of the “open” analogue. The affinity to the hH₁R and the gpH₁R was less affected, however, a decrease in a range of about one order of magnitude was observed (figure 4.30).

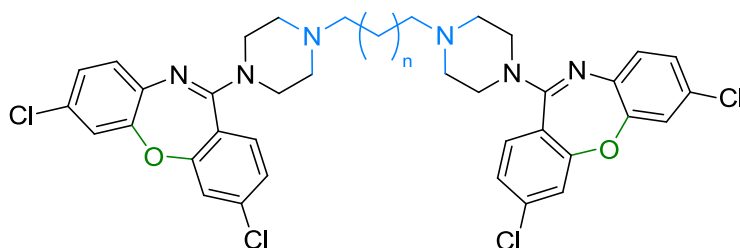


193	pK_i (hH₁R) = 8.23 ± 0.11	pK_i (hH₄R) = 5.92 ± 0.12	pA₂ (gpH₁R) = 7.97 ± 0.05
------------	--	--	---

Figure 4.30. Pharmacological data of compound **193** (*piperazine-bearing analogue of 159*).

With intent to address (homo- or hetero-) dimeric hH₁Rs / hH₄Rs and thus to increase the potency of compound **159**, several attempts to obtain dimeric molecules were carried out modifying the spacer length within the molecule. However, the affinity of the resulting dimeric molecules to the target receptors was significantly decreased compared to the monomer **159**. An exception marks **206**, maintaining an H₁R affinity (human and guinea pig) on a moderate high level: it is suggested that this compound addresses only monomeric H₁Rs and additionally interacts with the extracellular surface of the H₁R.

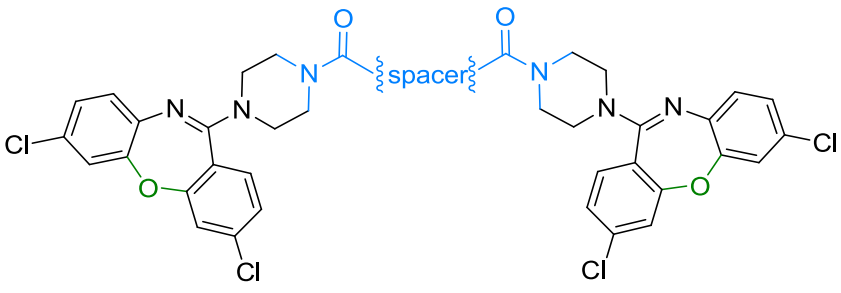
Regarding the hH₄R, a complete loss of affinity was the consequence of the dimerization. This can be traced back to the important role of a (free) *N*-methylpiperazine moiety in hH₄R binding, as it is prevalent in the H₄R antagonist JNJ7777120 (Jablonowski et al., 2003), in several 2-aminopyrimidines targeting the hH₄R (Altenbach et al., 2008) as well as in the VUF6884 molecule (Smits et al., 2006). (Figure 4.31)



213	n = 6	pK_i (hH₁R) = 5.87 ± 0.16	pK_i (hH₄R) = < 5	pA₂ (gpH₁R) = 6.67 ± 0.05
206	n = 7	pK_i (hH₁R) = 7.44 ± 0.16	pK_i (hH₄R) = < 5	pA₂ (gpH₁R) = 7.16 ± 0.09
210	n = 8	pK_i (hH₁R) = 5.02 ± 0.20	pK_i (hH₄R) = < 5	pA₂ (gpH₁R) = 6.22 ± 0.09
209	n = 10	pK_i (hH₁R) = 5.84 ± 0.09	pK_i (hH₄R) = < 5	pA₂ (gpH₁R) = 6.54 ± 0.05

Figure 4.31. Pharmacological data of compounds **206**, **209**, **210** and **213** (*dimeric analogues of 159 linked by nonpolar alkyl-spacers*).

Although the H₄R affinity was still on a very low level, the affinity to the H₁R profited from the insertion of polar piperazine or homopiperazine bearing spacers. Besides, the hH₁R revealed a slight preference for the piperazine-spacer type (**239**). (Figure 4.32)



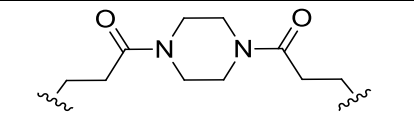
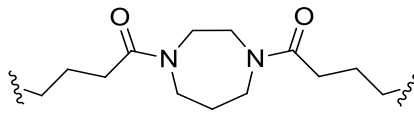
239		$\text{pK}_i (\text{hH}_1\text{R}) = 6.77 \pm 0.09$	$\text{pK}_i (\text{hH}_4\text{R}) = < 5$	$\text{pA}_2 (\text{gpH}_1\text{R}) = 7.03 \pm 0.11$
244		$\text{pK}_i (\text{hH}_1\text{R}) = 6.12 \pm 0.05$	$\text{pK}_i (\text{hH}_4\text{R}) = < 5$	$\text{pA}_2 (\text{gpH}_1\text{R}) = 7.12 \pm 0.06$

Figure 4.32. Pharmacological data of compounds **239** and **244** (*dimeric analogues of 159 linked by polar spacers*).

The last series of dimeric compounds derived from **159** is characterized by a free *N*-methylpiperazine moiety as the spacer is attached in position 3. Due to matters of synthesis, the 3-Cl substituent was replaced by an NH_2 group that made it easier to create dimers linked at this position of the molecule. As expected, the H_4R affinity returned to an at least $10 \mu\text{M}$ level. Both the H_1R and the H_4R revealed a preference for the homopiperazine spacer-type (**231**), reflected in an up to 0.5 orders of magnitude higher affinity. The use of a spacer without piperazine or homopiperazine moiety resulted in a significant decrease of affinity toward H_1Rs irrespective of species (**215**) ($p < 0.0001$). (Figure 4.33)

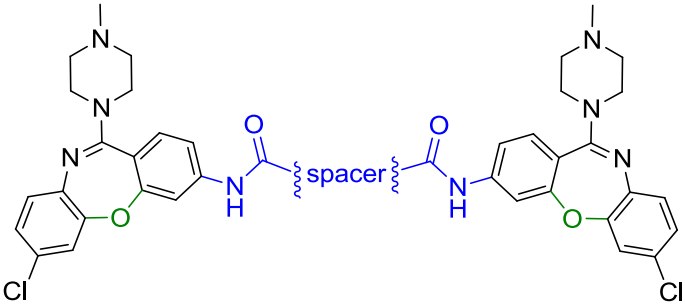
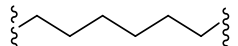
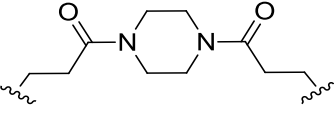
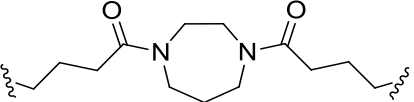
				
215		$pK_i (hH_1R) = 5.15 \pm 0.10$	$pK_i (hH_4R) = 5.06 \pm 0.18$	$pA_2 (gpH_1R) = 6.14 \pm 0.12$
227		$pK_i (hH_1R) = 6.17 \pm 0.22$	$pK_i (hH_4R) = 5.10 \pm 0.09$	$pA_2 (gpH_1R) = 6.96 \pm 0.12$
231		$pK_i (hH_1R) = 6.64 \pm 0.02$	$pK_i (hH_4R) = 5.74 \pm 0.21$	$pA_2 (gpH_1R) = 7.06 \pm 0.15$

Figure 4.33. Pharmacological data of compounds **215**, **227** and **231** (*dimeric analogues of 159 linked in position 3 / 3'*).

4.5.2. Structure activity relationships of H₁R and H₄R ligands

Within this study, some specific structure activity relationships (SARs) for VUF 6884 derived molecules were reported for H₁R and H₄R. As due to the continuous progress in pharmacological research (e.g., molecular modelling studies, scaffold hopping approaches) the four histamine receptors and their ligands have been intensively investigated throughout the last decades, a comparison of the results found in this work to previously described SARs of H₁R- and H₄R-ligands in literature will be given in the following. Moreover, as both H₁R- and H₄R-ligands reveal some key elements regarding their chemical structure, the SARs of these regions will find themselves in the spotlight of interest.

Aromatic rings and a **side chain with a basic nitrogen** were found to be the essential pharmacophoric requirements for H₁R antagonists. (Naruto et al., 1985, Ter Laak et al., 1995, Shishoo et al., 2000) These structural elements find themselves, e.g., in the well-known first generation H₁R antagonists mepyramine and doxepin, in the second generation antagonist cetirizine as well as in clozapine and related molecules (VUF

6884 and -derivatives synthesized in this work) (Naruto et al., 1985, Wieland et al., 1999, Smits et al., 2006, Shimamura et al., 2011). (Figure 4.34)

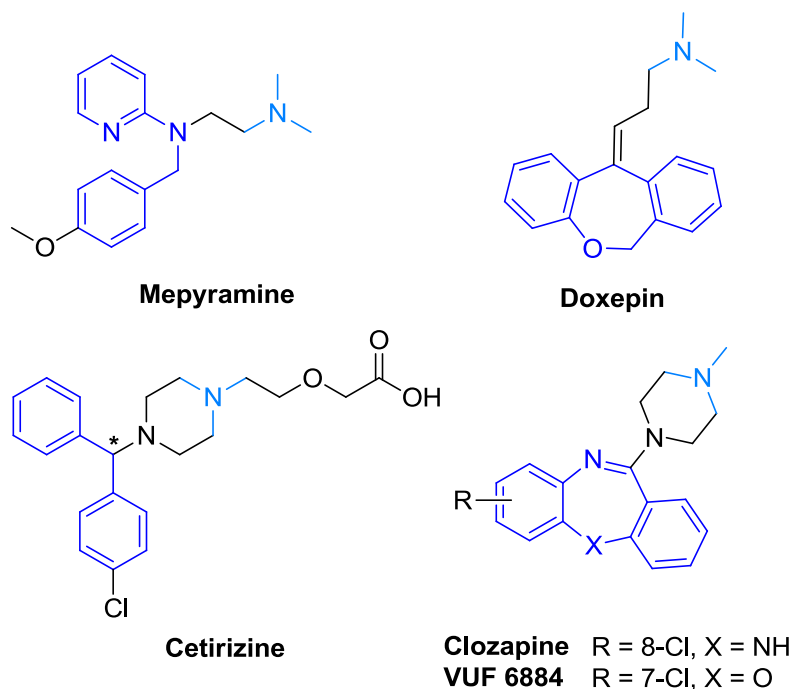


Figure 4.34. Pharmacophoric requirements of H₁R antagonists. (Naruto et al., 1985, Wieland et al., 1999, Smits et al., 2006, Shimamura et al., 2011)

On a molecular level, an interaction of the positively charged amine moiety with Asp^{3.32} in TM 3 of the H₁R as well as an interaction of the aromatic rings with aromatic amino acids (Trp^{4.56}, Phe^{6.52} and Phe^{6.55}) in TM 4 and TM 6 is postulated. (Ohta et al., 1994, Wieland et al., 1999, Strasser et al., 2008a, Strasser et al., 2013, Wagner et al., 2014) Focusing on tricyclic H₁R antagonists like doxepine or clozapine and analogues, an additional interaction of the hetero atom in the central heterocycle with the H₁R is suggested: therein, a water molecule may act as hydrogen bond mediator between amino acids in the binding pocket of H₁R (Thr^{3.37}) and the hetero atom in the aromatic core of the respective ligand, what could be a possible explanation for the higher H₁R affinity of “ring-closed” VUF 6884 derivatives compared to the corresponding “open” counterparts presented in this work. However, further studies have to be performed, in order to support this hypothesis.

The introduction of Cl substituents at the aromatic rings of the VUF 6884 derivatives revealed that the H₁R shows specific preferences for Cl substitution in position 3 / *p*-position of the benzoic acid moiety and *m*-position of the aniline moiety: the H₁R affinity of compounds bearing Cl substituents in these positions (*p*-position of the benzoic acid

moiety / position 3: **70**, **149**; *m*-position of the aniline moiety: **73**) was distinctly increased compared to the corresponding unsubstituted counterparts (**28**, **141**) (figure 4.35). It may be speculated that the lipophilic character of a Cl substituent in these positions provides a further possibility to interact with amino acids of the H₁R binding pocket. This is emphasized by the finding that within the series of the “open” compounds, Cl substituents in *m*-position of the aniline moiety are able to possess different positions in the binding pocket of H₁R and thus reveal an increase in H₁R affinity (see section 4.4.1.2).

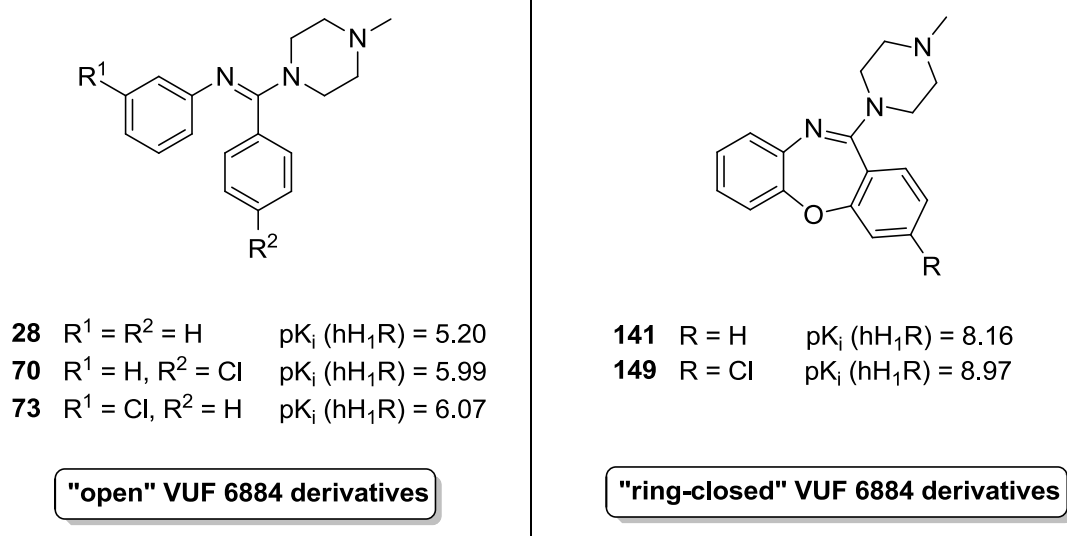


Figure 4.35. SARs of Cl substituents introduced at the aromatic rings of the VUF 6884 derived molecules.

Regarding the H₄R, the SARs determined within this study are in good agreement with previously published data in literature, e.g., by Jablonowski et al. (2003), Terzioglu et al. (2004), Smits et al. (2006, 2008) and Altenbach et al. (2008). The therein described molecules reveal some specific key elements for the interaction with the H₄R: an *N*-methylpiperazine moiety, a lipophilic substituent located at the left ring of the aromatic core structure as well as a basic nitrogen. (Figure 4.36)

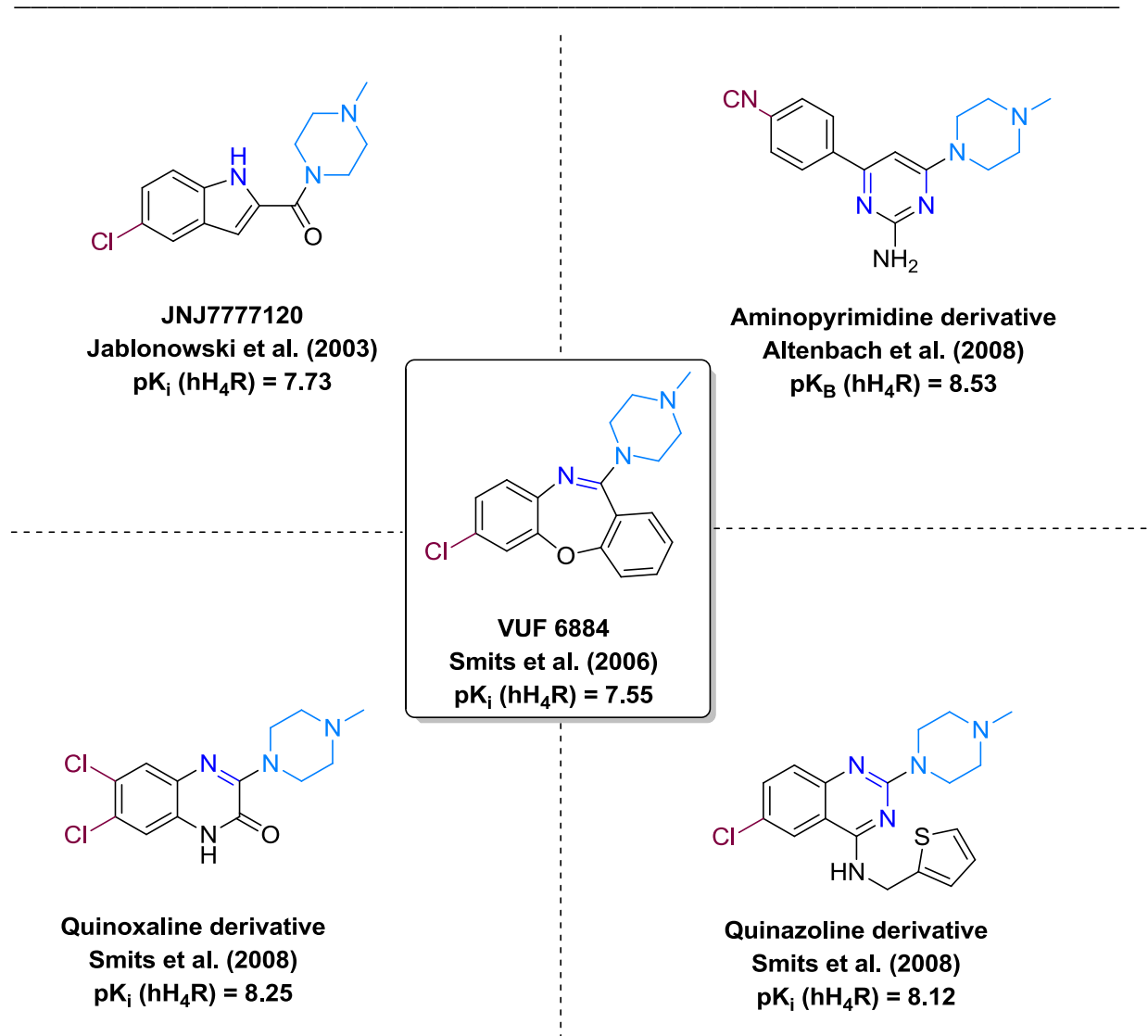


Figure 4.36. Pharmacophoric requirements and structural analogy of H₄R antagonists / inverse agonists

The *N*-methylpiperazine moiety turned out to be crucial for H₄R affinity as neither replacement by ethylenediamine-/ piperazine-elements nor connection to a spacer in this position was tolerated. This can be related to the recently described sensitivity of the H₄R to steric effects in this position of the molecule. (Jablonowski et al., 2003, Terzioglu et al., 2004, Smits et al., 2006) (Figure 4.37)

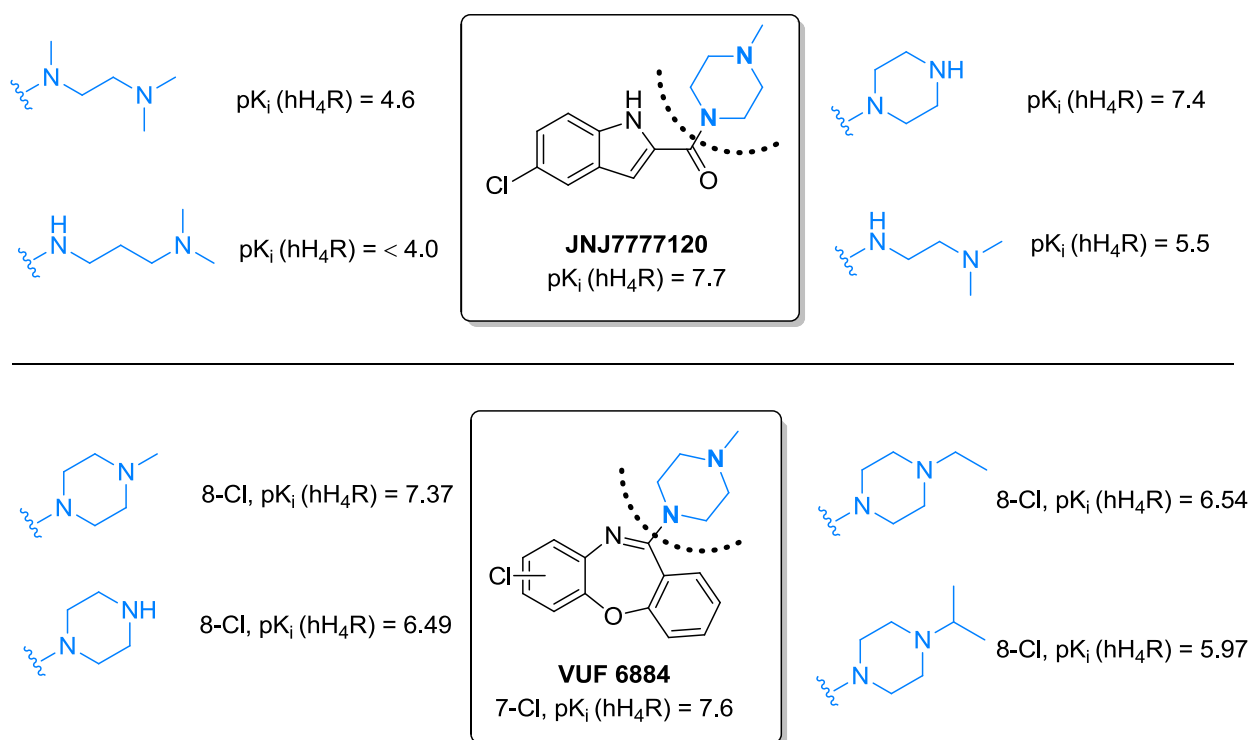


Figure 4.37. Modifications of the *N*-methylpiperazine moiety proving a sensitivity of the H_4R to steric effects in this region of the molecule. (Jablonowski et al., 2003, Terzioglu et al., 2004, Smits et al., 2006)

With regard to the nature and the position of the lipophilic substituent at the left aromatic ring, Cl substituents were found to reveal the most pronounced SAR profile of the characterized compounds. (Jablonowski et al., 2003, Terzioglu et al., 2004, Smits et al., 2006) Focusing on clozapine derived compounds, a distinct preference for Cl substitution in position 7 was reported in literature, what is congruent with the findings of our group. (Smits et al., 2006) The replacement of the Cl substituent by, e.g., a Br substituent, as it was carried out for two representatives within the series of the “open” compounds (**62**, **64**), led to no significant change of the hH_4R affinity compared to the Cl substituted analogues (**67**, **80**). This phenomenon was already observed within a SAR study of JNJ7777120 derived molecules. (Jablonowski et al., 2003, Terzioglu et al., 2004)

As a result, the SARs of the VUF 6884 derived compounds characterized within this study are in good agreement with the data of common ligands described in literature for both, the H₁R and the H₄R. Nevertheless, our results contribute to a better understanding of histamine receptors as they widen the H₄R-focused scope of Smits et al. (2006) to the H₁R. Moreover, a broader range of structural modifications within the synthesized compounds is comprised: not only slightly modified VUF 6884 derivatives were prepared (**88, 92, 128, 129, 136, 141, 149, 158, 159, 193, 196, 232 – 235**) but also reduced (**22, 23, 25, 28, 52, 56, 58, 62, 64, 67, 70, 73, 76, 80, 99, 103, 110, 111, 112, 114 – 117, 180, 181**) and distinctly enlarged analogues (**205 – 210, 212, 213, 215, 221, 225, 227, 229 – 231, 238 – 244**). The pharmacological characterization of these compounds at both, the H₁R and the H₄R provides a closer insight into H₁R and H₄R on a molecular level und represents a reasonable approach on the way to the development of dual action H₁R- / H₄R-ligands.

4.6. References

- ALTENBACH, R. J., ADAIR, R. M., BETTENCOURT, B. M., BLACK, L. A., FIX-STENZEL, S. R., GOPALAKRISHNAN, S. M., HSIEH, G. C., LIU, H., MARSH, K. C., MCPHERSON, M. J., MILICIC, I., MILLER, T. R., VORTHERMS, T. A., WARRIOR, U., WETTER, J. M., WISHART, N., WITTE, D. G., HONORE, P., ESBENSHADE, T. A., HANCOCK, A. A., BRIONI, J. D. & COWART, M. D. **2008**. Structure-activity studies on a series of a 2-aminopyrimidine-containing histamine H₄ receptor ligands. *J Med Chem*, **51**, 6571-6580.
- ARUNLAKSHANA, O. & SCHILD, H. O. **1959**. Some quantitative uses of drug antagonists. *Br J Pharmacol Chemother*, **14**, 48-58.
- ASGHARI, V., SANYAL, S., BUCHWALDT, S., PATERSON, A., JOVANOVIĆ, V. & VAN TOL, H. H. **1995**. Modulation of intracellular cyclic AMP levels by different human dopamine D₄ receptor variants. *J Neurochem*, **65**, 1157-1165.
- BALDESSARINI, R. J. & FRANKENBURG, F. R. **1991**. Clozapine. A novel antipsychotic agent. *N Engl J Med*, **324**, 746-754.
- BETTINETTI, L., SCHLOTTER, K., HÜBNER, H. & GMEINER, P. **2002**. Interactive SAR studies: rational discovery of super-potent and highly selective dopamine D₃ receptor antagonists and partial agonists. *J Med Chem*, **45**, 4594-4597.
- CARBONELL, L. F., KLOWDEN, M. J. & MILLER, L. K. **1985**. Baculovirus-mediated expression of bacterial genes in dipteran and mammalian cells. *J Virol*, **56**, 153-160.
- CARBONELL, L. F. & MILLER, L. K. **1987**. Baculovirus interaction with nontarget organisms: a virus-borne reporter gene is not expressed in two mammalian cell lines. *Appl Environ Microbiol*, **53**, 1412-1417.
- CHENG, Y. & PRUSOFF, W. H. **1973**. Relationship between the inhibition constant (K_i) and the concentration of inhibitor which causes 50 per cent inhibition (I₅₀) of an enzymatic reaction. *Biochem Pharmacol*, **22**, 3099-3108.
- DOLBY, V., COLLEN, A., LUNDQVIST, A. & CRONET, P. **2004**. Overexpression and functional characterisation of the human melanocortin 4 receptor in Sf9 cells. *Protein Expr Purif*, **37**, 455-461.
- ELZ, S., KRAMER, K., PERTZ, H. H., DETERT, H., TER LAAK, A. M., KÜHNE, R. & SCHUNACK, W. **2000**. Histaprodifens: synthesis, pharmacological in vitro evaluation, and molecular modeling of a new class of highly active and selective histamine H₁-receptor agonists. *J Med Chem*, **43**, 1071-1084.
- GADDUM, J., HAMEED, K. A., HATHWAY, D. & STEPHENS, F. **1955**. Quantitative studies of antagonists for 5-hydroxytryptamine. *QJ Exp Physiol Cogn Med Sci*, **40**, 49-74.
- HOUSTON, C., WENZEL-SEIFERT, K., BÜRCKSTÜMMER, T. & SEIFERT, R. **2002**. The human histamine H₂-receptor couples more efficiently to Sf9 insect cell Gs-proteins than to insect cell G_q-proteins: limitations of Sf9 cells for the analysis of receptor/G_q-protein coupling. *J Neurochem*, **80**, 678-696.

- HÜBNER, H., HAUBMANN, C., UTZ, W. & GMEINER, P. **2000**. Conjugated enynes as nonaromatic catechol bioisosteres: synthesis, binding experiments, and computational studies of novel dopamine receptor agonists recognizing preferentially the D₃ subtype. *J Med Chem*, **43**, 756-762.
- JABLONOWSKI, J. A., GRICE, C. A., CHAI, W., DVORAK, C. A., VENABLE, J. D., KWOK, A. K., LY, K. S., WEI, J., BAKER, S. M. & DESAI, P. J. **2003**. The first potent and selective non-imidazole human histamine H₄ receptor antagonists. *J Med Chem*, **46**, 3957-3960.
- JENKINSON, D. H., BARNARD, E. A., HOYER, D., HUMPHREY, P. P., LEFF, P. & SHANKLEY, N. P. **1995**. International Union of Pharmacology Committee on Receptor Nomenclature and Drug Classification. IX. Recommendations on terms and symbols in quantitative pharmacology. *Pharmacol Rev*, **47**, 255-266.
- JI, T. H., GROSSMANN, M. & JI, I. **1998**. G protein-coupled receptors I. Diversity of receptor-ligand interactions. *J Biol Chem*, **273**, 17299-17302.
- JONGEJAN, A., BRUYSTERS, M., BALLESTEROS, J. A., HAAKSMA, E., BAKKER, R. A., PARDO, L. & LEURS, R. **2005**. Linking agonist binding to histamine H₁ receptor activation. *Nat Chem Biol*, **1**, 98-103.
- JORDAN, M., SCHALLHORN, A. & WURM, F. M. **1996**. Transfecting mammalian cells: optimization of critical parameters affecting calcium-phosphate precipitate formation. *Nucleic Acids Res*, **24**, 596-601.
- KENAKIN, T., JENKINSON, S. & WATSON, C. **2006**. Determining the potency and molecular mechanism of action of insurmountable antagonists. *J Pharmacol Exp Ther*, **319**, 710-723.
- KNIGHT, P. J. & GRIGLIATTI, T. A. **2004**. Diversity of G proteins in Lepidopteran cell lines: partial sequences of six G protein α subunits. *Arch Insect Biochem Physiol*, **57**, 142-150.
- KÜHN, B., SCHMID, A., HARTENECK, C., GUDERMANN, T. & SCHULTZ, G. **1996**. G proteins of the Gq family couple the H₂ histamine receptor to phospholipase C. *Mol Endocrinol*, **10**, 1697-1707.
- LESCHKE, C., ELZ, S., GARBARG, M. & SCHUNACK, W. **1995**. Synthesis and histamine H₁ receptor agonist activity of a series of 2-phenylhistamines, 2-heteroarylhistamines, and analogues. *J Med Chem*, **38**, 1287-1294.
- LIÉGEOIS, J.-F., EYROLLES, L., ELLENBROEK, B. A., LEJEUNE, C., CARATO, P., BRUHWYLER, J., GÉCZY, J., DAMAS, J. & DELARGE, J. **2002**. New pyridobenzodiazepine derivatives: Modifications of the basic side chain differentially modulate binding to dopamine (D_{4.2}, D_{2L}) and serotonin (5-HT_{2A}) receptors. *J Med Chem*, **45**, 5136-5149.
- LOWRY, O. H., ROSEBROUGH, N. J., FARR, A. L. & RANDALL, R. J. **1951**. Protein measurement with the Folin phenol reagent. *J Biol Chem*, **193**, 265-275.
- NARUTO, S., MOTOC, I. & MARSHALL, G. **1985**. Computer-assisted analysis of bioactivity. I: Active conformation of histamine H₁ receptor antagonists. *Eur J Med Chem*, **20**, 529-532.
- OHTA, K., HAYASHI, H., MIZUGUCHI, H., KAGAMIYAMA, H., FUJIMOTO, K. & FUKUI, H. **1994**. Site-Directed Mutagenesis of the Histamine H₁ Receptor - Roles of Aspartic Acid(107), Asparagine(198) and Threonine(194). *Biochem Biophys Res Commun*, **203**, 1096-1101.

- PERTZ, H. & ELZ, S. **1995**. In-vitro pharmacology of sarpogrelate and the enantiomers of its major metabolite: 5-HT_{2A} receptor specificity, stereoselectivity and modulation of ritanserin-induced depression of 5-HT contractions in rat tail artery. *J Pharm Pharmacol*, **47**, 310-316.
- PREUSS, H., GHORAI, P., KRAUS, A., DOVE, S., BUSCHAUER, A. & SEIFERT, R. **2007**. Point mutations in the second extracellular loop of the histamine H₂ receptor do not affect the species-selective activity of guanidine-type agonists. *Naunyn Schmiedebergs Arch Pharmacol*, **376**, 253-264.
- SCHNEIDER, E. H., SCHNELL, D., PAPA, D. & SEIFERT, R. **2009**. High constitutive activity and a G-protein-independent high-affinity state of the human histamine H₄-receptor. *Biochemistry*, **48**, 1424-1438.
- SCHNEIDER, E. H. & SEIFERT, R. **2009**. Histamine H₄ receptor-RGS fusion proteins expressed in Sf9 insect cells: a sensitive and reliable approach for the functional characterization of histamine H₄ receptor ligands. *Biochem Pharmacol*, **78**, 607-616.
- SCHNEIDER, E. H. & SEIFERT, R. **2010**. Sf9 cells: a versatile model system to investigate the pharmacological properties of G protein-coupled receptors. *Pharmacol Ther*, **128**, 387-418.
- SCHNEIDER, E. H., STRASSER, A., THURMOND, R. L. & SEIFERT, R. **2010**. Structural Requirements for Inverse Agonism and Neutral Antagonism of Indole-, Benzimidazole-, and Thienopyrrole-Derived Histamine H₄ Receptor Ligands. *J Pharmacol Exp Ther*, **334**, 513-521.
- SCHNELL, D., BRUNSKOLE, I., LADOVA, K., SCHNEIDER, E. H., IGEL, P., DOVE, S., BUSCHAUER, A. & SEIFERT, R. **2011**. Expression and functional properties of canine, rat, and murine histamine H₄ receptors in Sf9 insect cells. *Naunyn Schmiedebergs Arch Pharmacol*, **383**, 457-470.
- SEIFERT, R., LEE, T. W., LAM, V. T. & KOBILKA, B. K. **1998**. Reconstitution of β_2 -adrenoceptor-GTP-binding-protein interaction in Sf9 cells--high coupling efficiency in a β_2 -adrenoceptor-G $\alpha_{s\alpha}$ fusion protein. *Eur J Biochem*, **255**, 369-382.
- SEIFERT, R., WENZEL-SEIFERT, K., BÜRKSTÜMMER, T., PERTZ, H. H., SCHUNACK, W., DOVE, S., BUSCHAUER, A. & ELZ, S. **2003**. Multiple differences in agonist and antagonist pharmacology between human and guinea pig histamine H₁-receptor. *J Pharmacol Exp Ther*, **305**, 1104-1115.
- SEIFERT, R. & WIELAND, T. **2005**. G Protein-Coupled Receptors as Drug Targets: Analysis of Activation and Constitutive Activity Vol. 24 Weinheim: Wiley-VCH. *Weinheim: Wiley-VCH.*, **Vol. 24**
- SHIMAMURA, T., SHIROISHI, M., WEYAND, S., TSUJIMOTO, H., WINTER, G., KATRITCH, V., ABAGYAN, R., CHEREZOV, V., LIU, W., HAN, G. W., KOBAYASHI, T., STEVENS, R. C. & IWATA, S. **2011**. Structure of the human histamine H₁ receptor complex with doxepin. *Nature*, **475**, 65-70.
- SHISHOO, C. J., SHIRSATH, V. S., RATHOD, I. S. & YANDE, V. D. **2000**. Design, synthesis and antihistaminic H₁-activity of some condensed 3-aminopyrimidin-4(3H)-ones. *Eur J Med Chem*, **35**, 351-358.
- SMITS, R. A., LIM, H. D., STEGINK, B., BAKKER, R. A., DE ESCH, I. J. & LEURS, R. **2006**. Characterization of the histamine H₄ receptor binding site. Part 1. Synthesis and pharmacological evaluation of dibenzodiazepine derivatives. *J Med Chem*, **49**, 4512-4516.
- SMRCKA, A. V. **2008**. G protein beta gamma subunits: Central mediators of G protein-coupled receptor signaling. *Cell Mol Life Sci*, **65**, 2191-2214.

- SOKOLOFF, P., ANDRIEUX, M., BESANCON, R., PILON, C., MARTRES, M. P., GIROS, B. & SCHWARTZ, J. C. **1992**. Pharmacology of human dopamine D₃ receptor expressed in a mammalian cell line: comparison with D₂ receptor. *Eur J Pharmacol*, **225**, 331-337.
- STRASSER, A., STRIEGL, B., WITTMANN, H. J. & SEIFERT, R. **2008**. Pharmacological profile of histaprodifens at four recombinant histamine H₁ receptor species isoforms. *J Pharmacol Exp Ther*, **324**, 60-71.
- STRASSER, A., WITTMANN, H. J., BUSCHAUER, A., SCHNEIDER, E. H. & SEIFERT, R. **2013**. Species-dependent activities of G-protein-coupled receptor ligands: lessons from histamine receptor orthologs. *Trends Pharmacol Sci*, **34**, 13-32.
- STRASSER, A., WITTMANN, H. J., **2014**. Personal communication about molecular dynamics simulations (unpublished data).
- TER LAAK, A. M., VENHORST, J., DENKELDER, G. M. D. O. & TIMMERMAN, H. **1995**. The Histamine H₁-Receptor Antagonist Binding-Site - a Stereoselective Pharmacophoric Model-Based Upon (Semi-)Rigid H₁-Antagonists and Including a Known Interaction Site on the Receptor. *J Med Chem*, **38**, 3351-3360.
- TERZIOGLU, N., VAN RIJN, R. M., BAKKER, R. A., DE ESCH, I. J. P. & LEURS, R. **2004**. Synthesis and structure-activity relationships of indole and benzimidazole piperazines as histamine H₄ receptor antagonists. *Bioorg Med Chem Lett*, **14**, 5251-5256.
- VAUQUELIN, G., VAN LIEFDE, I., BIRZBIER, B. & VANDERHEYDEN, P. **2002**. New insights in insurmountable antagonism. *Fund Clin Pharmacol*, **16**, 263-272.
- WAGNER, E., WITTMANN, H. J., ELZ, S. & STRASSER, A. **2014**. Pharmacological profile of astemizole-derived compounds at the histamine H-1 and H-4 receptor-H-1/H-4 receptor selectivity. *Naunyn-Schmiedeberg's Arch Pharmacol*, **387**, 235-250.
- WIELAND, K., TER LAAK, A. M., SMIT, M. J., KÜHNE, R., TIMMERMAN, H. & LEURS, R. **1999**. Mutational analysis of the antagonist-binding site of the histamine H₁ receptor. *J Biol Chem*, **274**, 29994-30000.

Chapter 5

Summary

5. Summary

Derived from the atypical antipsychotic drug clozapine and its structurally optimized derivative VUF 6884, several series of differently modified analogues were prepared with intent to get a closer insight into the H₁R and the H₄R on a molecular level as well as to improve the affinity to these receptors.

The synthesized compounds can be divided into three major groups (“truncated”, “ring-closed” and “dimeric” VUF 6884 derivatives) that in turn are subdivided into smaller subgroups with different characteristic modifications. An overview is given in figure 5.1.

The group of the truncated VUF 6884 derivatives is in general characterized by a ring opening of the central heterocycle, resulting in an increased flexibility of the two aromatic rings in the core of the molecule. Modifications regarding the rigid basic *N*-methylpiperazine moiety, the substitution pattern or the size of the inserted substituents led to three subgroups referred to as “ethylenediamine”, “open” or “acylamino” group. All truncated VUF 6884 derivatives revealed a decreased affinity to both the H₁R and the H₄R compared to clozapine or VUF 6884. However, when substituted with chlorine, special positions in the molecule turned out to have specific beneficial effects on either the affinity to the H₁R or the H₄R: *p*-Cl substitution of the left aromatic ring (the “aniline moiety”) was found to improve H₄R affinity, whereas *p*-Cl substitution of the right aromatic ring (the “benzoic acid moiety”) revealed advantageous effects on the H₁R affinity. Although all compounds among the “acylamino” group revealed rather weak affinity to the target receptors, the loss of affinity was more pronounced with regard to the H₁R. This emphasizes the influence of substituents in *p*-position of the benzoic acid moiety on the interaction with the H₁R. By contrast, among the “ethylenediamine” group, the dropped affinity toward the H₄R is particularly striking. As a consequence, a dependence of the H₄R affinity on the rigid basic *N*-methylpiperazine moiety is postulated. The group of the VUF derivatives is characterized by a closed central oxazepine ring, resulting in distinctly improved affinity to both the H₁R and the H₄R. The direct comparison to the corresponding “open” counterparts points out a key role of the closed central heterocycle in the ligand-receptor interaction.

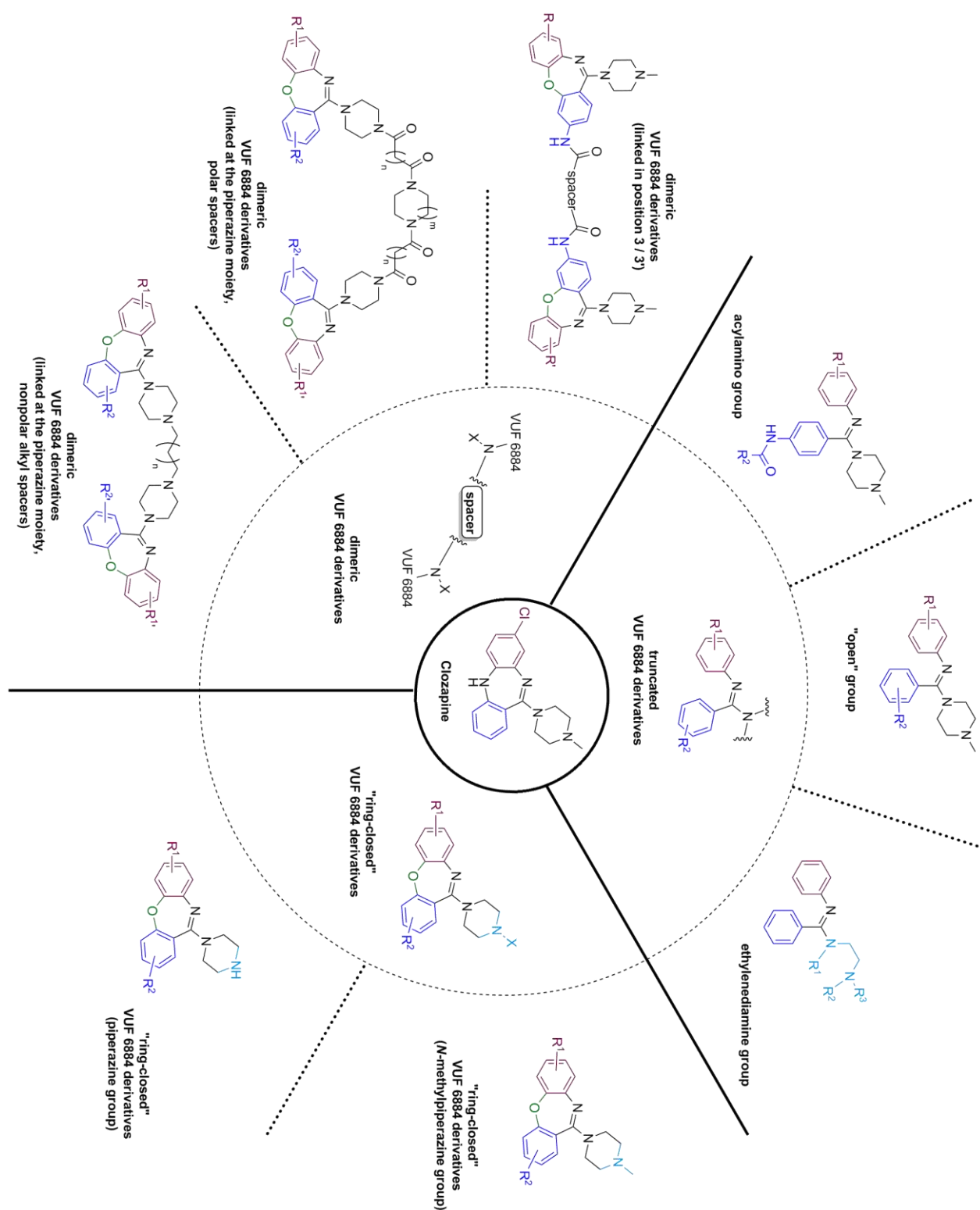


Figure 5.1. Overview of the structurally different clozapine derivatives synthesized in this work.

Two subgroups of “ring-closed” VUF 6884 derivatives were prepared differing in their piperazine moiety (referred to as piperazine and *N*-methylpiperazine group). Again, a dependence of the H₄R affinity on the rigid basic *N*-methylpiperazine moiety was revealed: in all cases, the “ring-closed” VUF 6884 derivatives of the piperazine group showed a reduced H₄R affinity compared to their “ring-closed” VUF 6884 derived counterparts of the *N*-methylpiperazine group. Moreover, the substituent-dependent structure-activity relationships (SARs) determined at the “open” counterparts could be proved: Cl substitution in position 3 improved the affinity to the H₁R, whereas Cl substitution in position 7 improved the affinity to the H₄R. A combination of Cl substituents in these two H₁R- and H₄R beneficial positions resulted in a new lead compound with distinctly improved affinity to both target receptors (compound **159**, pK_i (hH₁R) = 9.25 ± 0.16, pK_i (hH₄R) = 6.96 ± 0.16)). With intent to address homo- and heterodimeric H₁R- and H₄R or extracellular binding sites of monomeric H₁R and H₄R and hence to evoke a further increase of affinity, based on this compound and derivatives thereof a third group of molecules was prepared, referred to as “dimeric” VUF 6884 derivatives. The resulting compounds are linked with different spacers (polar or nonpolar) in different positions of the molecule (piperazine moiety or NH₂ group in position 3 / 3'). However, as the spacers turned out to be not of a sufficient length, an interaction with homo- or heterodimeric H₁R / H₄R was not achieved.

The dimeric compounds linked at the piperazine moiety either by nonpolar or polar spacers are characterized by a distinct decrease of affinity to the H₄R (pK_i (hH₄R) ≤ 5). This can again be traced back to the key role of the *N*-methylpiperazine moiety in H₄R interaction: the spacers either block the methyl group or decrease the basicity of the nitrogen and thus reduce the affinity to the H₄R. Moreover, as the H₄R was found to be sensitive to steric effects at the *N*-methylpiperazine moiety, a negative influence on the H₄R affinity is suggested. Regarding their H₁R affinity, compounds linked by polar spacers are slightly superior, however, compared to their monomeric counterparts, a distinct decrease was revealed in all cases. Among the “dimeric” VUF 6884 derivatives linked at the NH₂ group in position 3 / 3' at least some showed a H₄R affinity of a moderate range (pK_i (hH₄R) = 5 – 6) due to the free basic *N*-methylpiperazine moiety. The H₁R affinity in turn is decreased in comparison to the monomeric counterparts and showed almost no dependence on the substitution pattern (compounds without Cl substitution as most H₁R-potent representatives of this group). All compounds were additionally characterized at the isolated guinea pig ileum, however, the observed

SARs were comparatively equal to the findings in the hH₁R binding assays. Due to species differences and the disparity of the testing systems, the pA₂ values resulting from the organ bath experiments were mostly higher than the pK_i values detected in the binding assays. Moreover, some selected compounds were characterized at dopamine, serotonin and muscarine receptors, as clozapine as so called “dirty drug” shows affinity to a broad variety of GPCRs, dopamine, serotonin, muscarine and histamine receptors included. As a result, the Cl substituent in position 8 was found to play an important role in the interaction with GPCRs other than histamine receptors.

Taken together, due to the various structure modifications of the synthesized compounds, a detailed structure-activity relationship map of clozapine and its derivatives was set up in this work that contributes to a better understanding of the pharmacological profile on a molecular level. (Figure 5.2) Possible future investigations on this topic could start from further modifications of the aromatic core (e.g., insertion of heteroaromatic rings in the aniline or benzoic acid moiety) or from pursuing the dimerization strategy with optimized spacer length and type (e.g., inserting a further basic center in the spacer).

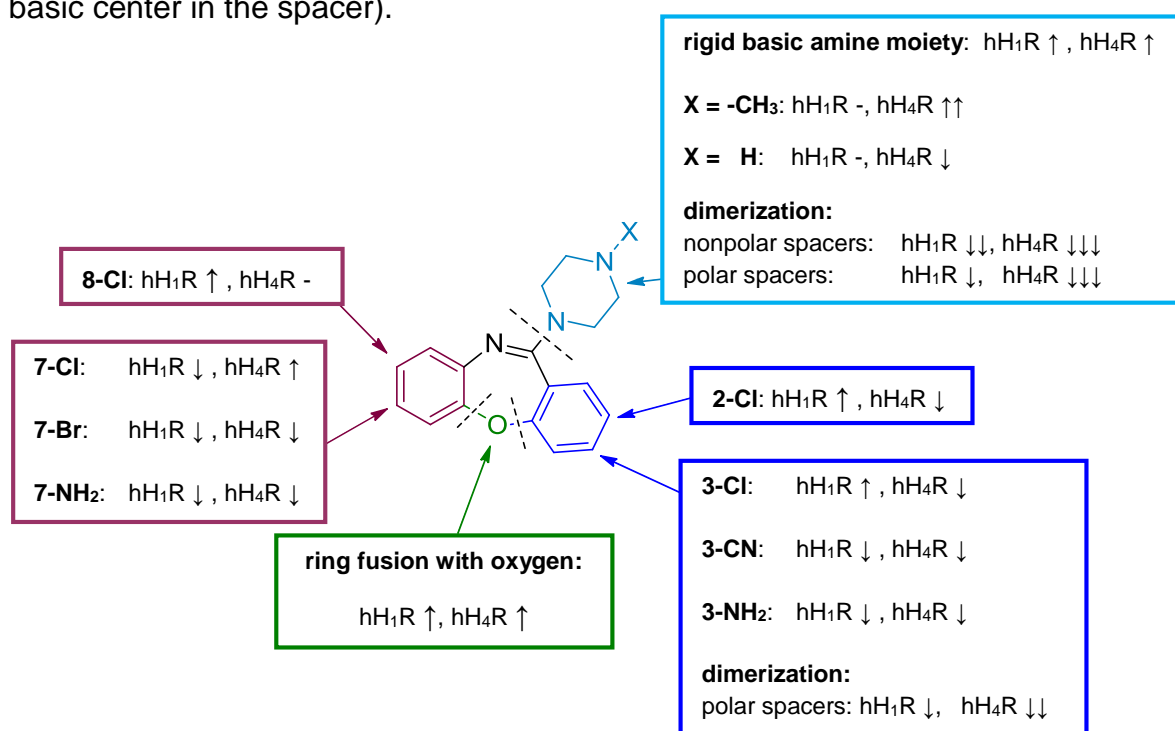


Figure 5.2. SARs of VUF 6884 derived compounds (truncated, “ring-closed” and dimeric) at hH₁R and hH₄R

Chapter 6

Experimental section

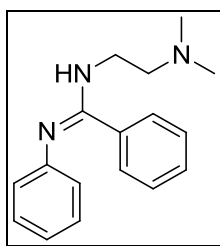
6. Experimental section

6.1. General chemical procedures

Commercially available reagents were purchased from Acros Organics (Geel, Belgium), Sigma-Aldrich Chemie GmbH (München, Germany), TCI Europe GmbH (Eschborn, Germany), Activate Scientific GmbH (Prien, Germany) or Merck KGaA (Darmstadt, Germany) and used as received. Column chromatography was carried out using Merck silica gel Geduran 60 (0.063-0.200). Reactions were monitored by thin layer chromatography (TLC) on Merck silica gel 60 F254 aluminium sheets and spots were visualized with UV light at 254 nm. Nuclear Magnetic Resonance (^1H -NMR and ^{13}C -NMR) spectra were recorded on a Bruker Avance 300 spectrometer using per-deuterated solvents (CDCl_3 , DMSO-d_6 , CD_3OD) (Deutero GmbH, Kastellaun, Germany). Nuclear Magnetic Resonance 2D spectra (HSQC, HMBC and COSY) were recorded using a Bruker Avance 400 spectrometer. The chemical shift δ is given in parts per million (ppm) with reference to the chemical shift of the residual protic solvent compared to tetramethylsilane ($\delta = 0$ ppm). Multiplicities were specified with the following abbreviations: s (singlet), bs (broad singlet), d (doublet), t (triplet), q (quartet) and m (multiplet) as well as combinations thereof. The multiplicity of carbon atoms (^{13}C -NMR) was determined by DEPT 135 and DEPT 90 (distortionless enhancement by polarization transfer): “+” primary and tertiary carbon atom (positive DEPT 135 signal), “-” secondary carbon atom (negative DEPT 135 signal), “quat” quaternary carbon atom. Mass spectrometry analysis (MS) was performed on a Finnigan MAT 95, a Finnigan SSY 710A and on a Finnigan ThermoQuest TSQ 7000 spectrometer. Melting points (mp) were measured on a BÜCHI B-545 melting point apparatus using an open capillary and are uncorrected. The elementary analysis (CHN) was performed with a Heraeus CHN Rapid. Chemical names were generated using ChemBioDraw Ultra 12.0. (Cambridgesoft). Purification of compounds **243** and **244** by preparative HPLC was performed by Dr. Rudolf Vasold and Simone Strauss (Institute of Organic Chemistry, Chair Prof. Dr. Burkhard König, University of Regensburg, Germany).

6.2. General procedure A:**Preparation of compounds 22, 23, 25**

To a solution of *N*-phenylbenzamide in benzene, one equivalent of PCl_5 was added and heated at reflux for 2 h. After cooling to room temperature the solvent and formed POCl_3 was removed under reduced pressure. The residue was re-dissolved in benzene and a 2-fold excess of substituted ethylenediamine was added dropwise. After stirring for 2 h at room temperature the solution was left over night without stirring. The precipitated solid was filtered and washed with acetone and the combined washing solutions were concentrated and dried in vacuo over night. The residue was purified by chromatography over silica gel (EtOAc / 7 N NH_3 in methanol (9 : 1)) to give compounds **22**, **23** and **25** as colorless solids.

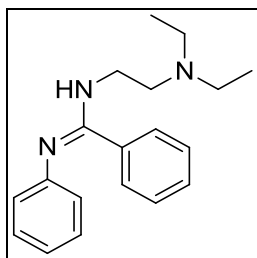
(*E*)-*N*-(2-(Dimethylamino)ethyl)-*N'*-phenylbenzimidamide (22**)**

$\text{C}_{17}\text{H}_{21}\text{N}_3$ ($M = 267.37$ g/mol)

22 was prepared according to *general procedure A* using *N*-phenylbenzamide (2.00 g, 10.10 mmol) in 10 ml benzene and *N,N*-dimethylethylenediamine (1.80 g, 20.20 mmol) and was obtained as a colorless solid (0.35 g, 1.31 mmol, 12.9 % yield).

$\text{C}_{17}\text{H}_{21}\text{N}_3$ ($M = 267.37$ g/mol), mp 53.2 °C. **$^1\text{H-NMR}$** (300 MHz, CDCl_3) δ 7.23 (s, 5H), δ 7.04 (t, 2H, $J = 7.3\text{Hz}$), δ 6.79 (t, 1H, $J = 7.0\text{Hz}$), δ 6.63 (d, 2H, $J = 7.1\text{Hz}$), δ 5.26 (s, 1H), δ 3.57 (bs, 2H), δ 2.58 (bs, 2H), δ 2.26 (s, 6H). **$^{13}\text{C-NMR}$** (75 MHz, CDCl_3) δ 157.80 (C_{quat}), 129.06 (+, 2 Ar-CH), 128.69 (+, 2 Ar-CH), 128.31 (+, Ar-CH), 128.18 (+, Ar-CH), 123.16 (+, 2 Ar-CH), 121.17 (+, 2 Ar-CH), 57.73 (-, CH_2), 45.18 (+, 2 CH_3), 39.14 (-, CH_2). **ESI-MS** m/z 268 [MH^+]. **CHN** ($\text{C}_{17}\text{H}_{21}\text{N}_3$) calc.: C 76.37; H 7.92; N 15.72; exp.: C 76.13; H 7.91; N 15.70.

(E)-N-(2-(Diethylamino)ethyl)-N'-phenylbenzimidamide (23)

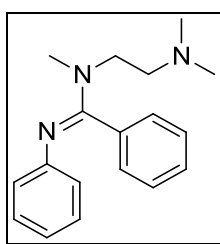


$C_{19}H_{25}N_3$ (M = 295.42 g/mol)

23 was prepared according to *general procedure A* using *N*-phenylbenzamide (4.00 g, 20.28 mmol) in 16 ml benzene and *N,N*-diethylethylenediamine (4.71 g, 40.56 mmol) and was obtained as a colorless solid (0.38 g, 1.29 mmol, 6.4 % yield).

$C_{19}H_{25}N_3$ (M = 295.42 g/mol), mp 55.2 °C. **1H -NMR** (300 MHz, $CDCl_3$) δ 7.24 (s, 5H), δ 7.05 (s, 2H), δ 6.81 (s, 1H), δ 6.64 (s, 2H), δ 5.45 (s, 1H), 3.57 (bs, 2H), δ 2.75 (bs, 2H), δ 2.59 (t, J = 5.1Hz, 4H), δ 1.05 (d, J = 5.8Hz, 6H). **^{13}C -NMR** (75 MHz, $CDCl_3$) δ 129.15 (C_{quat}), 128.67 (+, 2 Ar-CH), 128.36 (+, Ar-CH), 128.21 (+, Ar-CH), 123.12 (+, 4 Ar-CH), 121.21 (+, 2 Ar-CH), 46.72 (-, 4 CH_2), 11.75 (+, 2 CH_3). **ESI-MS** m/z 296.1 $[MH^+]$. **CHN** ($C_{19}H_{25}N_3 \cdot \frac{1}{7} H_2O$) calc.: C 76.58; H 8.55; N 14.10; exp.: C 76.20; H 8.16; N 14.03.

(E)-N-(2-(Dimethylamino)ethyl)-N-methyl-N'-phenylbenzimidamide (25)



$C_{18}H_{23}N_3$ (M = 281.40 g/mol)

25 was prepared according to *general procedure A* using *N*-phenylbenzamide (2.50 g, 12.68 mmol) in 10 ml benzene and *N,N,N'*-trimethylethylenediamine (2.59 g, 25.36 mmol) and was obtained as a colorless solid (1.60 g, 5.69 mmol, 44.9 % yield).

$C_{18}H_{23}N_3$ (M = 281.40 g/mol), mp 58.1 °C. **1H -NMR** (300 MHz, $CDCl_3$) δ 7.20 (t, J = 5.0Hz, 3H), δ 7.10 (d, J = 7.7Hz, 2H), δ 6.97 (m, 2H), δ 6.70 (t, J = 7.3Hz, 3H), δ 3.21

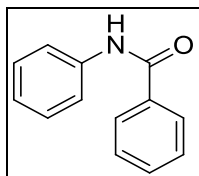
(s, 3H), δ 3.05 (bs, 2H), δ 2.48 (bs, 2H), δ 2.14 (m, 6H). **$^{13}\text{C-NMR}$** (75 MHz, CDCl_3) δ 151.40 (3 C_{quat}), 133.91 (+, 2 Ar-CH), 128.85 (+, 2 Ar-CH), 128.38 (+, Ar-CH), 128.01 (+, Ar-CH), 122.99 (+, 2 Ar-CH), 120.77 (+, 2 Ar-CH), 59.37 (-, 2 CH_2), 45.70 (+, 3 CH_3). **ESI-MS** m/z 282 [MH^+]. **CHN** ($\text{C}_{18}\text{H}_{23}\text{N}_3$) calc.: C 76.83; H 8.24; N 14.93; exp.: C 76.64; H 8.09; N 15.17.

6.3. General procedure B:

Preparation of compounds 4, 45 – 47, 53, 59, 65, 68, 71, 74, 77, 100, 104, 105, 176, 177

To a solution of substituted aniline (10 mmol) and triethylamine (15 mmol) in 200 ml DCM, substituted benzoylchloride (12 mmol) was added under nitrogen atmosphere and vigorous stirring. After stirring at room temperature for 6 h the mixture was heated at reflux over night. The next day the mixture was cooled to room temperature, the solvent was removed under reduced pressure and the resulting solid was washed with 3 M HCl. All compounds were re-crystallized from acetone and obtained as crystalline solids of different colours.

N-Phenylbenzamide (4)

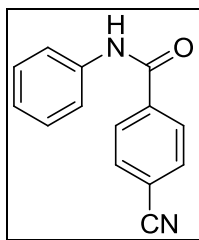


$\text{C}_{13}\text{H}_{11}\text{NO}$ ($M = 197.23$ g/mol)

4 was prepared according to *general procedure B* using aniline (0.93 g, 10 mmol) and benzoylchloride (1.69 g, 12 mmol) and was obtained as colorless crystalline solid (1.20 g, 6.08 mmol, 60.8 % yield).

$\text{C}_{13}\text{H}_{11}\text{NO}$ ($M = 197.23$ g/mol), mp 166.7 °C. **$^1\text{H-NMR}$** (300 MHz, DMSO-d_6) δ 10.25 (s, 1H), δ 7.96 (d, $J = 6.7\text{Hz}$, 2H), δ 7.78 (d, $J = 8.4\text{Hz}$, 2H), δ 7.56 (t, $J = 6.9\text{Hz}$, 3H), δ 7.36 (m, 2H), δ 7.10 (t, $J = 7.4\text{Hz}$, 1H). **EI-MS** (m/z) 197.1 [$\text{M}^{+\cdot}$]. **CHN** ($\text{C}_{13}\text{H}_{11}\text{NO}$) calc.: C 79.16; H 5.62; N 7.10; exp.: C 78.90; H 5.50; N 7.14.

4-Cyano-*N*-phenylbenzamide (47)

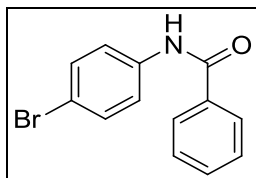


$C_{14}H_{10}N_2O$ ($M = 222.24$ g/mol)

47 was prepared according to *general procedure B* using aniline (0.93 g, 10 mmol) and 4-cyanobenzoylchloride (1.99 g, 12 mmol) and was obtained as a colorless crystalline solid (1.35 g, 6.07 mmol, 60.8 % yield).

$C_{14}H_{10}N_2O$ ($M = 222.24$ g/mol), mp 180.4 °C. **1H -NMR** (300 MHz, $CDCl_3$) δ 7.98 (d, $J = 8.5$ Hz, 2H), δ 7.80 (m, 3H), δ 7.63 (d, $J = 7.8$ Hz, 2H), δ 7.40 (m, 2H), δ 7.20 (t, $J = 7.4$ Hz, 1H). **ESI-MS** m/z 223 [MH^+]. **CHN** ($C_{14}H_{10}N_2O \cdot \frac{1}{2} H_2O$) calc.: C 74.79; H 4.61; N 12.46; exp.: C 74.89; H 4.31; N 12.50.

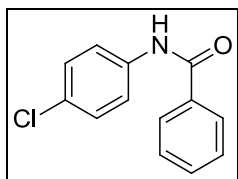
N-(4-Bromophenyl)benzamide (59)



$C_{13}H_{10}BrNO$ ($M = 276.13$ g/mol)

59 was prepared according to *general procedure B* using 4-bromoaniline (1.72 g, 10 mmol) and benzoylchloride (1.69 g, 12 mmol) and was obtained as a light rose crystalline solid (2.09 g, 7.57 mmol, 75.7 % yield).

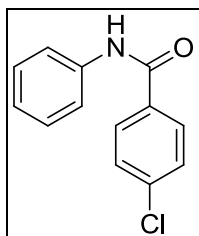
$C_{13}H_{10}BrNO$ ($M = 276.13$ g/mol), mp 205.9 °C. **1H -NMR** (300 MHz, $DMSO-d_6$) δ 10.37 (s, 1H), 7.95 (d, $J = 6.8$ Hz, 2H), 7.77 (d, $J = 8.9$ Hz, 2H), 7.56 (m, 5H). **EI-MS** m/z 51 (8), 63 (3), 77 (39), 91 (3), 105 (100), 145 (1), 167 (1), 195 (1), 275 (22) M^+ , 277 (21). **CHN** ($C_{13}H_{10}BrNO$) calc.: C 56.55; H 3.65; N 5.07; exp.: C 56.77; H 3.51; N 4.79.

***N*-(4-Chlorophenyl)benzamide (65)**

$C_{13}H_{10}ClNO$ ($M = 231.68$ g/mol)

65 was prepared according to *general procedure B* using 4-chloroaniline (1.27 g, 10 mmol) and benzoylchloride (1.69 g, 12 mmol) and was obtained as a colorless crystalline solid (1.46 g, 6.30 mmol, 63.0 % yield).

$C_{13}H_{10}ClNO$ ($M = 231.68$ g/mol), mp 197.7 °C. **1H -NMR** (300 MHz, DMSO- d_6) δ 10.37 (s, 1H), δ 7.95 (d, $J = 6.8$ Hz, 2H), δ 7.82 (d, $J = 8.9$ Hz, 2H), δ 7.57 (m, 3H), δ 7.41 (d, $J = 8.9$ Hz, 2H). **EI-MS** m/z 94 (1), 105 (5), 139 (1), 231 (77) M^+ , 249 (100) MNH_4^+ , 251 (32). **CHN** ($C_{13}H_{10}ClNO$) calc.: C 67.39; H 4.35; N 6.05; exp.: C 67.49; H 4.41; N 5.94.

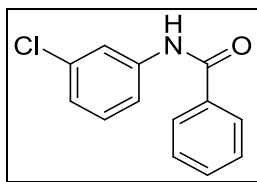
4-Chloro-*N*-phenylbenzamide (68)

$C_{13}H_{10}ClNO$ ($M = 231.68$ g/mol)

68 was prepared according to *general procedure B* using aniline (0.93 g, 10 mmol) and 4-chlorobenzoylchloride (2.10 g, 12 mmol) and was obtained as a colorless crystalline solid (1.57 g, 6.78 mmol, 67.8 % yield).

$C_{13}H_{10}ClNO$ ($M = 231.68$ g/mol), mp 200.9 °C. **1H -NMR** (300 MHz, $CDCl_3$) δ 7.82 (d, $J = 8.6$ Hz, 2H), δ 7.74 (s, 1H), δ 7.62 (d, $J = 7.6$ Hz, 2H), δ 7.47 (d, $J = 8.7$ Hz, 2H), δ 7.43 – 7.34 (m, 2H), δ 7.17 (t, $J = 7.4$ Hz, 1H). **EI-MS** m/z 94 (1), 105 (5), 139 (1), 231 (77) M^+ , 249 (100) MNH_4^+ , 251 (32). **CHN** $C_{13}H_{10}ClNO$ calc.: C 67.39; H 4.35; N 6.05; exp.: C 67.30; H 4.26; N 5.85.

***N*-(3-Chlorophenyl)benzamide (71)**

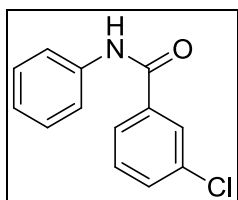


$\text{C}_{13}\text{H}_{10}\text{ClNO}$ ($M = 231.68 \text{ g/mol}$)

71 was prepared according to *general procedure B* using 3-chloroaniline (2.56 g, 20 mmol) and benzoylchloride (3.38 g, 24 mmol) and was obtained as a colorless crystalline solid (2.56 g, 11.0 mmol, 45.8 % yield).

$\text{C}_{13}\text{H}_{10}\text{ClNO}$ ($M = 231.68 \text{ g/mol}$), mp 128.1°C . **$^1\text{H-NMR}$** (300 MHz, DMSO-d_6) δ 10.42 (s, 1H), δ 7.96 (d, $J = 10.1\text{Hz}$, 3H), δ 7.72 (d, $J = 9.3\text{Hz}$, 1H), δ 7.57 (m, 3H), δ 7.39 (t, $J = 8.1\text{Hz}$, 1H) δ 7.16 (d, $J = 8.0\text{Hz}$, 1H). **CI-MS** m/z 105 (8) Ph-CO^+ , 232 (80) MH^+ , 249 (100) MNH_4^+ . **CHN** ($\text{C}_{13}\text{H}_{10}\text{ClNO}$) calc.: C 67.39; H 4.35; N 6.05; exp.: C 67.25; H 4.40; N 5.88.

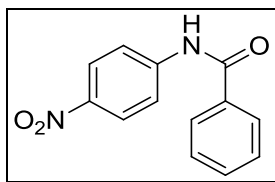
3-Chloro-*N*-phenylbenzamide (74)



$\text{C}_{13}\text{H}_{10}\text{ClNO}$ ($M = 231.68 \text{ g/mol}$)

74 was prepared according to *general procedure B* using aniline (0.93 g, 10 mmol) and 3-chlorobenzoylchloride (2.10 g, 12 mmol) and was obtained as a colorless crystalline solid (1.77 g, 7.64 mmol, 76.4 % yield).

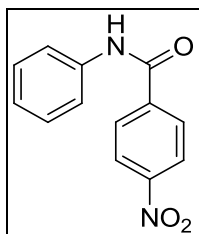
$\text{C}_{13}\text{H}_{10}\text{ClNO}$ ($M = 231.68 \text{ g/mol}$), mp 137.7°C . **$^1\text{H-NMR}$** (300 MHz, CDCl_3) δ 7.85 (t, $J = 1.9\text{Hz}$, 1H), δ 7.81 (s, 1H), δ 7.74 (d, $J = 7.7\text{Hz}$, 1H), δ 7.63 (d, $J = 7.6\text{Hz}$, 2H), δ 7.52 (d, $J = 8.9\text{Hz}$, 1H), δ 7.40 (m, 3H), δ 7.17 (t, $J = 7.4\text{Hz}$, 1H). **CI-MS** m/z 139 (1), 215 (1), 231 (4), 232 (33, MH^+), 233 (6), 234 (10), 235 (1), 249 (100, MNH_4^+), 250 (14), 251 (33), 252 (5), 266 (2). **CHN** ($\text{C}_{13}\text{H}_{10}\text{ClNO}$) calc.: C 67.39; H 4.35; N 6.05; exp.: C 67.46; H 4.40; N 6.05.

***N*-(4-Nitrophenyl)benzamide (45)**

$\text{C}_{13}\text{H}_{10}\text{N}_2\text{O}_3$ ($M = 242.23$ g/mol)

45 was prepared according to *general procedure B* using 4-nitroaniline (1.38 g, 10 mmol) and benzoylchloride (1.69 g, 12 mmol) and was obtained as a light brown crystalline solid. (1.41 g, 5.82 mmol, 58.2 % yield).

$\text{C}_{13}\text{H}_{10}\text{N}_2\text{O}_3$ ($M = 242.23$ g/mol), mp 201.9 °C. **$^1\text{H-NMR}$** (300 MHz, DMSO-d_6) δ 10.82 (s, 1H), δ 8.28 (d, $J = 9.3\text{Hz}$, 2H), δ 8.07 (d, $J = 9.3\text{Hz}$, 2H), δ 7.98 (d, $J = 6.9\text{Hz}$, 2H), δ 7.60 (m, 3H). **ESI-MS** m/z 240.9 $[(M-H)^-]$. **CHN** ($\text{C}_{13}\text{H}_{10}\text{N}_2\text{O}_3$) calc.: C 64.46; H 4.16; N 11.56; exp.: C 64.69; H 4.34; N 11.89.

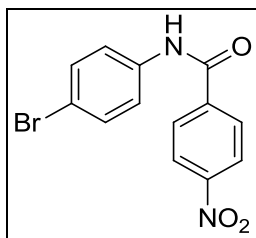
4-Nitro-*N*-phenylbenzamide (53)

$\text{C}_{13}\text{H}_{10}\text{N}_2\text{O}_3$ ($M = 242.23$ g/mol)

53 was prepared according to *general procedure B* using aniline (0.93 g, 10 mmol) and 4-nitrobenzoylchloride (2.23 g, 12 mmol) and was obtained as a yellow crystalline solid (1.75 g, 7.22 mmol, 72.3 % yield).

$\text{C}_{13}\text{H}_{10}\text{N}_2\text{O}_3$ ($M = 242.23$ g/mol), mp 218.8 °C. **$^1\text{H-NMR}$** (300 MHz, DMSO-d_6) δ 10.57 (s, 1H), δ 8.38 (d, $J = 8.9\text{Hz}$, 2H), δ 8.18 (d, $J = 8.9\text{Hz}$, 2H), δ 7.78 (d, $J = 7.6\text{Hz}$, 2H), δ 7.38 (t, $J = 6.9\text{Hz}$, 2H), δ 7.14 (t, $J = 7.4\text{Hz}$, 1H). **ESI-MS** m/z 242.9 $[\text{MH}^+]$. **CHN** ($\text{C}_{13}\text{H}_{10}\text{N}_2\text{O}_3$) calc.: C 64.46; H 4.16; N 11.56; exp.: C 64.41; H 3.83; N 11.65.

***N*-(4-Bromophenyl)-4-nitrobenzamide (46)**

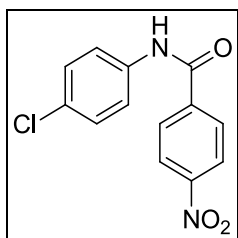


$C_{13}H_9BrN_2O_3$ ($M = 321.13$ g/mol)

46 was prepared according to *general procedure B* using 4-bromoaniline (1.72 g, 10 mmol) and 4-nitrobenzoylchloride (2.23 g, 12 mmol) and was obtained as a yellow crystalline solid. (0.93 g, 2.90 mmol, 29.0 % yield).

$C_{13}H_9BrN_2O_3$ ($M = 321.13$ g/mol), mp 248.9 °C. **1H -NMR** (300 MHz, DMSO- d_6) δ 10.69 (s, 1H), δ 8.38 (d, $J = 8.9$ Hz, 2H), δ 8.18 (d, $J = 8.9$ Hz, 2H), δ 7.77 (d, $J = 8.9$ Hz, 2H), δ 7.57 (d, $J = 8.9$ Hz, 2H). **ESI-MS** m/z 320.9 [(MH) $^-$]. **CHN** ($C_{13}H_9BrN_2O_3$) calc.: C 48.62; H 2.82; N 8.72; exp.: C 48.77; H 2.76; N 8.90.

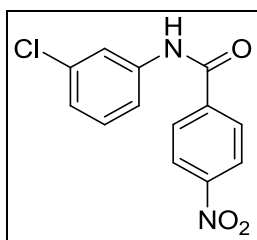
***N*-(4-Chlorophenyl)-4-nitrobenzamide (77)**



$C_{13}H_9ClN_2O_3$ ($M = 276.68$ g/mol)

77 was prepared according to *general procedure B* using 4-chloroaniline (1.28 g, 10 mmol) and 4-nitrobenzoylchloride (2.23 g, 12 mmol) and was obtained as a yellow crystalline solid (1.55 g, 5.60 mmol, 56.0 % yield).

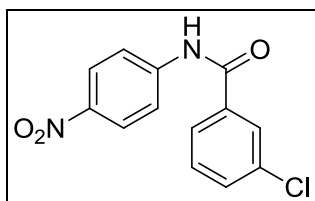
$C_{13}H_9ClN_2O_3$ ($M = 276.68$ g/mol), mp 231.0 °C. **1H -NMR** (300 MHz, DMSO- d_6) δ 10.69 (s, 1H), δ 8.38 (d, 2H, $J = 8.9$ Hz), δ 8.18 (d, 2H, $J = 8.9$ Hz), δ 7.82 (d, 2H, $J = 8.9$ Hz), δ 7.45 (d, 2H, $J = 8.9$ Hz). **CI-MS** m/z 120 (3), 247 (57), 248 (9), 249 (20), 250 (3), 264 (36), 265 (5), 266 (11), 276 (9), 277 (16, MH $^+$), 278 (6), 279 (5), 294 (100, MNH $_4^+$), 295 (14), 296 (33), 297 (4), 311 (4). **CHN** ($C_{13}H_9ClN_2O_3$) calc.: C 56.43; H 3.28; N 10.13; exp.: C 56.42; H 3.34; N 10.11.

***N*-(3-Chlorophenyl)-4-nitrobenzamide (100)**

$\text{C}_{13}\text{H}_9\text{ClN}_2\text{O}_3$ ($M = 276.68$ g/mol)

100 was prepared according to *general procedure B* using 3-chloroaniline (6.38 g, 50 mmol) and 4-nitrobenzoylchloride (11.13 g, 60 mmol) and was obtained as a light yellow crystalline solid (6.74 g, 24.36 mmol, 40.6 % yield).

$\text{C}_{13}\text{H}_9\text{ClN}_2\text{O}_3$ ($M = 276.68$ g/mol), mp 105.9 °C. **$^1\text{H-NMR}$** (300 MHz, DMSO-d_6) δ 10.76 (s, 1H), δ 8.38 (d, $J = 8.9\text{Hz}$, 2H), δ 8.19 (d, $J = 8.9\text{Hz}$, 2H), δ 7.98 (t, $J = 2.0\text{Hz}$, 1H), δ 7.72 (d, $J = 9.3\text{Hz}$, 1H) δ 7.42 (t, $J = 8.1\text{Hz}$, 1H) δ 7.21 (d, $J = 8.0\text{Hz}$, 1H). **EI-MS** m/z 50 (5), 75 (7), 76 (19), 92 (12), 104 (33), 120 (9), 134 (2), 150 (100), 276 (25) M^+ , 278 (8). **CHN** ($\text{C}_{13}\text{H}_9\text{ClN}_2\text{O}_3$) calc.: C 56.43; H 3.28; N 10.13; exp.: C 56.28; H 3.50; N 10.13.

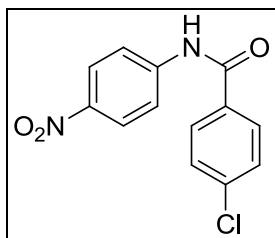
3-Chloro-*N*-(4-nitrophenyl)benzamide (105)

$\text{C}_{13}\text{H}_9\text{ClN}_2\text{O}_3$ ($M = 276.68$ g/mol)

105 was prepared according to *general procedure B* using 4-nitroaniline (6.91 g, 50 mmol) and 3-chlorobenzoylchloride (10.50 g, 60 mmol) and was obtained as light green crystalline solid (10.49 g, 37.91 mmol, 75.8 %).

$\text{C}_{13}\text{H}_9\text{ClN}_2\text{O}_3$ ($M = 276.68$ g/mol), mp 195.3°C. **$^1\text{H-NMR}$** (300 MHz, DMSO-d_6) δ 10.89 (s, 1H), δ 8.28 (d, $J = 9.3\text{Hz}$, 2H), δ 8.06 (d, $J = 9.3\text{Hz}$, 3H), δ 7.94 (d, $J = 7.8\text{Hz}$, 1H), δ 7.72 (d, $J = 9.0\text{Hz}$, 1H), δ 7.60 (t, $J = 7.9\text{Hz}$, 1H). **EI-MS** m/z 75 (11), 76 (4), 111 (38), 113 (12), 139 (100), 140 (7), 141 (30), 276 (9, M^+). **CHN** ($\text{C}_{13}\text{H}_9\text{ClN}_2\text{O}_3$) calc.: C 56.43; H 3.28; N 10.13; exp.: C 56.52; H 3.41; N 10.10.

4-Chloro-*N*-(4-nitrophenyl)benzamide (104)

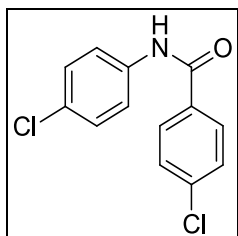


$C_{13}H_9ClN_2O_3$ ($M = 276.68$ g/mol)

104 was prepared according to *general procedure B* using 4-nitroaniline (6.91 g, 50 mmol) and 4-chlorobenzoylchloride (10.50 g, 60 mmol) and was obtained as green crystalline solid (12.11 g, 43.74 mmol, 87.5 % yield).

$C_{13}H_9ClN_2O_3$ ($M = 276.68$ g/mol), mp 214.9 °C. **1H -NMR** (300 MHz, DMSO- d_6) δ 10.87 (s, 1H), δ 8.28 (d, $J = 9.3$ Hz, 2H), δ 8.04 (m, 4H), δ 7.65 (d, $J = 8.6$ Hz, 2H). **EI-MS** m/z 40 (23), 44 (100), 75 (10), 111 (33), 113 (11), 139 (96), 140 (8), 141 (31), 276 (6) M^{+} . **CHN** ($C_{13}H_9ClN_2O_3$) calc.: C 56.43; H 3.28; N 10.13; exp.: C 56.47; H 3.47; N 9.98.

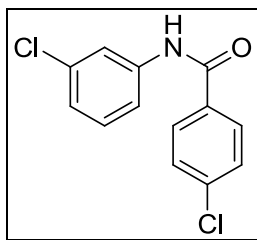
4-Chloro-*N*-(4-chlorophenyl)benzamide (176)



$C_{13}H_9Cl_2NO$ ($M = 266.12$ g/mol)

176 was prepared according to *general procedure B* using 4-chloroaniline (2.55 g, 20 mmol) and 4-chlorobenzoylchloride (4.20 g, 24 mmol) and was obtained as colorless crystalline solid (4.2 g, 15.78 mmol, 78.9 % yield).

$C_{13}H_9Cl_2NO$ ($M = 266.12$ g/mol), mp 212.6 °C. **1H -NMR** (300 MHz, DMSO- d_6) δ 10.44 (s, 1H), δ 7.98 (d, $J = 8.6$ Hz, 2H), δ 7.81 (d, $J = 8.9$ Hz, 2H), δ 7.62 (d, $J = 8.6$ Hz, 2H), δ 7.42 (d, $J = 8.9$ Hz, 2H). **EI-MS** m/z 265.0 [M^{+}]. **CHN** ($C_{13}H_9Cl_2NO$) calc.: C 58.67; H 3.41; N 5.26; exp.: C 58.52; H 3.50; N 5.11.

4-Chloro-*N*-(3-chlorophenyl)benzamide (177)

$\text{C}_{13}\text{H}_9\text{Cl}_2\text{NO}$ ($M = 266.12 \text{ g/mol}$)

177 was prepared according to *general procedure B* using 3-chloroaniline (2.55 g, 20 mmol) and 4-chlorobenzoylchloride (4.20 g, 24 mmol) and was obtained as colorless crystalline solid (1.89 g, 7.1 mmol, 35.5 % yield).

$\text{C}_{13}\text{H}_9\text{Cl}_2\text{NO}$ ($M = 266.12 \text{ g/mol}$), mp 114.6 °C. **$^1\text{H-NMR}$** (300 MHz, DMSO-d_6) δ 10.48 (s, 1H), δ 8.16 (d, $J = 8.6\text{Hz}$, 1H), δ 7.98 (m, 2H), δ 7.72 (d, $J = 8.6\text{Hz}$, 2H), δ 7.63 (d, $J = 8.6\text{Hz}$, 1H), δ 7.39 (t, $J = 8.1\text{Hz}$, 1H), δ 7.18 (d, $J = 8.0\text{Hz}$, 1H). **EI-MS** m/z 265.0 [M^+]. **CHN** ($\text{C}_{13}\text{H}_9\text{Cl}_2\text{NO}$) calc.: C 58.67; H 3.41; N 5.26; exp.: C 58.86; H 3.55; N 5.12.

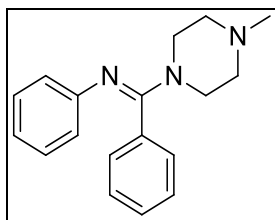
6.4. General procedure C:

Preparation of compounds 28, 50, 55, 58, 61, 64, 67, 70, 73, 76, 79, 102, 108, 109, 180, 181

To a solution of *N*-phenylbenzamide (**4, 45 – 47, 53, 59, 65, 68, 71, 74, 77, 100, 104, 105, 176, 177**) in acetonitrile and benzene (2 : 1) one equivalent of PCl_5 was added and the mixture was heated at reflux for 2 h. After the completion of the reaction the solvent was removed under reduced pressure and the resulting very reactive imidchloride was used in the next step without further purification.

To a solution of the imidchloride (1.5 mmol) and triethylamine (2.5 mmol) in acetonitrile and benzene (2:1), *N*-methylpiperazine (2.0 mmol) was added dropwise under vigorous stirring. The mixture was heated at reflux over night and the next day the solvent was removed under reduced pressure. The resulting solid was purified by column chromatography (ethyl acetate / methanol 1:1) and compounds **28, 50, 55, 58, 61, 64, 67, 70, 73, 76, 79, 102, 108, 109, 180, 181** were obtained as solids of different colours.

(E)-N-((4-Methylpiperazin-1-yl)(phenyl)methylen)aniline (28)

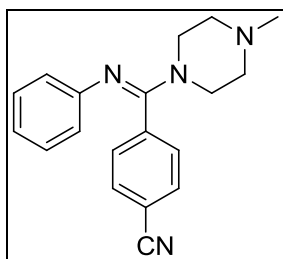


$C_{18}H_{21}N_3$ (M = 279.38 g/mol)

28 was prepared according to *general procedure C* from **4** (2.00 g, 10.14 mmol) in acetonitrile / benzene (90 ml) giving intermediate (*E*)-*N*-phenylbenzimidoyl chloride (2.18 g, 10.14 mmol) to which triethylamine (1.71 g, 16.9 mmol), *N*-methylpiperazine (1.35 g, 13.50 mmol) and acetonitrile / benzene (90 ml) were added to give **28** as colorless solid (1.33 g, 4.76 mmol, 46.9 % yield).

$C_{18}H_{21}N_3$ (M = 279.38 g/mol), mp 83.1 °C. **¹H-NMR** (300 MHz, $CDCl_3$) δ 7.22 (m, 3H), δ 7.11 (m, 2H), δ 6.99 (m, 2H), δ 6.74 (t, J = 7.4Hz, 1H), δ 6.55 (d, J = 8.2Hz, 2H), δ 3.47 (bs, 4H), δ 2.47 (bs, 4H), δ 2.35 (s, 3H). **¹³C-NMR** (75 MHz, $CDCl_3$) δ 160.48 (C_{quat}), 150.97 (C_{quat}), 133.42 (C_{quat}), 129.08 (+, 2 Ar-CH), 128.63 (+, 2 Ar-CH), 128.18 (+, Ar-CH), 128.13 (+, Ar-CH), 122.82 (+, 2 Ar-CH), 121.07 (+, 2 Ar-CH), 55.00 (-, 2 Pip-CH₂), 47.38 (-, 2 Pip-CH₂), 46.21(+, CH₃). **ESI-MS** *m/z* 280 [MH⁺]. **CHN** ($C_{18}H_{21}N_3$) calc.: C 77.38; H 7.58; N 15.04; exp.: 77.12; H 7.84; N 14.86.

(E)-4-((4-Methylpiperazin-1-yl)(phenylimino)methyl)benzonitrile (58)



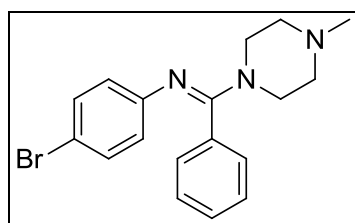
$C_{19}H_{20}N_4$ (M = 304.39 g/mol)

58 was prepared according to *general procedure C* from **47** (1.33 g, 6.00 mmol) in acetonitrile / benzene (60 ml) giving intermediate (*E*)-4-cyano-*N*-phenylbenzimidoyl chloride (1.44 g, 6.00 mmol) to which triethylamine (0.76 g, 7.50 mmol), *N*-

methylpiperazine (0.60 g, 6.00 mmol) and acetonitrile / benzene (60 ml) were added to give **58** as a colorless foam (0.69 g, 2.27 mmol, 37.8 % yield).

$C_{19}H_{20}N_4$ ($M = 304.39$ g/mol), mp 131.4 °C. **1H -NMR** (300 MHz, $CDCl_3$) δ 7.53 (d, $J = 8.4$ Hz, 2H), δ 7.23 (d, $J = 8.3$ Hz, 2H), δ 7.01 (t, $J = 7.8$ Hz, 2H), δ 6.77 (t, $J = 7.4$ Hz, 1H), δ 6.50 (d, $J = 7.3$ Hz, 2H), δ 3.41 (bs, 4H), δ 2.46 (bs, 4H), δ 2.35 (s, 3H). **^{13}C -NMR** (75 MHz, $CDCl_3$) δ 158.28 (C_{quat}), 150.08 (C_{quat}), 138.25 (C_{quat}), 132.05 (+, 2 Ar-CH), 129.76 (+, 2 Ar-CH), 128.45 (+, Ar-CH), 122.50 (+, 2 Ar-CH), 121.72 (+, 2 Ar-CH), 118.16 (C_{quat}), 112.55 (C_{quat} , $C\equiv N$), 54.78 (-, 2 Pip- CH_2), 46.12 (+, CH_3), 45.09 (-, 2 Pip- CH_2). **ESI-MS** m/z 304.9 [MH^+]. **CHN** ($C_{19}H_{20}N_4 \cdot \frac{1}{2} H_2O$) calc.: C 72.82; H 6.75; N 17.88; exp.: C 72.51; H 6.47; N 17.78.

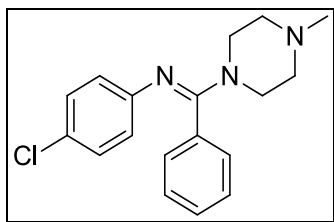
(*E*)-4-Bromo-*N*-((4-methylpiperazin-1-yl)(phenyl)methylene)aniline (64**)**



$C_{18}H_{20}BrN_3$ ($M = 358.28$ g/mol)

64 was prepared according to *general procedure C* from **59** (2.02 g, 7.32 mmol) in acetonitrile / benzene (60 ml) giving intermediate (*E*)-*N*-(4-bromophenyl)benzimidoyl chloride (2.15 g, 7.32 mmol) to which triethylamine (0.51 mmol, 5.00 mmol), *N*-methylpiperazine (0.73 g, 7.32 mmol) and acetonitrile / benzene (60 ml) were added to give **64** as a colorless solid (0.62 g, 1.73 mmol, 23.7 % yield).

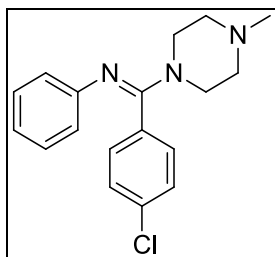
$C_{18}H_{20}BrN_3$ ($M = 358.28$ g/mol), mp 80.3 °C. **1H -NMR** (300 MHz, $CDCl_3$) δ 7.40 (s, 1H), δ 7.24 (d, $J = 3.6$ Hz, 2H), δ 7.08 (d, $J = 8.5$ Hz, 4H), δ 6.42 (d, $J = 8.6$ Hz, 2H), δ 3.44 (bs, 4H), δ 2.44 (bs, 4H), δ 2.34 (s, 3H). **^{13}C -NMR** (75 MHz, $CDCl_3$) δ 160.68 (C_{quat}), 150.09 (C_{quat}), 132.96 (C_{quat}), 131.07 (+, 2 Ar-CH), 128.95 (+, 2 Ar-CH), 128.41 (+, Ar-CH), 127.04 (+, 2 Ar-CH), 124.55 (+, 2 Ar-CH), 113.88 (C_{quat}), 54.88 (-, 2 Pip- CH_2), 46.36 (-, 2 Pip- CH_2), 46.07 (+, CH_3). **ESI-MS** m/z 357.8 [MH^+], 359.8. **CHN** ($C_{18}H_{20}BrN_3 \cdot \frac{3}{4} H_2O$) calc.: C 58.15; H 5.83; N 11.30; exp.: C 58.29; H 5.54; N 11.11.

(E)-4-Chloro-N-((4-methylpiperazin-1-yl)(phenyl)methylene)aniline (67)

$C_{18}H_{20}ClN_3$ (M = 313.82 g/mol)

67 was prepared according to *general procedure C* from **65** (1.39 g, 6.00 mmol) in acetonitrile / benzene (60 ml) giving intermediate (*E*)-*N*-(4-chlorophenyl)benzimidoyl chloride (1.50 g, 6.00 mmol) to which triethylamine (0.71 mmol, 7.00 mmol), *N*-methylpiperazine (0.60 g, 6.00 mmol) and acetonitrile / benzene (60 ml) were added to give **67** according to general procedure as a colorless solid (0.61 g, 1.95 mmol, 32.6 % yield).

$C_{18}H_{20}ClN_3$ (M = 313.82 g/mol), mp 74.1 °C. **¹H-NMR** (300 MHz, $CDCl_3$) δ 7.24 (d, J = 3.4Hz, 3H), δ 7.08 (d, J = 9.6Hz, 2H), δ 6.94 (d, J = 8.7Hz, 2H), δ 6.46 (d, J = 8.7Hz, 2H), δ 3.43 (bs, 4H), δ 2.45 (bs, 4H), δ 2.34 (s, 3H). **¹³C-NMR** (75 MHz, $CDCl_3$) δ 160.77 (C_{quat}), 149.67 (C_{quat}), 133.07 (C_{quat}), 128.96 (+, 2 Ar-CH), 128.85 (+, 2 Ar-CH), 128.37 (+, Ar-CH), 128.15 (+, Ar-CH), 127.05 (+, 2 Ar-CH), 126.14 (C_{quat}), 124.04 (+, Ar-CH), 54.90 (-, 2 Pip-CH₂), 46.10 (+, CH₃), 45.88 (-, 2 Pip-CH₂). **ESI-MS** *m/z* 313.9 [MH⁺]. **CHN** ($C_{18}H_{20}ClN_3 \cdot \frac{1}{10} H_2O$) calc.: C 68.45; H 6.45; N 13.30; exp.: C 68.45; H 6.78; N 13.47.

(E)-N-((4-Chlorophenyl)(4-methylpiperazin-1-yl)methylene)aniline (70)

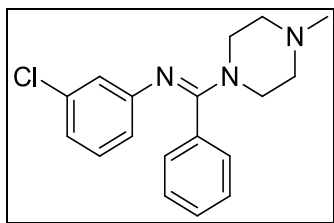
$C_{18}H_{20}ClN_3$ (M = 313.82 g/mol)

70 was prepared according to *general procedure C* from **68** (1.39 g, 6.00 mmol) in acetonitrile / benzene (60 ml) giving intermediate (*E*)-4-chloro-*N*-phenylbenzimidoyl

chloride (1.50 g, 6.00 mmol) to which triethylamine (0.71 mmol, 7.00 mmol), *N*-methylpiperazine (0.60 g, 6.00 mmol) and acetonitrile / benzene (60 ml) were added to give **70** as a colorless solid (0.42 g, 1.33 mmol, 22.2 % yield).

$C_{18}H_{20}ClN_3$ ($M = 313.82$ g/mol), mp 68.1 °C. **1H -NMR** (300 MHz, $CDCl_3$) δ 7.21 (d, $J = 8.4$ Hz, 2H), δ 7.03 (m, 4H), δ 6.77 (t, $J = 7.4$ Hz, 1H), δ 6.53 (d, $J = 7.3$ Hz, 2H), δ 3.42 (bs, 4H), δ 2.45 (bs, 4H), δ 2.34 (s, 3H). **^{13}C -NMR** (75 MHz, $CDCl_3$) δ 159.32 (C_{quat}), 150.67 (C_{quat}), 134.63 (C_{quat}), 131.83 (C_{quat}), 130.46 (+, 2 Ar-CH), 128.57 (+, 2 Ar-CH), 128.33 (+, Ar-CH), 122.67 (+, 2 Ar-CH), 121.31 (+, 2 Ar-CH), 54.91 (-, 2 Pip-CH₂), 46.18 (+, CH₃), 45.92 (-, 2 Pip-CH₂). **ESI-MS** m/z 313.9 [MH^+]. **CHN** ($C_{18}H_{20}ClN_3 \cdot \frac{1}{10} H_2O$) calc.: C 68.45; H 6.45; N 13.30; exp.: C 68.40; H 6.34; N 13.15.

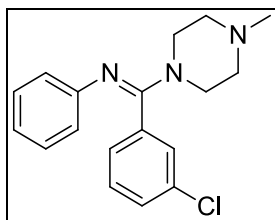
(*E*)-3-Chloro-*N*-((4-methylpiperazin-1-yl)(phenyl)methylene)aniline (73**)**



$C_{18}H_{20}ClN_3$ ($M = 313.82$ g/mol)

73 was prepared according to *general procedure C* from **71** (0.30 g, 1.30 mmol) in acetonitrile / benzene (30 ml) giving intermediate (*E*)-*N*-(3-chlorophenyl)benzimidoyl chloride (0.33 g, 1.30 mmol) to which triethylamine (0.20 g, 2.00 mmol), *N*-methylpiperazine (0.13 g, 1.30 mmol) and acetonitrile / benzene (30 ml) were added to give **73** according to general procedure as a colorless solid (0.08 g, 0.24 mmol, 18.5 % yield).

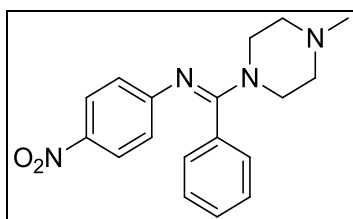
$C_{18}H_{20}ClN_3$ ($M = 313.82$ g/mol), mp 156.2 °C. **1H -NMR** (300 MHz, $CDCl_3$) δ 7.26 (m, 3H), δ 7.10 (d, $J = 9.6$ Hz, 2H), δ 6.89 (t, $J = 7.9$ Hz, 1H), δ 6.71 (d, $J = 7.9$ Hz, 1H), δ 6.59 (t, $J = 2.0$ Hz, 1H), δ 6.39 (d, $J = 8.6$ Hz, 1H), δ 3.50 (bs, 4H), δ 2.52 (bs, 4H), δ 2.40 (s, 3H). **^{13}C -NMR** (75 MHz, $CDCl_3$) δ 160.78 (C_{quat}), 152.40 (C_{quat}), 133.57 (C_{quat}), 132.84 (C_{quat}), 129.06 (+, 2 Ar-CH), 128.89 (+, 2 Ar-CH), 128.40 (+, Ar-CH), 123.00 (+, 2 Ar-CH), 121.06 (+, 2 Ar-CH), 54.84 (-, 2 Pip-CH₂), 46.03 (+, CH₃), 45.71 (-, 2 Pip-CH₂). **ESI-MS** m/z 313.9 [MH^+]. **CHN** ($C_{18}H_{20}ClN_3 \cdot \frac{1}{2} H_2O$) calc.: C 66.97; H 6.56; N 13.02; exp.: C 66.99; H 6.48; N 12.94.

(E)-N-((3-Chlorophenyl)(4-methylpiperazin-1-yl)methylene)aniline (76)

$C_{18}H_{20}ClN_3$ (M = 313.82 g/mol)

76 was prepared according to *general procedure C* from **74** (1.39 g, 6.00 mmol) in acetonitrile / benzene (60 ml) giving intermediate (*E*)-3-chloro-*N*-phenylbenzimidoyl chloride (1.50 g, 6.00 mmol) to which triethylamine (0.71 g, 7.00 mmol), *N*-methylpiperazine (0.60 g, 6.00 mmol) and acetonitrile / benzene (60 ml) were added to give **76** as a colorless solid (0.87 g, 2.76 mmol, 45.9 % yield).

$C_{18}H_{20}ClN_3$ (M = 313.82 g/mol), mp 93.0 °C. **¹H-NMR** (300 MHz, $CDCl_3$) δ 7.17 (m, 3H), δ 7.00 (m, 3H), δ 6.77 (t, J = 7.4 Hz, 1H), δ 6.54 (d, J = 8.1 Hz, 2H), δ 3.45 (bs, 4H), δ 2.48 (bs, 4H), δ 2.36 (s, 3H). **¹³C-NMR** (75 MHz, $CDCl_3$) δ 158.74 (C_{quat}), 150.44 (C_{quat}), 135.21 (C_{quat}), 134.34 (C_{quat}), 129.55 (+, 2 Ar-CH), 128.89 (+, 2 Ar-CH), 128.31 (+, Ar-CH), 127.27 (+, 2 Ar-CH), 122.62 (+, Ar-CH), 121.45 (+, Ar-CH), 54.86 (-, 2 Pip-CH₂), 46.12 (+, CH₃), 45.69 (-, 2 Pip-CH₂). **ESI-MS** m/z 313.9 [MH^+]. **CHN** ($C_{18}H_{20}ClN_3$) calc.: C 68.89; H 6.42; N 13.39; exp.: C 68.56; H 6.44; N 13.37.

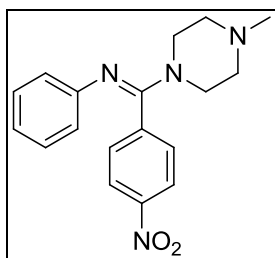
(E)-N-((4-Methylpiperazin-1-yl)(phenyl)methylene)-4-nitroaniline (50)

$C_{18}H_{20}N_4O_2$ (M = 324.38 g/mol)

50 was prepared according to *general procedure C* from **45** (0.36 g, 1.50 mmol) in acetonitrile / benzene (30 ml) giving intermediate (*E*)-*N*-(4-nitrophenyl)benzimidoyl chloride (0.39 g, 1.50 mmol) to which triethylamine (0.25 g, 2.50 mmol), *N*-methylpiperazine (0.20 g, 2.00 mmol) and acetonitrile / benzene (30 ml) were added to give **50** as a yellow hygroscopic foam (0.26 g, 0.79 mmol, 52.6 % yield).

$C_{18}H_{20}N_4O_2$ (M = 324.38 g/mol), mp 216.7 °C. **1H -NMR** (300 MHz, $CDCl_3$) δ 7.88 (d, J = 9.1Hz, 2H), δ 7.28 (m, 3H), δ 7.10 (d, J = 6.5Hz, 2H), δ 6.57 (d, J = 9.1Hz, 2H), δ 3.49 (bs, 4H), δ 2.47 (bs, 4H), δ 2.35 (s, 3H). **ESI-MS** m/z 325 $[MH^+]$. **CHN** ($C_{18}H_{20}N_4O_2 \cdot \frac{1}{2} H_2O$) calc.: C 64.85; H 6.35; N 16.81; exp.: C 64.59; H 6.12; N 16.83.

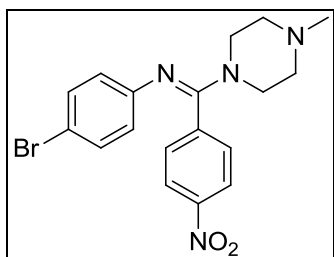
(E)-N-((4-Methylpiperazin-1-yl)(4-nitrophenyl)methylene)aniline (55)



$C_{18}H_{20}N_4O_2$ (M = 324.38 g/mol)

55 was prepared according to *general procedure C* from **53** (1.69 g, 7.00 mmol) in acetonitrile / benzene (60 ml) giving intermediate (*E*)-4-nitro-*N*-phenylbenzimidoyl chloride (1.82 g, 7.00 mmol) to which triethylamine (0.89 g, 8.75 mmol), *N*-methylpiperazine (0.70 g, 7.00 mmol) and acetonitrile / benzene (60 ml) were added to give **55** according to general procedure as a yellow hygroscopic foam (1.51 g, 4.66 mmol, 66.5 % yield).

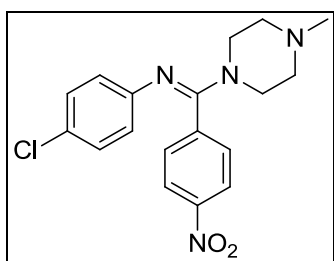
$C_{18}H_{20}N_4O_2$ (M = 324.38 g/mol), mp 146.5 °C. **1H -NMR** (300 MHz, $CDCl_3$) δ 8.09 (d, J = 8.8Hz, 2H), δ 7.30 (d, J = 8.7Hz, 2H), δ 7.01 (t, J = 7.8Hz, 2H), δ 6.77 (t, J = 7.4Hz, 1H), δ 6.52 (d, J = 7.3Hz, 2H), δ 3.43 (bs, 4H), δ 2.48 (bs, 4H), δ 2.36 (s, 3H). **ESI-MS** m/z 324.9 $[MH^+]$. **CHN** ($C_{18}H_{20}N_4O_2 \cdot \frac{1}{2} H_2O$) calc.: C 64.85; H 6.35; N 16.81; exp.: C 64.69; H 6.29; N 17.03.

(E)-4-Bromo-N-((4-methylpiperazin-1-yl)(4-nitrophenyl)methylene)aniline (61)

$C_{18}H_{19}BrN_4O_2$ (M = 403.27 g/mol)

61 was prepared according to *general procedure C* from **46** (0.64 g, 2.00 mmol) in acetonitrile / benzene (30 ml) giving intermediate (*E*)-*N*-(4-bromophenyl)-4-nitrobenzimidoyl chloride (0.68 g, 2.00 mmol) to which triethylamine (0.15 g, 1.50 mmol), *N*-methylpiperazine (0.20 g, 2.00 mmol) and acetonitrile / benzene (30 ml) were added to give **61** as a yellow solid (0.38 g, 0.94 mmol, 47.1 % yield).

$C_{18}H_{19}BrN_4O_2$ (M = 403.27 g/mol), mp 156.8 °C. **¹H-NMR** (300 MHz, $CDCl_3$) δ 8.13 (d, J = 8.8Hz, 2H), δ 7.29 (d, J = 8.8Hz, 2H), δ 7.11 (d, J = 8.6Hz, 2H), δ 6.39 (d, J = 8.6Hz, 2H), δ 3.40 (bs, 4H), δ 2.45 (bs, 4H), δ 2.34 (s, 3H). **ESI-MS** m/z 404.8 $[MH^+]$. **CHN** ($C_{18}H_{19}BrN_4O_2 \cdot H_2O$) calc.: C 51.32; H 5.02; N 13.30; exp.: C 51.33; H 4.77; N 13.14.

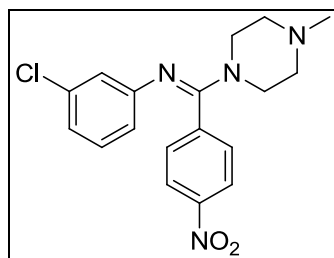
(E)-4-Chloro-N-((4-methylpiperazin-1-yl)(4-nitrophenyl)methylene)aniline (79)

$C_{18}H_{19}ClN_4O_2$ (M = 358.2 g/mol)

79 was prepared according to *general procedure C* from **77** (16.42 g, 59.35 mmol) in acetonitrile / benzene (300 ml) giving intermediate (*E*)-*N*-(4-chlorophenyl)-4-nitrobenzimidoyl chloride (17.50 g, 59.30 mmol) to which triethylamine (7.10 g, 70.00 mmol), *N*-methylpiperazine (5.94 g, 59.3 mmol) and acetonitrile / benzene (300 ml) were added to give **79** according to general procedure as a yellow hygroscopic foam (11.40 g, 31.77 mmol, 53.6 % yield).

$C_{18}H_{19}ClN_4O_2$ ($M = 358.82$ g/mol), mp 133.0 °C. **1H -NMR** (300 MHz, $CDCl_3$) δ 8.13 (d, $J = 8.8$ Hz, 2H), 7.29 (d, $J = 8.8$ Hz, 2H), 6.96 (d, $J = 8.7$ Hz, 2H), 6.44 (d, $J = 8.7$ Hz, 2H), 3.45 (bs, 4H), 2.47 (bs, 4H), 2.36 (s, 3H). **ESI-MS** m/z 358.9 $[MH^+]$. **CHN** ($C_{18}H_{19}ClN_4O_2$) calc.: C 60.25; H 5.34; N 15.61; exp.: C 60.33; H 5.51; N 15.61.

(*E*)-3-Chloro-*N*-((4-methylpiperazin-1-yl)(4-nitrophenyl)methylene)aniline (102)

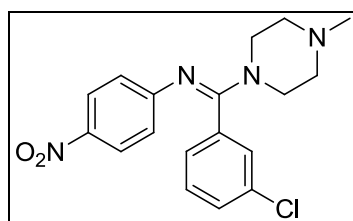


$C_{18}H_{19}ClN_4O_2$ ($M = 358.82$ g/mol)

102 was prepared according to *general procedure C* from **100** (6.00 g, 21.69 mmol) in acetonitrile / benzene (150 ml) giving intermediate (*E*)-*N*-(3-chlorophenyl)-4-nitrobenzimidoyl chloride (6.40 g, 21.69 mmol) to which triethylamine (2.74 g, 27.11 mmol), *N*-methylpiperazine (2.17 g, 21.69 mmol) and acetonitrile / benzene (150 ml) were added to give **102** as a yellow hygroscopic foam (2.97 g, 8.28 mmol, 38.2 % yield).

$C_{18}H_{19}ClN_4O_2$ ($M = 358.82$ g/mol), mp 113.6 °C. **1H -NMR** (300 MHz, $CDCl_3$) δ 8.15 (d, $J = 8.8$ Hz, 2H), δ 7.31 (d, $J = 8.7$ Hz, 2H), δ 6.92 (t, $J = 7.9$ Hz, 1H), δ 6.76 (d, $J = 6.0$ Hz, 1H), δ 6.58 (t, $J = 2.0$ Hz, 1H), δ 6.35 (d, $J = 8.9$ Hz, 1H), δ 3.49 (bs, 4H), δ 2.61 (bs, 4H), δ 2.45 (s, 3H). **ESI-MS** m/z 358.9 $[MH^+]$. **CHN** ($C_{18}H_{19}ClN_4O_2 \cdot H_2O$) calc.: C 59.26; H 5.43; N 15.36; exp.: C 59.21; H 5.68; N 15.28.

(*E*)-*N*-((3-Chlorophenyl)(4-methylpiperazin-1-yl)methylene)-4-nitroaniline (109)

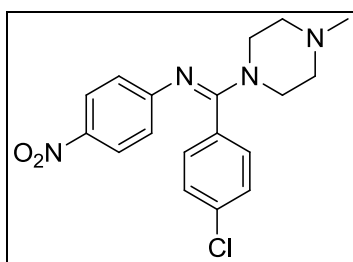


$C_{18}H_{19}ClN_4O_2$ ($M = 358.82$ g/mol)

109 was prepared according to *general procedure C* from **105** (8.48 g, 30.65 mmol) in acetonitrile / benzene (150 ml) giving intermediate (*E*)-3-chloro-*N*-(4-nitrophenyl)benzimidoyl chloride (9.05 g, 30.65 mmol) to which triethylamine (3.88 g, 38.31 mmol), *N*-methylpiperazine (3.07 g, 30.65 mmol) and acetonitrile / benzene (150 ml) were added to give **109** as a yellow hygroscopic foam (4.47 g, 12.46 mmol, 40.7 % yield).

$C_{18}H_{19}ClN_4O_2$ ($M = 358.82$ g/mol), mp 107.9 °C. **¹H-NMR** (300 MHz, $CDCl_3$) δ 7.92 (d, $J = 9.0$ Hz, 2H), δ 7.23 (m, 2H), δ 7.14 (t, $J = 1.7$ Hz, 1H), δ 6.96 (d, $J = 7.4$ Hz, 1H), δ 6.58 (d, $J = 9.0$ Hz, 2H), δ 3.49 (bs, 4H), δ 2.53 (bs, 4H), δ 2.40 (s, 3H). **ESI-MS** m/z 358.9 $[MH^+]$. **CHN** ($C_{18}H_{19}ClN_4O_2 \cdot \frac{1}{3} H_2O$) calc.: C 59.26; C 5.43; N 15.36; exp.: C 59.18; H 5.59; N 15.16.

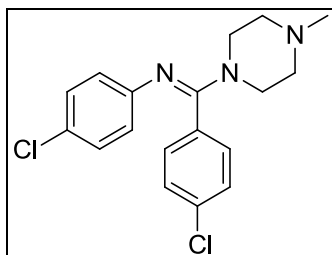
(*E*)-*N*-((4-Chlorophenyl)(4-methylpiperazin-1-yl)methylene)-4-nitroaniline (108**)**



$C_{18}H_{19}ClN_4O_2$ ($M = 358.82$ g/mol)

108 was prepared according to *general procedure C* from **104** (8.31 g, 30.03 mmol) in acetonitrile / benzene (150 ml) giving intermediate (*E*)-4-chloro-*N*-(4-nitrophenyl)benzimidoyl chloride (8.86 g, 30.03 mmol) to which triethylamine (3.80 g, 37.54 mmol), *N*-methylpiperazine (3.01 g, 30.03 g mmol) and acetonitrile / benzene (150 ml) were added to give **108** as a yellow hygroscopic foam (2.97 g, 8.27 mmol, 27.5 % yield).

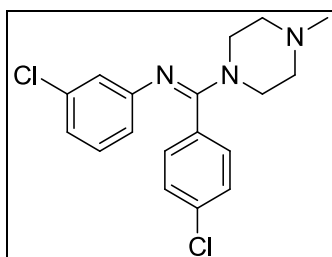
$C_{18}H_{19}ClN_4O_2$ ($M = 358.82$ g/mol), mp 113.1 °C. **¹H-NMR** (300 MHz, $CDCl_3$) δ 7.91 (d, $J = 9.0$ Hz, 2H), δ 7.26 (t, $J = 4.3$ Hz, 2H), δ 7.05 (d, $J = 8.5$ Hz, 2H), δ 6.56 (d, $J = 9.1$ Hz, 2H), δ 3.50 (bs, 4H), δ 2.51 (bs, 4H), δ 2.38 (s, 3H). **ESI-MS** m/z 358.9 $[MH^+]$. **CHN** ($C_{18}H_{19}ClN_4O_2 \cdot \frac{1}{3} H_2O$) calc.: C 59.26; H 5.43; N 15.63; exp.: C 59.24; H 5.51; N 15.33.

(E)-4-Chloro-N-((4-chlorophenyl)(4-methylpiperazin-1-yl)methylene)aniline (180)

$C_{18}H_{19}Cl_2N_3$ (M = 348.27 g/mol)

180 was prepared according to *general procedure C* from **176** (4.00 g, 15.03 mmol) in acetonitrile / benzene (105 ml) giving intermediate (*E*)-4-chloro-*N*-(4-chlorophenyl)benzimidoyl chloride (4.28 g, 15.03 mmol) to which triethylamine (1.90 g, 18.79 mmol), *N*-methylpiperazine (1.51 g, 15.03 g mmol) and acetonitrile / benzene (120 ml) were added to give **180** as a colorless solid (1.03 g, 3.07 mmol, 20.4 % yield).

$C_{18}H_{19}Cl_2N_3$ (M = 348.27 g/mol), mp 293.2 °C (decomposition). **¹H-NMR** (300 MHz, $CDCl_3$) δ 7.26 (d, J = 8.4Hz, 2H), δ 7.01 (m, 4H), δ 6.45 (d, J = 8.6Hz, 2H), δ 3.68 (bs, 4H), δ 2.82 (bs, 4H), δ 2.59 (s, 3H). **¹³C-NMR** (75 MHz, $CDCl_3$) δ 159.65 (C_{quat}), 149.36 (C_{quat}), 134.91 (C_{quat}), 131.44 (C_{quat}), 130.35 (+, 2 Ar-CH), 128.77 (+, 2 Ar-CH), 128.35 (+, 2 Ar-CH), 126.41 (C_{quat}), 123.91 (+, 2 Ar-CH), 54.86 (-, 2 Pip-CH₂), 46.15 (+, CH₃), 45.77 (-, 2 Pip-CH₂). **ESI-MS** *m/z* 348.1 [MH^+]. **CHN** ($C_{18}H_{19}Cl_2N_3 \cdot \frac{2}{3} H_2O$) calc.: C 60.01; H 5.69; N 11.66; exp.: C 59.91; H 5.33; N 11.55.

(E)-3-Chloro-N-((4-chlorophenyl)(4-methylpiperazin-1-yl)methylene)aniline (181)

$C_{18}H_{19}Cl_2N_3$ (M = 348.27 g/mol)

181 was prepared according to *general procedure C* from **177** (1.60 g, 6.01 mmol) in acetonitrile / benzene (90 ml) giving intermediate (*E*)-4-chloro-*N*-(3-chlorophenyl)benzimidoyl chloride (1.71 g, 6.01 mmol) to which triethylamine (0.76 g,

7.51 mmol), *N*-methylpiperazine (0.60 g, 6.01 mmol) and acetonitrile / benzene (75 ml) were added to give **181** as a colorless solid (470 mg, 1.35 mmol, 22.5 % yield).

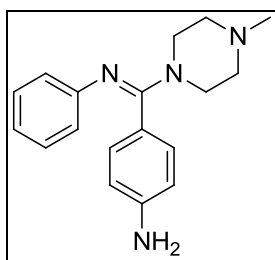
$C_{18}H_{19}Cl_2N_3$ ($M = 348.27$ g/mol), mp 97.1 °C **1H -NMR** (300 MHz, $CDCl_3$) δ 7.25 (d, $J = 7.4$ Hz, 2H), δ 7.05 (d, $J = 8.5$ Hz, 2H), δ 6.92 (t, $J = 7.9$ Hz, 1H), δ 6.75 (d, $J = 8.0$ Hz, 1H), δ 6.59 (t, $J = 2.0$ Hz, 1H), δ 6.36 (d, $J = 8.9$ Hz, 1H), δ 3.50 (bs, 4H), δ 2.55 (bs, 4H), δ 2.41 (s, 3H). **^{13}C -NMR** (75 MHz, $CDCl_3$) δ 159.59 (C_{quat}), 152.09 (C_{quat}), 135.03 (C_{quat}), 133.76 (C_{quat}), 131.23 (C_{quat}), 130.28 (+, 2 Ar-CH), 129.28 (+, 2 Ar-CH), 128.80 (+, Ar-CH), 122.86 (+, Ar-CH), 121.39 (+, Ar-CH), 120.86 (+, Ar-CH), 54.77 (-, 2 Pip-CH₂), 46.03 (+, CH₃), 45.81 (-, 2 Pip-CH₂). **ESI-MS** m/z 348.1 [MH^+]. **CHN** ($C_{18}H_{19}Cl_2N_3 \cdot \frac{4}{3} H_2O$) calc.: C 58.07; H 5.87; N 11.29; exp.: C 58.28; H 5.48; N 10.94.

6.5. General procedure D:

Preparation of compounds **52**, **56**, **62**, **80**, **103**, **110**, **111**

To a solution of **50**, **55**, **61**, **79**, **102**, **108**, or **109** in ethanol the 5-fold excess of $SnCl_2 \cdot 2 H_2O$ was added and the mixture was heated at reflux over night. The next day the mixture was cooled to room temperature and the solvent was evaporated under reduced pressure. Water and DCM (1 : 3) were added to the resulting solid and the pH was adjusted to 7 using a saturated solution of Na_2CO_3 . The aqueous layer was extracted with DCM and the combined organic layers were dried over Na_2SO_4 . Evaporation of the solvent yielded the crude product, which was purified by column chromatography (EtOAc / methanol (1 : 1)) to give the title compounds **52**, **56**, **62**, **80**, **103**, **110**, **111**.

(*E*)-*N*-((4-Aminophenyl)(4-methylpiperazin-1-yl)methylene)aniline (**56**)

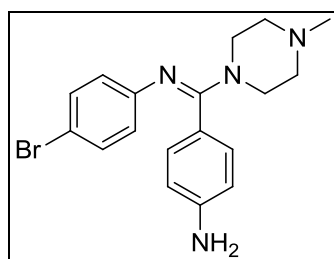


$C_{18}H_{22}N_4$ ($M = 294.39$ g/mol)

56 was prepared according to *general procedure D* from **55** (0.50 g, 1.54 mmol) in 60 ml ethanol and was obtained as a light yellow foam (0.19 g, 0.64 mmol, 41.7 % yield).

$C_{18}H_{22}N_4$ ($M = 294.39$ g/mol), mp 140.0 °C. **1H -NMR** (300 MHz, $CDCl_3$) δ 7.02 (t, $J = 7.8$ Hz, 2H), δ 6.90 (d, $J = 8.4$ Hz, 2H), δ 6.75 (t, $J = 7.3$ Hz, 1H), δ 6.57 (d, $J = 7.3$ Hz, 2H), δ 6.49 (d, $J = 8.5$ Hz, 2H), δ 4.52 (s, 2H), δ 3.45 (bs, 4H), δ 2.48 (bs, 4H), δ 2.35 (s, 3H). **^{13}C -NMR** (75 MHz, $CDCl_3$) δ 161.23 (C_{quat}), 151.08 (C_{quat}), 146.90 (2 C_{quat}), 130.72 (+, 2 Ar-CH), 128.18 (+, Ar-CH), 122.93 (+, 2 Ar-CH), 120.94 (+, 2 Ar-CH), 114.38 (+, 2 Ar-CH), 54.85 (-, 2 Pip-CH₂), 46.07 (-, 2 Pip-CH₂), 45.93 (+, CH₃). **ESI-MS** m/z 295.0 [MH^+]. **CHN** ($C_{18}H_{22}N_4 \cdot H_2O$) calc.: C 69.20; H 7.74; N 17.93; exp.: C 69.09; H 7.86; N 17.78.

(*E*)-*N*-((4-Aminophenyl)(4-methylpiperazin-1-yl)methylene)-4-bromoaniline (62**)**

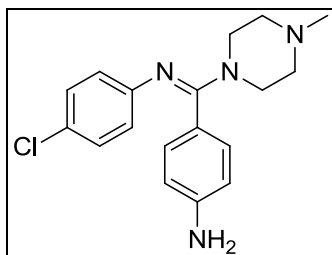


$C_{18}H_{21}BrN_4$ ($M = 373.29$ g/mol)

62 was prepared according to *general procedure D* from **61** (0.81 g, 2.00 mmol) in 60 ml ethanol and was obtained as a light yellow foam (0.20 g, 0.53 mmol, 37.9 % yield).

$C_{18}H_{21}BrN_4$ ($M = 373.29$ g/mol), mp 162.2 °C. **1H -NMR** (300 MHz, $CDCl_3$) δ 7.10 (d, $J = 8.6$ Hz, 2H), δ 6.87 (d, $J = 8.4$ Hz, 2H), δ 6.51 (d, $J = 8.5$ Hz, 2H), δ 6.43 (d, $J = 8.6$ Hz, 2H), δ 3.73 (s, 2H), δ 3.44 (bs, 4H), δ 2.44 (bs, 4H), δ 2.33 (s, 3H). **^{13}C -NMR** (75 MHz, $CDCl_3$) δ 161.45 (C_{quat}), 150.71 (C_{quat}), 146.98 (C_{quat}), 131.06 (+, 2 Ar-CH), 130.62 (+, 2 Ar-CH), 124.64 (+, 2 Ar-CH), 122.44 (C_{quat}), 114.47 (+, 2 Ar-CH), 113.47 (C_{quat}), 55.01 (-, 2 Pip-CH₂), 46.16 (+, CH₃), 45.80 (-, 2 Pip-CH₂). **ESI-MS** m/z 372.8 [MH^+], 374.8. **CHN** ($C_{18}H_{21}BrN_4 \cdot \frac{1}{3} H_2O$) calc.: C 57.35; H 5.86; N 14.59; exp.: C 57.48; H 5.60; N 14.40.

(E)-N-((4-Aminophenyl)(4-methylpiperazin-1-yl)methylene)-4-chloroaniline (80)

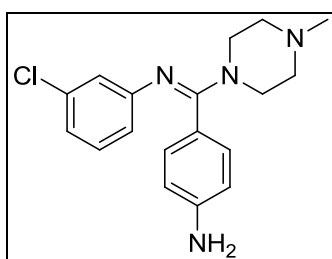


$C_{18}H_{21}ClN_4$ (M = 328.84 g/mol)

80 was prepared according to *general procedure D* from **79** (2.18 g, 6.08 mmol) in 80 ml ethanol and was obtained as a very light yellow foam (0.76 g, 2.32 mmol, 38.1 % yield).

$C_{18}H_{21}ClN_4$ (M = 328.84 g/mol), mp 158.3 °C. **1H -NMR** (300 MHz, $CDCl_3$) δ 6.96 (d, J = 8.6Hz, 2H), δ 6.87 (d, J = 8.4Hz, 2H), δ 6.49 (t, J = 8.9Hz, 4H), δ 3.73 (s, 2H), δ 3.44 (bs, 4H), δ 2.44 (bs, 4H), δ 2.34 (s, 3H). **^{13}C -NMR** (75 MHz, $CDCl_3$) δ 161.51 (C_{quat}), 150.05 (C_{quat}), 147.02 (C_{quat}), 130.64 (+, 2 Ar-CH), 128.15 (+, 2 Ar-CH), 125.83 (C_{quat}), 124.13 (+, 2 Ar-CH), 122.37 (C_{quat}), 114.45 (+, 2 Ar-CH), 55.03 (-, 2 Pip-CH₂), 46.17 (+, CH₃), 45.79 (-, 2 Pip-CH₂). **ESI-MS** m/z 328.9 [MH^+]. **CHN** ($C_{18}H_{21}ClN_4$) calc.: C 65.74; H 6.44; N 17.04; exp.: C 65.38; H 6.29; N 17.03.

(E)-N-((4-Aminophenyl)(4-methylpiperazin-1-yl)methylene)-3-chloroaniline (103)



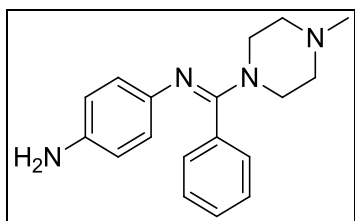
$C_{18}H_{21}ClN_4$ (M = 328.84 g/mol)

103 was prepared according to *general procedure D* from **102** (1.50 g, 4.18 mmol) in 60 ml ethanol and was obtained as a very light yellow foam (0.43 g, 1.31 mmol, 31.3 % yield).

$C_{18}H_{21}ClN_4$ (M = 328.84 g/mol), mp 152.4°C. **1H -NMR** (300 MHz, $CDCl_3$) δ 6.90 (m, 3H), δ 6.72 (d, J = 9.0Hz, 1H), δ 6.60 (t, J = 2.0Hz, 1H), δ 6.52 (d, J = 8.5Hz, 2H), δ

6.41 (d, $J = 8.9\text{Hz}$, 1H), δ 3.73 (s, 2H), δ 3.46 (bs, 4H), δ 2.46 (bs, 4H), δ 2.34 (s, 3H). **$^{13}\text{C-NMR}$** (75 MHz, CDCl_3) δ 161.53 (C_{quat}), 153.06 (C_{quat}), 147.04 (C_{quat}), 133.53 (C_{quat}), 130.58 (+, 2 Ar-CH), 129.05 (+, 2 Ar-CH), 123.05 (+, Ar-CH), 122.38 (C_{quat}), 121.14 (+, Ar-CH), 120.69 (+, Ar-CH), 114.47 (+, Ar-CH), 54.99 (-, 2 Pip- CH_2), 46.15 (+, CH_3), 45.74 (-, 2 Pip- CH_2). **ESI-MS** m/z 328.9 [MH^+]. **CHN** ($\text{C}_{18}\text{H}_{21}\text{ClN}_4 \cdot \frac{2}{3} \text{CH}_3\text{OH}$) calc.: C 64.02; H 6.67; N 16.16; exp.: C 63.97; H 6.75; N 16.24.

(*E*)- N' -((4-Methylpiperazin-1-yl)(phenyl)methylen)benzene-1,4-diamine (52)

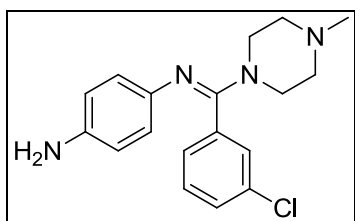


$\text{C}_{18}\text{H}_{22}\text{N}_4$ ($M = 294.39 \text{ g/mol}$)

52 was prepared according to *general procedure D* from **50** (0.43 g, 1.33 mmol) in 60 ml ethanol and was obtained as a light yellow foam (0.19 g, 0.64 mmol, 47.8 % yield).

$\text{C}_{18}\text{H}_{22}\text{N}_4$ ($M = 294.39 \text{ g/mol}$), mp 140.3°C . **$^1\text{H-NMR}$** (300 MHz, CDCl_3) δ 7.86 (d, $J = 9.0\text{Hz}$, 2H), δ 7.25 (m, 3H), δ 7.08 (d, $J = 6.4\text{Hz}$, 2H), δ 6.55 (d, $J = 9.0\text{Hz}$, 2H), δ 3.71 (s, 2H), δ 3.49 (bs, 4H), δ 2.47 (bs, 4H), δ 2.35 (s, 3H). **$^{13}\text{C-NMR}$** (75 MHz, CDCl_3) δ 160.66 (C_{quat}), 142.79 (C_{quat}), 140.14 (C_{quat}), 133.83 (C_{quat}), 129.16 (+, 2 Ar-CH), 128.43 (+, 2 Ar-CH), 128.17 (+, Ar-CH), 123.52 (+, 2 Ar-CH), 115.55 (+, 2 Ar-CH), 55.02 (-, 2 Pip- CH_2), 46.19 (+, CH_3), 45.89 (-, 2 Pip- CH_2). **ESI-MS** m/z 280 [MH^+]. **CHN** ($\text{C}_{18}\text{H}_{21}\text{N}_3 \cdot \frac{1}{3} \text{H}_2\text{O}$) calc.: C 71.97; H 7.61; N 18.65; exp.: C 72.05; H 7.52; N 18.42.

(*E*)- N' -((3-Chlorophenyl)(4-methylpiperazin-1-yl)methylene)benzene-1,4-diamine (110)

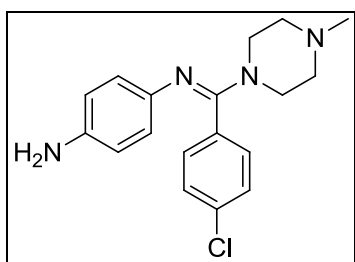


$\text{C}_{18}\text{H}_{21}\text{ClN}_4$ ($M = 328.84 \text{ g/mol}$)

110 was prepared according to *general procedure D* from **109** (2.30 g, 6.41 mmol) in 60 ml ethanol and was obtained as a light yellow foam (0.16 g, 0.48 mmol, 3.6 % yield).

$C_{18}H_{21}ClN_4$ ($M = 328.84$ g/mol), mp 128.4 °C. **1H -NMR** (300 MHz, $CDCl_3$) δ 7.90 (d, $J = 9.1$ Hz, 2H), δ 7.22 (m, 2H), δ 7.13 (t, $J = 1.5$ Hz, 1H), δ 6.94 (d, $J = 7.2$ Hz, 1H), δ 6.56 (d, $J = 9.1$ Hz, 2H), δ 3.79 (s, 2H), δ 3.49 (bs, 4H), δ 2.53 (bs, 4H), δ 2.40 (s, 3H). **^{13}C -NMR** (75 MHz, $CDCl_3$) δ 159.01 (C_{quat}), 142.29 (C_{quat}), 140.41 (C_{quat}), 135.71 (C_{quat}), 134.30 (C_{quat}), 129.54 (+, 2 Ar-CH), 128.95 (+, 2 Ar-CH), 128.69 (+, Ar-CH), 127.39 (+, Ar-CH), 123.38 (+, Ar-CH), 115.67 (+, Ar-CH), 54.89 (-, 2 Pip-CH₂), 46.14 (+, CH₃), 46.02 (-, 2 Pip-CH₂). **ESI-MS** m/z 328.9 [MH^+]. **CHN** ($C_{18}H_{21}ClN_4 \cdot \frac{3}{4} CH_3OH$) calc.: C 62.49; H 7.14; N 15.08; exp.: C 62.31; H 6.73; N 15.11.

(*E*)- N' -((4-Chlorophenyl)(4-methylpiperazin-1-yl)methylene)benzene-1,4-diamine (111)



$C_{18}H_{21}ClN_4$ ($M = 328.84$ g/mol)

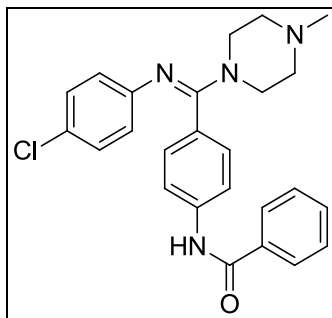
111 was prepared according to *general procedure D* from **108** (1.08 g, 3.01 mmol) in 60 ml ethanol and was obtained as a light yellow solid (0.13 g, 0.40 mmol, 4.4 % yield).

$C_{18}H_{21}ClN_4$ ($M = 328.84$ g/mol), mp 126.4 °C. **1H -NMR** (300 MHz, $CDCl_3$) δ 7.21 (d, $J = 8.5$ Hz, 2H), δ 7.04 (d, $J = 8.4$ Hz, 2H), δ 6.38 (m, 4H), δ 3.40 (s, 2H), δ 2.68 (bs, 4H), δ 2.45 (bs, 4H), δ 2.34 (s, 3H). **^{13}C -NMR** (75 MHz, $CDCl_3$) δ 159.54 (C_{quat}), 142.48 (C_{quat}), 140.36 (C_{quat}), 134.41 (C_{quat}), 132.25 (C_{quat}), 130.55 (+, 2 Ar-CH), 128.54 (+, 2 Ar-CH), 123.40 (+, 2 Ar-CH), 115.66 (+, 2 Ar-CH), 54.93 (-, 2 Pip-CH₂), 46.16 (+, CH₃), 46.06 (-, 2 Pip-CH₂). **ESI-MS** m/z 328.9 [MH^+]. **CHN** ($C_{18}H_{21}ClN_4 \cdot \frac{4}{5} CH_3OH$) calc.: C 63.70; H 6.88; N 15.81; exp.: C 63.74; H 6.75; N 15.93.

6.6. General procedure E:**Preparation of compounds 99, 112, 114 - 117**

To a solution of **80** or **103** (2.0 mmol) and triethylamine (3.0 mmol) in 100 ml DCM a substituted acid chloride (2.4 mmol) was added under nitrogen atmosphere and vigorous stirring. After stirring at room temperature for 6 h the mixture was heated at reflux over night. The next day the solution was cooled to room temperature, concentrated and purified by column chromatography (ethyl acetate / methanol 1 : 1) to give the title compounds **99, 112, 114 - 117**.

(E)-N-(4-((4-Chlorophenylimino)(4-methylpiperazin-1-yl)methyl)phenyl)benzamide (99)

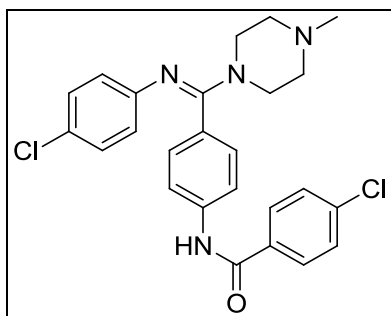


$C_{25}H_{25}ClN_4O$ ($M = 432.95$ g/mol)

99 was prepared according to *general procedure E* from **30** (2.00 g, 6.10 mmol) and benzoylchloride (1.03 g, 7.32 mmol) and was obtained as a light yellow foam (1.19 g, 2.75 mmol, 45.0 % yield).

$C_{25}H_{25}ClN_4O$ ($M = 432.95$ g/mol), mp 95.9 °C. **1H -NMR** (300 MHz, $CDCl_3$) δ 7.84 (d, $J = 7.0$ Hz, 3H), δ 7.52 (m, 5H), δ 7.10 (d, $J = 8.5$ Hz, 2H), δ 6.97 (d, $J = 8.6$ Hz, 2H), δ 6.49 (d, $J = 8.6$ Hz, 2H), δ 3.48 (bs, 4H), δ 2.49 (bs, 4H), δ 2.37 (s, 3H). **^{13}C -NMR** (75 MHz, $CDCl_3$) δ 165.90 (C_{quat} , $C=O$), 160.36 (C_{quat}), 149.53 (C_{quat}), 138.55 (C_{quat}), 134.60 (C_{quat}), 132.11 (+, 2 Ar-CH), 129.99 (+, 2 Ar-CH), 128.85 (+, 2 Ar-CH), 128.74 (C_{quat}), 128.28 (+, Ar-CH), 127.06 (+, 2 Ar-CH), 126.27 (C_{quat}), 124.07 (+, 2 Ar-CH), 119.85 (+, 2 Ar-CH), 54.84 (-, 2 Pip- CH_2), 46.00 (+, CH_3), 45.90 (-, 2 Pip- CH_2). **ESI-MS** m/z 433.0 [MH^+]. **CHN** ($C_{25}H_{25}ClN_4O \cdot \frac{1}{2} H_2O$) calc.: C 67.94; H 5.93; N 12.68; exp.: C 67.67; H 6.18; N 12.43.

(E)-4-Chloro-N-(4-((4-chlorophenylimino)(4-methylpiperazin-1-yl)methyl)phenyl)-benzamide (112)

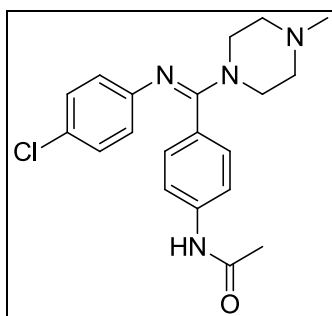


$C_{25}H_{24}Cl_2N_4O$ (M = 467.39 g/mol)

112 was prepared according to *general procedure E* from **80** (0.72 g, 2.19 mmol) and 4-chlorobenzoylchloride (0.46 g, 2.63 mmol) and was obtained as a light yellow solid (0.41 g, 0.88 mmol, 40.2 % yield).

$C_{25}H_{24}Cl_2N_4O$ (M = 467.39 g/mol), mp 75.0 °C. **1H -NMR** (300 MHz, $CDCl_3$) δ 7.78 (d, J=8.6Hz, 3H), δ 7.49 (m, 4H), δ 7.10 (d, J=8.5Hz, 2H), δ 6.96 (d, J=8.6Hz, 2H), δ 6.48 (d, J=8.6Hz, 2H), δ 3.46 (bs, 4H), δ 2.47 (bs, 4H), δ 2.35 (s, 3H). **^{13}C -NMR** (75 MHz, $CDCl_3$) δ 164.83 (C_{quat} , C=O), 160.33 (C_{quat}), 149.74 (C_{quat}), 138.41 (C_{quat}), 138.18 (C_{quat}), 132.96 (C_{quat}), 130.00 (+, 2 Ar-CH), 129.20 (C_{quat}), 129.11 (+, 2 Ar-CH), 128.49 (+, 2 Ar-CH), 128.25 (+, 2 Ar-CH), 126.17 (C_{quat}), 124.05 (+, 2 Ar-CH), 119.88 (+, 2 Ar-CH), 54.89 (-, 2 Pip-CH₂), 46.19 (-, 2 Pip-CH₂), 46.13 (+, CH₃). **ESI-MS** m/z 466.9 [MH⁺]. **CHN** ($C_{25}H_{24}Cl_2N_4O \cdot \frac{2}{3} H_2O$) calc.: C 62.63; H 5.33; N 11.69; exp.: C 62.59; H 5.59; N 11.40.

(E)-N-(4-((4-Chlorophenylimino)(4-methylpiperazin-1-yl)methyl)phenyl)acetamide (114)

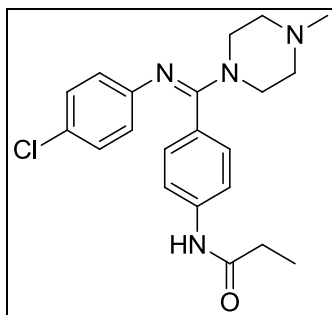


$C_{20}H_{23}ClN_4O$ (M = 370.88 g/mol)

114 was prepared according to *general procedure E* from **80** (0.95 g, 2.89 mmol) and acetylchloride (0.27 g, 3.47 mmol) and was obtained as colorless foam (0.59 g, 1.59 mmol, 55.0 % yield).

$C_{20}H_{23}ClN_4O$ (M = 370.88 g/mol), mp 82.1 °C. **¹H-NMR** (300 MHz, $CDCl_3$) δ 7.40 (d, J = 8.4Hz, 2H), δ 7.20 (s, 1H), δ 7.04 (d, J = 8.5Hz, 2H), δ 6.94 (d, J = 8.6Hz, 2H), δ 6.46 (d, J = 8.6Hz, 2H), δ 3.44 (bs, 4H), δ 2.46 (bs, 4H), δ 2.34 (s, 3H), δ 2.15 (s, 3H). **¹³C-NMR** (75 MHz, $CDCl_3$) δ 168.53 (C_{quat} , C=O), 160.50 (C_{quat}), 149.76 (C_{quat}), 138.43 (C_{quat}), 129.89 (+, 2 Ar-CH), 128.60 (C_{quat}), 128.21 (+, 2 Ar-CH), 126.10 (C_{quat}), 124.06 (+, 2 Ar-CH), 119.31 (+, 2 Ar-CH), 54.91 (-, 2 Pip-CH₂), 46.13 (+, CH₃), 46.07 (-, 2 Pip-CH₂), 24.58 (+, CH₃). **ESI-MS** *m/z* 370.9 [MH⁺]. **CHN** ($C_{20}H_{23}ClN_4O \cdot \frac{3}{4} H_2O$) calc.: C 62.49; H 6.42; N 14.58; exp.: C 62.22; H 6.51; N 14.23.

(E)-N-(4-((4-Chlorophenylimino)(4-methylpiperazin-1-yl)methyl)phenyl)propionamide (115)



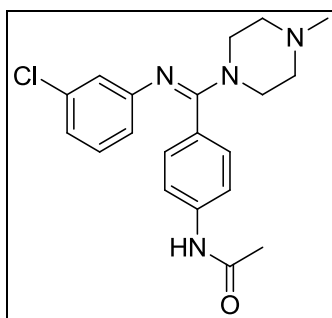
$C_{21}H_{25}ClN_4O$ (M = 384.90 g/mol)

115 was prepared according to *general procedure E* from **80** (0.88 g, 2.68 mmol) and propionylchloride (0.28 g, 3.21 mmol) and was obtained as colorless foam (0.25 g, 0.64 mmol, 23.9 % yield).

$C_{21}H_{25}ClN_4O$ (M = 384.90 g/mol), mp 94.1 °C. **¹H-NMR** (300 MHz, $CDCl_3$) δ 7.42 (d, J = 8.4Hz, 2H), δ 7.15 (s, 1H), δ 7.04 (d, J = 8.6Hz, 2H), δ 6.95 (d, J = 8.6Hz, 2H), δ 6.46 (d, J = 8.6Hz, 2H), δ 3.46 (bs, 4H), δ 2.49 (bs, 4H), δ 2.36 (m, 5H), δ 1.23 (t, 3H, J = 7.5Hz). **¹³C-NMR** (75 MHz, $CDCl_3$) δ 172.18 (C_{quat} , C=O), 160.49 (C_{quat}), 149.76 (C_{quat}), 138.47 (C_{quat}), 129.90 (+, 2 Ar-CH), 128.47 (C_{quat}), 128.21 (+, 2 Ar-CH), 126.10 (C_{quat}), 124.05 (+, 2 Ar-CH), 119.25 (+, 2 Ar-CH), 54.84 (-, 2 Pip-CH₂), 46.19 (-, 2 Pip-CH₂),

46.06 (+, CH₃), 30.74 (-, CH₂), 9.58 (+, CH₃). **ESI-MS** *m/z* 385.0 [MH⁺]. **CHN** (C₂₁H₂₅ClN₄O · H₂O) calc.: C 63.60; H 6.75; N 13.91; exp.: C 63.93; H 6.58; N 13.64.

(E)-N-(4-((3-Chlorophenylimino)(4-methylpiperazin-1-yl)methyl)phenyl)acetamide (116)

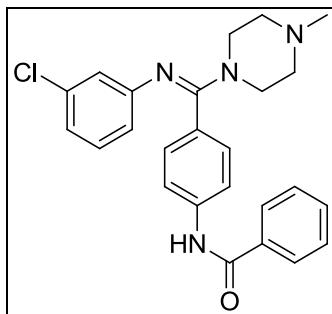


C₂₀H₂₃ClN₄O (M = 370.88 g/mol)

116 was prepared according to *general procedure E* from **103** (1.54 g, 4.68 mmol) and acetylchloride (0.44 g, 5.62 mmol) and was obtained as colorless foam (0.16 g, 0.44 mmol, 9.4 % yield).

C₂₀H₂₃ClN₄O (M = 370.88 g/mol), mp 179.6 °C. **¹H-NMR** (300 MHz, CDCl₃) δ 7.42 (d, J = 8.4Hz, 2H), δ 7.28 (s, 1H), δ 7.06 (d, J = 8.5Hz, 2H), δ 6.90 (t, J = 7.9Hz, 1H), δ 6.72 (d, J = 7.9Hz, 1H), δ 6.58 (t, J = 1.9Hz, 1H), δ 6.39 (d, J = 8.1Hz, 1H), δ 3.49 (bs, 4H), δ 2.53 (bs, 4H), δ 2.39 (s, 3H), δ 2.15 (s, 3H). **¹³C-NMR** (75 MHz, CDCl₃) δ 168.50 (C_{quat}, C=O), 160.44 (C_{quat}), 152.58 (C_{quat}), 138.44 (C_{quat}), 133.59 (C_{quat}), 129.86 (+, 2 Ar-CH), 129.16 (+, 2 Ar-CH), 128.51 (C_{quat}), 122.94 (+, Ar-CH), 121.09 (+, Ar-CH), 121.03 (+, Ar-CH), 119.33 (+, Ar-CH), 54.92 (-, 2 Pip-CH₂), 46.15 (+, CH₃), 45.99 (-, 2 Pip-CH₂), 24.60 (+, CH₃). **ESI-MS** *m/z* 371.2 [MH⁺]. **CHN** (C₂₀H₂₃ClN₄O · 4/5 H₂O) calc.: C 62.35; H 6.44; N 14.54; exp.: C 62.60; H 6.10; N 14.25.

(E)-N-(4-((3-Chlorophenylimino)(4-methylpiperazin-1-yl)methyl)phenyl)benzamide (117)



$C_{25}H_{25}ClN_4O$ ($M = 432.95$ g/mol)

117 was prepared according to *general procedure E* from **103** (0.97 g, 2.95 mmol) and benzoylchloride (0.50 g, 3.54 mmol) and was obtained as colorless foam (0.26 g, 0.61 mmol, 20.7 % yield).

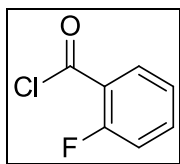
$C_{25}H_{25}ClN_4O$ ($M = 432.95$ g/mol), mp 91.9 °C. **1H -NMR** (300 MHz, $CDCl_3$) δ 7.83 (d, $J = 8.6$ Hz, 3H), δ 7.51 (m, 5H), δ 7.13 (d, $J = 8.5$ Hz, 2H), δ 6.92 (t, $J = 7.9$ Hz, 1H), δ 6.73 (d, $J = 7.1$ Hz, 1H), δ 6.62 (t, $J = 2.0$ Hz, 1H), δ 6.41 (d, $J = 8.9$ Hz, 1H), δ 3.48 (bs, 4H), δ 2.52 (bs, 4H), δ 2.39 (s, 3H). **^{13}C -NMR** (75 MHz, $CDCl_3$) δ 165.80 (C_{quat} , $C=O$), 160.33 (C_{quat}), 152.52 (C_{quat}), 138.45 (C_{quat}), 134.62 (C_{quat}), 133.66 (C_{quat}), 132.12 (+, 2 Ar-CH), 129.97 (+, 2 Ar-CH), 129.19 (+, 2 Ar-CH), 128.89 (+, 2 Ar-CH), 128.82 (C_{quat}), 127.00 (+, Ar-CH), 122.98 (+, Ar-CH), 121.12 (+, Ar-CH), 121.06 (+, Ar-CH), 119.78 (+, Ar-CH), 54.86 (-, 2 Pip- CH_2), 46.17 (-, 2 Pip- CH_2), 46.07 (+, CH_3). **ESI-MS** m/z 433.0 [MH^+]. **CHN** ($C_{25}H_{25}ClN_4O \cdot 2 H_2O$) calc.: C 67.48; H 5.97; N 12.59; exp.: C 67.34; H 6.16; N 12.25.

6.7. General procedure F:

Preparation of compounds **84**, **118**, **145**

To a solution of substituted 2-fluorobenzoic acid in THF, one equivalent of thionylchloride was added dropwise and heated at reflux for 2 h. After cooling to room temperature, the solvent as well as excess thionylchloride were removed under reduced pressure yielding the crude product. Compounds **84**, **118**, and **145** were used in the next step without further purification.

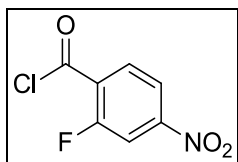
2-Fluorobenzoyl chloride (84)



$\text{C}_7\text{H}_4\text{ClFO}$ ($M = 158.56 \text{ g/mol}$)

84 was prepared according to *general procedure F* using 2-fluorobenzoic acid (1.40 g, 10 mmol) in 30 ml THF yielding a light yellow solid (1.59 g, 10 mmol, 100 % yield).

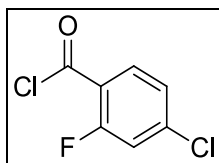
2-Fluoro-4-nitrobenzoyl chloride (118)



$\text{C}_7\text{H}_3\text{ClFNO}_3$ ($M = 203.56 \text{ g/mol}$)

118 was prepared according to *general procedure F* using 2-fluoro-4-nitrobenzoic acid (6.66 g, 36 mmol) in 75 ml THF yielding a light yellow solid (7.33 g, 36 mmol, 100 % yield).

4-Chloro-2-fluorobenzoyl chloride (145)

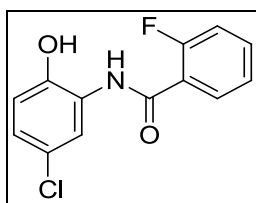


$\text{C}_7\text{H}_3\text{Cl}_2\text{FO}$ ($M = 193.00 \text{ g/mol}$)

145 was prepared according to *general procedure F* using 4-chloro-2-fluorobenzoic acid (5.16 g, 29.55 mmol) in 50 ml THF yielding a light yellow solid (5.70 g, 29.55 mmol, 100 % yield).

6.8. General procedure G:**Preparation of compounds 85, 89, 119, 120, 132, 138, 146, 152, 153**

To a solution of substituted 2-aminophenol (50 mmol) and triethylamine (100 mmol) in 100 ml dry THF, substituted 2-fluorobenzoyl chloride (50 mmol) was added dropwise at 0 °C. After the complete adding of the acid chloride, the mixture was allowed to warm to room temperature while stirring under a nitrogen atmosphere over night. The next day the mixture was diluted with 400 ml water and adjusted with HCl (w = 4 %) to pH 7. The precipitated solid was then filtered over a glass filter and washed with HCl (w = 4 %) and water and was afterwards dried in vacuo over night to give the title compounds **85, 89, 119, 120, 132, 138, 146, 152, 153** as solids of different colour that were used in the next step without further purification.

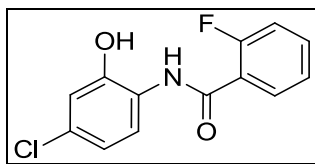
***N*-(5-Chloro-2-hydroxyphenyl)-2-fluorobenzamide (85)**

$C_{13}H_9ClFNO_2$ (M = 265.67 g/mol)

85 was prepared according to *general procedure G* using 2-amino-4-chlorophenol (7.18 g, 50.00 mmol) and 2-fluorobenzoyl chloride (8.00 g, 50.00 mmol) and was obtained as a light brown solid (12.54 g, 47.20 mmol, 94.4 % yield).

$C_{13}H_9ClFNO_2$ (M = 265.67 g/mol), mp 235.3 °C. **¹H-NMR** (300 MHz, DMSO- d_6) δ 10.47 (s, 1H), δ 9.48 (d, J = 9.2 Hz, 1H), δ 8.21 (s, 1H), δ 7.90 (t, J = 7.8 Hz, 1H), δ 7.64 (m, 1H), δ 7.39 (m, 2H), δ 7.05 (d, J = 8.6 Hz, 1H), δ 6.92 (d, J = 8.6 Hz, 1H). **CI-MS** m/z 123 (7), 140 (2), 157 (2), 180 (2), 248 (2), 266 (89, MH^+), 267 (14), 268 (27), 269 (4), 283 (100, MNH_4^+), 284 (14), 285 (31), 286 (4), 300 (1). **CHN** ($C_{13}H_9ClFNO_2$) calc.: C 58.77; H 3.41; N 5.27; exp.: C 58.66; H 3.47; N 5.13.

***N*-(4-Chloro-2-hydroxyphenyl)-2-fluorobenzamide (89)**

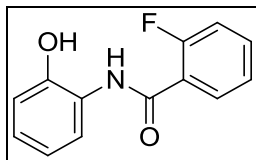


$\text{C}_{13}\text{H}_9\text{ClFNO}_2$ ($M = 265.67$ g/mol)

89 was prepared according to *general procedure G* using 2-amino-5-chlorophenol (3.62 g, 25.20 mmol) and 2-fluorobenzoyl chloride (4.00 g, 25.20 mmol) and was obtained as a red-brown solid (3.45 g, 12.99 mmol, 51.6 % yield).

$\text{C}_{13}\text{H}_9\text{ClFNO}_2$ ($M = 265.67$ g/mol), mp 142.7 °C. **$^1\text{H-NMR}$** (300 MHz, DMSO-d_6) δ 10.63 (s, 1H), δ 9.45 (d, $J = 8.3\text{Hz}$, 1H), δ 8.07 (d, $J = 8.5\text{Hz}$, 1H), δ 7.88 (t, $J = 7.3\text{Hz}$, 1H), δ 7.63 (m, 1H), δ 7.38 (m, 2H), δ 6.91 (d, $J = 12.4\text{Hz}$, 2H). **GC-MS** m/z 123 (3), 180.1 (4), 265.9 (82, MH^+), 267.1 (12), 268 (25), 269.1 (3), 283 (100), 284.1 (14), 285 (33), 286.1 (4). **CHN** ($\text{C}_{13}\text{H}_9\text{ClFNO}_2$) calc.: C 58.77; H 3.41; N 5.27; exp.: C 58.89; H 3.46; N 5.02.

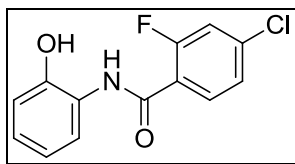
2-Fluoro-*N*-(2-hydroxyphenyl)benzamide (138)



$\text{C}_{13}\text{H}_{10}\text{FNO}_2$ ($M = 231.22$ g/mol)

138 was prepared according to *general procedure G* using 2-aminophenol (3.93 g, 36.00 mmol) and 2-fluorobenzoylchloride (5.71 g, 36.00 mmol) and was obtained as a colorless solid after re-crystallization from acetone (7.98 g, 34.51 mmol, 95.9 % yield).

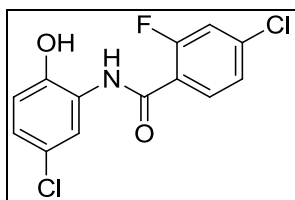
$\text{C}_{13}\text{H}_{10}\text{FNO}_2$ ($M = 231.22$ g/mol), mp 166.8 °C. **$^1\text{H-NMR}$** (300 MHz, DMSO-d_6) δ 10.06 (s, 1H), 9.44 (d, $J = 9.0\text{Hz}$, 1H), 8.12 (d, $J = 12.4\text{Hz}$, 1H), 7.97 (m, 2H), 7.48 (m, 3H), 6.73 (m, 2H). **ESI-MS** m/z 232.0 [MH^+]. **CHN** ($\text{C}_{13}\text{H}_{10}\text{FNO}_2$) calc.: C 67.53; H 4.36; N 6.06; exp.: C 67.47; H 4.38; N 5.86.

5-Chloro-2-fluoro-*N*-(2-hydroxyphenyl)benzamide (146)

$C_{13}H_9ClFNO_2$ ($M = 265.67$ g/mol)

146 was prepared according to *general procedure G* using 2-aminophenol (3.22 g, 29.55 mmol) and **145** (5.70 g, 29.55 mmol) and was obtained as a colorless solid after re-crystallization from acetone (5.03 g, 18.93 mmol, 64.1 % yield).

$C_{13}H_9ClFNO_2$ ($M = 265.67$ g/mol), mp 191.6 °C. **1H -NMR** (300 MHz, DMSO- d_6) δ 10.05 (s, 1H), δ 9.49 (d, $J = 7.6$ Hz, 1H), δ 8.02 (d, $J = 7.4$ Hz, 1H), δ 7.89 (t, $J = 8.3$ Hz, 1H), δ 7.65 (d, $J = 12.9$ Hz, 1H), δ 7.47 (d, $J = 8.4$ Hz, 1H), δ 6.92 (m, 3H). **GC-MS** m/z 266 [MH^+]. **CHN** ($C_{13}H_9ClFNO_2$) calc.: C 58.77; H 3.41; N 5.27; exp.: C 58.72; H 3.52; N 5.11.

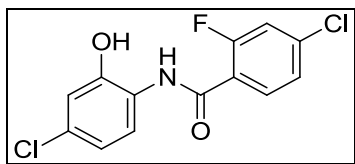
4-Chloro-*N*-(5-chloro-2-hydroxyphenyl)-2-fluorobenzamide (152)

$C_{13}H_8Cl_2FNO_2$ ($M = 300.11$ g/mol)

152 was prepared according to *general procedure G* using 2-amino-4-chlorophenol (4.47 g, 31.11 mmol) and **145** (6.00 g, 31.11 mmol) and was obtained as a colorless crystalline solid after re-crystallization from acetone (2.09 g, 6.96 mmol, 22.4 % yield).

$C_{13}H_8Cl_2FNO_2$ ($M = 300.11$ g/mol), mp 208.5 °C. **1H -NMR** (300 MHz, DMSO- d_6) δ 10.63 (s, 1H), δ 9.48 (d, $J = 7.0$ Hz, 1H), δ 8.01 (d, $J = 8.2$ Hz, 1H), δ 7.77 (t, $J = 8.1$ Hz, 1H), δ 7.64 (d, $J = 10.8$ Hz, 1H), δ 7.46 (d, $J = 10.1$ Hz, 1H), δ 6.89 (m, 2H). **ESI-MS** m/z 300.0 [MH^+]. **CHN** ($C_{13}H_8Cl_2FNO_2$) calc.: C 52.03; H 2.69; N 4.67; exp.: C 52.18; H 2.76; N 4.57.

4-Chloro-*N*-(4-chloro-2-hydroxyphenyl)-2-fluorobenzamide (**153**)

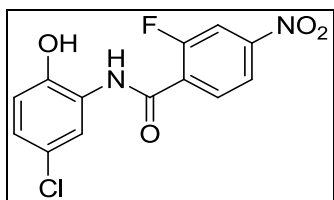


$C_{13}H_8Cl_2FNO_2$ ($M = 300.11$ g/mol)

153 was prepared according to *general procedure G* using 2-amino-5-chlorophenol (4.25 g, 29.62 mmol) and **145** (5.72 g, 29.62 mmol) and was obtained as a light purple crystalline solid after re-crystallization from acetone (7.47 g, 24.89 mmol, 84.0 % yield).

$C_{13}H_8Cl_2FNO_2$ ($M = 300.11$ g/mol), mp 230.9 °C. **1H -NMR** (300 MHz, DMSO- d_6) δ 10.61 (s, 1H), δ 9.51 (d, $J = 7.1$ Hz, 1H), δ 8.03 (d, $J = 8.5$ Hz, 1H), δ 7.86 (t, $J = 8.3$ Hz, 1H), δ 7.64 (d, $J = 11.0$ Hz, 1H), δ 7.46 (d, $J = 10.2$ Hz, 1H), δ 6.91 (m, 2H). **ESI-MS** m/z 300.0 [MH^+]. **CHN** ($C_{13}H_8Cl_2FNO_2$) calc.: C 52.03; H 2.69; N 4.67; exp.: C 51.98; H 2.82; N 4.38.

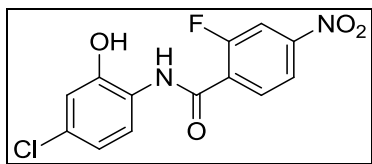
N-(5-Chloro-2-hydroxyphenyl)-2-fluoro-4-nitrobenzamide (**119**)



$C_{13}H_8ClFN_2O_4$ ($M = 310.67$ g/mol)

119 was prepared according to *general procedure G* using 2-amino-4-chlorophenol (5.17 g, 36.00 mmol) and **118** (7.33 g, 36.00 mmol) and was obtained as a light yellow crystalline solid after re-crystallization from acetone (1.74 g, 5.60 mmol, 15.5 % yield).

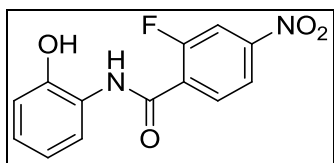
$C_{13}H_8ClFN_2O_4$ ($M = 310.67$ g/mol), mp 273.5 °C. **1H -NMR** (300 MHz, DMSO- d_6) δ 10.41 (s, 1H), δ 9.90 (d, $J = 8.9$ Hz, 1H), δ 8.28 (d, $J = 12.3$ Hz, 1H), δ 8.19 (d, $J = 10.6$ Hz, 1H), δ 8.10 (d, $J = 2.5$ Hz, 1H), δ 8.03 (m, 1H), δ 7.08 (d, $J = 11.3$ Hz, 1H), δ 6.93 (d, $J = 8.6$ Hz, 1H). **ESI-MS** m/z 309.0 [$(M-H)^-$]. **CHN** ($C_{13}H_8ClFN_2O_4$) calc.: C 50.26; H 2.60; N 9.02; exp.: C 50.24; H 2.70; N 9.03.

***N*-(4-Chloro-2-hydroxyphenyl)-2-fluoro-4-nitrobenzamide (120)**

$\text{C}_{13}\text{H}_8\text{ClFN}_2\text{O}_4$ ($M = 310.67$ g/mol)

120 was prepared according to *general procedure G* using 2-amino-5-chlorophenol (5.17 g, 36.00 mmol) and **118** (7.33 g, 36.00 mmol) and was obtained as a brown solid (3.30 g, 10.60 mmol, 29.5 % yield).

$\text{C}_{13}\text{H}_8\text{ClFN}_2\text{O}_4$ ($M = 310.67$ g/mol), mp 247.7 °C. **$^1\text{H-NMR}$** (300 MHz, DMSO-d_6) δ 10.57 (s, 1H), δ 9.86 (d, $J = 8.6\text{Hz}$, 1H), δ 8.23 (d, $J = 5.1\text{Hz}$, 2H), δ 8.00 (m, 2H), δ 6.92 (d, $J = 13.7\text{Hz}$, 2H). **ESI-MS** m/z 309.0 $[(M-H)^-]$. **CHN** ($\text{C}_{13}\text{H}_8\text{ClFN}_2\text{O}_4$) calc.: C 50.26; H 2.60; N 9.02; exp.: C 50.37; H 2.78; N 8.82.

***N*-(2-hydroxyphenyl)-2-fluoro-4-nitrobenzamide (132)**

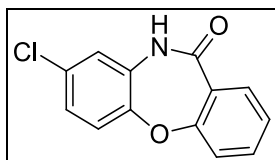
$\text{C}_{13}\text{H}_9\text{FN}_2\text{O}_4$ ($M = 276.22$ g/mol)

132 was prepared according to *general procedure G* using 2-aminophenol (3.15 g, 28.9 mmol) and **118** (5.88 g, 28.9 mmol) and was obtained as a yellow solid (5.62 g, 20.35 mmol, 70.42 % yield).

$\text{C}_{13}\text{H}_9\text{FN}_2\text{O}_4$ ($M = 276.22$ g/mol), mp 245.2 °C. **$^1\text{H-NMR}$** (300 MHz, DMSO-d_6) δ 10.02 (s, 1H), δ 9.79 (d, $J = 4.5\text{Hz}$, 1H), δ 8.27 (d, $J = 10.3\text{Hz}$, 1H), δ 8.20 (d, $J = 8.6\text{Hz}$, 1H), δ 8.04 (m, 1H), δ 7.95 (d, $J = 9.3\text{Hz}$, 1H), δ 7.03 (m, 1H), δ 6.93 (d, $J = 9.4\text{Hz}$, 1H), δ 6.84 (t, $J = 8.3\text{Hz}$, 1H). **ESI-MS** m/z 276.0 $[M]$. **CHN** ($\text{C}_{13}\text{H}_9\text{FN}_2\text{O}_4 \cdot \frac{1}{3} \text{H}_2\text{O}$) calc.: C 55.32; H 3.45; N 9.92; exp.: C 55.67; H 3.42; N 9.52.

6.9. General procedure H:**Preparation of compounds 86, 90, 122, 123, 133, 139, 147, 154, 155**

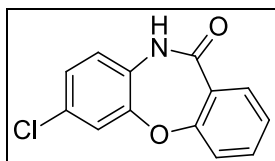
Compounds **85**, **89**, **119**, **120**, **132**, **138**, **146**, **152**, or **153** (10 mmol) were dissolved in 40 ml DMF and one equivalent of freshly powdered NaOH (10 mmol) was added. The mixture was heated at reflux for 5 h and after re-cooling to room temperature it was diluted with 300 ml water. The precipitated solid was filtered over a glass filter, washed with NaOH (w = 5%) and water and then dried in vacuo over night. Compounds **86**, **90**, **122**, **123**, **133**, **139**, **147**, **154**, or **155** were obtained as solids of different colours and were used in the next step without further purification.

8-Chlorodibenzo[*b,f*][1,4]oxazepin-11(10*H*)-one (86)

$C_{13}H_8ClNO_2$ ($M = 245.66$ g/mol)

86 was prepared according to *general procedure H* from **85** (7.97 g, 30.00 mmol) and was obtained as a very light brown solid (5.96 g, 24.26 mmol, 80.9 % yield).

$C_{13}H_8ClNO_2$ ($M = 245.66$ g/mol), mp 255.3 °C (decomposition). **¹H-NMR** (300 MHz, DMSO- d_6) δ 10.63 (s, 1H), δ 7.78 (d, $J = 9.3$ Hz, 1H), δ 7.63 (t, $J = 7.7$ Hz, 1H), δ 7.36 (m, 3H), δ 7.19 (d, $J = 6.8$ Hz, 2H). **GC-MS** m/z 230 (1), 245 (4), 246 (28, MH^+), 247 (5), 248 (9), 249 (1), 263 (100, MNH_4^+), 264 (15), 265 (32), 266 (4), 280 (5), 282 (2). **CHN** ($C_{13}H_8ClNO_2 \cdot \frac{1}{4} H_2O$) calc.: C 62.41; H 3.42; N 5.60; exp.: C 62.45; H 3.28; N 5.66.

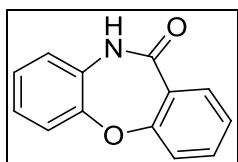
7-Chlorodibenzo[*b,f*][1,4]oxazepin-11(10*H*)-one (90)

$C_{13}H_8ClNO_2$ ($M = 245.66$ g/mol)

90 was prepared according to *general procedure H* from **89** (3.45 g, 13.00 mmol) and was obtained as a violett solid (3.0 g, 12.20 mmol, 93.9 % yield).

$C_{13}H_8ClNO_2$ ($M = 245.66$ g/mol), mp 286.2 °C (decomposition). **1H -NMR** (300 MHz, DMSO- d_6) δ 10.63 (s, 1H), δ 7.77 (d, $J = 9.4$ Hz, 1H), δ 7.64 (m, 1H), δ 7.51 (d, $J = 2.3$ Hz, 1H), δ 7.33 (m, 3H), δ 7.17 (d, $J = 8.6$ Hz, 1H). **GC-MS** m/z 50.1 (31), 63.1 (35), 76.1 (40), 154.1 (33), 182.1 (55), 210.1 (100), 245 (99, MH^+), 247.1 (33). **CHN** ($C_{13}H_8ClNO_2 \cdot \frac{1}{4} H_2O$) calc.: C 62.41; H 3.42; N 5.60; exp.: C 62.27; H 3.60; N 5.73.

Dibenzo[*b,f*][1,4]oxazepin-11(10*H*)-one (**139**)

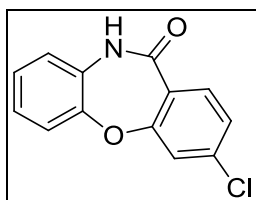


$C_{13}H_9NO_2$ ($M = 211.22$ g/mol)

139 was prepared according to *general procedure H* from **138** (3.98 g, 18.84 mmol) and was obtained as light brown solid (3.51 g, 16.62 mmol, 88.2 % yield).

$C_{13}H_9NO_2$ ($M = 211.22$ g/mol), mp 213.9 °C (decomposition). **1H -NMR** (300 MHz, DMSO- d_6) δ 10.54 (s, 1H), δ 7.77 (d, $J = 9.4$ Hz, 1H), δ 7.61 (m, 1H), δ 7.33 – 7.27 (m, 3H), δ 7.16 – 7.11 (m, 3H). **ESI-MS** m/z 212.0 [MH^+]. **CHN** ($C_{13}H_9NO_2$) calc.: C 73.92; H 4.29; N 6.63; exp.: C 73.69; H 4.33; N 6.61.

3-Chlorodibenzo[*b,f*][1,4]oxazepin-11(10*H*)-one (**147**)

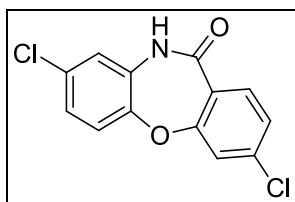


$C_{13}H_8ClNO_2$ ($M = 245.66$ g/mol)

147 was prepared according to *general procedure H* from **146** (4.94 g, 18.59 mmol) and was obtained as light brown solid (4.12 g, 16.77 mmol, 90.2 % yield).

$C_{13}H_8ClNO_2$ ($M = 245.66$ g/mol), mp 252.9 °C (decomposition). **1H -NMR** (300 MHz, DMSO- d_6) δ 8.54 (s, 1H), δ 7.72 (d, $J = 8.4$ Hz, 1H), δ 7.47 (s, 1H), δ 7.32 (m, 2H), δ 7.07 (m, 3H). **GC-MS** m/z 246 [MH^+]. **CHN** ($C_{13}H_8ClNO_2 \cdot \frac{1}{4} H_2O$) calc.: C 62.41; H 3.42; N 5.60; exp.: C 62.24; H 3.46; N 5.36.

3,8-Dichlorodibenzo[*b,f*][1,4]oxazepin-11(10*H*)-one (154)

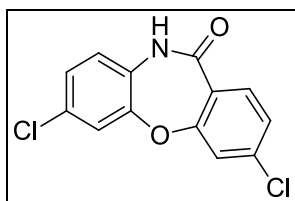


$C_{13}H_7Cl_2NO_2$ ($M = 280.11$ g/mol)

154 was prepared according to *general procedure H* from **152** (2.00 g, 6.66 mmol) and was obtained as light brown solid (1.25 g, 4.46 mmol, 67.0 % yield).

$C_{13}H_7Cl_2NO_2$ ($M = 280.11$ g/mol), mp 271.9 °C (decomposition). **1H -NMR** (300 MHz, DMSO- d_6) δ 8.53 (s, 1H), δ 7.60 (d, $J = 8.3$ Hz, 1H), δ 7.29 (m, 2H), δ 7.13 (d, $J = 8.5$ Hz, 1H), δ 6.95 (s, 1H), δ 6.81 (d, $J = 10.8$ Hz, 1H). **ESI-MS** m/z 280.0 [MH^+]. **CHN** ($C_{13}H_7Cl_2NO_2 \cdot \frac{1}{3} H_2O$) calc.: C 54.57; H 2.70; N 4.90; exp.: C 54.68; H 2.57; N 4.67.

3,7-Dichlorodibenzo[*b,f*][1,4]oxazepin-11(10*H*)-one (155)



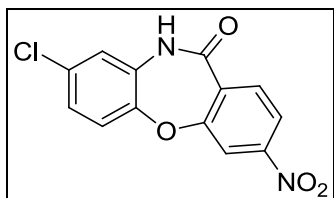
$C_{13}H_7Cl_2NO_2$ ($M = 280.11$ g/mol)

155 was prepared according to *general procedure H* from **153** (6.75 g, 22.49 mmol) and was obtained as red-brown solid (6.19 g, 22.10 mmol, 98.3 % yield).

$C_{13}H_7Cl_2NO_2$ ($M = 280.11$ g/mol), mp 310.2 °C (decomposition). **1H -NMR** (300 MHz, DMSO- d_6) δ 10.72 (s, 1H), δ 7.78 (d, $J = 8.4$ Hz, 1H), δ 7.57 (d, $J = 13.2$ Hz, 2H), δ 7.43 (d, $J = 10.5$ Hz, 1H), δ 7.30 (d, $J = 10.9$ Hz, 1H), δ 7.18 (d, $J = 8.6$ Hz, 1H). **EI-MS** m/z

278.9 [M⁺]. **CHN** (C₁₃H₇Cl₂NO₂ · 1/3 H₂O) calc.: C 54.57; H 2.70; N 4.90; exp.: C 54.80; H 2.65; N 4.67.

8-Chloro-3-nitrodibenzo[*b,f*][1,4]oxazepin-11(10*H*)-one (**122**)

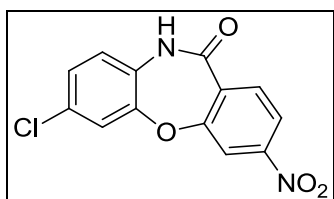


C₁₃H₇ClN₂O₄ (M = 290.66 g/mol)

122 was prepared according to *general procedure H* from **119** (1.59 g, 5.12 mmol) and was obtained as light brown solid (1.46 g, 5.02 mmol, 98.1 % yield).

C₁₃H₇ClN₂O₄ (M = 290.66 g/mol), mp 297.9 °C (decomposition). **¹H-NMR** (300 MHz, DMSO-*d*₆) δ 10.67 (s, 1H), δ 8.21 (d, J = 2.2Hz, 1H), δ 8.12 (d, J = 10.8Hz, 1H), δ 7.97 (d, J = 8.6Hz, 1H), δ 7.47 (d, J = 9.0Hz, 1H), δ 7.15 (d, J = 7.3Hz, 2H). **EI-MS** *m/z* 289.9 [M⁺]. **CHN** (C₁₃H₇ClN₂O₄ · H₂O) calc.: C 50.58; H 2.94; N 9.08; exp.: C 50.92; H 2.57; N 9.00.

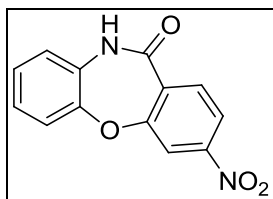
7-Chloro-3-nitrodibenzo[*b,f*][1,4]oxazepin-11(10*H*)-one (**123**)



C₁₃H₇ClN₂O₄ (M = 290.66 g/mol)

123 was prepared according to *general procedure H* from **120** (3.24 g, 10.43 mmol) and was obtained as grey-brown solid (2.79 g, 9.60 mmol, 92.0 % yield).

C₁₃H₇ClN₂O₄ (M = 290.66 g/mol), mp 320.0 °C (decomposition). **¹H-NMR** (300 MHz, DMSO-*d*₆) δ 11.03 (s, 1H), δ 8.28 (s, 1H), δ 8.15 (d, J = 8.6Hz, 1H), δ 8.00 (d, J = 8.6Hz, 1H), δ 7.69 (s, 1H), δ 7.25 (d, J = 7.5Hz, 2H). **EI-MS** *m/z* 290.0 [M⁺]. **CHN** (C₁₃H₇ClN₂O₄ · H₂O) calc.: C 50.58; H 2.94; N 9.08; exp.: C 50.28; H 2.60; N 8.76.

3-Nitrodibenzo[*b,f*][1,4]oxazepin-11(10*H*)-one (133)

$C_{13}H_8N_2O_4$ ($M = 256.21$ g/mol)

133 was prepared according to *general procedure H* from **132** (4.00 g, 14.48 mmol) and was obtained as light brown solid (3.41 g, 13.31 mmol, 91.9 % yield).

$C_{13}H_8N_2O_4$ ($M = 256.21$ g/mol), mp 286.0 °C (decomposition). **1H -NMR** (300 MHz, DMSO- d_6) δ 10.88 (s, 1H), δ 8.24 (d, $J = 1.8$ Hz, 1H), δ 8.14 (d, $J = 10.5$ Hz, 1H), δ 8.02 (d, $J = 8.6$ Hz, 1H), δ 7.49 (d, $J = 7.5$ Hz, 1H), δ 7.21 (t, 3H, $J = 7.7$ Hz). **EI-MS** m/z 63 (27), 75 (27), 77 (17), 127 (30), 153 (16), 154 (21), 182 (34), 183 (18), 210 (35), 256 (100) (M^+). **CHN** ($C_{13}H_8N_2O_4 \cdot \frac{1}{3} H_2O$) calc.: C 59.55; H 3.33; N 10.68; exp.: C 59.70; H 3.39; N 10.46.

6.10. General procedure I:

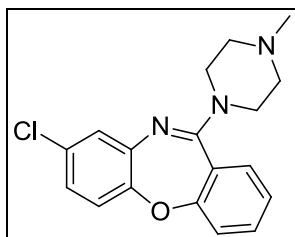
Preparation of compounds 88, 92, 126, 127, 135, 141, 149, 158, 159 and 193, 196, 232 - 235

A solution of **86, 90, 122, 123, 133, 139, 147, 154, or 155** in $POCl_3$ and acetonitrile was heated at reflux over night. Solvent and formed $POCl_3$ were removed under reduced pressure and the resulting 11-chlorodibenzo[*b,f*][1,4]oxazepin intermediates were used in the next step without further purification.

To a solution of the 11-chlorodibenzo[*b,f*][1,4]oxazepin intermediates in toluene the 10-fold excess of *N*-methylpiperazine (compounds **88, 92, 128, 129, 136, 141, 149, 158, 159**) or piperazine (compounds **193, 196, 232 – 235**; piperazine dissolved in CH_3OH quantum satis) was added and the resulting mixture was then heated at reflux for 4 h. After cooling to room temperature, the mixture was added to ethyl acetate and a solution of Na_2CO_3 in water (3 : 2). The aqueous layer was extracted with ethyl acetate and the combined organic layers were dried over Na_2SO_4 . After concentration in vacuo, the crude product was purified by column chromatography (EtOAc / methanol (1 : 1))

to give the title compounds **88**, **92**, **128**, **129**, **136**, **141**, **149**, **158**, **159**, **193**, **196**, **232** - **235** as solids of different colours.

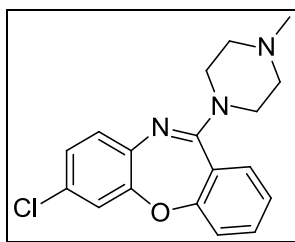
8-Chloro-11-(4-methylpiperazin-1-yl)dibenzo[*b,f*][1,4]oxazepine (**88**)



$C_{18}H_{18}ClN_3O$ ($M = 327.81$ g/mol)

88 was prepared according to *general procedure I* from **86** (3.00 g, 12.20 mmol) in 15 ml $POCl_3$ and 30 ml acetonitrile giving intermediate 8,11-dichloro-dibenzo[*b,f*][1,4]oxazepine (3.22 g, 12.20 mmol) to which *N*-methylpiperazine (12.22 g, 122.00 mmol) and 60 ml toluene were added to give **88** as a light yellow solid (0.64 g, 1.95 mmol, 16.0 % yield).

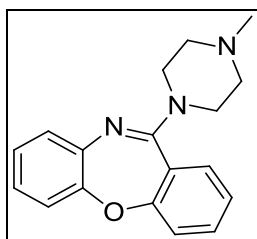
$C_{18}H_{18}ClN_3O$ ($M = 327.81$ g/mol), mp 166.3 °C. **1H -NMR** (300 MHz, $CDCl_3$) δ 7.42 (t, $J = 8.2, 7.3, 1.7$ Hz, 1H), δ 7.32 (d, $J = 7.7$ Hz, 1H), δ 7.22 (d, $J = 8.2$ Hz, 1H), 7.17 (t, $J = 7.6, 1.2$ Hz 1H), δ 7.12 (d, $J = 2.5$ Hz, 1H), δ 7.01 (d, $J = 8.5$ Hz, 1H), δ 6.88 (d, $J = 11.1$ Hz, 1H), δ 3.61 (bs, 4H), δ 2.55 (bs, 4H), δ 2.38 (s, 3H). **^{13}C -NMR** (400 MHz, $CDCl_3$) δ 160.63 (C_{quat}), 150.69 (C_{quat}), 141.81 (C_{quat}), 132.75 (+, Ar-CH), 130.29 (C_{quat}), 129.50 (+, Ar-CH), 126.5 (+, Ar-CH), 124.93 (+, Ar-CH), 123.47 (+, Ar-CH), 123.31 (C_{quat}), 121.14 (+, Ar-CH), 120.96 (+, Ar-CH), 54.91 (-, 2 Pip-CH₂), 47.18 (-, 2 Pip-CH₂), 46.10 (+, CH₃). **ESI-MS** m/z 328.9 [MH^+]. **CHN** ($C_{18}H_{18}ClN_3O$) calc.: C 65.95; H 5.53; N 12.82; exp.: C 65.63; H 5.63; N 12.67.

7-Chloro-11-(4-methylpiperazin-1-yl)dibenzo[*b,f*][1,4]oxazepine (92)

$C_{18}H_{18}ClN_3O$ ($M = 327.81$ g/mol)

92 was prepared according to *general procedure I* from **90** (3.22 g, 12.20 mmol) in 15 ml $POCl_3$ and 30 ml acetonitrile giving intermediate intermediate 7,11-dichlorodibenzo[*b,f*][1,4]oxazepine (3.22 g, 12.20 mmol) to which *N*-methylpiperazine (12.22 g, 122.00 mmol) and 60 ml toluene were added to give **90** as a light red solid (0.68 g, 2.08 mmol, 17.1 %).

$C_{18}H_{18}ClN_3O$ ($M = 327.81$ g/mol), mp 149.7 °C. **1H -NMR** (300 MHz, $CDCl_3$) δ 7.47 (m, 1H), δ 7.34 (d, $J = 9.4$ Hz, 1H), δ 7.21 (m, 1H), δ 7.13 (m, 2H), δ 7.04 (d, $J = 1.1$ Hz, 2H), δ 3.69 (bs, 4H), δ 2.67 (bs, 4H), δ 2.45 (s, 3H). **^{13}C -NMR** (75 MHz, $CDCl_3$) δ 160.52 (C_{quat}), 160.34 (C_{quat}), 152.08 (C_{quat}), 139.46 (C_{quat}), 132.84 (+, Ar-CH), 129.61 (+, Ar-CH), 128.52 (C_{quat}), 127.54 (+, Ar-CH), 125.67 (+, Ar-CH), 125.15 (+, Ar-CH), 123.40 (C_{quat}), 121.29 (+, Ar-CH), 120.60 (+, Ar-CH), 54.90 (-, 2 Pip-CH₂), 47.20 (-, 2 Pip-CH₂), 46.09 (+, CH₃). **ESI-MS** m/z 327.9 [MH^+]. **CHN** ($C_{18}H_{18}ClN_3O$) calc.: C 65.95; H 5.53; N 12.82; exp.: C 65.74; H 5.58; N 12.76.

11-(4-Methylpiperazin-1-yl)dibenzo[*b,f*][1,4]oxazepine (141)

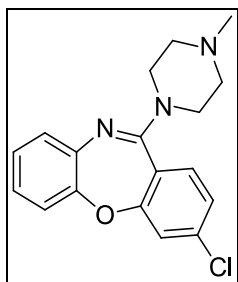
$C_{18}H_{19}N_3O$ ($M = 293.36$ g/mol)

141 was prepared according to *general procedure I* from **139** (3.0 g, 14.20 mmol) in 15 ml $POCl_3$ and a mixture of 100 ml acetonitrile and 40 ml toluene giving intermediate 11-chlorodibenzo[*b,f*][1,4]oxazepine (3.26 g, 14.20 mmol) to which *N*-methylpiperazine

(14.22 g, 142.90 mmol) and a mixture of 100 ml acetonitrile and 40 ml toluene were added to give **141** as a light yellow hygroscopic foam (0.97 g, 3.31 mmol, 23.3 % yield).

$C_{18}H_{19}N_3O$ (M = 293.36 g/mol), mp 60.2 °C. **1H -NMR** (300 MHz, $CDCl_3$) δ 7.43 (m, 1H), δ 7.35 (d, J = 9.4 Hz, 1H), δ 7.14 (m, 5H), δ 6.98 (m, 1H), δ 3.61 (bs, 4H), δ 2.58 (bs, 4H), δ 2.39 (s, 3H). **^{13}C -NMR** (75 MHz, $CDCl_3$) δ 161.01 (C_{quat}), 160.37 (C_{quat}), 152.18 (C_{quat}), 140.61 (C_{quat}), 132.62 (+, Ar-CH), 129.59 (+, Ar-CH), 126.95 (+, Ar-CH), 125.54 (+, Ar-CH), 124.79 (+, Ar-CH), 124.18 (+, Ar-CH), 123.66 (C_{quat}), 121.29 (+, Ar-CH), 120.20 (+, Ar-CH), 54.99 (-, 2 Pip-CH₂), 47.29 (-, 2 Pip-CH₂), 46.16 (+, CH₃). **ESI-MS** m/z 294.1 [MH^+]. **CHN** ($C_{18}H_{19}N_3O \cdot \frac{1}{3} H_2O$) calc.: C 72.22; H 6.62; N 14.04; exp.: C 72.46; H 6.35; N 13.76.

3-Chloro-11-(4-methylpiperazin-1-yl)dibenzo[*b,f*][1,4]oxazepine (**149**)



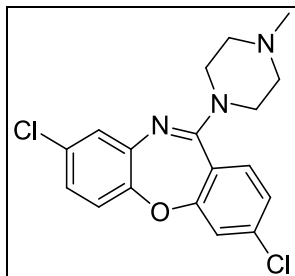
$C_{18}H_{18}ClN_3O$ (M = 327.81 g/mol)

149 was prepared according to *general procedure I* from **147** (3.75 g, 15.27 mmol) in 15 ml $POCl_3$ and a mixture of 100 ml acetonitrile and 30 ml toluene giving intermediate 3,11-dichlorodibenzo[*b,f*][1,4]oxazepine (4.03 g, 15.27 mmol) to which *N*-methylpiperazine (15.29 g, 152.7 mmol) and a mixture of 100 ml acetonitrile and 40 ml toluene were added to give **149** as a light yellow hygroscopic foam (0.59 g, 1.80 mmol, 12.6 % yield).

$C_{18}H_{18}ClN_3O$ (M = 327.81 g/mol), mp 65.6 °C. **1H -NMR** (300 MHz, $CDCl_3$) δ 7.30 (s, 1H), δ 7.27 (m, 2H), δ 7.18 (d, J = 10.4 Hz, 1H), δ 7.10 – 7.01 (m, 3H), δ 3.60 (bs, 4H), δ 2.60 (bs, 4H), δ 2.41 (s, 3H). **^{13}C -NMR** (75 MHz, $CDCl_3$) δ 161.10 (C_{quat}), 159.37 (C_{quat}), 151.72 (C_{quat}), 140.29 (C_{quat}), 137.90 (C_{quat}), 130.33 (+, Ar-CH), 127.09 (+, Ar-CH), 125.87 (+, Ar-CH), 125.33 (+, Ar-CH), 124.47 (+, Ar-CH), 122.21 (C_{quat}), 121.91 (+, Ar-CH), 120.22 (+, Ar-CH), 54.89 (-, 2 Pip-CH₂), 47.28 (-, 2 Pip-CH₂), 46.11 (+,

CH₃). **ESI-MS** m/z 328.0 [MH⁺]. **CHN** (C₁₈H₁₈ClN₃O · ¼ H₂O) calc.: C 65.06; H 5.61; N 12.64; exp.: C 65.30; H 5.61; N 12.50.

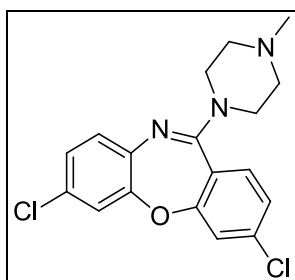
3,8-Dichloro-11-(4-methylpiperazin-1-yl)dibenzo[*b,f*][1,4]oxazepine (**158**)



C₁₈H₁₇Cl₂N₃O (M = 362.25 g/mol)

158 was prepared according to *general procedure I* from **154** (1.00 g, 3.57 mmol) in 5 ml POCl₃ and a mixture of 40 ml acetonitrile and 20 ml toluene giving intermediate 3,8,11-trichlorodibenzo[*b,f*][1,4]oxazepine (1.07 g, 3.57 mmol) to which *N*-methylpiperazine (3.58 g, 35.70 mmol) and a mixture of 40 ml acetonitrile and 20 ml toluene were added to give **158** according to general procedure as a light brown solid (0.64 g, 1.77 mmol, 49.6 % yield).

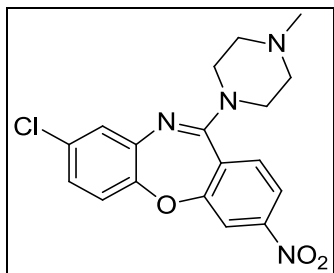
C₁₈H₁₇Cl₂N₃O (M = 362.25 g/mol), mp 155.8 °C. **¹H-NMR** (300 MHz, CDCl₃) δ 7.26 (s, 2H), δ 7.20 (d, J = 10.1Hz, 1H), δ 7.12 (d, J = 2.4Hz, 1H), δ 7.02 (d, J = 8.5Hz, 1H), δ 6.93 (d, J = 11.0Hz, 1H), δ 3.62 (bs, 4H), δ 2.59 (bs, 4H), δ 2.40 (s, 3H). **¹³C-NMR** (75 MHz, CDCl₃) δ 160.58 (C_{quat}), 159.41 (C_{quat}), 151.60 (C_{quat}), 139.19 (C_{quat}), 138.12 (C_{quat}), 130.36 (+, Ar-CH), 128.81 (C_{quat}), 127.68 (+, Ar-CH), 126.02 (+, Ar-CH), 125.68 (+, Ar-CH), 121.95 (C_{quat}), 121.90 (+, Ar-CH), 120.60 (+, Ar-CH), 54.84 (-, 2 Pip-CH₂), 47.30 (-, 2 Pip-CH₂), 46.08 (+, CH₃). **ESI-MS** m/z 362.1 [MH⁺]. **CHN** (C₁₈H₁₇Cl₂N₃O · ⅓ H₂O) calc.: C 58.71; H 4.84; N 11.41; exp.: C 58.71; H 4.81; N 11.20.

3,7-Dichloro-11-(4-methylpiperazin-1-yl)dibenzo[*b,f*][1,4]oxazepine (159)

$C_{18}H_{17}Cl_2N_3O$ ($M = 362.25$ g/mol)

159 was prepared according to *general procedure I* from **155** (5.50 g, 19.64 mmol) in 20 ml $POCl_3$ and a mixture of 100 ml acetonitrile and 40 ml toluene giving intermediate 3,7,11-trichlorodibenzo[*b,f*][1,4]oxazepine (5.86 g, 19.64 mmol) to which *N*-methylpiperazine (19.67 g, 196.40 mmol) and a mixture of 100 ml acetonitrile and 40 ml toluene were added to give **159** as a red-brown solid (124 mg, 3.42 mmol, 17.4 % yield).

$C_{18}H_{17}Cl_2N_3O$ ($M = 362.25$ g/mol), mp 154.3 °C. **1H -NMR** (300 MHz, $CDCl_3$) δ 7.26 (s, 2H), δ 7.21 (d, $J = 1.9$ Hz, 1H), δ 7.12 (m, 1H), δ 7.05 (d, $J = 1.3$ Hz, 2H), δ 3.59 (bs, 4H), δ 2.57 (bs, 4H), δ 2.43 (s, 3H). **^{13}C -NMR** (75 MHz, $CDCl_3$) δ 160.59 (C_{quat}), 159.38 (C_{quat}), 151.59 (C_{quat}), 139.15 (C_{quat}), 138.14 (C_{quat}), 130.35 (+, Ar-CH), 128.82 (C_{quat}), 127.69 (+, Ar-CH), 126.01 (+, Ar-CH), 125.68 (+, Ar-CH), 121.96 (C_{quat}), 121.91 (+, Ar-CH), 120.62 (+, Ar-CH), 54.82 (-, 2 Pip- CH_2), 47.19 (-, 2 Pip- CH_2), 46.06 (+, CH_3). **ESI-MS** m/z 362.1 [MH^+]. **CHN** ($C_{18}H_{17}Cl_2N_3O \cdot \frac{1}{3} H_2O$) calc.: C 58.71; H 4.84; N 11.41; exp.: C 58.74; H 4.89; N 11.06.

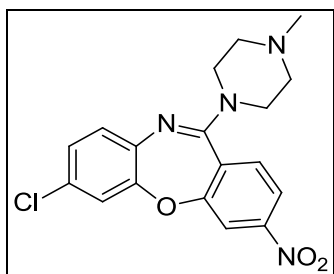
8-Chloro-11-(4-methylpiperazin-1-yl)-3-nitrodibenzo[*b,f*][1,4]oxazepine (126)

$C_{18}H_{17}ClN_4O_3$ ($M = 372.81$ g/mol)

126 was prepared according to *general procedure I* from **122** (1.35 g, 4.64 mmol) in 7 ml POCl₃ and 20 ml acetonitrile giving intermediate 8,11-dichloro-3-nitrodibenzo[*b,f*][1,4]oxazepine (1.43 g, 4.64 mmol) to which *N*-methylpiperazine (4.65 g, 46.4 mmol) and 100 ml toluene were added to give **126** as a light yellow oil (0.40 g, 1.22 mmol, 26.3 % yield).

C₁₈H₁₇ClN₄O₃ (M = 372.81 g/mol). **¹H-NMR** (300 MHz, CDCl₃) δ 8.10 (d, J = 5.5Hz, 2H), δ 7.52 (d, J = 9.1Hz, 1H), δ 7.16 (d, J = 2.5Hz, 1H), δ 7.10 (d, J = 8.6Hz, 1H), δ 7.01 (m, 1H), δ 3.80 (bs, 4H), δ 2.82 (bs, 4H), δ 2.55 (s, 3H). **ESI-MS** *m/z* 373.0 [MH⁺].

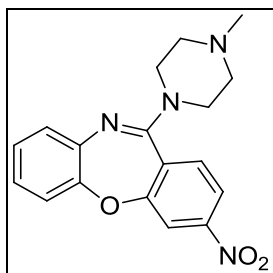
7-Chloro-11-(4-methylpiperazin-1-yl)-3-nitrodibenzo[*b,f*][1,4]oxazepine (**127**)



C₁₈H₁₇ClN₄O₃ (M = 372.81 g/mol)

127 was prepared according to *general procedure I* from **123** (2.60 g, 8.95 mmol) in 14 ml POCl₃ and 50 ml acetonitrile giving intermediate 7,11-dichloro-3-nitrodibenzo[*b,f*][1,4]oxazepine (2.77 g, 8.95 mmol) to which *N*-methylpiperazine (8.96 g, 89.50 mmol) and 120 ml toluene were added to give **127** as a light yellow oil (0.24 g, 0.64 mmol, 7.2 % yield).

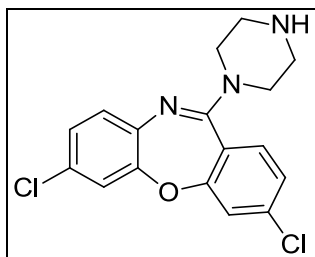
C₁₈H₁₇ClN₄O₃ (M = 372.81 g/mol). **¹H-NMR** (300 MHz, CDCl₃) δ 8.10 (m, 2H), δ 7.53 (d, J = 9.1Hz, 1H), δ 7.19 (d, J = 1.8Hz, 1H), δ 7.09 (d, J = 2.4Hz, 2H), δ 3.70 (bs, 4H), δ 2.72 (bs, 4H), δ 2.49 (s, 3H). **ESI-MS** *m/z* 373.0 [MH⁺].

11-(4-Methylpiperazin-1-yl)-3-nitrodibenzo[*b,f*][1,4]oxazepine (135)

$C_{18}H_{18}N_4O_3$ (M = 338.36 g/mol)

135 was prepared according to *general procedure I* from **133** (3.14 g, 12.26 mmol) in 13 ml $POCl_3$ and a mixture of 120 ml acetonitrile and 30 ml toluene giving intermediate 11-chloro-3-nitrodibenzo[*b,f*][1,4]oxazepine (3.37 g, 12.26 mmol) to which *N*-methylpiperazine (12.28 g, 122.60 mmol) and a mixture of 100 ml acetonitrile and 40 ml toluene were added to give **135** as yellow hygroscopic solid (1.70 g, 5.02 mmol, 41.0 % yield).

$C_{18}H_{18}N_4O_3$ (M = 338.36 g/mol), mp 177.8°C. **¹H-NMR** (300 MHz, $CDCl_3$) δ 8.08 (m, 2H), δ 7.53 (d, *J* = 8.5 Hz, 1H), δ 7.14 (m, 3H), δ 7.04 (m, 1H), δ 3.62 (bs, 4H), δ 2.63 (bs, 4H), δ 2.42 (s, 3H). **ESI-MS** *m/z* 339.0 [MH^+]. **CHN** ($C_{18}H_{18}N_4O_3 \cdot \frac{1}{4} H_2O$) calc.: C 63.05; H 5.44; N 16.34; exp.: C 63.16; H 5.41; N 15.94.

3,7-Dichloro-11-(piperazin-1-yl)dibenzo[*b,f*][1,4]oxazepine (193)

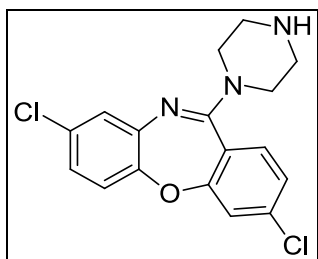
$C_{17}H_{15}Cl_2N_3O$ (M = 348.23 g/mol)

193 was prepared according to *general procedure I* from **155** (4.50 g, 16.07 mmol) in 12 ml $POCl_3$ and a mixture of 100 ml acetonitrile and 50 ml toluene giving intermediate 3,7,11-trichlorodibenzo[*b,f*][1,4]oxazepine (4.75 g, 16.07 mmol) to which piperazine (13.84 g, 160.70 mmol, dissolved in 35 ml CH_3OH) and a mixture of 100 ml acetonitrile

and 50 ml toluene were added to give **193** as yellow hygroscopic solid (2.62 g, 7.52 mmol, 46.8 % yield).

$C_{17}H_{15}Cl_2N_3O$ (M = 348.23 g/mol), mp 69.8 °C. **1H -NMR** (300 MHz, $CDCl_3$) δ 7.24 (m, 2H), 7.20 (dd, J = 8.6, 1.8 Hz, 1H), 7.15 – 7.08 (t, 1H), 7.06 (d, J = 4.4 Hz, 2H), 3.48 (bs, 4H), 3.02 (bs, 4H), 1.86 (s, 1H). **^{13}C -NMR** (75 MHz, $CDCl_3$) δ 160.61 (C_{quat}), 159.68 (C_{quat}), 151.61 (C_{quat}), 139.14 (C_{quat}), 138.11 (C_{quat}), 130.36 (+, Ar-CH), 128.80 (C_{quat}), 127.68 (+, Ar-CH), 126.01 (+, Ar-CH), 125.69 (+, Ar-CH), 121.96 (C_{quat}), 121.91 (+, Ar-CH), 120.61 (+, Ar-CH), 48.63 (-, 2 Pip-CH₂), 45.89 (-, 2 Pip-CH₂). **ESI-MS** m/z 348.1 [MH⁺]. **CHN** ($C_{17}H_{15}Cl_2N_3O \cdot CH_3OH$) calc. C 56.85; H 5.04; N 11.05; exp. C 56.75; H 4.74; N 11.21.

3,8-Dichloro-11-(piperazin-1-yl)dibenzo[*b,f*][1,4]oxazepine (**196**)



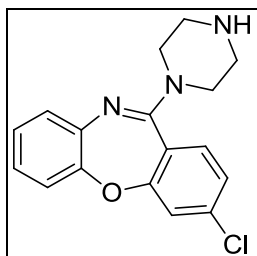
$C_{17}H_{15}Cl_2N_3O$ (M = 348.23 g/mol)

196 was prepared according to *general procedure I* from **154** (10.46 g, 37.34 mmol) in 25 ml $POCl_3$ and a mixture of 120 ml acetonitrile and 60 ml toluene giving intermediate 3,8,11-trichlorodibenzo[*b,f*][1,4]oxazepine (11.15 g, 37.34 mmol) to which piperazine (32.16 g, 373.40 mmol, dissolved in 50 ml CH_3OH) and a mixture of 120 ml acetonitrile and 60 ml toluene were added to give **196** as yellow hygroscopic foam (5.38 g, 15.45 mmol, 41.4 % yield).

$C_{17}H_{15}Cl_2N_3O$ (M = 348.23 g/mol), mp 55.6 °C. **1H -NMR** (300 MHz, $CDCl_3$) δ 7.26 (m, J = 4.8 Hz, 2H), 7.20 (dd, J = 8.4, 3.7 Hz, 1H), 7.12 (d, J = 2.5 Hz, 1H), 7.02 (d, J = 8.6 Hz, 1H), 6.92 (dd, J = 8.5, 2.5 Hz, 1H), 3.51 (bs, 4H), 3.00 (bs, 4H), 2.01 (s, 1H). **^{13}C -NMR** (75 MHz, $CDCl_3$) δ 160.83 (C_{quat}), 159.95 (C_{quat}), 150.29 (C_{quat}), 141.51 (C_{quat}), 138.14 (C_{quat}), 130.76 (C_{quat}), 130.32 (+, Ar-CH), 126.71 (+, Ar-CH), 125.59 (+, Ar-CH), 123.87 (+, Ar-CH), 121.88 (+, Ar-CH), 121.09 (+, Ar-CH), 48.54 (-, 2 Pip-CH₂), 45.82 (-, 2 Pip-

CH₂). **ESI-MS** m/z 348.1 [MH⁺]. **CHN** (C₁₇H₁₅Cl₂N₃O · ³/₅CH₃OH) calc. C 57.41; H 4.82; N 11.37; C 57.41; H 4.60; N 11.00

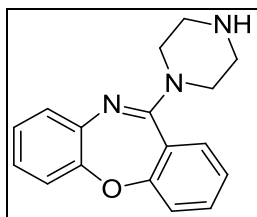
3-Chloro-11-(piperazin-1-yl)dibenzo[*b,f*][1,4]oxazepine (**232**)



C₁₇H₁₆ClN₃O (M = 313.78 g/mol)

232 was prepared according to *general procedure I* from **147** (10.46 g, 42.58 mmol) in 25 ml POCl₃ and a mixture of 200 ml acetonitrile and 100 ml toluene giving intermediate 3,11-dichlorodibenzo[*b,f*][1,4]oxazepine (11.25 g, 42.58 mmol) to which piperazine (25.84 g, 300.00 mmol, dissolved in 40 ml CH₃OH) and a mixture of 100 ml acetonitrile and 100 ml toluene were added to give **232** as a yellow solid that was re-crystallized from EtOAc (6.16 g, 19.63 mmol, 46.1 % yield).

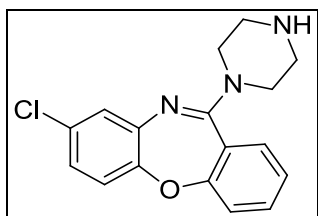
C₁₇H₁₆ClN₃O (M = 313.78 g/mol), mp 154.9 °C. **¹H-NMR** (300 MHz, CDCl₃) δ 7.29 – 7.24 (m, 2H), 7.17 (d, J = 8.3Hz, 1H), 7.15 – 7.04 (m, 3H), 6.95 (m, 1H), 3.49 (bs, 4H), 2.99 (bs, 4H), 1.72 (s, 1H). **¹³C-NMR** (75 MHz, CDCl₃) δ 161.12 (C_{quat}), 159.69 (C_{quat}), 151.75 (C_{quat}), 140.28 (C_{quat}), 137.87 (C_{quat}), 130.34 (+, Ar-CH), 127.07 (+, Ar-CH), 125.87 (+, Ar-CH), 125.33 (+, Ar-CH), 124.45 (+, Ar-CH), 122.22 (C_{quat}), 121.89 (+, Ar-CH), 120.21 (+, Ar-CH), 48.69 (-, 2 Pip-CH₂), 45.95 (-, 2 Pip-CH₂). **ESI-MS** m/z 314.1 [MH⁺]. **CHN** (C₁₇H₁₆ClN₃O · ¹/₅ H₂O) calc. C 64.33; H 5.21; N 13.24; exp. 64.55; H 5.26; N 13.46

11-(Piperazin-1-yl)dibenzo[*b,f*][1,4]oxazepine (233)

C₁₇H₁₇N₃O (M = 279.34 g/mol)

233 was prepared according to *general procedure I* from **139** (7.02 g, 33.24 mmol) in 20 ml POCl₃ and a mixture of 150 ml acetonitrile and 150 ml toluene giving intermediate 11-chlorodibenzo[*b,f*][1,4]oxazepine (7.63 g, 33.24 mmol) to which piperazine (21.54 g, 250.00 mmol, dissolved in 40 ml CH₃OH) and a mixture of 150 ml acetonitrile and 150 ml toluene were added to give **233** as yellow hygroscopic foam (2.69 g, 9.63 mmol, 29.0 % yield).

C₁₇H₁₇N₃O (M = 279.34 g/mol), mp 62.2 °C. **¹H-NMR** (300 MHz, CDCl₃) δ 7.43 (m, 1H), 7.35 (dd, J = 7.8, 1.7 Hz, 1H), 7.30 – 7.11 (m, 5H), 7.01 – 6.92 (m, 1H), 3.29 (bs, 4H), 2.99 (bs, 4H), 1.93 (s, 1H). **¹³C-NMR** (75 MHz, CDCl₃) δ 161.03 (C_{quat}), 160.66 (C_{quat}), 152.20 (C_{quat}), 140.61 (C_{quat}), 132.59 (+, Ar-CH), 129.61 (+, Ar-CH), 126.94 (+, Ar-CH), 125.53 (+, Ar-CH), 124.80 (+, Ar-CH), 124.16 (+, Ar-CH), 123.67 (C_{quat}), 121.28 (+, Ar-CH), 120.19 (+, Ar-CH), 48.70 (-, 2 Pip-CH₂), 46.03 (-, 2 Pip-CH₂). **ESI-MS** *m/z* 280.2 [MH⁺]. **CHN** (C₁₇H₁₇N₃O · ¼ H₂O) calc. C 71.94; H 6.21; N 14.80; exp. C 72.04; H 5.95; N 14.57.

8-Chloro-11-(piperazin-1-yl)dibenzo[*b,f*][1,4]oxazepine (234)

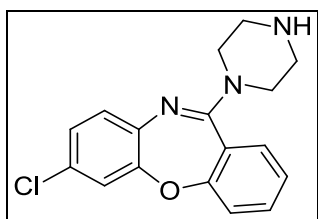
C₁₇H₁₆ClN₃O (M = 313.78 g/mol)

234 was prepared according to *general procedure I* from **86** (5.34 g, 21.74 mmol) in 15 ml POCl₃ and a mixture of 75 ml acetonitrile and 75 ml toluene giving intermediate 8,11-dichlorodibenzo[*b,f*][1,4]oxazepine (5.74 g, 21.74 mmol) to which piperazine

(15.51 g, 180.00 mmol, dissolved in 40 ml CH₃OH) and a mixture of 100 ml acetonitrile and 100 ml toluene were added to give **234** as light brown hygroscopic foam (1.79 g, 5.70 mmol, 26.2 % yield).

C₁₇H₁₆ClN₃O (M = 313.78 g/mol), mp 59.8 °C. **¹H-NMR** (300 MHz, CDCl₃) δ 7.44 (m, 1H), 7.33 (dd, J = 7.7, 1.7 Hz, 1H), 7.28 – 7.15 (m, 2H), 7.12 (d, J = 2.5 Hz, 1H), 7.03 (d, J = 8.5 Hz, 1H), 6.90 (dd, J = 8.5, 2.6 Hz, 1H), 3.51 (bs, 4H), 2.98 (bs, 4H), 1.81 (s, 1H). **¹³C-NMR** (75 MHz, CDCl₃) δ 160.97 (C_{quat}), 160.73 (C_{quat}), 150.77 (C_{quat}), 141.86 (C_{quat}), 132.81 (+, Ar-CH), 130.38 (C_{quat}), 129.59 (+, Ar-CH), 126.55 (+, Ar-CH), 125.03 (+, Ar-CH), 123.55 (+, Ar-CH), 123.39 (C_{quat}), 121.23 (+, Ar-CH), 121.03 (+, Ar-CH), 48.54 (-, 2 Pip-CH₂), 46.04 (-, 2 Pip-CH₂). **ESI-MS** *m/z* 314.1 [MH⁺]. **CHN** (C₁₇H₁₆ClN₃O · 7/3 H₂O) calc. C 63.51; H 5.28; N 13.07; exp. C 63.76; H 5.24; N 12.68.

7-Chloro-11-(piperazin-1-yl)dibenzo[*b,f*][1,4]oxazepine (**235**)



C₁₇H₁₆ClN₃O (M = 313.78 g/mol)

235 was prepared according to *general procedure I* from **90** (7.32 g, 29.80 mmol) in 15 ml POCl₃ and a mixture of 75 ml acetonitrile and 75 ml toluene giving intermediate 7,11-dichlorodibenzo[*b,f*][1,4]oxazepine (7.87 g, 29.80 mmol) to which piperazine (21.54 g, 250.00 mmol, dissolved in 40 ml MeOH) and a mixture of 100 ml acetonitrile and 100 ml toluene were added to give **235** as grey-violet hygroscopic foam (6.28 g, 20.01 mmol, 67.2 % yield).

C₁₇H₁₆ClN₃O (M = 313.78 g/mol), mp 60.2 °C. **¹H-NMR** (300 MHz, CDCl₃) δ 7.45 (m, 1H), 7.34 (d, J = 7.7 Hz, 1H), 7.29 – 7.16 (m, 2H), 7.12 (m, 2H), 7.04 (m, 1H), 3.66 (bs, 4H), 2.99 (bs, 4H), 1.84 (s, 1H). **¹³C-NMR** (75 MHz, CDCl₃) δ 160.64 (C_{quat}), 160.55 (C_{quat}), 152.10 (C_{quat}), 139.49 (C_{quat}), 132.78 (+, Ar-CH), 129.62 (+, Ar-CH), 128.46 (C_{quat}), 127.53 (+, Ar-CH), 125.66 (+, Ar-CH), 125.13 (+, Ar-CH), 123.45 (C_{quat}), 121.27 (+, Ar-CH), 120.57 (+, Ar-CH), 48.67 (-, 2 Pip-CH₂), 46.02 (-, 2 Pip-CH₂). **ESI-MS** *m/z*

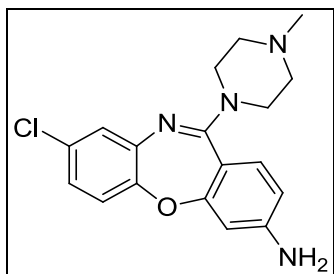
314.1 [MH⁺]. **CHN** (C₁₇H₁₆ClN₃O · ¼ H₂O) calc. C 64.15; H 5.23; N 13.20; exp. C 64.26; H 5.26; N 12.89.

6.11. General procedure J:

Preparation of compounds 128, 129, 136

To a solution of **126**, **127**, or **135** in ethanol the 5-fold excess of SnCl₂ · 2 H₂O was added and the mixture was heated at reflux over night. The next day the mixture was cooled to room temperature and the solvent was evaporated under reduced pressure. Water and DCM (2 : 7) were added to the resulting solid and the pH was adjusted to 7 using a saturated solution of Na₂CO₃. The aqueous layer was then extracted with DCM and the combined organic layers were dried over Na₂SO₄. Evaporation of the solvent yielded the crude product, which was purified by column chromatography (EtOAc / methanol (1 : 1)) to give the title compounds **128**, **129**, **136**.

8-Chloro-11-(4-methylpiperazin-1-yl)dibenzo[b,f][1,4]oxazepin-3-amine (**128**)



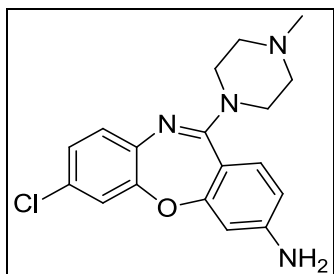
C₁₈H₁₉ClN₄O (M = 342.82 g/mol)

128 was prepared according to *general procedure J* from **126** (0.40 g, 1.22 mmol) in 50 ml ethanol and was obtained as a colorless solid (0.11 g, 0.33 mmol, 26.8 % yield).

C₁₈H₁₉ClN₄O (M = 342.82 g/mol), mp 209.5 °C. **¹H-NMR** (300 MHz, CDCl₃) δ 7.08 (d, J = 7.7Hz, 2H), δ 6.96 (d, J = 8.5Hz, 1H), δ 6.88 (d, J = 11.0Hz, 1H), δ 6.46 (m, 2H), δ 3.96 (s, 2H), δ 3.56 (bs, 4H), δ 2.52 (bs, 4H), δ 2.35 (s, 3H). **¹³C-NMR** (75 MHz, CDCl₃) δ 162.20 (C_{quat}), 161.23 (C_{quat}), 151.05 (C_{quat}), 150.85 (C_{quat}), 142.32 (C_{quat}), 130.87 (+, Ar-CH), 130.22 (C_{quat}), 126.57 (+, Ar-CH), 123.31 (+, Ar-CH), 121.10 (+, Ar-CH), 112.91 (C_{quat}), 111.26 (+, Ar-CH), 106.12 (+, Ar-CH), 54.99 (-, 2 Pip-CH₂), 47.37 (-, 2

Pip-CH₂), 46.09 (+, CH₃). **ESI-MS** m/z 342.9 [MH⁺]. **CHN** (C₁₈H₁₉ClN₄O · 1/3 H₂O) calc.: C 61.98; H 5.68; N 16.06; exp.: C 61.65; H 5.66; N 15.68.

7-Chloro-11-(4-methylpiperazin-1-yl)dibenzo[*b,f*][1,4]oxazepin-3-amine (129)

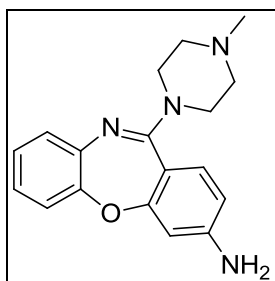


C₁₈H₁₉ClN₄O (M = 342.82 g/mol)

129 was prepared according to *general procedure J* from **127** (0.24 g, 0.64 mmol) in 35 ml ethanol and was obtained as colorless solid (0.08 g, 0.23 mmol, 35.9 % yield).

C₁₈H₁₉ClN₄O (M = 342.82 g/mol), mp 222.2 °C. **¹H-NMR** (300 MHz, CDCl₃) δ 7.07 (m, 4H), δ 6.46 (m, 2H), δ 3.98 (s, 2H), δ 3.62 (bs, 4H), δ 2.61 (bs, 4H), δ 2.41 (s, 3H). **¹³C-NMR** (75 MHz, CDCl₃) δ 162.00 (C_{quat}), 160.91 (C_{quat}), 152.18 (C_{quat}), 151.03 (C_{quat}), 139.95 (C_{quat}), 130.90 (+, Ar-CH), 128.13 (C_{quat}), 127.54 (+, Ar-CH), 125.52 (+, Ar-CH), 120.63 (+, Ar-CH), 112.95 (C_{quat}), 111.35 (+, Ar-CH), 106.15 (+, Ar-CH), 55.03 (-, 2 Pip-CH₂), 47.35 (-, 2 Pip-CH₂), 46.12 (+, CH₃). **ESI-MS** m/z 342.9 [MH⁺]. **CHN** (C₁₈H₁₉ClN₄O · 1/3 H₂O) calc.: C 61.98; H 5.68; N 16.06; exp.: C 61.82; H 5.68; N 15.69.

11-(4-Methylpiperazin-1-yl)dibenzo[*b,f*][1,4]oxazepin-3-amine (136)



C₁₈H₂₀N₄O (M = 308.38 g/mol)

136 was prepared according to *general procedure J* from **135** (1.70 g, 5.02 mmol) in 140 ml ethanol and was obtained as colorless solid (1.07 g, 3.47 mmol, 69.1 % yield).

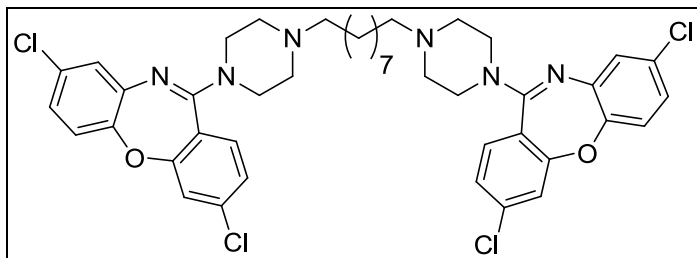
$C_{18}H_{20}N_4O$ ($M = 308.38$ g/mol), mp 191.4 °C. **1H -NMR** (300 MHz, $CDCl_3$) δ 7.08 (m, 4H), δ 6.95 (m, 1H), δ 6.50 (d, $J=2.3$ Hz, 1H), δ 6.43 (d, $J=10.6$ Hz, 1H), δ 3.95 (s, 2H), δ 3.61 (bs, 4H), δ 2.60 (bs, 4H), δ 2.40 (s, 3H). **^{13}C -NMR** (75 MHz, $CDCl_3$) δ 162.47 (C_{quat}), 160.88 (C_{quat}), 152.24 (C_{quat}), 150.91 (C_{quat}), 141.04 (C_{quat}), 130.85 (+, Ar-CH), 126.95 (+, Ar-CH), 125.42 (+, Ar-CH), 123.91 (+, Ar-CH), 120.24 (+, Ar-CH), 113.28 (C_{quat}), 111.12 (+, Ar-CH), 106.25 (+, Ar-CH), 55.08 (-, 2 Pip-CH₂), 47.44 (-, 2 Pip-CH₂), 46.16 (+, CH₃). **ESI-MS** m/z 309.1 [MH^+]. **CHN** ($C_{18}H_{20}N_4O \cdot \frac{1}{4} CH_3OH$) calc.: C 69.28; H 6.69; N 17.71; exp.: C 69.48; H 6.50; N 17.37.

6.12. General procedure K:

Preparation of compounds 205 – 210, 212, 213

To a solution of two equivalents of **193**, or **196** in acetonitrile, one equivalent of 1,w-dibromo or 1,w-diiodo alkane of different length was added dropwise in presence of one equivalent of K_2CO_3 . The reaction mixture was heated at reflux for 12 h under nitrogen atmosphere. The reaction status was monitored by TLC and if after 12 h any starting material remained, further 0.5 equivalents of 1,w-dibromo or 1,w-diiodo alkane was added and the reaction was continued for at least further 6 h. When the reaction was completed, the solvent was evaporated and the remaining oil was poured into water. The aqueous layer was extracted with $CHCl_3$ and the combined organic layers were dried over Na_2SO_4 . The solvent was removed under reduced pressure and the remaining foam was purified by column chromatography over silica gel using three different solvents (gradual modification of the solvent within one column chromatography run): *solvent 1*: EtOAc / HX (3 : 2); *solvent 2*: EtOAc; *solvent 3*: EtOAc / 7 N NH_3 in methanol (9 : 1).

1,9-Bis(4-(3,8-dichlorodibenzo[*b,f*][1,4]oxazepin-11-yl)piperazin-1-yl)nonane (205)

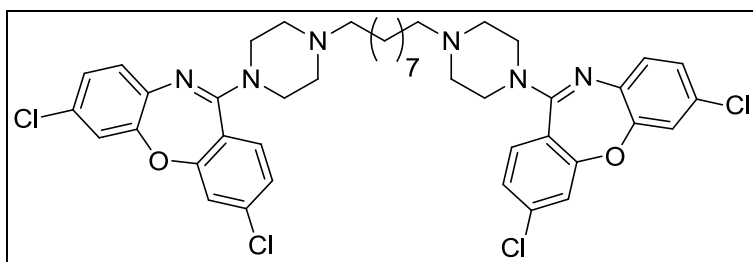


$C_{43}H_{46}Cl_4N_6O_2$ ($M = 820.68$ g/mol)

205 was prepared according to *general procedure K* using **196** (600 mg, 1.73 mmol) and 1,9-dibromononane (246 mg, 0.86 mmol) and was obtained as a light yellow foam (440 mg, 0.54 mmol, 62.3 % yield).

$C_{43}H_{46}Cl_4N_6O_2$ ($M = 820.68$ g/mol), mp 82.5 – 82.9 °C. **1H -NMR** (300 MHz, $CDCl_3$) δ 7.29 – 7.23 (m, 3H), δ 7.19 (dd, $J = 8.4, 1.9$ Hz, 2H), δ 7.12 (d, $J = 2.5$ Hz, 2H), δ 7.02 (d, $J = 8.5$ Hz, 2H), δ 6.92 (dd, $J = 8.5, 2.5$ Hz, 3H), δ 3.51 (bs, 8H), δ 2.51 (bs, 8H), δ 2.45 – 2.31 (m, 4H), δ 1.58 (s, 4H), δ 1.30 (s, 10H). **^{13}C -NMR** (75 MHz, $CDCl_3$) δ 160.79 (2 C_{quat}), 159.64 (2 C_{quat}), 150.28 (2 C_{quat}), 141.55 (2 C_{quat}), 138.14 (2 C_{quat}), 130.77 (2 C_{quat}), 130.35 (+, 2 Ar-CH), 126.71 (+, 2 Ar-CH), 125.56 (+, 2 Ar-CH), 123.84 (+, 2 Ar-CH), 121.87 (+, 2 Ar-CH), 121.08 (+, 2 Ar-CH), 58.74 (-, 4 Pip-CH₂), 53.01 (-, 4 Pip-CH₂), 31.96 (-, 2 CH₂), 29.48 (-, 2 CH₂), 27.92 (-, CH₂), 27.51 (-, 2 CH₂), 26.67 (-, 2 CH₂). **ESI-MS** m/z 274.4 [($M+3H$)³⁺]; 411.1 [($M+2H$)²⁺]; 821.3 [MH^+]. **CHN** ($C_{43}H_{46}Cl_4N_6O_2$) calc. C 62.93; H 5.65; N 10.24; exp. C 62.85; H 5.79; N 9.95.

1,9-Bis(4-(3,7-dichlorodibenzo[*b,f*][1,4]oxazepin-11-yl)piperazin-1-yl)nonane (206)

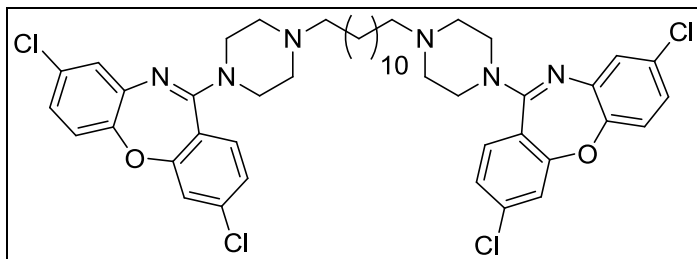


$C_{43}H_{46}Cl_4N_6O_2$ ($M = 820.68$ g/mol)

206 was prepared according to *general procedure K* using **193** (500 mg, 1.44 mmol) and 1,9-dibromononane (205 mg, 0.72 mmol) and was obtained as a light red solid (240 mg, 0.29 mmol, 40.8 % yield).

$C_{43}H_{46}Cl_4N_6O_2$ ($M = 820.68$ g/mol), mp 75.7 – 76.0 °C. **1H -NMR** (300 MHz, $CDCl_3$) δ 7.29 – 7.24 (m, 4H), δ 7.19 (dd, $J = 8.4, 1.9$ Hz, 2H), δ 7.12 (t, $J = 7.3$ Hz, 2H), δ 7.07 – 7.03 (m, 4H), δ 3.61 (bs, 8H), δ 2.62 (bs, 8H), δ 2.45 (s, 4H), δ 1.56 (s, 4H), δ 1.21 (s, 10H). **^{13}C -NMR** (75 MHz, $CDCl_3$) δ 160.57 (2 C_{quat}), 159.25 (2 C_{quat}), 151.58 (2 C_{quat}), 139.15 (2 C_{quat}), 138.15 (2 C_{quat}), 130.37 (+, 2 Ar-CH), 128.81 (2 C_{quat}), 127.67 (+, 2 Ar-CH), 126.02 (+, 2 Ar-CH), 125.68 (+, 2 Ar-CH), 121.91 (+, 2 Ar-CH), 120.62 (+, 2 Ar-CH), 58.70 (-, 4 Pip-CH₂), 52.92 (-, 4 Pip-CH₂), 31.19 (-, 2 CH₂), 29.43 (-, 2 CH₂), 27.97 (-, CH₂), 27.46 (-, 2 CH₂), 26.52 (-, 2 CH₂). **ESI-MS** m/z 274.4 [($M+3H$)³⁺]; 411.1 [($M+2H$)²⁺]; 821.2 [MH^+]. **CHN** ($C_{43}H_{46}Cl_4N_6O_2 \cdot \frac{8}{5} H_2O$) calc. C 60.71; H 5.85; N 9.88; exp. C 60.51; H 5.79; N 9.84.

1,12-Bis(4-(3,8-dichlorodibenzo[*b,f*][1,4]oxazepin-11-yl)piperazin-1-yl)dodecane (207)



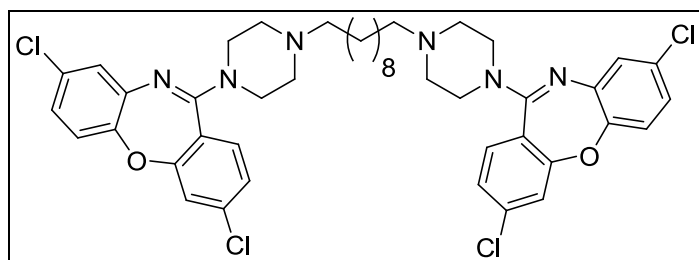
$C_{46}H_{52}Cl_4N_6O_2$ ($M = 862.76$ g/mol)

207 was prepared according to *general procedure K* using **196** (600 mg, 1.73 mmol) and 1,12-dibromododecane (283 mg, 0.86 mmol) and was obtained as a light yellow solid (440 mg, 0.51 mmol, 59.3 % yield).

$C_{46}H_{52}Cl_4N_6O_2$ ($M = 862.76$ g/mol), 179.1 – 179.4 °C. **1H -NMR** (300 MHz, $CDCl_3$) δ 7.30 – 7.23 (m, 4H), δ 7.19 (dd, $J = 8.4, 1.9$ Hz, 2H), δ 7.12 (d, $J = 2.5$ Hz, 2H), δ 7.02 (d, $J = 8.5$ Hz, 2H), δ 6.93 (dd, $J = 8.5, 2.5$ Hz, 2H), δ 3.61 (bs, 8H), δ 2.54 (bs, 8H), δ 2.49 – 2.34 (m, 4H), δ 1.54 (s, 4H), δ 1.33 (s, 16H). **^{13}C -NMR** (75 MHz, $CDCl_3$) δ 160.79 (2 C_{quat}), 159.64 (2 C_{quat}), 150.28 (2 C_{quat}), 141.57 (2 C_{quat}), 138.12 (2 C_{quat}), 130.76 (2 C_{quat}), 130.34 (+, 2 Ar-CH), 126.71 (+, 2 Ar-CH), 125.54 (+, 2 Ar-CH), 123.81 (+, 2 Ar-

CH), 121.91 (2 C_{quat}), 121.86 (+, 2 Ar-CH), 121.07 (+, 2 Ar-CH), 58.77 (-, 4 Pip-CH₂), 53.02 (-, 4 Pip-CH₂), 31.14 (-, 2 CH₂), 29.61 (-, 2 CH₂), 29.58 (-, 2 CH₂), 27.54 (-, 2 CH₂), 26.78 (-, 2 CH₂), 26.70 (-, 2 CH₂). **ESI-MS** *m/z* 288.4 [(M+3H)³⁺]; 432.1 [(M+2H)²⁺]; 863.3 [MH⁺]. **CHN** (C₄₆H₅₂Cl₄N₆O₂) calc. C 64.04; H 6.08; N 9.74; exp. C 63.78; H 6.14; N 9.44.

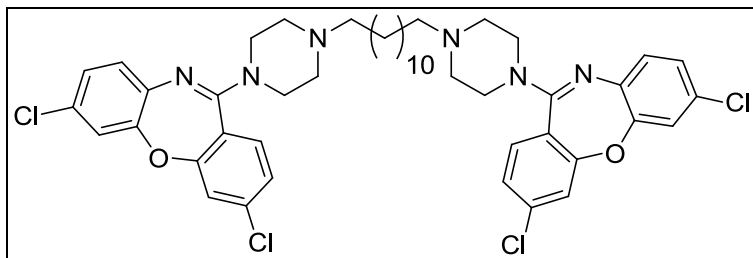
1,10-Bis(4-(3,8-dichlorodibenzo[*b,f*][1,4]oxazepin-11-yl)piperazin-1-yl)decane (208)



C₄₄H₄₈Cl₄N₆O₂ (M = 834.70 g/mol)

208 was prepared according to *general procedure K* using **196** (600 mg, 1.73 mmol) and 1,10-diiododecane (339 mg, 0.86 mmol) and was obtained as a light yellow solid (510 mg, 0.61 mmol, 71.0 % yield).

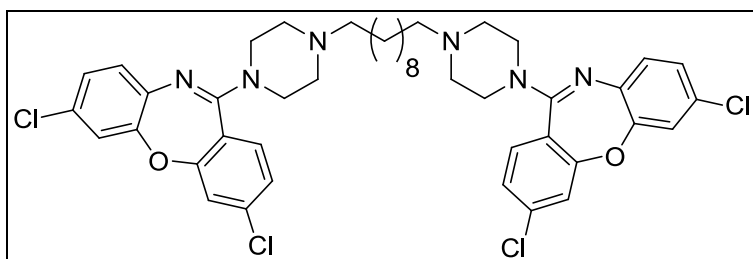
C₄₄H₄₈Cl₄N₆O₂ (M = 834.70 g/mol), mp 161.5 – 162.2 °C. **¹H-NMR** (300 MHz, CDCl₃) δ 7.31 – 7.23 (m, 4H), δ 7.19 (dd, J = 8.4, 1.9Hz, 2H), δ 7.12 (d, J = 2.5Hz, 2H), δ 7.02 (d, J = 8.5Hz, 2H), δ 6.93 (dd, J = 8.5, 2.5Hz, 2H), δ 3.61 (bs, 8H), δ 2.53 (bs, 8H), δ 2.42 – 2.31 (m, 4H), δ 1.54 (s, 4H), δ 1.36 (s, 12H). **¹³C-NMR** (75 MHz, CDCl₃) δ 160.80 (2 C_{quat}), 159.64 (2 C_{quat}), 150.28 (2 C_{quat}), 141.56 (2 C_{quat}), 138.14 (2 C_{quat}), 130.77 (2 C_{quat}), 130.34 (+, 2 Ar-CH), 126.71 (+, 2 Ar-CH), 125.54 (+, 2 Ar-CH), 123.83 (+, 2 Ar-CH), 121.90 (2 C_{quat}), 121.86 (+, 2 Ar-CH), 121.08 (+, 2 Ar-CH), 58.75 (-, 4 Pip-CH₂), 53.00 (-, 4 Pip-CH₂), 29.50 (-, 2 CH₂), 29.38 (-, 2 CH₂), 27.52 (-, 2 CH₂), 26.67 (-, 2 CH₂), 26.59 (-, 2 CH₂). **ESI-MS** *m/z* 279.1 [(M+3H)³⁺]; 418.1 [(M+2H)²⁺]; 835.3 [MH⁺]. **CHN** (C₄₄H₄₈Cl₄N₆O₂ · 2/3 H₂O) calc. C 62.41; H 5.87; N 9.93; exp. C 62.69; H 5.97; N 9.57.

1,12-Bis(4-(3,7-dichlorodibenzo[*b,f*][1,4]oxazepin-11-yl)piperazin-1-yl)dodecane (209)


$C_{46}H_{52}Cl_4N_6O_2$ ($M = 862.76$ g/mol)

209 was prepared according to *general procedure K* using **193** (380 mg, 1.09 mmol) and 1,12-dibromododecane (179 mg, 0.55 mmol) and was obtained as a light red solid (200 mg, 0.54 mmol, 42.5 % yield).

$C_{46}H_{52}Cl_4N_6O_2$ ($M = 862.76$ g/mol), mp 145.9 – 146.3 °C. **1H -NMR** (300 MHz, $CDCl_3$) δ 7.29 – 7.23 (m, 4H), δ 7.19 (dd, $J = 8.4, 1.9$ Hz, 2H), δ 7.14 – 7.09 (m, 2H), δ 7.05 (d, $J = 1.2$ Hz, 4H), δ 3.59 (bs, 8H), 2.60 (bs, 8H), δ 2.44 – 2.32 (m, 4H), δ 1.54 (s, 4H), δ 1.33 (s, 16H). **^{13}C -NMR** (75 MHz, $CDCl_3$) δ 160.58 (2 C_{quat}), 159.28 (2 C_{quat}), 151.58 (2 C_{quat}), 139.19 (2 C_{quat}), 138.11 (2 C_{quat}), 130.37 (+, 2 Ar-CH), 128.77 (2 C_{quat}), 127.68 (+, 2 Ar-CH), 126.02 (+, 2 Ar-CH), 125.66 (+, 2 Ar-CH), 121.95 (2 C_{quat}), 121.91 (+, 2 Ar-CH), 120.62 (+, 2 Ar-CH), 58.78 (-, 4 Pip-CH₂), 53.01 (-, 4 Pip-CH₂), 31.07 (-, 2 CH₂), 29.57 (-, 2 CH₂), 29.49 (-, 2 CH₂), 27.54 (-, 2 CH₂), 26.74 (-, 2 CH₂), 26.67 (-, 2 CH₂). **ESI-MS** m/z 288.4 [(M+3H)³⁺]; 432.2 [(M+2H)²⁺]; 863.3 [MH⁺]. **CHN** ($C_{46}H_{52}Cl_4N_6O_2 \cdot \frac{1}{3} H_2O$) calc. C 63.60; H 6.11; N 9.67; exp. C 63.53; H 6.14; N 9.44.

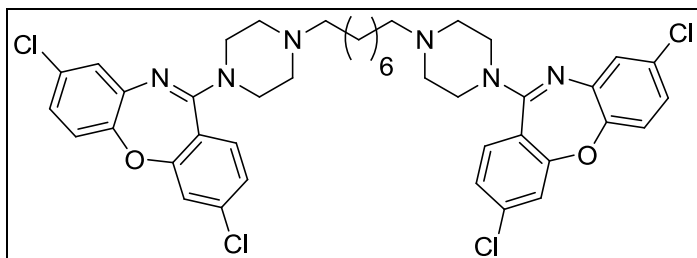
1,10-Bis(4-(3,7-dichlorodibenzo[*b,f*][1,4]oxazepin-11-yl)piperazin-1-yl)decane (210)


$C_{44}H_{48}Cl_4N_6O_2$ ($M = 834.70$ g/mol)

210 was prepared according to *general procedure K* using **193** (600 mg, 1.73 mmol) and 1,10-diiododecane (339 mg, 0.86 mmol) and was obtained as a light yellow solid (440 mg, 0.53 mmol, 61.9 % yield).

$C_{44}H_{48}Cl_4N_6O_2$ ($M = 834.70$ g/mol), mp 178.7 – 179.0 °C. **1H -NMR** (300 MHz, $CDCl_3$) δ 28 – 7.24 (m, 4H), δ 7.19 (dd, $J = 8.4, 1.9$ Hz, 2H), δ 7.14 – 7.09 (m, 2H), δ 7.05 (d, $J = 1.8$ Hz, 4H), δ 3.60 (bs, 8H), δ 2.61 (bs, 8H), δ 2.45 (s, 4H), δ 1.55 (s, 4H), δ 1.30 (s, 12H). **^{13}C -NMR** (75 MHz, $CDCl_3$) δ 160.57 (2 C_{quat}), 159.29 (2 C_{quat}), 151.58 (2 C_{quat}), 139.19 (2 C_{quat}), 138.11 (2 C_{quat}), 130.37 (+, 2 Ar-CH), 128.76 (2 C_{quat}), 127.67 (+, 2 Ar-CH), 126.01 (+, 2 Ar-CH), 125.65 (+, 2 Ar-CH), 121.95 (2 C_{quat}), 121.90 (+, 2 Ar-CH), 120.62 (+, 2 Ar-CH), 58.77 (-, 4 Pip-CH₂), 53.02 (-, 4 Pip-CH₂), 29.51 (-, 2 CH₂), 29.43 (-, 2 CH₂), 27.53 (-, 2 CH₂), 26.69 (-, 2 CH₂), 26.57 (-, 2 CH₂). **ESI-MS** m/z 279.1 [(M+3H)³⁺]; 418.1 [(M+2H)²⁺]; 835.3 [MH⁺]. **CHN** ($C_{44}H_{48}Cl_4N_6O_2 \cdot \frac{1}{6} H_2O$) calc. 63.09; H 5.82; N 10.03; exp. C 63.23; H 6.03; N 9.65.

1,8-Bis(4-(3,8-dichlorodibenzo[*b,f*][1,4]oxazepin-11-yl)piperazin-1-yl)octane (212)



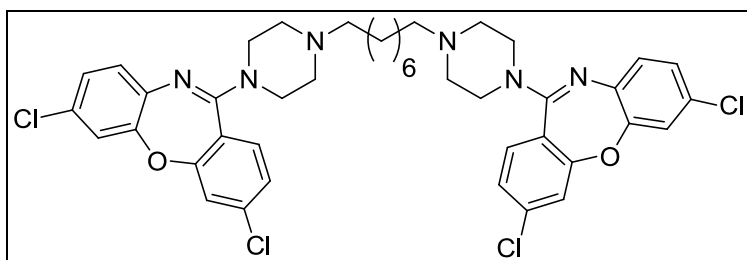
$C_{42}H_{44}Cl_4N_6O_2$ ($M = 806.65$ g/mol)

212 was prepared according to *general procedure K* using **196** (600 mg, 1.73 mmol) and 1,8-diiodooctane (315 mg, 0.86 mmol) and was obtained as a light yellow solid (400 mg, 0.50 mmol, 57.6 % yield).

$C_{42}H_{44}Cl_4N_6O_2$ ($M = 806.65$ g/mol), 176.7 – 177.2 °C. **1H -NMR** (300 MHz, $CDCl_3$) δ 7.30 - 7.23 (m, 4H), δ 7.19 (dd, $J = 8.4, 1.9$ Hz, 2H), δ 7.12 (d, $J = 2.5$ Hz, 2H), δ 7.02 (d, $J = 8.5$ Hz, 2H), δ 6.93 (dd, $J = 8.5, 2.5$ Hz, 2H), δ 3.61 (bs, 8H), δ 2.59 (bs, 8H), δ 2.43 (s, 4H), δ 1.55 (s, 4H), δ 1.28 (s, 8H). **^{13}C -NMR** (75 MHz, $CDCl_3$) δ 160.79 (2 C_{quat}), 159.64 (2 C_{quat}), 150.28 (2 C_{quat}), 141.55 (2 C_{quat}), 138.13 (2 C_{quat}), 130.77 (2 C_{quat}), 130.34 (+, 2 Ar-CH), 126.71 (+, 2 Ar-CH), 125.55 (+, 2 Ar-CH), 123.83 (+, 2 Ar-

CH), 121.87 (+, 2 Ar-CH), 121.08 (+, 2 Ar-CH), 58.74 (-, 4 Pip-CH₂), 53.02 (-, 4 Pip-CH₂), 29.45 (-, 2 CH₂), 27.47 (-, 2 CH₂), 26.72 (-, 2 CH₂), 26.67 (-, 2 CH₂). **ESI-MS** *m/z* 269.8 [(M+3H)³⁺]; 404.1 [(M+2H)²⁺]; 807.2 [MH⁺]. **CHN** (C₄₂H₄₄Cl₄N₆O₂ · 1/7 EtOAc) calc. C 62.41; H 5.55; N 10.26; exp. C 62.40; H 5.78; N 9.92.

1,8-Bis(4-(3,7-dichlorodibenzo[*b,f*][1,4]oxazepin-11-yl)piperazin-1-yl)octane (213)



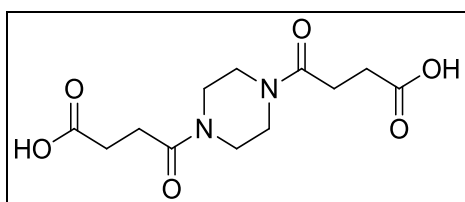
C₄₂H₄₄Cl₄N₆O₂ (M = 806.65 g/mol)

213 was prepared according to *general procedure K* using **193** (600 mg, 1.73 mmol) and 1,8-diiodooctane (315 mg, 0.86 mmol) and was obtained as a light yellow solid (350 mg, 0.43 mmol, 50.4 % yield).

C₄₂H₄₄Cl₄N₆O₂ (M = 806.65 g/mol), 148.3 – 148.7 °C. **¹H-NMR** (300 MHz, CDCl₃) δ 7.26 (m, 4H), δ 7.19 (dd, J = 8.4, 1.9Hz, 2H), δ 7.12 (t, J = 7.1Hz, 2H), δ 7.05 (d, J = 1.2Hz, 4H), δ 3.57 (bs, 8H), δ 2.58 (bs, 8H), δ 2.48 – 2.33 (m, 4H), δ 1.53 (s, 4H), δ 1.27 (s, 8H). **¹³C-NMR** (75 MHz, CDCl₃) δ 160.71 (2 C_{quat}), 159.22 (2 C_{quat}), 151.48 (2 C_{quat}), 139.18 (2 C_{quat}), 138.20 (2 C_{quat}), 130.37 (+, 2 Ar-CH), 128.79 (2 C_{quat}), 127.67 (+, 2 Ar-CH), 126.02 (+, 2 Ar-CH), 125.67 (+, 2 Ar-CH), 121.92 (+, 2 Ar-CH), 120.62 (+, 2 Ar-CH), 58.73 (-, 4 Pip-CH₂), 53.13 (-, 4 Pip-CH₂), 29.43 (-, 2 CH₂), 27.45 (-, 2 CH₂), 26.24 (-, 2 CH₂), 26.20 (-, 2 CH₂). **ESI-MS** *m/z* 269.8 [(M+3H)³⁺]; 404.1 [(M+2H)²⁺]; 807.2 [MH⁺]. **CHN** (C₄₂H₄₄Cl₄N₆O₂) calc. C 62.54; H 5.50; N 10.42; exp. C 62.40; H 5.66; N 10.13.

6.13. General procedure L:**Preparation of compounds 217, 224**

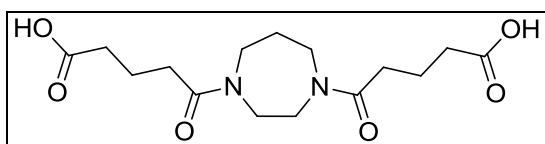
Piperazine or homopiperazine was dissolved in dioxane under gentle warming. A solution of succinic or glutaric anhydride in 15 ml dioxane was added dropwise and under constant stirring and the reaction mixture was heated at reflux for 24 h. After cooling to room temperature the solvent was evaporated in vacuo yielding the title compounds **217**, **224** which were used in the next step without further purification.

4,4'-(Piperazine-1,4-diyl)bis(4-oxobutanoic acid) (217)

$C_{12}H_{18}N_2O_6$ (M = 286.28 g/mol)

217 was prepared according to *general procedure L* using piperazine (1.00 g, 11.61 mmol, dissolved in 25 ml dioxane) and succinic anhydride (2.28 g, 22.83 mmol, dissolved in 15 ml dioxane) and was obtained as colorless crystalline solid after re-crystallization from ethanol (2.39 g, 8.35 mmol, 71.9 % yield).

$C_{12}H_{18}N_2O_6$ (M = 286.28 g/mol), 171.2 °C. **¹H-NMR** (300 MHz, CD₃OD) δ 4.92 (s, 2H), δ 3.78 (d, J = 7.8 Hz, 8H), δ 2.48 (bs, 8H). **ESI-MS** *m/z* 287.1 [MH⁺]. **CHN** ($C_{12}H_{18}N_2O_6$) calc. C 50.35; H 6.34; N 9.79; exp. C 50.28; H 6.45; N 9.82.

5,5'-(1,4-Diazepane-1,4-diyl)bis(5-oxopentanoic acid) (224)

$C_{15}H_{24}N_2O_6$ (M = 328.36 g/mol)

224 was prepared according to *general procedure L* using homopiperazine (500 mg, 4.99 mmol, dissolved in 15 ml dioxane) and glutaric anhydride (1.15 g, 10.12 mmol,

dissolved in 10 ml dioxane) and was obtained as a light yellow oil (1.31 g, 4.00 mmol, 79.5 % yield).

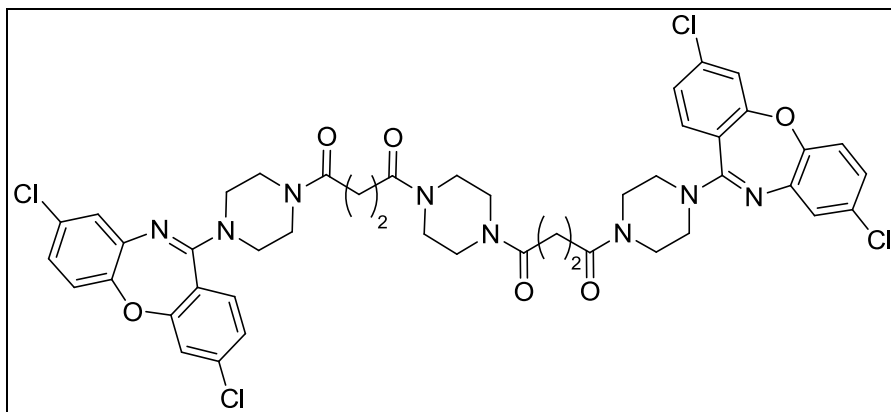
$C_{15}H_{24}N_2O_6$ ($M = 328.36$ g/mol). **1H -NMR** (300 MHz, CD_3OD) δ 4.98 (s, 2H), δ 3.80 – 3.67 (m, 12H), δ 2.54 (bs, 8H), δ 1.56 (m, 2H). **ESI-MS** m/z 329.2 [MH^+].

6.14. General procedure M:

Preparation of compounds 225, 238 – 242, 244

The dioic acid **217** or **224** was suspended in DCM under nitrogen atmosphere. A drop of DMF and 2.2 equivalents of oxalylchlorid were added and the reaction mixture was stirred at room temperature for 1 h. As soon as the reaction was completed (colour turned deeply yellow) the solution was carefully added to a solution of **193**, **196**, **232**, **233**, **234**, or **235** that was prepared in the meantime and to which a drop of pyridine and 2.5 equivalents of DIPEA were added. The mixture was stirred at room temperature over night and the next day partitioned between ethyl acetate and aqueous Na_2CO_3 solution. The organic layer was separated and the aqueous layer was extracted with ethyl acetate. The combined organic layers were washed with water and brine and afterwards dried over Na_2SO_4 . The solvent was evaporated in vacuo and the resulting crude product was purified by column chromatography over silica gel (gradual modification of the solvent within one column chromatography run, *solvent 1*: EtOAc / HX (3 : 2), *solvent 2*: EtOAc, *solvent 3*: methanol).

4,4'-(Piperazine-1,4-diyl)bis(1-(4-(3,8-dichlorodibenzo[*b,f*][1,4]oxazepin-11-yl)piperazin-1-yl)butane-1,4-dione) (225)

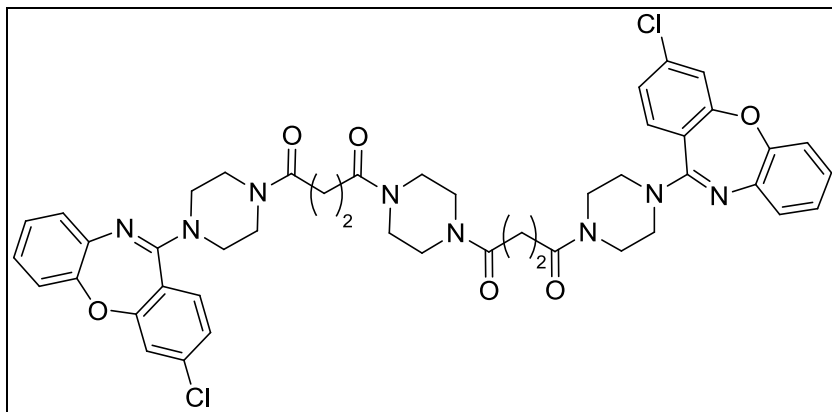


$C_{46}H_{44}Cl_4N_8O_6$ ($M = 946.70$ g/mol)

225 was prepared according to *general procedure M* using **196** (600 mg, 1.72 mmol) and **217** (421 mg, 1.47 mmol) and was obtained as a light yellow solid (273 mg, 0.29 mmol, 33.5 % yield).

$C_{46}H_{44}Cl_4N_8O_6$ ($M = 946.70$ g/mol), mp 164.2 – 165.0 °C. **1H -NMR** (300 MHz, $CDCl_3$) δ 7.30 – 7.25 (m, 4H), δ 7.22 (dd, $J = 8.4, 1.8$ Hz, 2H), δ 7.14 (d, $J = 2.3$ Hz, 2H), δ 7.03 (d, $J = 8.5$ Hz, 2H), δ 6.96 (dd, $J = 8.6, 2.5$ Hz, 2H), δ 3.74 – 3.44 (m, 16H), δ 2.72 (s, 8H), δ 1.89 (bs, 8H). **^{13}C -NMR** (75 MHz, $CDCl_3$) δ 170.70 (2 C_{quat} , $C=O$), 170.68 (2 C_{quat} , $C=O$), 160.88 (2 C_{quat}), 159.60 (2 C_{quat}), 150.24 (2 C_{quat}), 141.18 (2 C_{quat}), 138.54 (2 C_{quat}), 130.96 (2 C_{quat}), 130.09 (+, 2 Ar-CH), 126.76 (+, 2 Ar-CH), 125.79 (+, 2 Ar-CH), 124.35 (+, 2 Ar-CH), 122.03 (+, 2 Ar-CH), 121.66 (2 C_{quat}), 121.18 (+, 2 Ar-CH), 45.07 (-, 4 Pip-CH₂), 45.02 (-, 4 Pip-CH₂), 41.61 (-, 4 Pip-CH₂), 28.07 (-, 2 CH₂), 28.00 (-, 2 CH₂). **ESI-MS** m/z 474.1 [($M+2H$)²⁺]; 947.2 [MH^+]. **CHN** ($C_{46}H_{44}Cl_4N_8O_6 \cdot 3 H_2O$) calc. C 55.21, H 5.04, N 11.20; exp.: C 55.13, H 4.74, N 10.92

4,4'-(Piperazine-1,4-diyl)bis(1-(4-(3-chlorodibenzo[*b,f*][1,4]oxazepin-11-yl)-piperazin-1-yl)butane-1,4-dione) (238)



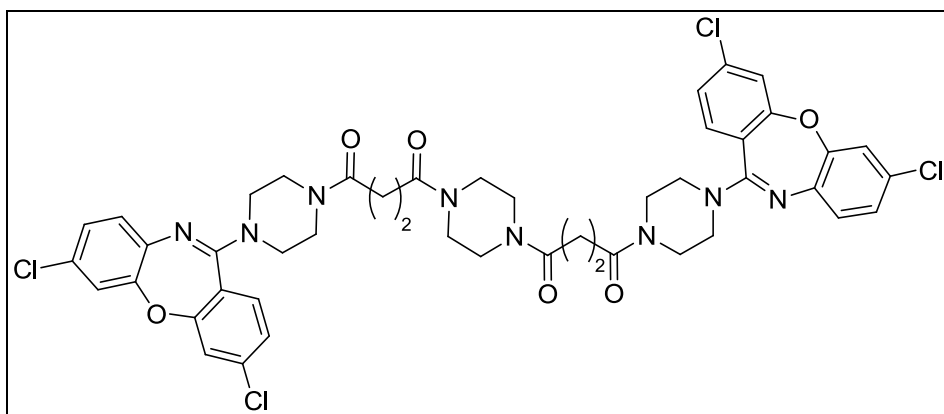
$C_{46}H_{46}Cl_2N_8O_6$ ($M = 877.81$ g/mol)

238 was prepared according to *general procedure M* using **232** (600 mg, 1.91 mmol) and **217** (467 mg, 1.63 mmol) and was obtained as a light yellow solid (258 mg, 0.29 mmol, 30.8 % yield).

$C_{46}H_{46}Cl_2N_8O_6$ ($M = 877.81$ g/mol), 159.8 – 160.1 °C. **1H -NMR** (300 MHz, $CDCl_3$) δ 7.31 – 7.25 (m, 4H), δ 7.21 (d, $J = 1.9$ Hz, 2H), δ 7.16 (dd, $J = 6.8, 3.3$ Hz, 2H), δ 7.15 – 7.12 (m, 2H), δ 7.11 – 7.06 (m, 2H), δ 7.02 (m, 2H), δ 3.64 – 3.51 (m, 14H), δ 3.47 (bs, 4H), δ 2.64 (s, 8H), δ 2.12 (bs, 6H). **^{13}C -NMR** (75 MHz, $CDCl_3$) δ 170.71 (2 C_{quat} ,

C=O), 170.69 (2 C_{quat}, C=O), 160.90 (2 C_{quat}), 159.62 (2 C_{quat}), 150.28 (2 C_{quat}), 138.61 (2 C_{quat}), 130.88 (2 C_{quat}), 130.13 (+, 2 Ar-CH), 126.76 (+, 2 Ar-CH), 125.81 (+, 2 Ar-CH), 124.46 (+, 2 Ar-CH), 124.42 (+, 2 Ar-CH), 122.05 (+, 2 Ar-CH), 121.59 (2 C_{quat}), 121.19 (+, 2 Ar-CH), 45.12 (-, 4 Pip-CH₂), 45.08 (-, 4 Pip-CH₂), 41.59 (-, 4 Pip-CH₂), 28.05 (-, 2 CH₂), 28.01 (-, 2 CH₂). **ESI-MS** *m/z* 439.15 [(M+2H)²⁺]; 877.30 [MH⁺]. **CHN** (C₄₆H₄₆Cl₂N₈O₆ · 5/2 H₂O) calc. C 59.87, H 5.57, N 12.14; exp. C 59.81, H 5.40, N 12.23.

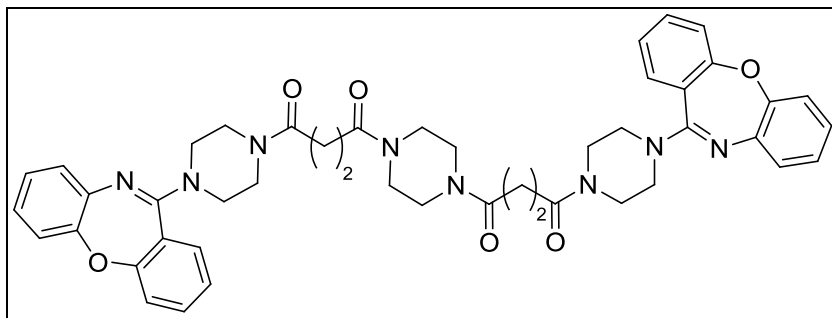
4,4'-(Piperazine-1,4-diyl)bis(1-(4-(3,7-dichlorodibenzo[*b,f*][1,4]oxazepin-11-yl)piperazin-1-yl)butane-1,4-dione) (239)



C₄₆H₄₄Cl₄N₈O₆ (M = 946.70 g/mol)

239 was prepared according to general *procedure M* using **193** (250 mg, 0.73 mmol) and **217** (175 mg, 0.61 mmol) and was obtained as a light yellow solid (127 mg, 0.13 mmol, 37.32 % yield).

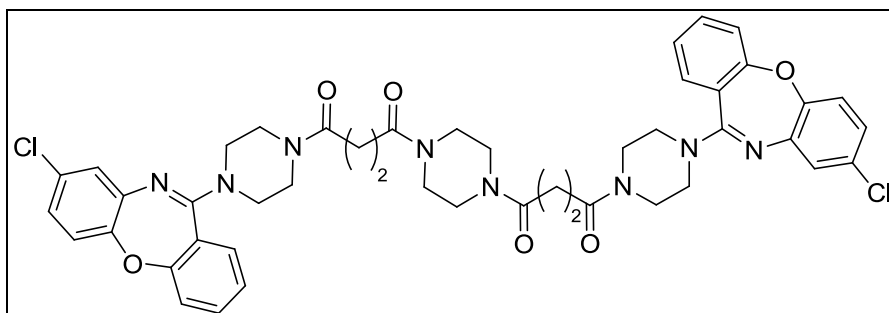
C₄₆H₄₄Cl₄N₈O₆ (M = 946.70 g/mol), 160.4 – 160.8 °C. **¹H-NMR** (300 MHz, CDCl₃) δ 7.31 – 7.24 (m, 4H), δ 7.22 (dd, *J* = 8.4, 1.9Hz, 2H), δ 7.15 – 7.10 (m, 2H), δ 7.06 (d, *J* = 1.6Hz, 4H), δ 3.62 – 3.54 (m, 12H), δ 3.46 (bs, 4H), δ 2.72 (s, 8H), δ 1.76 (bs, 8H). **¹³C-NMR** (75 MHz, CDCl₃) δ 170.78 (2 C_{quat}, C=O), 170.68 (2 C_{quat}, C=O), 160.66 (2 C_{quat}), 159.22 (2 C_{quat}), 151.54 (2 C_{quat}), 138.77 (2 C_{quat}), 138.51 (2 C_{quat}), 130.12 (+, 2 Ar-CH), 129.32 (2 C_{quat}), 127.73 (+, 2 Ar-CH), 126.11 (+, 2 Ar-CH), 125.90 (+, 2 Ar-CH), 122.08 (+, 2 Ar-CH), 121.72 (2 C_{quat}), 120.71 (+, 2 Ar-CH), 45.29 (-, 4 Pip-CH₂), 45.02 (-, 4 Pip-CH₂), 41.57 (-, 4 Pip-CH₂), 28.04 (-, 2 CH₂), 28.00 (-, 2 CH₂). **ESI-MS** *m/z* 474.1 [(M+2H)²⁺]; 947.2 [MH⁺]. **CHN** (C₄₆H₄₄Cl₄N₈O₆ · 4 H₂O) calc. C 54.32, H 5.14, N 11.00; exp. C 54.70, H 4.76, N 10.66.

4,4'-(Piperazine-1,4-diyl)bis(1-(4-(dibenzo[*b,f*][1,4]oxazepin-11-yl)piperazin-1-yl)butane-1,4-dione) (240)


$C_{46}H_{48}N_8O_6$ ($M = 808.92$ g/mol)

240 was prepared according to *general procedure M* using **233** (300 mg, 1.07 mmol) and **217** (261 mg, 0.91 mmol) and was obtained as a light yellow solid (152 mg, 0.19 mmol, 35.1 % yield).

$C_{46}H_{48}N_8O_6$ ($M = 808.92$ g/mol), mp 164.2 – 164.9 °C. **1H -NMR** (300 MHz, $CDCl_3$) δ 7.50 – 7.41 (m, 2H), δ 7.35 (dd, $J = 7.7, 1.6$ Hz, 2H), δ 7.30 – 7.04 (m, 10H), δ 7.03 – 6.95 (m, 2H), δ 3.67 – 3.61 (m, 10H), δ 3.46 (bs, 8H), δ 2.73 (s, 8H), δ 2.06 (s, 1H), δ 1.76 (bs, 4H), δ 1.25 (s, 1H). **^{13}C -NMR** (75 MHz, $CDCl_3$) δ 170.81 (2 C_{quat} , C=O), 170.64 (2 C_{quat} , C=O), 161.07 (2 C_{quat}), 160.16 (2 C_{quat}), 152.11 (2 C_{quat}), 140.22 (2 C_{quat}), 132.96 (+, 2 Ar-CH), 129.36 (+, 2 Ar-CH), 126.96 (+, 2 Ar-CH), 125.62 (+, 2 Ar-CH), 125.03 (+, 2 Ar-CH), 124.64 (+, 2 Ar-CH), 123.38 (2 C_{quat}), 121.45 (+, 2 Ar-CH), 120.29 (+, 2 Ar-CH), 45.33 (-, 4 Pip-CH₂), 45.11 (-, 4 Pip-CH₂), 41.67 (-, 4 Pip-CH₂), 28.03 (-, 2 CH₂), 28.01 (-, 2 CH₂). **ESI-MS** m/z 405.2 [(M+2H)²⁺]; 809.4 [MH⁺]. **CHN** ($C_{46}H_{48}N_8O_6 \cdot 4 H_2O$) calc. C 62.71, H 6.41, N 12.72; exp. C 62.63, H 6.09, N 12.52.

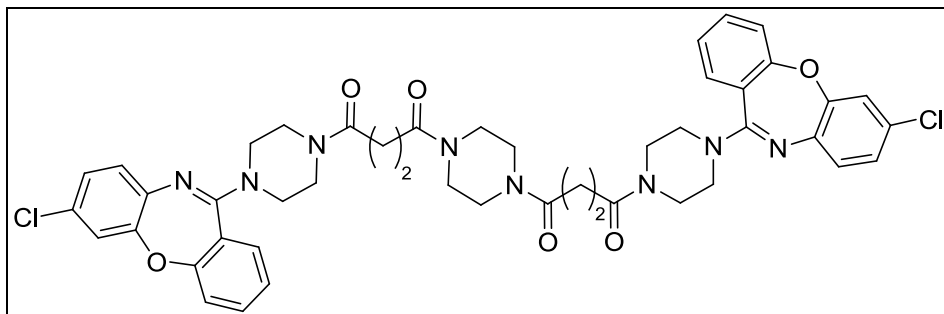
4,4'-(Piperazine-1,4-diyl)bis(1-(4-(8-chlorodibenzo[*b,f*][1,4]oxazepin-11-yl)piperazin-1-yl)butane-1,4-dione) (241)


$C_{46}H_{46}Cl_2N_8O_6$ ($M = 877.81$ g/mol)

241 was prepared according to *general procedure M* using **234** (300 mg, 0.96 mmol) and **217** (234 mg, 0.82 mmol) and was obtained as a colorless solid (148 mg, 0.17 mmol, 35.4 % yield).

$C_{46}H_{46}Cl_2N_8O_6$ ($M = 877.81$ g/mol), mp 161.1 – 162.0 °C. **1H -NMR** (300 MHz, $CDCl_3$) δ 7.53 – 7.42 (m, 2H), δ 7.33 (dd, $J = 7.7, 1.6$ Hz, 2H), δ 7.28 – 7.17 (m, 4H), δ 7.13 (d, $J = 2.5$ Hz, 2H), δ 7.03 (d, $J = 8.5$ Hz, 2H), δ 6.93 (dd, $J = 8.5, 2.6$ Hz, 2H), δ 3.78 – 3.60 (m, 10H), δ 3.53 (bs, 8H), δ 2.72 (s, 8H), δ 1.67 (bs, 6H). **^{13}C -NMR** (75 MHz, $CDCl_3$) δ 170.78 (2 C_{quat} , C=O), 170.66 (2 C_{quat} , C=O), 160.78 (2 C_{quat}), 160.57 (2 C_{quat}), 150.71 (2 C_{quat}), 141.43 (2 C_{quat}), 133.19 (+, 2 Ar-CH), 130.48 (2 C_{quat}), 129.36 (+, 2 Ar-CH), 126.61 (+, 2 Ar-CH), 125.27 (+, 2 Ar-CH), 124.08 (+, 2 Ar-CH), 123.10 (2 C_{quat}), 121.40 (+, 2 Ar-CH), 121.15 (+, 2 Ar-CH), 45.24 (-, 4 Pip-CH₂), 45.09 (-, 4 Pip-CH₂), 41.63 (-, 4 Pip-CH₂), , 28.04 (-, 2 CH₂), 28.01 (-, 2 CH₂). **ESI-MS** m/z 439.2 [($M+2H$)²⁺]; 877.3 [MH^+]. **CHN** ($C_{46}H_{46}Cl_2N_8O_6 \cdot 3 H_2O$) calc. C 59.29, H 5.62, N 12.02; exp. C 59.20, H 5.65, N 11.82.

4,4'-(Piperazine-1,4-diyl)bis(1-(4-(7-chlorodibenzo[*b,f*][1,4]oxazepin-11-yl)piperazin-1-yl)butane-1,4-dione) (242)



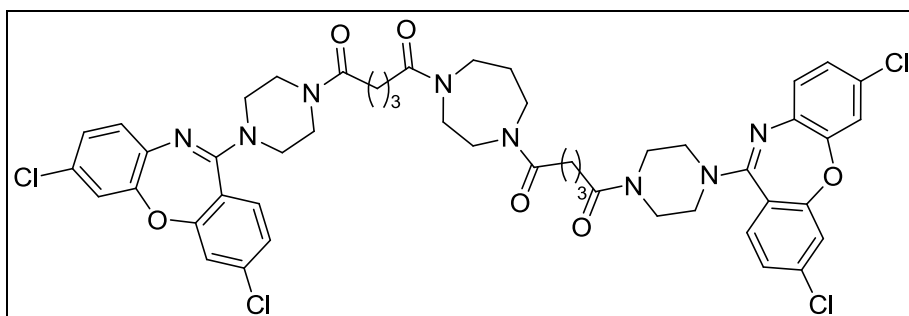
$C_{46}H_{46}Cl_2N_8O_6$ ($M = 877.81$ g/mol)

242 was prepared according to *general procedure M* using **235** (500 mg, 1.59 mmol) and **217** (386 mg, 1.35 mmol) and was obtained as a colorless solid (193 mg, 0.22 mmol, 27.7 % yield).

$C_{46}H_{46}Cl_2N_8O_6$ ($M = 877.81$ g/mol), mp 165.3 °C. **1H -NMR** (300 MHz, $CDCl_3$) δ 7.31 (m, 2H), δ 7.29 – 7.25 (m, 4H), δ 7.22 (dd, $J = 8.2, 2.3$ Hz, 2H), δ 7.15 – 7.11 (m, 2H), δ 7.03 (d, $J = 8.5$ Hz, 2H), δ 6.95 (dd, $J = 7.8, 2.6$ Hz, 2H), δ 3.74 – 3.60 (m, 10H), δ 3.51 (bs, 8H), δ 2.72 (s, 8H), δ 1.70 (bs, 6H). **^{13}C -NMR** (75 MHz, $CDCl_3$) δ 170.79 (2 C_{quat} , C=O), 170.69 (2 C_{quat} , C=O), 160.90 (2 C_{quat}), 159.62 (2 C_{quat}), 150.28 (2 C_{quat}),

130.88 (2 C_{quat}), 130.13 (+, 2 Ar-CH), 127.06 (2 C_{quat}), 126.76 (+, 2 Ar-CH), 125.82 (+, 2 Ar-CH), 124.43 (+, 2 Ar-CH), 122.06 (+, 2 Ar-CH), 121.19 (+, 2 Ar-CH), 121.07 (+, 2 Ar-CH), 45.23 (-, 4 Pip-CH₂), 45.08 (-, 4 Pip-CH₂), 41.58 (-, 4 Pip-CH₂), 28.05 (-, 2 CH₂), 28.02 (-, 2 CH₂). **ESI-MS** *m/z* 439.2 [(M+2H)²⁺]; 877.3 [MH⁺]. **CHN** (C₄₆H₄₆Cl₂N₈O₆ · 3 H₂O) calc. C 59.29, H 5.62, N 12.02; exp. C 59.46, H 5.48, N 12.08.

5,5'-(1,4-Diazepane-1,4-diyl)bis(1-(4-(3,7-dichlorodibenzo[*b,f*][1,4]oxazepin-11-yl)piperazin-1-yl)pentane-1,5-dione) (244)



C₄₉H₅₀Cl₄N₈O₆ (M = 988.76 g/mol)

244 was prepared according to *general procedure M* using **193** (300 mg, 0.86 mmol) and **224** (240 mg, 0.73 mmol). After additional purification by preparative HPLC*, **244** was obtained as trifluoroacetate salt that was extracted with EtOAc to give the free base of **244** as a light yellow solid (116 mg, 0.12 mmol, 27.2 % yield).

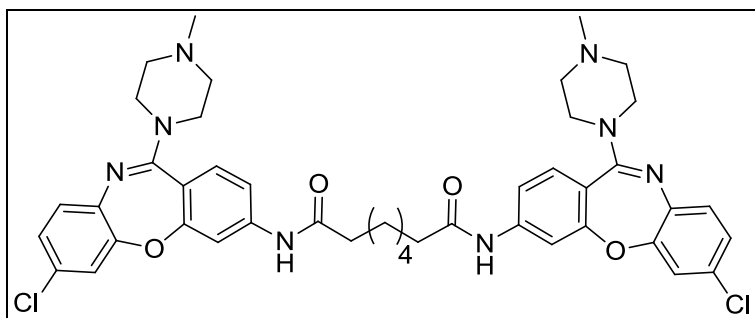
C₄₉H₅₀Cl₄N₈O₆ (M = 988.76 g/mol), mp 139.4 – 139.8 °C. **¹H NMR** (300 MHz, CDCl₃) δ 7.29 – 7.26 (m, 4H), 7.22 (d, *J* = 8.4 Hz, 2H), 7.11 (m, 2H), 7.07 (m, 4H), 3.73 – 3.37 (m, 12H), 2.42 (d, *J* = 6.7 Hz, 8H), 2.04 – 1.80 (m, 8H), 1.36 – 1.14 (m, 8H), 1.11 – 1.04 (m, 2H). **¹³C-NMR** (75 MHz, CDCl₃) δ 172.17 (2 C_{quat}, C=O), 171.53 (C_{quat}, C=O), 171.41 (C_{quat}, C=O), 160.64 (2 C_{quat}), 159.25 (2 C_{quat}), 151.53 (2 C_{quat}), 138.78 (2 C_{quat}), 138.51 (2 C_{quat}), 130.14 (+, 2 Ar-CH), 129.29 (2 C_{quat}), 127.73 (+, 2 Ar-CH), 126.10 (+, 2 Ar-CH), 125.90 (+, 2 Ar-CH), 122.06 (+, 2 Ar-CH), 121.71 (2 C_{quat}), 120.70 (+, 2 Ar-CH), 47.40 (-, 4 Pip-CH₂), 47.31 (-, 4 Pip-CH₂), 45.19 (-, 2 HomPip-CH₂), 41.29 (-, 2 HomPip-CH₂), 32.81 (-, 2 CH₂), 31.85 (-, 2 CH₂), 27.14 (-, 2 CH₂), 20.62 (-, HomPip-CH₂). **ESI-MS** *m/z* 495.1 [(M+2H)²⁺]; 989.3 [MH⁺]. **CHN** (C₄₉H₅₀Cl₄N₈O₆ · 3 H₂O) calc. C 56.44, H 5.41, N 10.75; exp. C 56.53, H 5.48, N 10.57.

* = see section 6.17 (Appendix) for experimental details

6.15. General procedure N:**Preparation of compounds 215, 221, 227, 229 – 231, 243**

The dioic acid (1,8-octanedioic acid, **217**, **224**) was suspended in DCM under nitrogen atmosphere. A drop of DMF and 2.2 equivalents of oxalylchlorid were added and the reaction mixture was stirred at room temperature for 2 h. As soon as the reaction was completed (colour turned deeply yellow) the solution was carefully added to a solution of **128**, **129**, or **136** that was prepared in the meantime and to which a drop of pyridine and 2.5 equivalents of DIPEA were added. The mixture was stirred at room temperature for 1 - 6 h (monitored by TLC) and afterwards partitioned between ethyl acetate and aqueous Na₂CO₃ solution. The organic layer was separated and the aqueous layer was extracted with ethyl acetate. The combined organic layers were washed with water and brine and afterwards dried over Na₂SO₄. The solvent was evaporated in vacuo and the resulting crude product was purified by column chromatography over silica gel (*solvent 1*: CH₃OH, *solvent 2*: 7 N NH₃ in CH₃OH).

***N'*,*N*⁸-Bis(7-chloro-11-(4-methylpiperazin-1-yl)dibenzo[*b,f*][1,4]oxazepin-3-yl)-octanedioicacid diamide (**215**)**



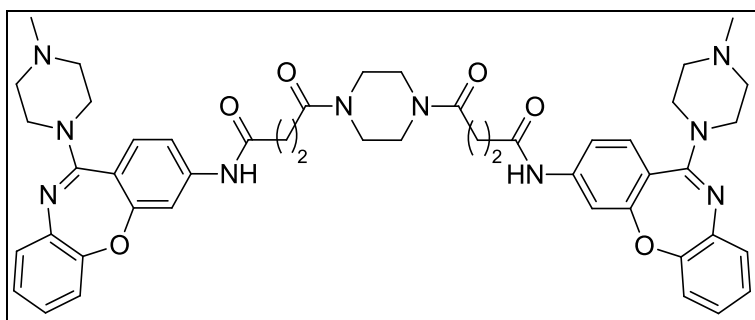
C₄₄H₄₈Cl₂N₈O₄ (M = 823.81 g/mol)

215 was prepared according to *general procedure N* using **129** (250 mg, 0.73 mmol) and 1,8-octanedioic acid (120 mg, 0.69 mmol) and was obtained as a colorless solid (83 mg, 0.10 mmol, 27.7 % yield).

C₄₄H₄₈Cl₂N₈O₄ (M = 823.81 g/mol), mp 152.7 – 153.4 °C. **¹H-NMR** (300 MHz, CD₃OD) δ 7.73 (d, J = 1.9Hz, 2H), δ 7.46 (dt, J = 15.3, 5.2Hz, 4H), δ 7.20 (d, J = 1.2Hz, 2H), δ 7.15 (t, J = 5.0Hz, 4H), δ 3.82 (bs, 2H), δ 3.42 (bs, 8H), δ 3.30 (dt, J = 3.2, 1.6 Hz, 8H), δ 2.97 (s, 6H), δ 2.40 (t, J = 7.4Hz, 4H), δ 1.70 (m, 4H), δ 1.39 (m, 4H). **¹³C-NMR** (75 MHz, CD₃OD) δ 175.08 (2 C_{quat}, C=O), 162.65 (2 C_{quat}), 161.39 (2 C_{quat}), 153.94 (2

C_{quat}), 145.79 (2 C_{quat}), 131.45 (+, 2 Ar-CH), 131.40 (2 C_{quat}), 128.79 (+, 2 Ar-CH), 127.02 (+, 2 Ar-CH), 121.98 (+, 2 Ar-CH), 117.89 (2 C_{quat}), 117.70 (+, 2 Ar-CH), 112.81 (+, 2 Ar-CH), 54.13 (-, 4 Pip-CH₂), 48.19 (-, 4 Pip-CH₂), 43.70 (+, 2 CH₃), 37.94 (-, 2 CH₂), 30.00 (-, 2 CH₂), 26.47 (-, 2 CH₂). **ESI-MS** *m/z* 275.1 [(M+3H)³⁺]; 412.2 [(M+2H)²⁺]; 823.3 [MH⁺]. **CHN** (C₄₄H₄₈Cl₂N₈O₄ · 3 H₂O) calc.: C 60.20, H 6.20, N 12.76; exp.: C 60.49, H 6.34, N 12.65.

4,4'-(Piperazine-1,4-diyl)bis(*N*-(11-(4-methylpiperazin-1-yl)dibenzo[*b,f*][1,4]-oxazepin-3-yl)-4-oxobutanamide) (221)

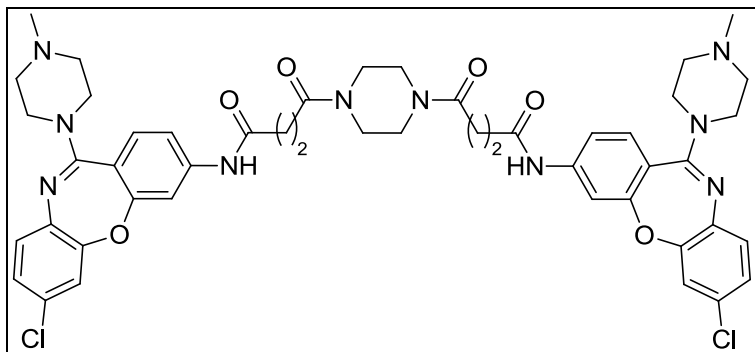


C₄₈H₅₄N₁₀O₆ (M = 867.01 g/mol)

221 was prepared according to *general procedure N* using **136** (200 mg, 0.65 mmol) and **217** (159 mg, 0.56 mmol) and was obtained as a colorless solid (70 mg, 0.08 mmol, 25.0 % yield).

C₄₈H₅₄N₁₀O₆ (M = 867.01 g/mol), 175.1 – 175.5 °C. **¹H-NMR** (300 MHz, CD₃OD) δ 7.74 (s, 2H), δ 7.44 (d, J = 0.9 Hz, 4H), δ 7.32 – 7.02 (m, 8H), 3.70 (bs, 2H), δ 3.66 – 3.57 (m, 8H), δ 3.50 (s, 8H), δ 3.42 (bs, 8H), δ 2.96 (s, 6H), δ 2.84 – 2.68 (m, 8H). **¹³C-NMR** (75 MHz, CD₃OD) δ 175.26 (2 C_{quat}, C=O), 172.68 (2 C_{quat}, C=O), 171.02, 161.39 (2 C_{quat}), 159.97 (2 C_{quat}), 142.24 (2 C_{quat}), 140.57 (2 C_{quat}), 130.01 (+, 2 Ar-CH), 127.01 (+, 2 Ar-CH), 125.60 (+, 2 Ar-CH), 124.59 (+, 2 Ar-CH), 121.71 (2 C_{quat}), 120.39 (+, 2 Ar-CH), 118.73 (2 C_{quat}), 115.55 (+, 2 Ar-CH), 111.76 (+, 2 Ar-CH), 54.92 (-, 4 Pip-CH₂), 48.17 (-, 4 Pip-CH₂), 45.97 (+, 2 CH₃), 41.52 (-, 4 Pip-CH₂), 32.52 (-, 2 CH₂), 28.77 (-, 2 CH₂). **ESI-MS** *m/z* 289.8 [(M+3H)³⁺]; 434.2 [(M+2H)²⁺]; 867.4 [MH⁺]. **CHN** (C₄₈H₅₄N₁₀O₆ · 3 H₂O) calc.: C 62.59, H 6.57, N 13.21; exp.: C 62.98, H 6.60, N 13.37.

**4,4'-(Piperazine-1,4-diyl)bis(*N*-(7-chloro-11-(4-methylpiperazin-1-yl)dibenzo-
[*b,f*][1,4]oxazepin-3-yl)-4-oxobutanamide) (227)**

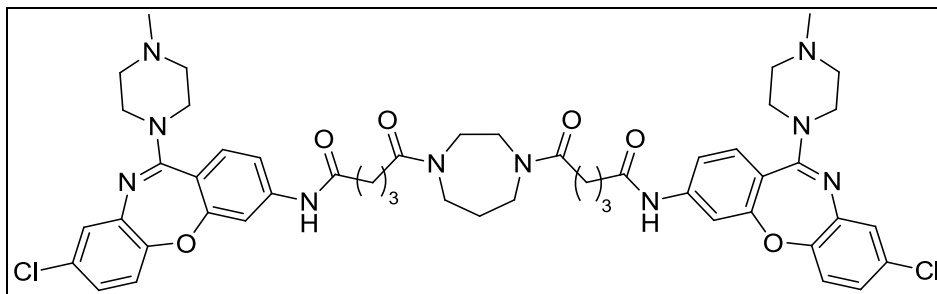


$C_{48}H_{52}Cl_2N_{10}O_6$ ($M = 935.90$ g/mol)

227 was prepared according to *general procedure N* using **129** (200 mg, 0.59 mmol) and **217** (143 mg, 0.50 mmol) and was obtained as a light yellow solid (79 mg, 0.08 mmol, 28.8 % yield).

$C_{48}H_{52}Cl_2N_{10}O_6$ ($M = 935.90$ g/mol), 162.4 – 162.8 °C. **1H -NMR** (300 MHz, CD_3OD) δ 7.68 (s, 2H), δ 7.52 – 7.24 (m, 6H), δ 7.13 – 6.97 (m, 4H), δ 6.93 (dd, $J = 8.6, 2.5$ Hz, 2H), δ 3.72 – 3.51 (m, 16H), δ 2.74 (d, $J = 8.0$ Hz, 8H), δ 2.54 (bs, 8H), δ 2.33 (s, 6H). **^{13}C -NMR** (75 MHz, CD_3OD) δ 173.51 (2 C_{quat} , C=O), 172.86 (2 C_{quat} , C=O), 162.68 (2 C_{quat}), 152.46 (2 C_{quat}), 143.23 (2 C_{quat}), 131.43 (2 C_{quat}), 131.34 (+, 2 Ar-CH), 127.32 (+, 2 Ar-CH), 126.31 (2 C_{quat}), 125.68 (2 C_{quat}), 124.96 (+, 2 Ar-CH), 122.53 (+, 2 Ar-CH), 118.97 (2 C_{quat}), 117.10 (+, 2 Ar-CH), 112.51 (+, 2 Ar-CH), 55.71 (-, 4 Pip-CH₂), 48.09 (-, 4 Pip-CH₂), 46.32 (+, 2 CH₃), 46.12 (-, 4 Pip-CH₂), 32.64 (-, 2 CH₂), 28.78 (-, 2 CH₂). **ESI-MS** m/z 312.5 [(M+3H)³⁺]; 468.2 [(M+2H)²⁺]; 935.4 [MH⁺]. **CHN** ($C_{48}H_{52}Cl_2N_{10}O_6 \cdot 4 H_2O$) calc. C 57.20, H 6.00, N 13.90; exp. C 57.31, H 5.75, N 13.62.

**5,5'-(1,4-Diazepane-1,4-diyl)bis(*N*-(8-chloro-11-(4-methylpiperazin-1-yl)dibenzo-
[*b*,*f*][1,4]oxazepin-3-yl)-5-oxopentanamide) (229)**

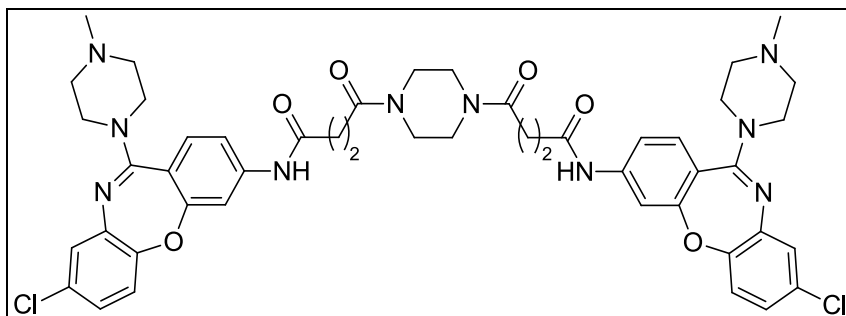


$C_{51}H_{58}Cl_2N_{10}O_6$ ($M = 977.98$ g/mol)

229 was prepared according to *general procedure N* using **128** (200 mg, 0.58 mmol) and **224** (164 mg, 0.50 mmol) and was obtained as a light yellow solid (81 mg, 0.08 mmol, 28.5 % yield).

$C_{51}H_{58}Cl_2N_{10}O_6$ ($M = 977.98$ g/mol), 168.7 – 169.3 °C. **1H -NMR** (300 MHz, CD_3OD) δ 7.66 (dd, $J = 8.0, 3.5$ Hz, 2H), δ 7.46 – 7.13 (m, 4H), δ 7.11 – 6.72 (m, 6H), δ 3.65–3.39 (m, 16H), δ 2.76 – 2.33 (m, 16H), δ 2.32 (s, 6H), δ 1.93 (dd, $J = 15.3, 8.5$ Hz, 4H), δ 1.75 (bs, 2H), δ 1.28 (bs, 2H). **^{13}C -NMR** (75 MHz, CD_3OD) δ 174.17 (2 C_{quat} , C=O), 173.96 (2 C_{quat} , C=O), 165.96 (2 C_{quat}), 162.41 (2 C_{quat}), 152.37 (2 C_{quat}), 144.81 (+, 2 Ar-CH), 143.18 (2 C_{quat}), 131.35 (+, 2 Ar-CH), 127.35 (+, 2 Ar-CH), 124.96 (+, 2 Ar-CH), 122.51 (+, 2 Ar-CH), 119.12 (2 C_{quat}), 117.21 (2 C_{quat}), 112.78 (+, 2 Ar-CH), 112.64 (2 C_{quat}), 55.71 (-, 4 Pip-CH₂), 48.12 (-, 4 Pip-CH₂), 46.12 (+, 2 CH₃), 37.04 (-, 2 HomPip-CH₂), 33.29 (-, 2 HomPip-CH₂), 32.61 (-, 2 CH₂), 28.16 (-, 2 CH₂), 23.65 (-, HomPip-CH₂), 22.06 (-, 2 CH₂). **ESI-MS** m/z 326.5 [(M+3H)³⁺]; 489.2 [(M+2H)²⁺]; 977.4 [MH⁺]. **CHN** ($C_{51}H_{58}Cl_2N_{10}O_6 \cdot 3 H_2O$) calc. C 59.35, H 6.25, N 13.57; exp. C 59.29, H 6.19, N 13.21.

4,4'-(Piperazine-1,4-diyl)bis(*N*-(8-chloro-11-(4-methylpiperazin-1-yl)dibenzo-[*b,f*][1,4]oxazepin-3-yl)-4-oxobutanamide) (230)

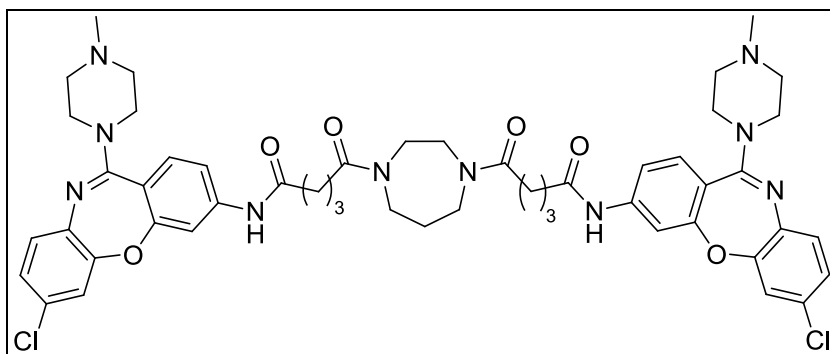


$C_{48}H_{52}Cl_2N_{10}O_6$ ($M = 935.90$ g/mol)

230 was prepared according to *general procedure N* using **128** (250 mg, 0.73 mmol) and **217** (179 mg, 0.62 mmol) and was obtained as a light yellow solid (95 mg, 0.10 mmol, 28.0 % yield).

$C_{48}H_{52}Cl_2N_{10}O_6$ ($M = 935.90$ g/mol), 173.4 – 173.9 °C. **1H -NMR** (300 MHz, CD_3OD) δ 7.69 (s, 2H), δ 7.51 – 7.24 (m, 6H), δ 7.15 – 6.99 (m, 4H), δ 6.91 (dd, $J = 8.4, 2.2$ Hz, 2H), δ 3.65 – 3.48 (m, 16H), δ 2.72 (d, $J = 8.2$ Hz, 8H), δ 2.50 (bs, 8H), δ 2.31 (s, 6H). **^{13}C -NMR** (75 MHz, CD_3OD) δ 172.71 (2 C_{quat} , C=O), 172.16 (2 C_{quat} , C=O), 160.17 (2 C_{quat}), 151.20 (2 C_{quat}), 143.01 (2 C_{quat}), 131.97 (2 C_{quat}), 131.44 (+, 2 Ar-CH), 127.12 (+, 2 Ar-CH), 126.56 (2 C_{quat}), 125.71 (2 C_{quat}), 124.80 (+, 2 Ar-CH), 122.35 (+, 2 Ar-CH), 118.81 (2 C_{quat}), 117.02 (+, 2 Ar-CH), 112.47 (+, 2 Ar-CH), 55.74 (-, 4 Pip-CH₂), 48.16 (-, 4 Pip-CH₂), 46.29 (+, 2 CH₃), 46.11 (-, 4 Pip-CH₂), 32.48 (-, 2 CH₂), 28.80 (-, 2 CH₂). **ESI-MS** m/z 312.5 [($M+3H$)³⁺]; 468.2 [($M+2H$)²⁺]; 935.4 [MH^+]. **CHN** ($C_{48}H_{52}Cl_2N_{10}O_6 \cdot 4 H_2O$) calc. C 57.20, H 6.00, N 13.90; exp. 57.16, H 5.98, N 13.68.

**5,5'-(1,4-Diazepane-1,4-diyl)bis(*N*-(7-chloro-11-(4-methylpiperazin-1-yl)dibenzo-
[*b*,*f*][1,4]oxazepin-3-yl)-5-oxopentanamide) (231)**

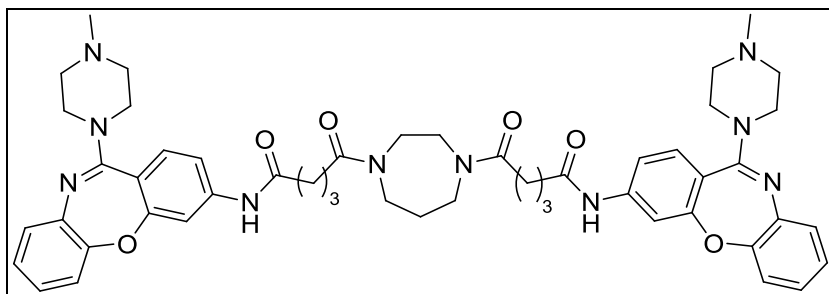


$C_{51}H_{58}Cl_2N_{10}O_6$ ($M = 977.98$ g/mol)

231 was prepared according to *general procedure N* using **129** (220 mg, 0.64 mmol) and **224** (180 mg, 0.55 mmol) and was obtained as a light yellow solid (94 mg, 0.10 mmol, 29.9 % yield).

$C_{51}H_{58}Cl_2N_{10}O_6$ ($M = 977.98$ g/mol), 159.1 – 159.8 °C. **1H -NMR** (300 MHz, CD_3OD) δ 7.67 (s, 2H), δ 7.45 – 7.18 (m, 4H), δ 7.13 – 6.97 (m, 6H), δ 3.61 – 3.39 (m, 16H), δ 2.70 – 2.36 (m, 16H), δ 2.32 (s, 6H), δ 2.05 – 1.86 (m, 4H), δ 1.72 (bs, 2H), δ 1.28 (bs, 2H). **^{13}C -NMR** (75 MHz, CD_3OD) δ 174.65 (2 C_{quat} , C=O), 174.03 (2 C_{quat} , C=O), 162.37 (2 C_{quat}), 162.01 (2 C_{quat}), 153.75 (2 C_{quat}), 144.79 (2 C_{quat}), 140.80 (2 C_{quat}), 131.34 (+, 2 Ar-CH), 129.86 (2 C_{quat}), 128.75 (+, 2 Ar-CH), 126.72 (+, 2 Ar-CH), 121.65 (+, 2 Ar-CH), 119.18 (2 C_{quat}), 117.38 (+, 2 Ar-CH), 112.64 (+, 2 Ar-CH), 55.71 (-, 4 Pip-CH₂), 48.13 (-, 4 Pip-CH₂), 46.14 (+, 2 CH₃), 41.55 (-, 2 HomPip-CH₂), 36.82 (-, 2 HomPip-CH₂), 33.31 (-, 2 CH₂), 32.69 (-, 2 CH₂), 23.51 (-, HomPip-CH₂), 22.13 (-, 2 CH₂). **ESI-MS** m/z 326.5 [(M+3H)³⁺]; 489.2 [(M+2H)²⁺]; 977.4 [MH⁺]. **CHN** ($C_{51}H_{58}Cl_2N_{10}O_6 \cdot 3 CH_3OH$) calc. C 60.38; H 6.57; N 13.04; exp. C 60.11; H 6.29; N 12.99.

5,5'-(1,4-Diazepane-1,4-diyl)bis(*N*-(11-(4-methylpiperazin-1-yl)dibenzo[*b,f*][1,4]-oxazepin-3-yl)-5-oxopentanamide) (243**)**



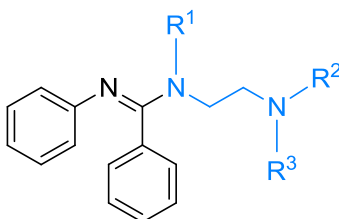
C₅₁H₆₀N₁₀O₆ (M = 909.09 g/mol)

243 was prepared according to *general procedure N* using **136** (80 mg, 0.26 mmol) and **224** (72 mg, 0.22 mmol). After additional purification by preparative HPLC*, **243** was obtained as trifluoroacetate salt that was extracted with EtOAc to give the free base of **243** as a colorless solid (32 mg, 0.04 mmol, 27.0 % yield).

C₅₁H₆₀N₁₀O₆ (M = 909.09 g/mol), 156.2 – 156.7 °C. **¹H NMR** (300 MHz, CD₃OD) δ 7.67 (dd, J = 8.2, 6.3 Hz, 2H), δ 7.41 – 7.21 (m, 4H), δ 7.18 – 6.90 (m, 8H), δ 3.70 – 3.49 (m, 16H), δ 2.64 (bs, 6H), δ 2.57 – 2.36 (m, 12H), δ 2.00 – 1.86 (m, 4H), δ 1.76 (bs, 2H), δ 0.91 (m, 6H). **¹³C-NMR** (75 MHz, CD₃OD) δ 176.13 (2 C_{quat}, C=O), 174.02 (2 C_{quat}, C=O), 167.51 (2 C_{quat}), 162.12 (2 C_{quat}), 153.82 (2 C_{quat}), 152.52 (2 C_{quat}), 147.31 (2 C_{quat}), 141.61 (+, 2 Ar-CH), 138.72 (+, 2 Ar-CH), 131.36 (+, 2 Ar-CH), 129.43 (+, 2 Ar-CH), 126.65 (+, 2 Ar-CH), 125.76 (+, 2 Ar-CH), 121.40 (2 C_{quat}), 117.02 (+, 2 Ar-CH), 55.75 (-, 4 Pip-CH₂), 48.09 (-, 4 Pip-CH₂), 46.15 (+, 2 CH₃), 43.16 (-, 2 HomPip-CH₂), 36.83 (-, 2 HomPip-CH₂), 32.81 (-, 2 CH₂), 30.85 (-, 2 CH₂), 30.29 (-, 2 CH₂), 23.81 (-, HomPip-CH₂). **ESI-MS** *m/z* 303.8 [(M+3H)³⁺]; 455.2 [(M+2H)²⁺]; 909.5 [MH⁺]. **CHN** (C₅₁H₆₀N₁₀O₆) calc. C 67.38, H 6.65, N 15.41; exp. C 62.24, H 7.46, N 9.28. Although the experimental CHN data did not match the calculated, the compound was used in the pharmacological assays without further purification.

* = see section 6.17 (*Appendix*) for experimental details

6.16. Overview

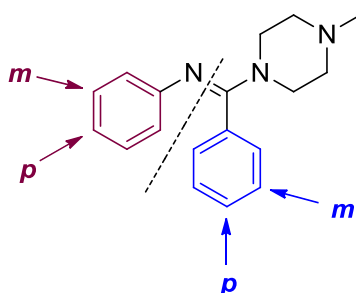


→ **6.2. General procedure A**

SG-22

SG-23

SG-25



→ **6.4. General procedure C**

SG-28

SG-58

SG-64

SG-67

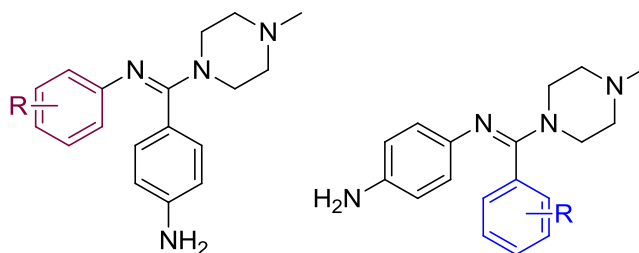
SG-70

SG-73

SG-76

SG-180

SG-181



→ **6.5. General procedure D**

SG-52

SG-56

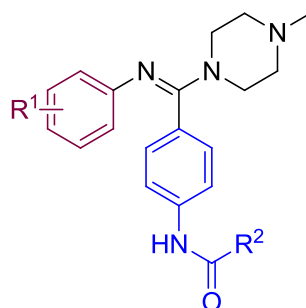
SG-62

SG-80

SG-103

SG-110

SG-111



→ **6.6. General procedure E**

SG-99

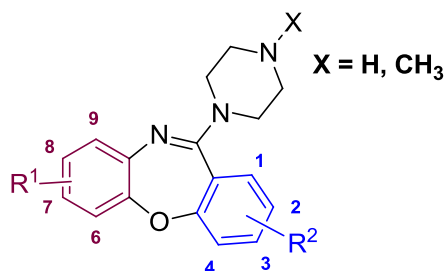
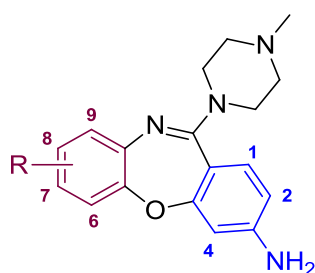
SG-112

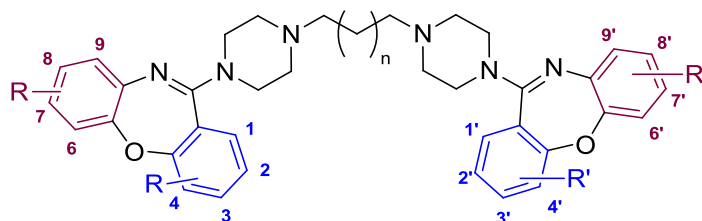
SG-114

SG-115

SG-116

SG-117

**→ 6.10. General procedure I****SG-88****SG-92****SG-141****SG-149****SG-158****SG-159****SG-193****SG-196****SG-232****SG-233****SG-234****SG-235****→ 6.11. General procedure J****SG-128****SG-129****SG-136**



→ **6.12. General procedure K**

SG-205

SG-206

SG-207

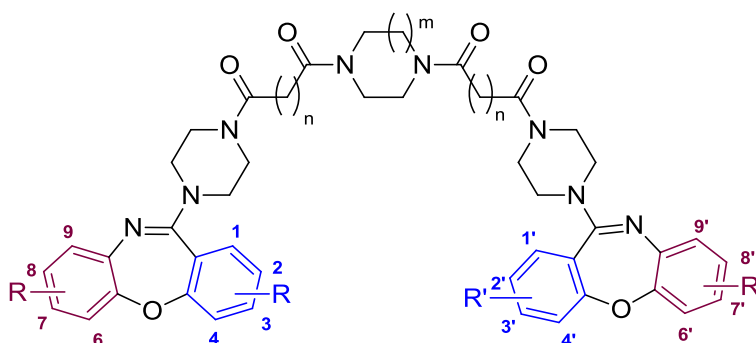
SG-208

SG-209

SG-210

SG-212

SG-213



→ **6.14. General procedure M**

SG-225

SG-238

SG-239

SG-240

SG-241

SG-242

SG-244

6.17. Appendix

6.17.1. HPLC parameters for compounds 243 and 244

Preparative HPLC was performed by Dr. Rudolf Vasold and Simone Strauss (Institute of Organic Chemistry, Chair Prof Dr. Burkhard König, University of Regensburg, Germany). Method Information:

Column:

LabID 90 / Phenomenex Luna 10 μ m C18 (2) 100A, 250 x 21.2 mm / [Part 00G-4253-PO-AX [Ser 453159-3] / B/N 5293-46; column temperature 25 °C

LC-System:

Agilent1100 Series: G1361A PrepPump [DE23900589]

G1316A PrepPump [DE23900591] / G1364A AFC [DE23900834] / G1365B MWD [DE30502172] / G1329A ALS [DE33211203] / G1330B ALS Therm [DE 13205892] / HPLC Column Chiller/Heater C030: Echo Therm Torrey Pines Scientific

Software:

ChemStation for LC 3D Systems Rev. B03.02 [341]

Compound 243

0 min w = 15% MeCN / H₂O [w = 0.059% TFA]

20 min w = 25% MeCN / H₂O [w = 0.059% TFA]

24 min w= 98% MeCN / H₂O [w = 0.059% TFA]

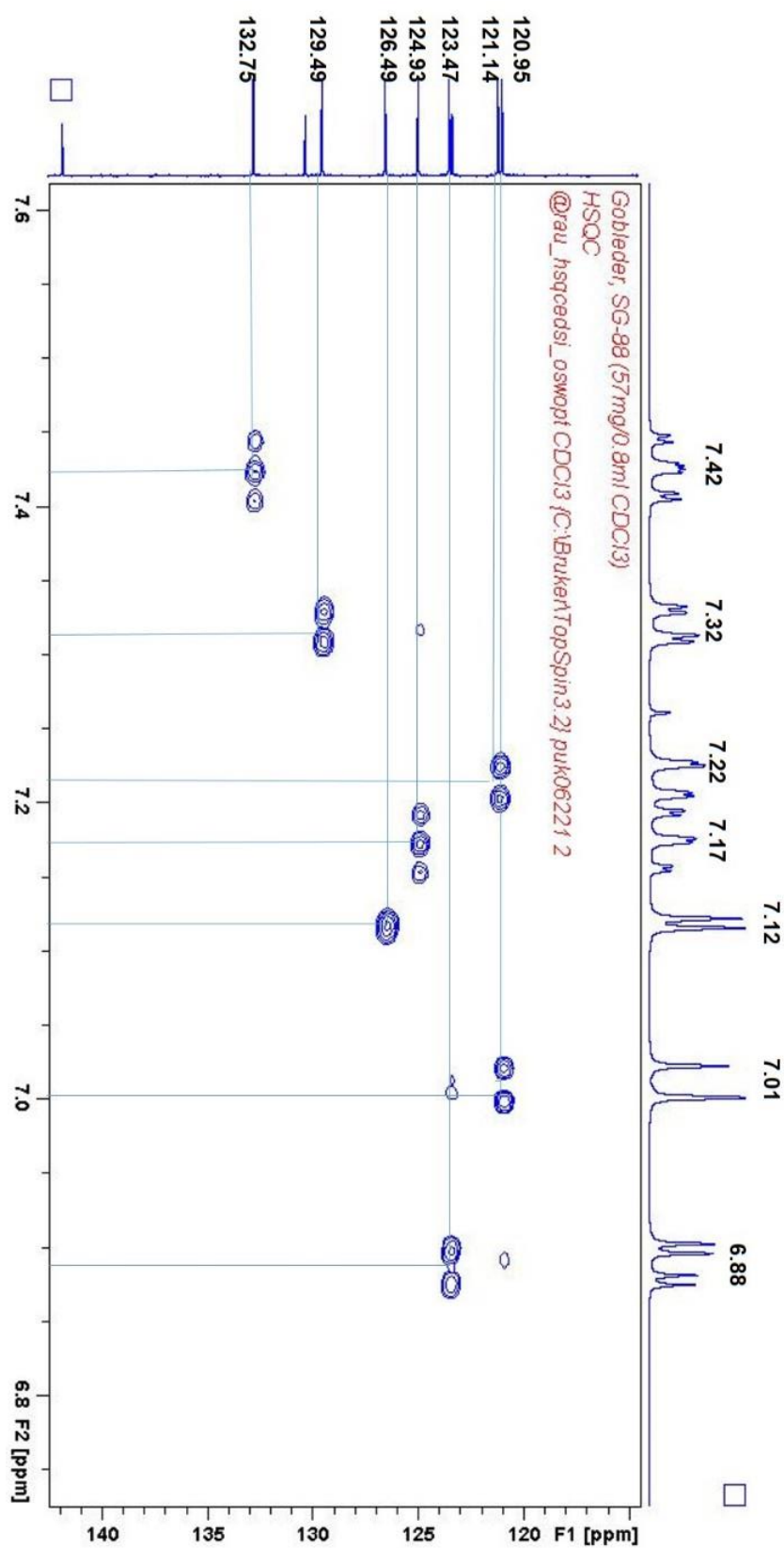
Inj. Vol. 300 μ l / Flow: 21 ml/min

Compound 244

0 min w = 5% MeCN / H₂O [w = 0.059% TFA]

20 min w = 98% MeCN / H₂O [w = 0.059% TFA]

Inj. Vol. 900 μ l / Flow: 21 ml/min

6.17.2. HSQC-, HMBC- and COSY-NMR spectra of compound **88****Figure 6.1.** Heteronuclear single quantum correlation spectrum (HSQC) of **88**, spread.

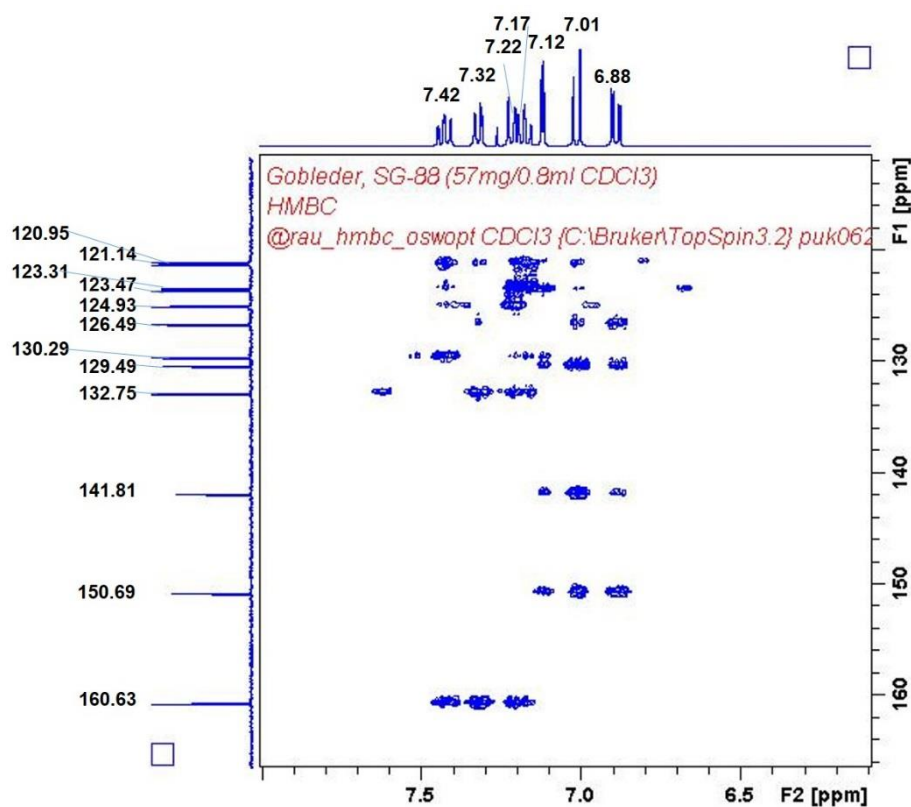


Figure 6.2. Heteronuclear multiple bond correlation spectrum (HMBC) of **88**, spread.

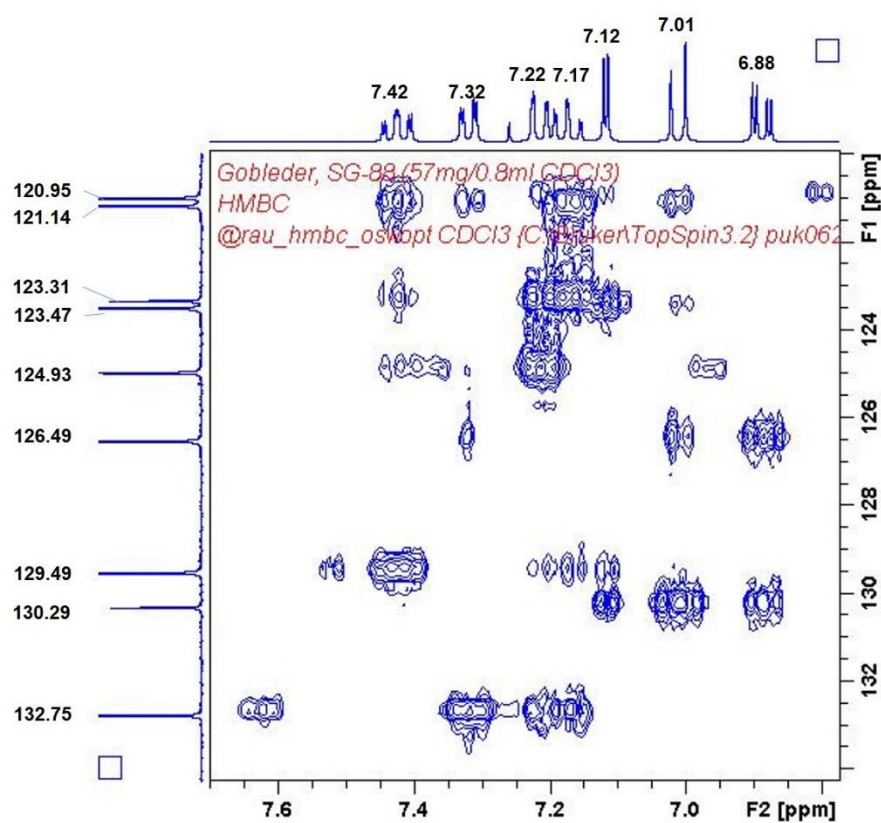


Figure 6.3. Heteronuclear multiple bond correlation spectrum (HMBC) of **88**, spread.

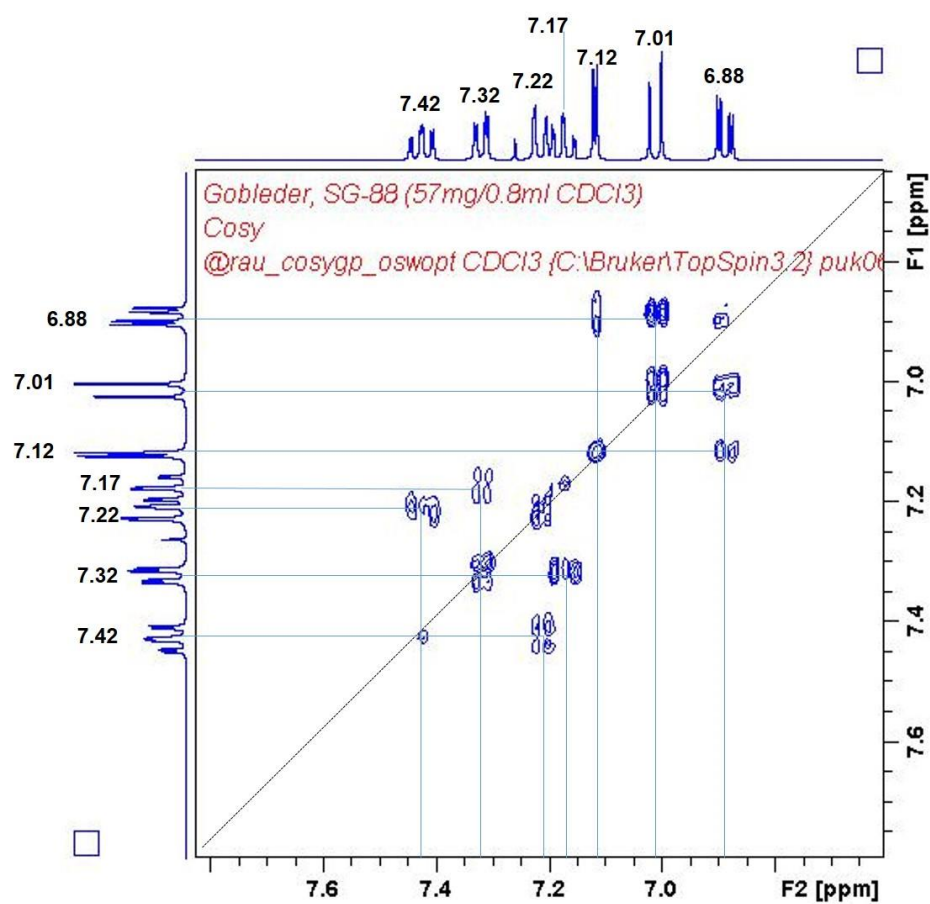


Figure 6.4. Correlation spectroscopy spectrum (COSY) of **88**, spread.

Analytical details for compound **88** (= compound **7a**, *J. Med. Chem.*, **49**, 15, 4512 – 16, Smits et al. (**2006**)):

Compound **7a**, Smits et al. (2006)

¹H-NMR

(200 MHz, DMSO-*d*₆) δ 7.62-7.54 (m, 1H), 7.42-7.28 (m, 3H), 7.19 (d, *J* = 8.4, 1H), 7.06-6.97 (m, 2H) 3.49 (m, 4H), 2.38 (m, 4H), 2.22 (s, 3H);

¹³C-NMR

(200 MHz, DMSO-*d*₆) δ 159.88, 159.53, 150.10, 141.75, 133.12, 129.34, 129.05, 125.38, 125.29, 122.84, 122.32, 121.39, 120.91, 54.08, 46.38, 45.43

Compound **88**:

¹H-NMR

(300 MHz, CDCl₃) δ 7.42 (t, *J* = 8.2, 7.3, 1.7Hz, 1H), δ 7.32 (d, *J* = 7.7Hz, 1H), δ 7.22 (d, *J* = 8.2 Hz, 1H), 7.17 (t, *J* = 7.6, 1.2Hz, 1H), δ 7.12 (d, *J* = 2.5Hz, 1H), δ 7.01 (d, *J* = 8.5Hz, 1H), δ 6.88 (d, *J* = 11.1Hz, 1H), δ 3.61 (bs, 4H), δ 2.55 (bs, 4H), δ 2.38 (s, 3H).

¹³C-NMR

(400 MHz, CDCl₃) δ 160.63 (C_{quat}), 150.69 (C_{quat}), 141.81 (C_{quat}), 132.75 (+, Ar-CH), 130.29 (C_{quat}), 129.49 (+, Ar-CH), 126.49 (+, Ar-CH), 124.93 (+, Ar-CH), 123.47 (+, Ar-CH), 123.31 (C_{quat}), 121.14 (+, Ar-CH), 120.96 (+, Ar-CH), 54.91 (-, 2 Pip-CH₂), 47.18 (-, 2 Pip-CH₂), 46.10 (+, CH₃).

The ¹H- and ¹³C-NMR data obtained within this study are in good agreement with the data published in literature (Smits et al., 2006). However, one discrepancy was found within the ¹³C-NMR data: the ¹³C-NMR signal of one quaternary carbon atom (marked in light blue) could not be detected with our methods. As the chemical shifts of this carbon atom are very similar to the vicinated carbon atom marked in green, an overlay of the ¹³C-NMR signals is assumed. Derived from the **HSQC**, **HMBC** and **COSY** spectra shown above (figures 6.1 – 6.4), the following correlation between the detected ¹H- and ¹³C-NMR signals and the chemical structure of compound **88** is suggested (figure 6.5):

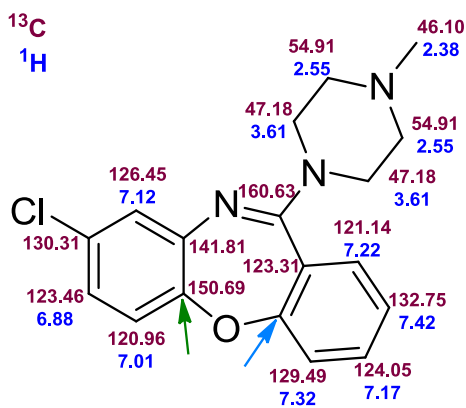


Figure 6.5. Correlation between the detected ^1H - and ^{13}C -NMR signals and the chemical structure of **88**.

Eidesstattliche Erklärung

Ich erkläre hiermit an Eides statt, dass ich die vorliegende Arbeit ohne unzulässige Hilfe Dritter und ohne Benutzung anderer als der angegebenen Hilfsmittel angefertigt habe; die aus anderen Quellen direkt oder indirekt übernommenen Daten und Konzepte sind unter Angabe des Literaturzitats gekennzeichnet.

Weitere Personen waren an der inhaltlich-materiellen Herstellung der vorliegenden Arbeit nicht beteiligt. Insbesondere habe ich hierfür nicht die entgeltliche Hilfe eines Promotionsberaters oder anderer Personen in Anspruch genommen. Niemand hat von mir weder unmittelbar noch mittelbar geldwerte Leistungen für Arbeiten erhalten, die im Zusammenhang mit dem Inhalt der vorgelegten Dissertation stehen.

Die Arbeit wurde bisher weder im In- noch im Ausland in gleicher oder ähnlicher Form einer anderen Prüfungsbehörde vorgelegt

Regensburg, im Mai 2014

(Susanne Gobleder)